



# University of HUDDERSFIELD

## University of Huddersfield Repository

Leivers, Shaun

Characterisation of Bacterial Exopolysaccharides

### Original Citation

Leivers, Shaun (2011) Characterisation of Bacterial Exopolysaccharides. Doctoral thesis, University of Huddersfield.

This version is available at <http://eprints.hud.ac.uk/12014/>

The University Repository is a digital collection of the research output of the University, available on Open Access. Copyright and Moral Rights for the items on this site are retained by the individual author and/or other copyright owners. Users may access full items free of charge; copies of full text items generally can be reproduced, displayed or performed and given to third parties in any format or medium for personal research or study, educational or not-for-profit purposes without prior permission or charge, provided:

- The authors, title and full bibliographic details is credited in any copy;
- A hyperlink and/or URL is included for the original metadata page; and
- The content is not changed in any way.

For more information, including our policy and submission procedure, please contact the Repository Team at: [E.mailbox@hud.ac.uk](mailto:E.mailbox@hud.ac.uk).

<http://eprints.hud.ac.uk/>

# Characterisation of Bacterial Exopolysaccharides

Shaun Leivers MSci



A thesis submitted to the University of Huddersfield in partial fulfilment of the  
requirements for the degree of Doctor of Philosophy

Department of Chemical and Biological Sciences

The University of Huddersfield

May 2011

## ABSTRACT

In this project, the structures of exopolysaccharides (EPS) produced by bacterial strains were characterised. The current techniques utilised for structural elucidation were also investigated.

The structure of the novel EPS isolated from the fermentation of the lactic acid bacteria (LAB) strain, *Lactobacillus helveticus* Rosyjski, has been characterised. The strain of LAB was grown on skimmed milk supplemented with glucose; the subsequent EPS produced was isolated using established protocols. The <sup>1</sup>H NMR spectrum identified the presence of five anomeric monosaccharide signals corresponding to the existence of a pentasaccharide repeating unit oligosaccharide. HP-SEC-MALLS analysis revealed the EPS has a weight average molecular weight of less than  $1.4 \times 10^6 \text{ g mol}^{-1}$ . A combination of GC-MS and HPAEC-PAD analysis confirmed that the structure was composed of D-glucose, D-galactose and D-N-acetyl mannosamine in a molar ratio of 2:2:1. Linkage analysis of the EPS, by GC-MS and 2D-NMR experiments showed that the repeating unit contains two terminal, one di-linked and two tri-linked monosaccharides. All of the data obtained allowed for the elucidation of the structure of the EPS produced by *Lactobacillus helveticus* Rosyjski.

The current techniques used for the determination of the monomers and linkages present in EPS structures were investigated. Monomer analysis was studied by using the previously characterised EPS, *Lactobacillus acidophilus* 5e2 as a model. A variety of acids were used to catalyse the hydrolysis of the polysaccharide. The monosaccharides liberated from the EPS were analysed by HPAEC-PAD. It was determined that hydrolysis with TFA was the simplest technique to employ whilst also providing reliable results. Linkage analysis was investigated by the production of a number of disaccharide-derived model linkage standard compounds. This resulted in the creation of a number of terminally and di-linked linkage standards which can be used as model reference compounds when characterising previously unidentified EPS.

The bacterial strain *Bifidobacterium animalis* subsp. *lactis* A1dOxR produces EPS. Initial inspection of the <sup>1</sup>H NMR spectrum however displayed a complex anomeric region with many overlapping signals. Analysis by HP-SEC-MALLS revealed multiple peaks, further adding to the evidence of the presence of more than one EPS in the recovered 'crude' sample. The crude sample was subjected to dialysis and a fraction (over 100,000 Da) was recovered and denoted as high molecular weight (HMW) EPS. Examination of the <sup>1</sup>H NMR spectrum from HMW EPS indicated a hexasaccharide repeating unit oligosaccharide, whilst HPAEC-PAD and GC-MS analysis confirmed that the structure was composed of L-rhamnose, D-galactose and D-glucose in a molar ratio of 3:2:1. Further analysis determined that one of the galactose monosaccharides was present in the furanose form as oppose to the more commonly observed pyranose configuration. Linkage analysis of the EPS, by GC-MS and 2D-NMR experiments, showed that the repeating unit contains one terminal, four di-linked and one tri-linked monosaccharide. All of the data obtained allowed for the elucidation of the structure of the HMW EPS from by *Bifidobacterium animalis* subsp. *lactis* A1dOxR.

Solubilising EPSs has been a constant challenge, however, it was hoped with the advent of ionic liquids (IL) this issue could be solved. Ultimately, dissolution of EPS in ionic liquids though proved to be unsuccessful, so attention was turned to combining derivatisation and dissolution, as a method for solubilising polysaccharides. Derivatisation of a number of model systems of di- and polysaccharides were explored. By studying both 1D- and 2D-NMR coupled with GC-MS analysis it has demonstrated that polysaccharides such as cellulose along with a number of common disaccharides can be successfully dissolved and modified in ionic liquids.

## **Acknowledgements**

Firstly I would like to thank my director of studies Dr. Andrew Laws for his help, assistance and guidance throughout my project. I would like to extend a great deal of thanks to Dr. Neil McLay for running the NMR experiments. I would also like to thank Dr. Marcus Chadha for his constant help and knowledgeable advice on numerous occasions. I would like to thank Dr. Paul Humphreys and his team of microbiologists for their assistance with fermentations. I would also like to thank Dr. Richard Hughes and Mr. Paul Shaw for their help with aspects of chromatography. I would like to thank my friends for the continual support they have shown during my studies. Finally I would like to thank my family – Mum, Dad, Sam (and Sparky), I simply wouldn't be where I am today without their constant support and encouragement.

## Glossary

### Chemical / Reagent Terms

Ac	Acetyl
Ac <sub>2</sub> O	Acetic anhydride
ADP	Adenosine diphosphate
ATP	Adenosine triphosphate
<i>B.</i>	<i>Bifidobacterium</i>
BMIMCl	1-Butyl-3-methylimidazolium chloride
CoA	acetyl-Coenzyme A
CPS	Capsular polysaccharide
CDM	Chemically Defined Medium
D <sub>2</sub> O	Deuterium oxide
DMSO	Dimethyl Sulfoxide
DMSO-d <sub>6</sub>	Deuterated Dimethyl Sulfoxide
DNA	Deoxyribonucleic acid
EDTA	Ethylenediaminetetraacetic acid
EMIMAc	1-Ethyl-3-methylimidazolium acetate
EPS	Exopolysaccharide
<i>f</i>	Furanose
GalA	Galacturonic acid
GalNAc	<i>N</i> -acetylgalactosamine
GAP	Glyceraldehyde-3-phosphate
GIT	Gastrointestinal tract
GlcA	Glucuronic acid
GlcNAc/NAG	<i>N</i> -acetylglucosamine
GRAS	Generally regarded as safe
HCl	Hydrochloric acid
H <sub>2</sub> SO <sub>4</sub>	Sulphuric acid
HPr	Histidine protein
IL	Ionic liquid

RTIL	Room temperature ionic liquid
IBD	Irritable bowel disease
LAB	Lactic acid bacteria
<i>Lb.</i>	<i>Lactobacillus</i>
LPS	Lipopolysaccharide
Me	Methyl
MeI	Methyl iodide
MRS	de Man, Rogosa, Sharpe media
NAD	Nicotinamide adenine dinucleotide
NAM	<i>N</i> -acetylmuramic acid
NaBH <sub>4</sub>	Sodium borohydride
NADH <sub>4</sub>	Sodium borodeuteride
NH <sub>2</sub>	Amine
NaOH	Sodium hydroxide
OH	Hydroxyl
<i>p</i>	Pyranose
PEP	Phosphoenolpyruvate
PGM	Phosphoglucomutases
P <sub>i</sub>	Inorganic phosphate
PTS	PEP transport system
PMAAs	Partially- <i>O</i> -methylated alditol acetates
RTIL	Room temperature ionic liquid
<i>St.</i>	<i>Streptococcus</i>
SDM	Semi-defined media
TCA	Trichloroacetic acid
TFA	Trifluoroacetic acid
UDP	Uridine diphosphate
VOC	Volatile organic solvent

## Experimental Terms

1D	One dimensional
2D	Two dimensional
Cfu mL <sup>-1</sup>	Colony forming units per millilitre
COSY	Correlation spectroscopy
DEPT	Distortionless enhancement by polarisation transfer
DP	Degree of polymerisation
DS	Degree of substitution
GC	Gas chromatography
GC-MS	Gas chromatography mass spectrometry
GPC	Gel permeation chromatography
g/L <sup>-1</sup>	Grams per litre
h	Hours
HMBC	Heteronuclear multiple bond correlation
HMQC/HSQC	Heteronuclear single/multiple quantum coherence
HPAEC-PAD	High performance anion exchange chromatography pulsed amperometric detection
HP-SEC	High performance size exclusion chromatography
MALLS	Multi-angle laser light scattering
Hz	Hertz
M	Molar (mol/dm <sup>-3</sup> )
mg/L <sup>-1</sup>	Milligrams per litre
Mins	Minutes
Mpt.	Melting point
<i>M<sub>w</sub></i>	Weight-average molecular weight
NMR	Nuclear magnetic resonance
ppm	Parts per million
ROESY/NOESY	Rotating frame/nuclear overhauser enhancement spectroscopy
RI	Refractive index
rpm	Revolutions per minute

TOCSY	Total correlation spectroscopy
UV	Ultraviolet
w/v	Weight per volume
w/w	weight per weight



## Table of Contents

<b>1. General Introduction</b> .....	1
1.1 Carbohydrates.....	1
1.1.1 Monosaccharides .....	1
1.1.2 Monosaccharide Derivatives .....	6
1.1.3 Disaccharides.....	6
1.2 Polysaccharides .....	7
1.3 Bacterial Polysaccharides .....	9
1.3.1 Bacteria .....	9
1.3.2 Bacterial Growth.....	10
1.3.3 Bacterial Cell Walls .....	11
1.3.4 Bacterial Polysaccharides .....	13
1.4 LAB.....	14
1.4.1 Homolactic Fermentation .....	14
1.4.2 Heterolactic Fermentation .....	16
1.4.3 LAB in the Food Industry and Possible Health Affects .....	19
1.5 Bifidobacteria.....	22
1.5.1 Heterolactic Fermentation of Bifidobacterium .....	23
1.5.2 Bifidobacteria – Uses, Benefits and Problems.....	25
1.6 Exopolysaccharides .....	26
1.6.1 Exopolysaccharide Biosynthesis.....	28
1.6.2 Exopolysaccharide Production and Isolation .....	32
1.7 Characterisation of Exopolysaccharides.....	35
1.7.1 Monosaccharide Analysis .....	36
1.7.2 Linkage Analysis .....	39
1.7.3 NMR Analysis.....	42
1.7.4 Weight-average Molecular Weight Determination .....	45
1.8 Dissolution of Polysaccharides .....	46
1.8.1 Ionic Liquids .....	46
1.8.2 Ionic Liquids and Carbohydrates.....	47
1.9 Research Aims.....	48
<b>2. Experimental</b> .....	49
2.1 General Reagents .....	49
2.2 Fermentation of <i>Lactobacillus helveticus</i> Rosyjski.....	49
2.2.1. Bacterial Cultures .....	49

2.2.2	Media.....	50
2.2.3	Batch Fermentation of <i>Lactobacillus helveticus</i> Rosyjski .....	51
2.2.4	Isolation of <i>Lactobacillus helveticus</i> Rosyjski .....	51
2.2.5	Isolation of HMW EPS from Crude <i>Bifidobacterium animalis</i> subsp. <i>lactis</i> A1dOxR....	52
2.3	Structural Characterisation of Exopolysaccharides .....	53
2.3.1	NMR Analysis.....	53
2.3.2	Molecular Weight Determination .....	54
2.3.3	Monomer Analysis.....	55
2.3.4	Linkage Analysis .....	59
2.3.5	Absolute Configuration .....	61
2.4	Analysis of Carbohydrates in Ionic Liquids .....	62
2.4.1	Dissolution of Carbohydrates .....	62
2.4.2	Acetylation of Carbohydrates in Ionic Liquids .....	63
2.4.3	Extraction of Carbohydrates from Ionic Liquids .....	63
2.4.4	NMR Analysis.....	63
2.4.5	GC-MS Analysis of Acetylated Carbohydrates .....	63
2.4.6	MS with MS/MS Analysis .....	64
2.4.7	Recycling of Ionic Liquids.....	65
<b>3.</b>	<b>Structural Characterisation of the Novel EPS from <i>Lactobacillus helveticus</i> Rosyjski .....</b>	<b>67</b>
3.1	Introduction.....	67
3.2	Production and Isolation of Rosyjski .....	67
3.2.1	Production and Isolation of EPS .....	67
3.2.2	Initial Observations.....	68
3.3	Monomer and Linkage Analysis for Rosyjski .....	71
3.3.1	Monomer Analysis Techniques .....	72
3.3.2	Linkage Analysis Techniques.....	76
3.3	Structural Characterisation.....	81
3.3.1	Structural Analysis Using NMR.....	81
3.3.2	Structural Analysis using GC-MS and HPAEC-PAD.....	92
3.3.3	Absolute Configuration .....	96
3.3.4	Structure of the EPS produced by <i>Lactobacillus helveticus</i> Rosyjski .....	97
3.4	Future Work.....	98
3.5	Appendices.....	99
3.5.1	HPAEC-PAD Monomer Standard Curves .....	99
3.5.2	Anomeric Configuration Determination .....	101
3.5.3	GC-MS Monomer Analysis.....	101
3.5.4	GC-MS Linkage Analysis .....	102

<b>4. Structural Characterisation of the Novel EPS from <i>Bifidobacterium animalis</i> subsp. <i>lactis</i></b>	
<b>IPLA-R1 (A1dOxR)</b> .....	103
4.1 Introduction.....	103
4.2 Isolation and Preparation of A1dOxR .....	103
4.2.1 Analysis of Crude Sample.....	103
4.2.2 Isolation of High Molecular Weight material from Crude A1dOxR.....	106
4.3 Structural Characterisation.....	109
4.3.1 Structural Analysis using NMR.....	110
4.3.2 Structural Analysis using GC-MS and HPAEC-PAD.....	123
4.3.3 Absolute Configuration .....	128
4.3.4 Proposed Structure of the HMW EPS produced by <i>Bifidobacterium animalis</i> subsp. <i>lactis</i> IPLA-R1 (A1dOxR) .....	130
4.4 Initial Analysis of LMW Fraction of Crude Material from <i>Bifidobacterium animalis</i> subsp. <i>lactis</i> A1dOxR.....	131
4.4.1 Comparison and Examination of LMW, HMW and the Original Crude EPS Sample .	131
4.4.2 Comparison and Examination of A1, A1dOx and A1dOxR.....	133
4.5 Future Work.....	134
4.6 Appendices.....	136
4.6.1 Anomeric Configuration Determination .....	136
4.6.2 HPAEC-PAD Monomer Standard Curves.....	137
4.6.3 GC-MS Linkage Analysis .....	138
4.6.4 Absolute Configuration Analysis .....	139
<b>5. Ionic Liquids and Carbohydrates</b> .....	140
5.1 Introduction.....	140
5.1.1 EPS and Ionic Liquids .....	140
5.2 Cellulose Dissolution and Modification in Ionic Liquids .....	143
5.2.1 Cellulose Dissolution.....	143
5.2.2 Cellulose Modification to Improve Dissolution .....	147
5.2.2 Ionic Liquid Recycling .....	152
5.3 Disaccharide Dissolution and Modification .....	153
5.3.1 Analysis of Cellobiose in Ionic Liquid Systems – A Simplified Model for Derivatisation Reactions .....	153
5.3.2 Acetylation of Other Disaccharides in BMIMCl .....	160
5.4 Appendices.....	165
5.4.1 <sup>1</sup> H NMR Spectra of Recycled Ionic Liquids.....	165
5.4.2 α-Cellobiose Octaacetate Standard .....	166
5.4.3 Cellobiose Acetylated in BMIMCl with Pyridine .....	167

5.4.4	Zinc Chloride and Sodium Acetate Catalysed Acetylation Products .....	168
5.4.5	Trehalose Acetylated in BMIMCl with Pyridine .....	169
5.4.6	$\alpha$ -Lactose Octaacetate Standard .....	169
5.4.7	$^1\text{H}$ NMR Spectrum of Sucrose Octaacetate Standard with $\text{CDCl}_3$ at $25^\circ\text{C}$ .....	170
<b>6. References</b>	.....	<b>171</b>
<b>7. Publications</b>	.....	<b>181</b>

## Table of Figures and Tables

### Figures

Figure 1: Structure of Cellulose – a highly abundant polysaccharide.....	1
Figure 2: General Formulas for Aldoses and Ketoses.....	2
Figure 3: Furanose and Pyranose Forms of D-glucose.....	2
Figure 4: Absolute Configurations of Glucose.....	3
Figure 5: The Anomeric Effect.....	3
Figure 6: The Anomeric Effect in D-glucose.....	4
Figure 7: Tautomeric forms of D-glucose in solution.....	5
Figure 8: Two Possible Chair forms of Glucopyranose.....	5
Figure 9: Sugar Derivatives.....	6
Figure 10: Example of Two Common Disaccharides.....	7
Figure 11: Amylopectin (Bottom) and $\alpha$ -amylose (Top).....	8
Figure 12: Xanthan Gum.....	9
Figure 13: Batch Culture Bacterial Growth Curve.....	11
Figure 14: Cross Section of a Gram-Positive Bacterial Cell Wall.....	12
Figure 15: Cross Section of a Gram-Negative Bacterial Cell Wall.....	13
Figure 16: Homolactic Fermentation Pathway.....	15
Figure 17: Heterolactic Fermentation Pathway.....	17
Figure 18: Heterolactic Fermentation Pathway of <i>Bifidobacteria</i> .....	24
Figure 19: Generalised diagram of the conversion of lactose, galactose and glucose to EPS and to glycolysis in LAB (Reproduced from Welman and Maddox, 2003 <sup>96</sup> ).....	29
Figure 20: Model of EPS Biosynthesis in <i>Lactococcus lactis</i> NIZO B40 (Reproduced from Welman and Maddox, 2003 <sup>96</sup> ).....	31
Figure 21: Tetrasaccharide Repeating Unit Structure of the Isolated EPS from <i>St. thermophilus</i> .....	35
Figure 22: Alditol Acetate Formation for Monosaccharide Analysis.....	36
Figure 23: Methylated Alditol Acetate Formation for Linkage Analysis.....	40
Figure 24: Demonstration of the Dihedral Angle - Coupling Constant Relationship.....	43
Figure 25: Examples of Ionic Liquids.....	47
Figure 26: <sup>1</sup> H NMR Spectrum of EPS from <i>Lactobacillus helveticus</i> Rosyjski in D <sub>2</sub> O at 70°C (Batch XN286).....	68
Figure 27: <sup>1</sup> H NMR Spectrum of EPS from <i>Lactobacillus helveticus</i> Rosyjski in D <sub>2</sub> O at 70°C (Batch XN361).....	69
Figure 28: A Chromatogram of the Pullulan Standard (800,000 M <sub>w</sub> ).....	70
Figure 29: A Chromatogram of EPS Produced By Fermentation of Rosyjski Batch XN361.....	71
Figure 30: Line Drawing Structure of EPS produced by <i>Lactobacillus acidophilus</i> 5e2.....	74
Figure 31: MS Fragmentation for PMAA Linkage Standards – A) Terminal Glucose/Galactose/Mannose; B) 1-2 Linked Mannose; C) 1-3 Linked Galactose; D) 1-4 Linked Glucose; E) 1-6 Linked Glucose.....	79
Figure 32: DEPT 135 <sup>13</sup> C NMR Spectrum of <i>Lactobacillus helveticus</i> Rosyjski (Main) Magnified Region showing Anomeric C1's (Inset Bottom Left) Magnified Region showing C6's (Inset Bottom Right).....	83

Figure 33: COSY Spectrum of EPS from <i>Lactobacillus helveticus</i> Rosyjski .....	84
Figure 34: TOCSY Spectra of EPS from <i>Lactobacillus helveticus</i> Rosyjski .....	85
Figure 35: $^1\text{H}$ - $^{13}\text{C}$ HSQC Spectrum of EPS from <i>Lactobacillus helveticus</i> Rosyjski .....	87
Figure 36: $^1\text{H}$ - $^{13}\text{C}$ HSQC Spectrum Anomeric Region of EPS from <i>Lactobacillus helveticus</i> Rosyjski	88
Figure 37: $^1\text{H}$ - $^{13}\text{C}$ HMBC Spectra of EPS from <i>Lactobacillus helveticus</i> Rosyjski.....	89
Figure 38: 2D- $^1\text{H}$ - $^1\text{H}$ ROESY Spectrum of EPS from <i>Lactobacillus helveticus</i> Rosyjski .....	91
Figure 39: MS Fragmentation for Sugar Alditol Acetate Monomers of A) Glucose and B) Mannosamine.....	93
Figure 40: HPAEC-PAD Chromatogram of EPS from <i>Lactobacillus helveticus</i> Rosyjski Monomers... 94	
Figure 41: Mass Spectra Fragmentation A) Terminal Glucose/Galactose; B) 1-4 Linked Glucose/Galactose; C) 1, 3, 4 Linked Glucose/Galactose; D) 1-4 Linked <i>N</i> -acetylmannosamine.....	95
Figure 42: Line Drawing of EPS Repeating Unit Structure from <i>Lactobacillus helveticus</i> Rosyjski .....	97
Figure 43: Structure of EPS produced by <i>Lactobacillus helveticus</i> Rosyjski.....	97
Figure 44: $^1\text{H}$ NMR Spectrum of Crude EPS from <i>Bifidobacterium animalis</i> subsp. <i>lactis</i> A1dOxR in $\text{D}_2\text{O}$ at $70^\circ\text{C}$ .....	104
Figure 45: Expanded Anomeric Region $^1\text{H}$ NMR Spectrum of EPS Crude EPS from <i>Bifidobacterium animalis</i> subsp. <i>lactis</i> A1dOxR .....	104
Figure 46: A Chromatogram of Crude EPS from <i>Bifidobacterium animalis</i> subsp. <i>lactis</i> A1dOxR ....	105
Figure 47: $^1\text{H}$ NMR Spectrum of High Molecular Weight Material Recovered from Vivaspin 20 (Main) Magnified Anomeric region (Inset) .....	106
Figure 48: $^1\text{H}$ NMR Spectrum of High Molecular Weight Material Recovered from Spectra/Por Float-A-Lyzer.....	108
Figure 49: A Chromatogram of High Molecular Weight material isolated from Crude A1dOxR using Spectra/Por Float-A-Lyzer.....	109
Figure 50: DEPT 135 $^{13}\text{C}$ NMR Spectrum of High Molecular Weight EPS from <i>Bifidobacterium animalis</i> subsp. <i>lactis</i> A1dOxR (Main) Magnified Region showing $\text{CH}_3\text{s}$ (Inset Top) Magnified Region showing C6s (Inset Bottom) .....	111
Figure 51: COSY Spectrum of High Molecular Weight EPS from <i>Bifidobacterium animalis</i> subsp. <i>lactis</i> A1dOxR.....	112
Figure 52: Overlaid TOCSY Spectra of High Molecular Weight EPS from <i>Bifidobacterium animalis</i> subsp. <i>lactis</i> A1dOxR.....	113
Figure 53: TOCSY (150 ms) Spectrum with COSY Spectrum Overlaid of High Molecular Weight EPS from <i>Bifidobacterium animalis</i> subsp. <i>lactis</i> A1dOxR .....	114
Figure 54: $^1\text{H}$ - $^{13}\text{C}$ HSQC Spectrum of High Molecular Weight EPS from <i>Bifidobacterium animalis</i> subsp. <i>lactis</i> A1dOxR.....	116
Figure 55: $^1\text{H}$ - $^{13}\text{C}$ HSQC Spectrum – Anomeric Region of High Molecular Weight EPS from <i>Bifidobacterium animalis</i> subsp. <i>lactis</i> A1dOxR.....	116
Figure 56: $^1\text{H}$ - $^{13}\text{C}$ HMBC Spectrum of High Molecular Weight EPS from <i>Bifidobacterium animalis</i> subsp. <i>lactis</i> A1dOxR.....	118
Figure 57: 2D- $^1\text{H}$ - $^1\text{H}$ NOESY Spectrum of High Molecular Weight EPS from <i>Bifidobacterium animalis</i> subsp. <i>lactis</i> A1dOxR.....	119
Figure 58: $^1\text{H}$ NMR Spectra of Acid Hydrolysed High Molecular Weight EPS from <i>Bifidobacterium animalis</i> subsp. <i>lactis</i> A1dOxR (Spectra 1) Pre-hydrolysis (Spectra 2-10) Post-hydrolysis 1 – 9 hours (Spectra 11) Post-hydrolysis 24 hours.....	121
Figure 59: Mild Acid Hydrolysis Effect on EPS Repeat Unit Structure .....	122
Figure 60: GC-MS Chromatogram of HMW EPS Monomers .....	123

Figure 61: MS Fragmentation for Sugar Alditol Acetate Monomers of A) Rhamnose and B) Glucose .....	124
Figure 62: HPAEC-PAD Chromatogram of HMW EPS Monomers .....	125
Figure 63: Mass Spectra Fragmentation A) 1-2 Linked deoxy hexose; B) 1-4 Linked hexose; C) 1, 2, 3 Linked deoxy hexose; D) Terminal hexose (f) .....	127
Figure 64: Acetylated Butyl ((S)-(+)-2-butanol) Glycosides .....	129
Figure 65: Structure of HMW EPS produced by <i>Bifidobacterium animalis</i> subsp. <i>lactis</i> A1dOxR .....	130
Figure 66: Line Drawing Structure of HMW EPS produced by <i>Bifidobacterium animalis</i> subsp. <i>lactis</i> A1dOxR.....	131
Figure 67: Anomeric Region <sup>1</sup> H NMR Spectra of Crude (Black), HMW (Red) and LMW (Green) material from <i>Bifidobacterium animalis</i> subsp. <i>lactis</i> A1dOxR .....	132
Figure 68: Anomeric Region <sup>1</sup> H NMR Spectra of LMW material isolated from Crude A1dOxR (Black), A1 (Red) and A1dOx (Green) .....	133
Figure 69: <sup>1</sup> H NMR Spectrum of BMIMCl with D <sub>2</sub> O Insert at 70°C .....	141
Figure 70: <sup>13</sup> C NMR Spectrum of BMIMCl with D <sub>2</sub> O Insert at 70°C .....	142
Figure 71: <sup>1</sup> H NMR Spectrum of EMIMAc with D <sub>2</sub> O Insert at 25°C .....	142
Figure 72: <sup>13</sup> C NMR Spectrum of EMIMAc with D <sub>2</sub> O Insert at 25°C .....	143
Figure 73: Cellulose Supramolecular Structure .....	144
Figure 74: <sup>13</sup> C NMR Spectra of Cellulose in Solution BMIMCl/DMSO-d <sub>6</sub> 5% w/w at 90°C – adapted from Moulthrop <i>et al</i> 2005 <sup>151</sup> ; B) BMIMCl/DMSO-d <sub>6</sub> 10% w/w at 70°C; C) EMIMAc/DMSO-d <sub>6</sub> 10% w/w at 70°C .....	145
Figure 75: Cellulose Hydrogen Bonding Disruption by BMIMCl .....	147
Figure 76: <sup>1</sup> H NMR Spectrum of Cellulose Acetylated in BMIMCl at 70°C in CDCl <sub>3</sub> .....	148
Figure 77: <sup>13</sup> C NMR Spectrum of Cellulose Acetylated in BMIMCl at 70°C in CDCl <sub>3</sub> .....	149
Figure 78: COSY Spectrum of Ring Proton Region of Cellulose Acetylated in BMIMCl at 70°C in CDCl <sub>3</sub> .....	150
Figure 79: <sup>1</sup> H- <sup>13</sup> C HSQC Spectrum of Ring Proton Region of Cellulose Acetylated in BMIMCl at 70°C in CDCl <sub>3</sub> .....	151
Figure 80: Cellobiose Displayed in Both Reducing End Conformations (Above) <sup>13</sup> C NMR Spectra of Cellobiose in Solution BMIMCl/DMSO-d <sub>6</sub> 10% w/w at 70°C (Below) .....	154
Figure 81: <sup>1</sup> H NMR Spectrum of Cellobiose Acetylated in BMIMCl with Pyridine at 70°C in CDCl <sub>3</sub> ; Inset - Magnified Region showing Reducing End anomeric Signals .....	156
Figure 82: GC-MS Chromatogram of Cellobiose Acetylated in BMIMCl with Pyridine.....	157
Figure 83: MS Spectrum of Cellobiose in BMIMCl with Pyridine .....	158
Figure 84: Anomeric Region of <sup>1</sup> H NMR Spectrum of Cellobiose Acetylated in BMIMCl A) Sodium Acetate and B) Zinc Chloride at 70°C in CDCl <sub>3</sub> .....	159
Figure 85: <sup>1</sup> H NMR Spectrum of Trehalose Acetylated in BMIMCl with Pyridine at 70°C in CDCl <sub>3</sub> ; Inset - Magnified Region showing Single Anomeric Signal .....	160
Figure 86: <sup>1</sup> H NMR Spectrum of Lactose Acetylated in BMIMCl with Pyridine at 70°C in CDCl <sub>3</sub> ; Inset - Magnified Anomeric Region .....	161
Figure 87: GC-MS Chromatogram of Acetylated Lactose in BMIMCl with Pyridine .....	162
Figure 88: Sucrose .....	163
Figure 89: <sup>1</sup> H NMR Spectrum of Sucrose Acetylated in BMIMCl with Pyridine at 70°C in CDCl <sub>3</sub> ; Inset – Magnified Anomeric Region .....	163
Figure 90: GC-MS Chromatogram of Acetylated Sucrose in BMIMCl with Pyridine .....	164

## **Tables**

Table 1: Homopolysaccharides Produced by Lactic Acid Bacteria.....	18
Table 2: Mesophilic and Thermophilic LAB Strains Producing Heteropolysaccharides .....	19
Table 3: Monomer Ratio Analysis Utilising Differing Hydrolysis Techniques .....	75
Table 4: Disaccharide Sugars studied for Model Compounds for Linkage Analysis .....	78
Table 5: Anomeric Proton Chemical Shifts and $^3J_{1,2}$ and $^1J_{H-C}$ Coupling Constants .....	82
Table 6: $^1H$ NMR Chemical Shifts of EPS Recorded in $D_2O$ at $70\text{ }^\circ C$ .....	86
Table 7: $^{13}C$ NMR Chemical Shifts of EPS Recorded in $D_2O$ at $70\text{ }^\circ C$ .....	88
Table 8: Anomeric Proton Chemical Shifts and $^3J_{1,2}$ and $^1J_{H-C}$ Coupling Constants .....	110
Table 9: $^1H$ NMR Chemical Shifts of EPS Recorded in $D_2O$ at $70\text{ }^\circ C$ .....	115
Table 10: $^{13}C$ NMR Chemical Shifts of EPS Recorded in $D_2O$ at $70\text{ }^\circ C$ .....	117
Table 11: Recorded $^{13}C$ Chemical Shift Values for C1 and C4 for Samples A), B) and C) .....	146
Table 12: $^1H$ and $^{13}C$ NMR Shifts of Cellulose Acetate in $CDCl_3$ at $70\text{ }^\circ C$ .....	151



## 1. General Introduction

### 1.1 Carbohydrates

Polysaccharides are macromolecules more specifically described by the term complex carbohydrates. They exist as either linear or branched chains and consist of a large number (tens, hundreds or even thousands) of simple sugars known as monosaccharides (or their simple derivatives) linked together through glycosidic bonds<sup>1</sup>. Structurally, polysaccharides (Figure 1) are encountered in a wide variety of forms, this is attributed to the fact that they are produced by a vast assortment of species including microbes, algae, plants and animals<sup>2</sup>.

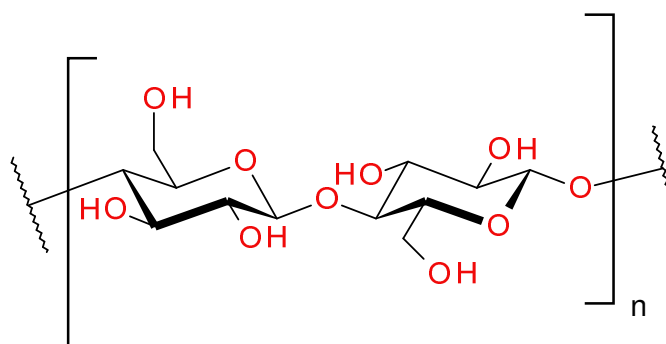


**Figure 1: Structure of Cellulose – a highly abundant polysaccharide**

#### 1.1.1 *Monosaccharides*

Carbohydrates are the most abundant class of molecules found in the natural environment<sup>3</sup>. Monosaccharides (with the basic empirical formula  $C_n (H_2O)_n$ , for the most basic monosaccharides) are the simplest form of carbohydrates as they are not able to be hydrolysed into smaller (simpler) compounds. These smaller carbohydrates are also commonly referred to as sugars. They are categorised as either aldoses or ketoses (Figure 2).

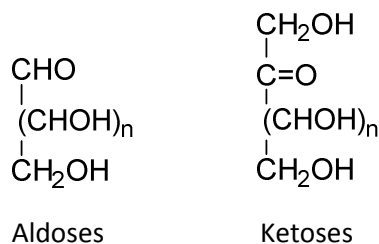


**Figure 2: General Formulas for Aldoses and Ketoses**

For the purpose of this introduction, the main focus will be concerned with monosaccharides containing five or six carbon atoms; these monomers are termed pentoses and hexoses. These are of particular importance as they can exist in a variety of different conformational structures. Using glucose as an example, it can be observed that the pentoses and hexoses can cyclize to form either a pyranose (*p*) or a furanose (*f*) structure as demonstrated by the Haworth projections in Figure 3. It should also be noted though that there are a number of important 7-9 carbon atom containing sugars found in nature such as sedoheptulose (heptose) and neuraminic acid (nonose).

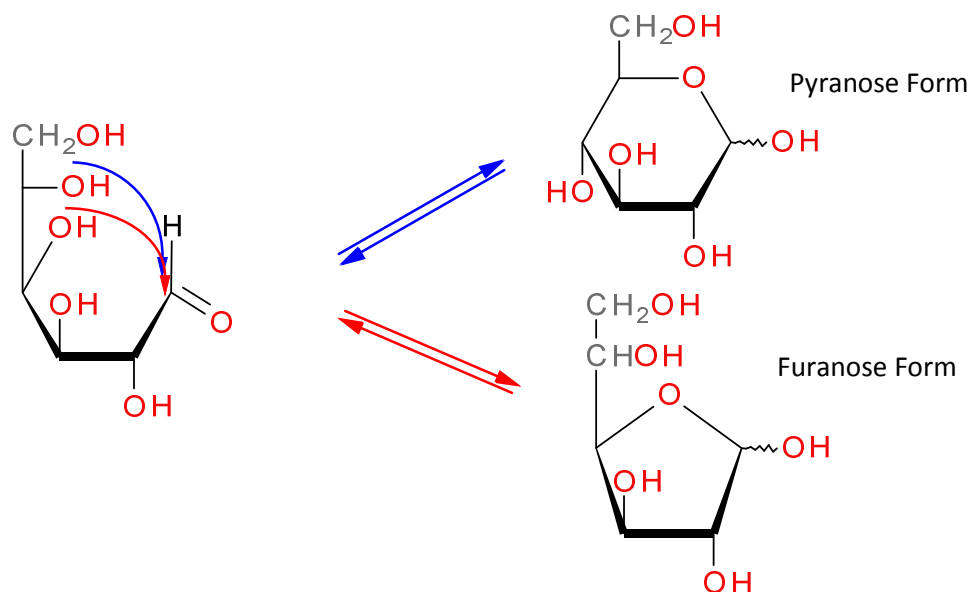


**Figure 3: Furanose and Pyranose Forms of D-glucose**

Which form is more stable (i.e. preferred) is determined by structural factors including the nature of the substituent groups on the carbonyl and/or hydroxyl groups and the

configuration about the asymmetric carbon will establish whether a given monosaccharide prefers the pyranose or furanose arrangement.

As the group of carbohydrates being studied have more than one chiral centre, their absolute configuration is denoted by the prefix D- or L-; this is determined by the absolute configuration of the secondary alcohol at the highest numbered stereogenic centre (Figure 4).

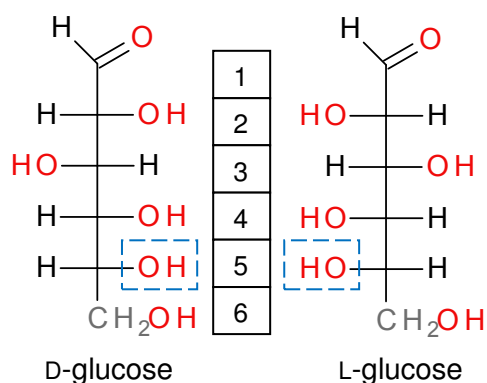


**Figure 4: Absolute Configurations of Glucose**

Alcohols react readily with aldehydes (aldoses) and ketones (ketoses). When the straight chain structures cyclise to form their favoured pyranose or furanose conformation they also form a combination of either  $\alpha$  and  $\beta$  anomers. This is determined by a phenomenon known as the anomeric effect; a term first coined by Riiber and Sørensen in 1933<sup>4</sup> (Figure 5).

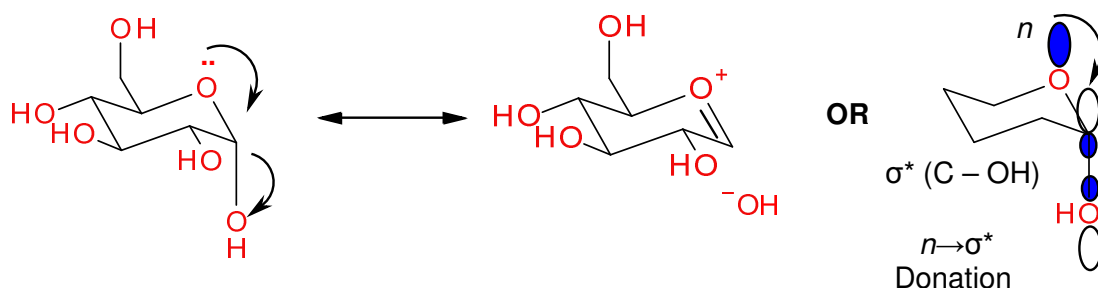


**Figure 5: The Anomeric Effect**

Unequivocal support for the conformational preferences of sugars and their derivatives was first expressed in 1958 by Lemieux *et al*<sup>6</sup>. Electronegative substituents on a pyranose ring prefer to occupy an axial rather than an equatorial orientation (Figure 6)<sup>6</sup>. This occurs as one

of the lone pairs of electrons are anti-periplanar to the C – OH bond, this causes a stabilising effect as it can participate in a two electron interaction, represented by the resonance structures displayed in Figure 5. At a molecular level this can be explained by the formation of an  $n - \sigma^*$  interaction, occurring via the partial donation of the oxygen lone pair (in an  $n$  orbital) into the anti-bonding ( $\sigma^*$ ) orbital of the C – OH. This causes electronic delocalisation resulting in the observed stabilisation<sup>7,6</sup>.

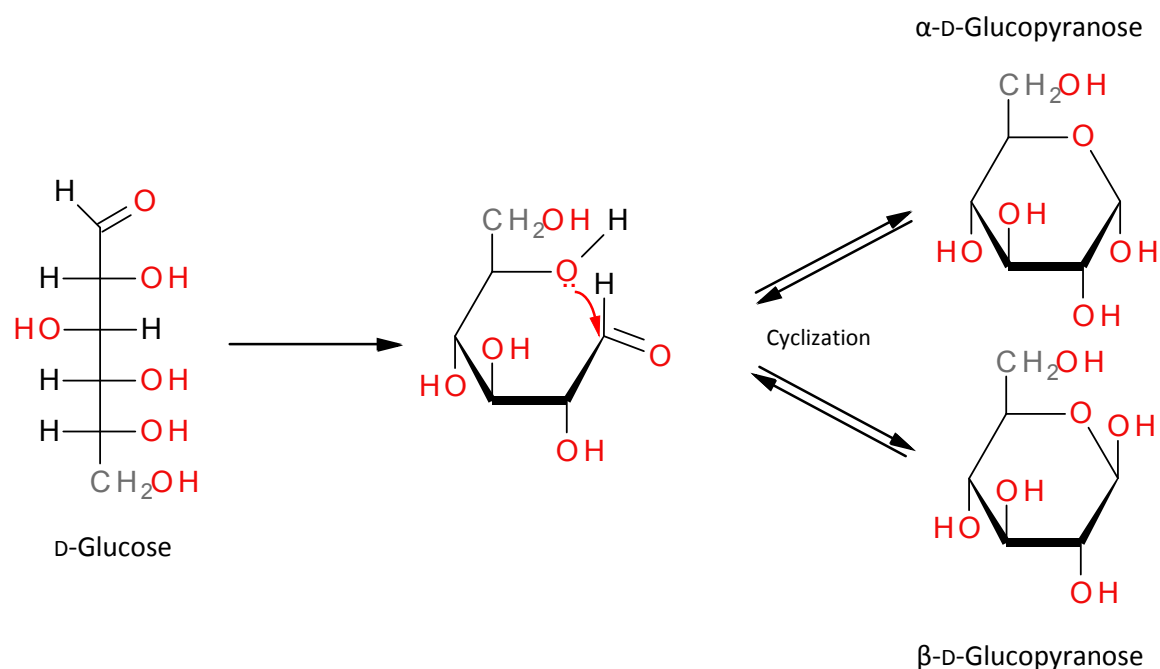


**Figure 6: The Anomeric Effect in D-glucose**

For glucose in water, however, the ratio is approximately 37%  $\alpha$ -glucopyranose and 62%  $\beta$ -glucopyranose, clearly not complying with the anomeric effect. This is thought to be due in part to the counteraction of the anomeric effect by steric effects which force the equilibrium of glucose in water to favour the equatorial position for the substituents over the axial positions (Figure 7).

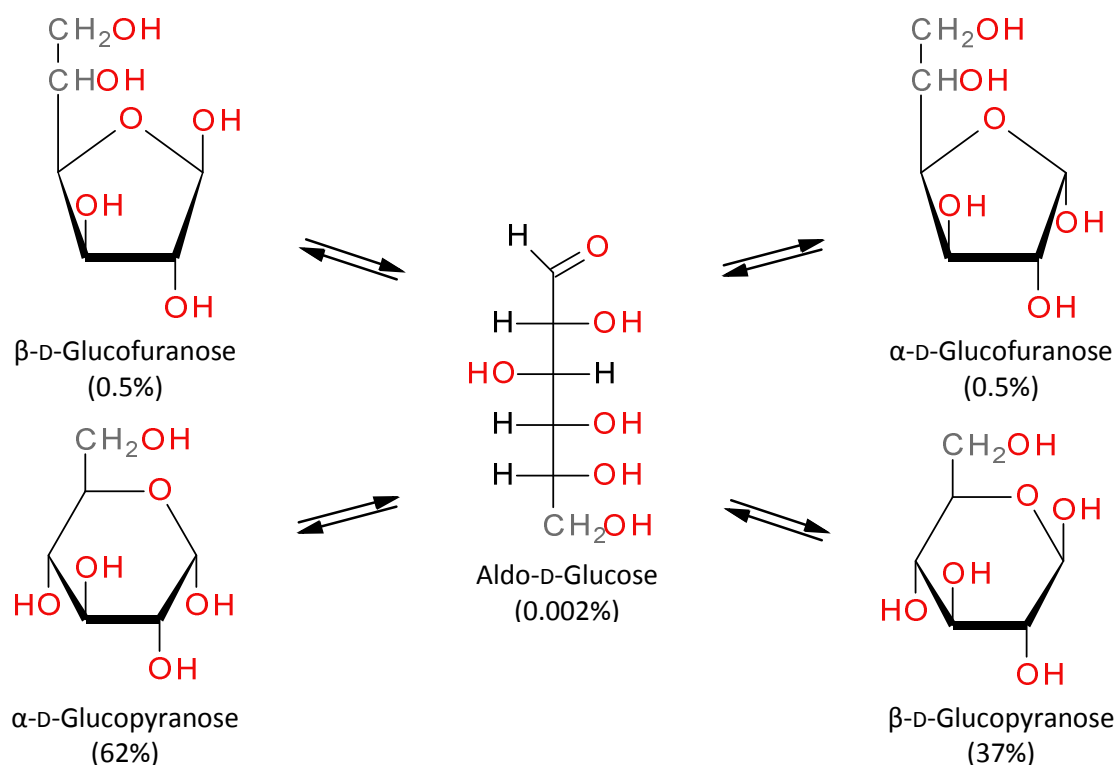


**Figure 7: Tautomeric forms of D-glucose in solution**

Although Haworth projections are useful for portraying monosaccharide structures; they do not however accurately represent the true conformations of pyranose and furanose rings. Thus the chair conformations are employed (as previously encountered in Figure 5); these provide an accurate view of the axial and equatorial substituents (Figure 8). The most stable conformation of glucopyranose is  ${}^4C_1$  (4 representing the highest part of the chair when viewed from a clockwise numbered face). A number of other, less favoured conformations are also available through interconversion of the other conformers by way of ring flipping.

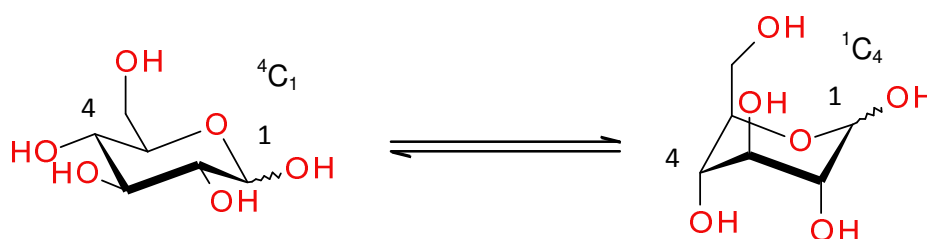


**Figure 8: Two Possible Chair forms of Glucopyranose**

### 1.1.2 Monosaccharide Derivatives

Many derivatives of simple monosaccharides are regularly encountered; a select few will be discussed in the section below (Figure 9).

Sugar acids are formed by either oxidation at C1 resulting in an aldonic acid or at C6 leading to the formation of an uronic acid. Certain uronic acid monomers, such as D-glucuronic acid, play key roles in the xenobiotic metabolism of substances in the body<sup>8</sup>. Sugar alcohols occur by reduction of the carbonyl group of the aldose or ketose forming alditols. Sugar alcohols, such as sorbitol and mannitol have been commonly utilised as artificial food additives for many years<sup>9</sup>. Deoxy sugars are an especially abundant class of sugar derivatives. They occur when one or more of the hydroxyl groups are replaced by hydrogens, thus forming a methyl substituent in its place. The most universally acknowledged deoxy sugar is 2-deoxy-D-ribose, a constituent of DNA. L-Rhamnose is another common deoxy sugar, often found in high abundance in polysaccharides<sup>10</sup>. Amino sugars contain an amino group (either NH<sub>2</sub> or NAc) in place of the hydroxyl group at the C2 position. Both glucosamine and *N*-acetyl glucosamine are found in bacterial cell walls<sup>11</sup>.

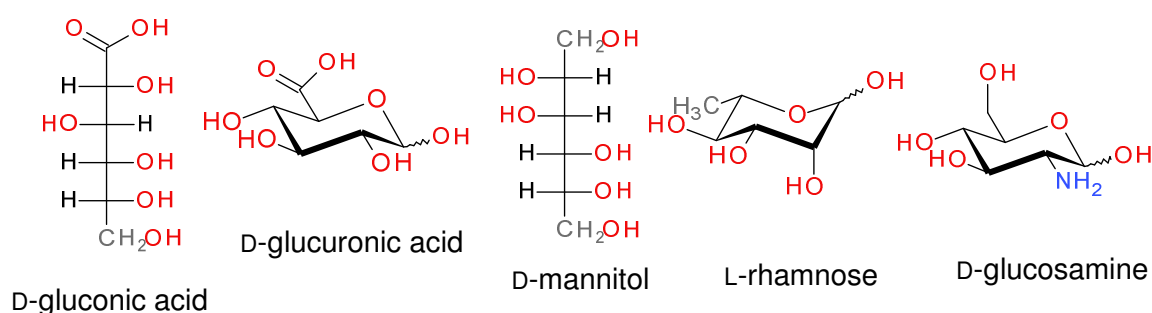


**Figure 9: Sugar Derivatives**

As it can be observed, monosaccharides can be present in a wide variety of forms; this further underlines the diversity and extensive range of polysaccharides that exist.

### 1.1.3 Disaccharides

Monosaccharides are joined together by glycosidic bonds (C – O – C) to form disaccharides (Figure 10). Lactose ( $\beta$ -D-galactopyranosyl-(1 $\rightarrow$ 4)-D-glucose), the principal carbohydrate in

milk for example is formed from  $\beta$ -D-galactopyranose C1 linked to glucose at the C4 position. Whilst sucrose ( $\beta$ -D-fructofuranosyl-(2 $\rightarrow$ 1)- $\alpha$ -D-glucopyranoside), known universally as common table sugar is formed by linking  $\alpha$ -D-glucopyranose C1 to fructose at the C2 position. It should be noted there are two different types of disaccharide, reducing and non-reducing. Lactose is an example of a reducing sugar as one monomer (reducing sugar) of the disaccharide still possesses a free hemiacetal moiety, whilst sucrose is an example of a non-reducing disaccharide as the two monomers involved bond through their anomeric centres, subsequently causing neither monomer to have a free hemiacetal unit.

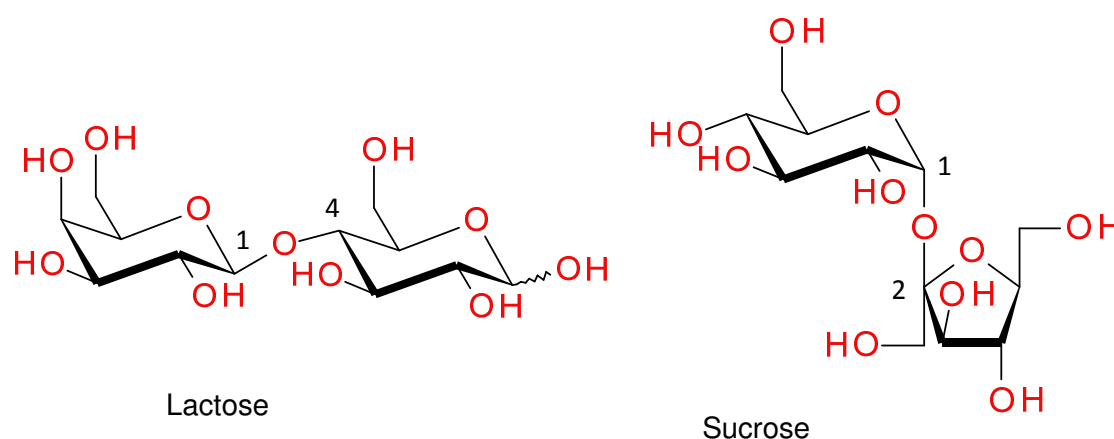


**Figure 10: Example of Two Common Disaccharides**

The continual addition of monomeric sugar residues through glycosidic bonds leads to the formation of trisaccharides (3 sugar units), oligosaccharides (3 – 9 sugar units) and finally to polysaccharides.

## **1.2 Polysaccharides**

It is estimated that approximately  $4 \times 10^{11}$  tonnes of carbohydrates are biosynthesised each year on earth by plants, animals, bacteria and other microorganisms. The majority of these carbohydrates are produced as polysaccharides<sup>2</sup>.

Polysaccharides, also referred to as glycans, play many vital roles in the natural world being used as storage, structural or protective materials. The most abundant of which being cellulose (Figure 1), the major structural component of plant cell walls. Cellulose is a linear

structure consisting of  $\beta$ -(1 $\rightarrow$ 4) linked D-glucopyranose units; it is therefore termed a homopolysaccharide<sup>12</sup> as it is comprised of only one type of monosaccharide. More specifically, cellulose is categorised as a glucan – a polymer containing only glucose monomers. Starch is a mixture of two glucans,  $\alpha$ -amylose ( $\alpha$ -(1 $\rightarrow$ 4) D-glucose) and amylopectin (Figure 11), both of which are present in high abundance in plants acting as the main, most common, storage material. In contrast to cellulose and  $\alpha$ -amylose, amylopectin is a highly branched polysaccharide, consisting of an  $\alpha$ -(1 $\rightarrow$ 4) linked D-glucose backbone with branches of  $\alpha$ -(1 $\rightarrow$ 4) linked D-glucose chains, (attached at the C6 position), occurring every 12-30 residues.

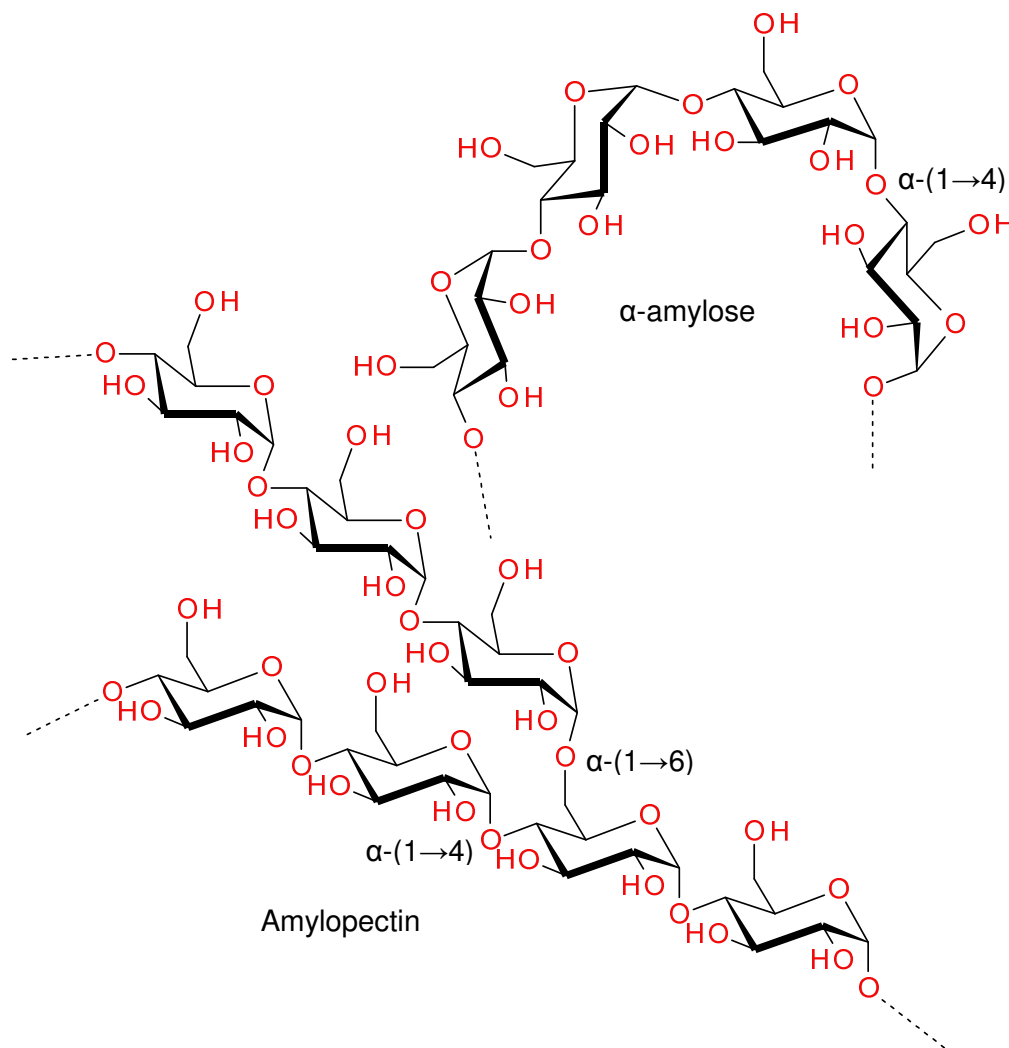


**Figure 11: Amylopectin (Bottom) and  $\alpha$ -amylose (Top)**



Xanthan gum (Figure 12) is classified as a heteropolysaccharide as it consists of more than one type of monosaccharide. It is used as a food additive and is mainly employed as a rheological modifier due to its ability to produce large increases in viscosity<sup>13</sup>.

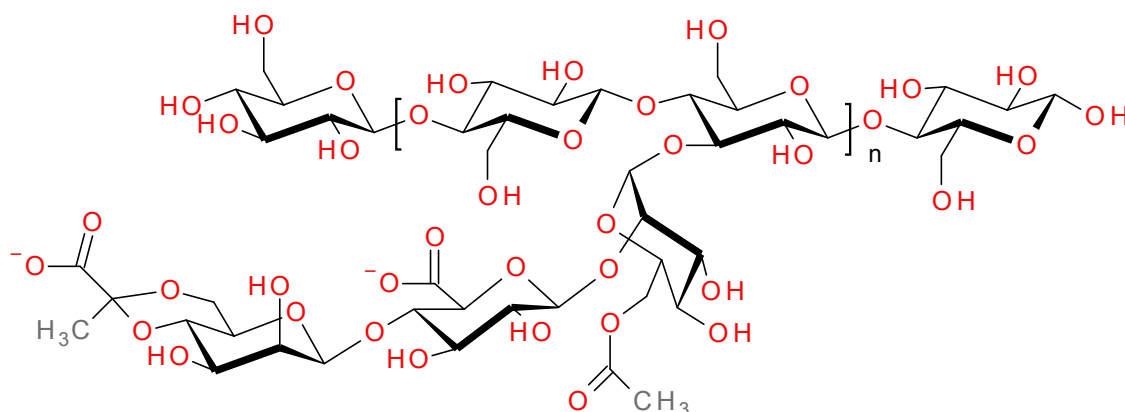


**Figure 12: Xanthan Gum**

Xanthan is composed of a β-D-glucose backbone with a trisaccharide unit consisting of mannose (with an acetyl substituent on carbon 6), glucuronic acid, and mannose (pyruvic acid linked to carbons 4 and 6) linked at every second glucose unit. Pyruvate and acetate however are not present on all side chains. Xanthan is produced by the fermentation of glucose or sucrose by the bacteria *Xanthomonas Campestris*<sup>14</sup>.

### **1.3 Bacterial Polysaccharides**

A range of highly complex polysaccharides are commonly biosynthesised by different bacterial families. The exact physical nature and indeed sometimes the chemical composition can depend on the substance or substrates available to the bacteria and to the growth conditions utilised<sup>15</sup>.

#### *1.3.1 Bacteria*

Bacteria are single cell microorganisms that are found all over the earth. They are typically spherical, rod or spiral shaped cells and are a few micrometres long<sup>16</sup>. Typically, there are 40 million bacterial cells in one gram of soil and around a million in a millilitre of fresh water.

It is estimated that there are approximately five nonillion bacteria on Earth, forming much of the world's biomass product<sup>17</sup>.

### 1.3.2 Bacterial Growth

Bacterial growth, when considered under the conditions of a closed or batch culture system can be separated into four phases<sup>18</sup> as represented in Figure 13. Bacteria are grown on a solid or in a liquid medium. The cell concentration (recorded as Log of the colony forming units (cfu) mL<sup>-1</sup>) is measured periodically with the number of cells determined and being measured against time; a bacterial growth curve is then plotted.

When a microbial population is inoculated into a fresh medium; initially cell growth is very slow, this slow phase of growth is termed the lag phase; the length of this period is dependent on the culture history and the growth conditions present. In this stage cells adapt to the new environment and therefore require time to synthesise essential constituents. As more nutrients become available for uptake, growth in volume and then in number begins to increase.

Once the lag phase is complete cell growth increases and cells enter the exponential (or log) phase where cell division and consequently population doubling is at its greatest. The number of new cells forming per unit time is proportional to the present growth. Again the rate of growth is controlled by the growth conditions (temperature, composition of culture medium) as well as the genetic characteristics of the specific organism itself. At some point cell growth slows and the system enters into the stationary phase.

The stationary phase occurs when the available nutrient resources are depleted and often also because of a build up of toxic products. No net increase or decrease in cell numbers is observed as bacterial growth is equal to the rate of bacterial death (cryptic growth)<sup>11</sup>. Ultimately new cell production ceases and the system enters the death phase.

Death phase occurs when the bacteria have exhausted the nutrients and begin to die. The death phase of the growth cycle is also exponential. The rate of cell death though is usually much slower than that of cell growth in the exponential phase.

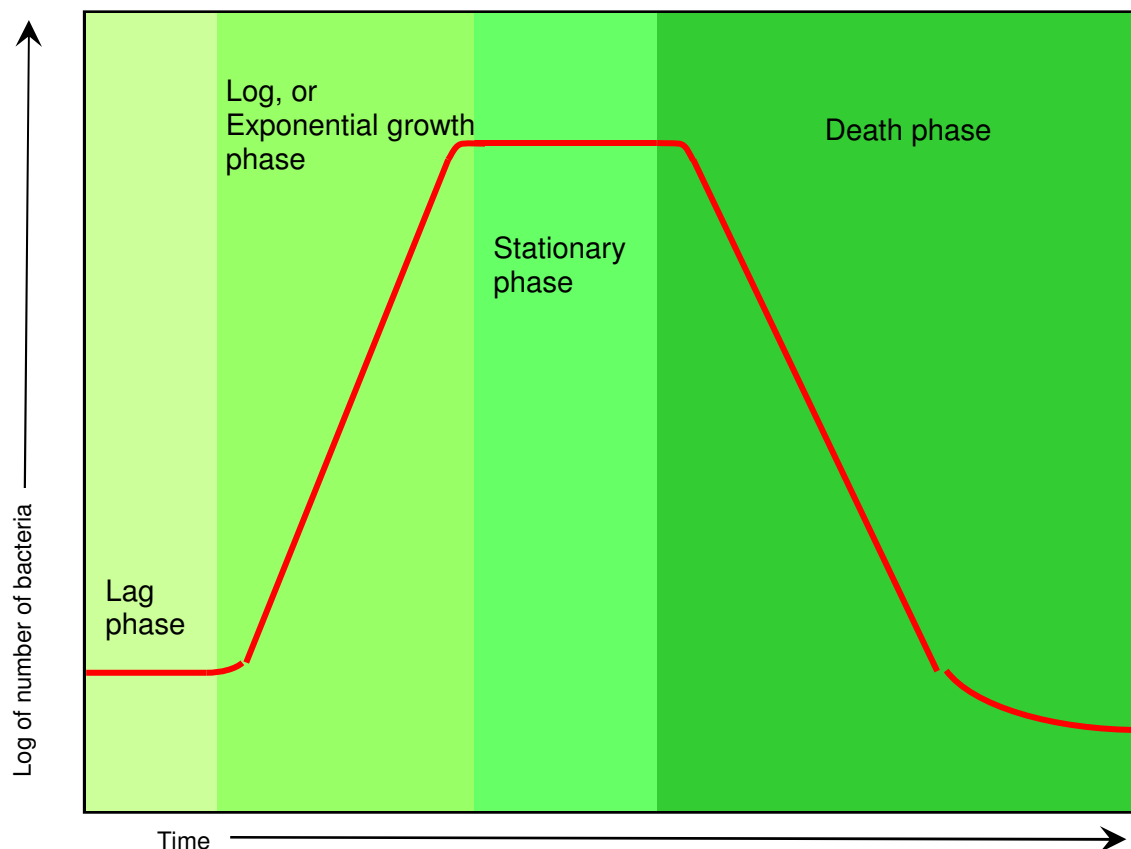


**Figure 13: Batch Culture Bacterial Growth Curve**

### 1.3.3 Bacterial Cell Walls

Almost all bacterial cell walls have a strong protective peptide-polysaccharide layer called peptidoglycan. This material provides rigidity and gives bacteria their characteristic shapes whilst protecting the cellular contents. The polysaccharide repeating unit component of peptidoglycan consists of linear chains of alternating  $\beta$ -(1 $\rightarrow$ 4) linked *N*-acetylglucosamine (NAG) and *N*-acetylmuramic acid (NAM)<sup>19</sup>.

Bacteria are classified into two sub-groups as either Gram-negative or Gram-positive, depending on the chemical and physical properties of their cell walls. The differentiation is achieved by subjecting bacteria to the Gram staining method developed in 1884<sup>20</sup>. Heat-fixed cells are repeatedly treated with a crystal violet dye and iodine, they are then destained

with either ethanol or acetone. Gram-positive cell walls (Figure 14) are thicker (containing 50 – 90% peptidoglycan) and therefore retain the dye more strongly – staining the cells purple.

Gram-positive bacterial cell walls are much less complex than Gram-negative cell walls. Gram-positive are a great deal thicker as they contain a larger amount of peptidoglycan to compensate for the lack of an outer membrane<sup>21</sup>. The cell walls also have acidic polysaccharides called teichoic acids embedded in them. Teichoic acids that are associated with the phospholipids are termed lipoteichoic acids. The peptidoglycan layer is also populated with wall associated/surface proteins.

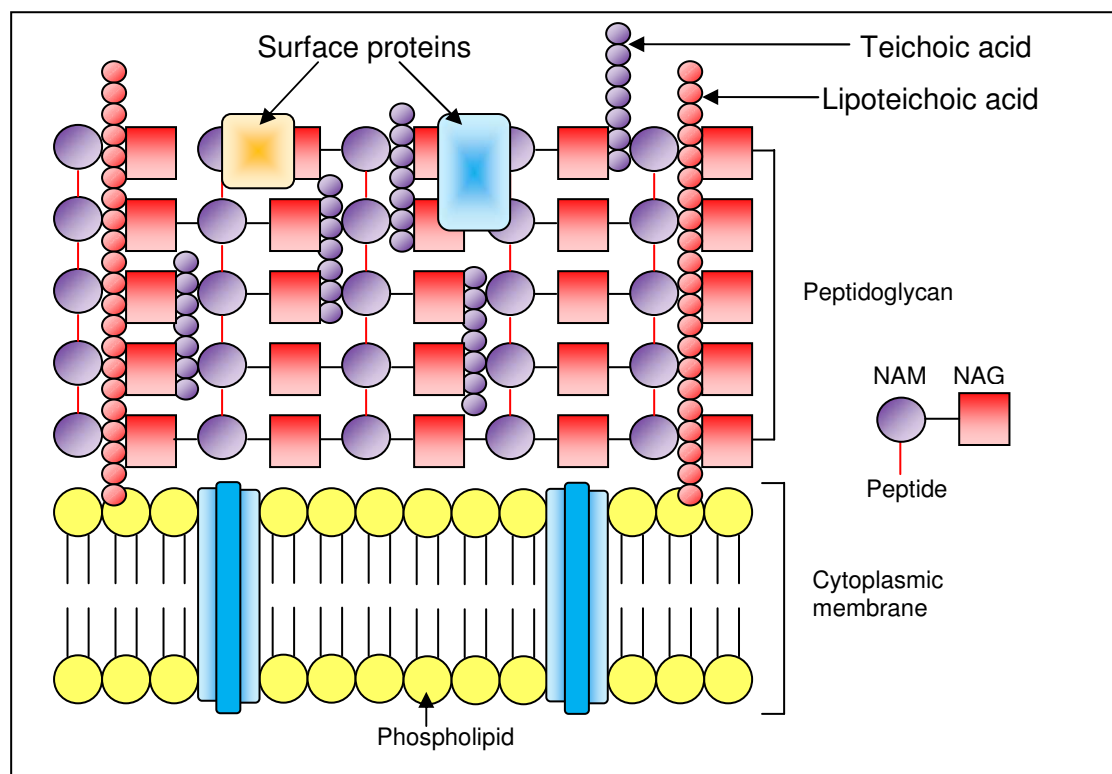


**Figure 14: Cross Section of a Gram-Positive Bacterial Cell Wall**

Gram-negative cell walls (Figure 15) however contain much less peptidoglycan (~10%); resulting in a much lighter pink stain being observed<sup>22</sup>.

As stated Gram-negative bacterial cell walls contain much less peptidoglycan, this is compensated for by the presence of an additional (outer) membrane which is coated with highly complex bacterial polysaccharides known as lipopolysaccharides (LPS)<sup>3</sup>. They

incorporate a lipid group which is inserted into the outer membrane and connected to a polysaccharide made up of repeating unit structures composed of a variety of different monosaccharides. Presently a substantial number of these LPS have been isolated and characterised<sup>23</sup>. The inner side of the outer membrane contains lipoprotein complexes which are small proteins that act as an anchor between the outer membrane and the peptidoglycan.

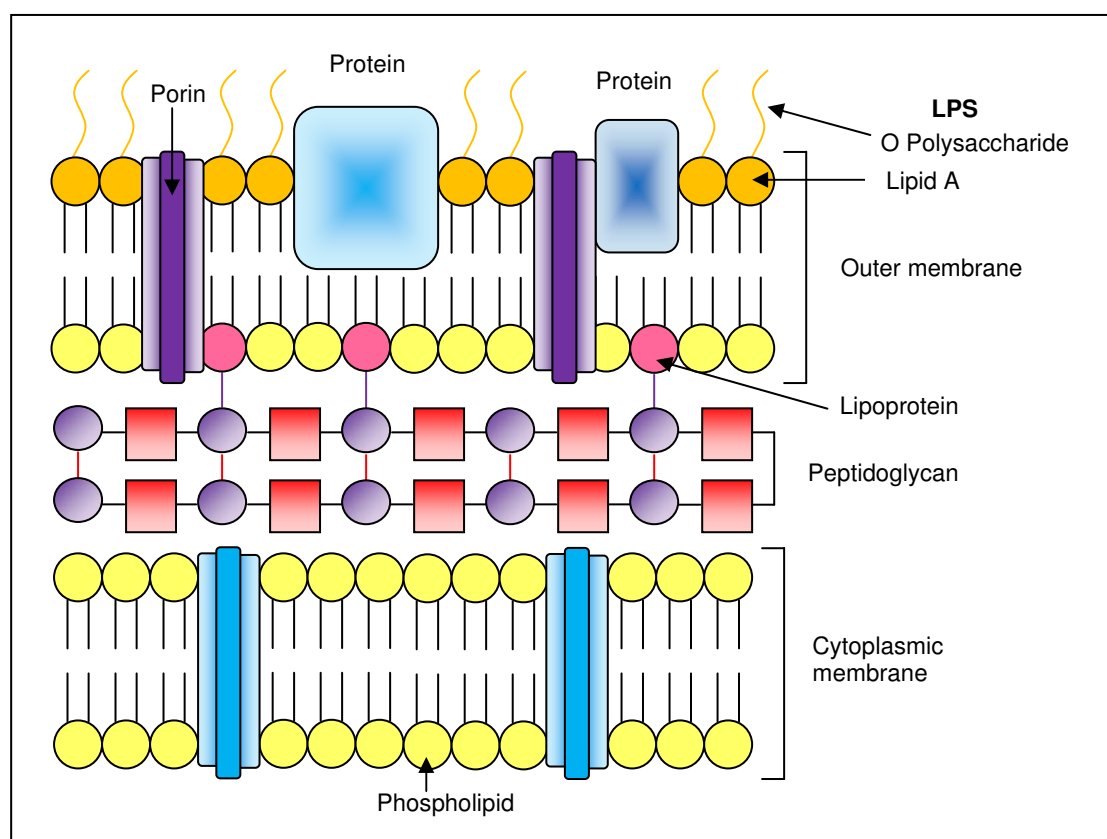


**Figure 15: Cross Section of a Gram-Negative Bacterial Cell Wall**

#### 1.3.4 Bacterial Polysaccharides

The majority of bacterial species when grown under appropriate culture conditions secrete mucoid substances external to the rigid cell wall structures, this material is normally of polysaccharide nature<sup>24</sup> and of high molecular weight<sup>25</sup>. This material may either be attached to the cell surface in the form of capsular polysaccharides<sup>26</sup> (CPS) or completely separated from the cell in the form of exopolysaccharides<sup>27</sup> (EPS).

Bacterial polysaccharide species represent a diverse range of macromolecules that include peptidoglycan, LPS, CPS and EPS. There is a tremendous amount of variation observed in the structure and function (many of which are yet to be determined) of this class of polysaccharides<sup>11</sup>.

Initially many structural studies on EPS focused on polysaccharides produced by Gram-negative species and some Gram-positive bacteria. Much work originally centred on pathogenic organisms though presently, the interest has shifted towards the analysis of Gram-positive bacteria such as lactic acid bacteria (LAB); which has recently produced a large number of structures<sup>28</sup>. For the purpose of this project, only the structure, function and characterisation of EPS produced from Gram-positive bacteria will be explored.

#### **1.4    LAB**

Lactic acid bacteria are classified as non-sporulating, low GC (DNA guanine + cytosine base ratio well below 50 %), Gram-positive bacteria. They appear as either rod or cocci in shape and produce lactic acid as a sole or major product of their fermentation process. They are widespread in nature and are also found in the human digestive system. LAB grow anaerobically, but unlike a large proportion of anaerobes most LAB are not sensitive to O<sub>2</sub> and can grow and thrive in its presence or absence alike. They have complex nutritional requirements and are dependent on the presence of fermentable carbohydrates in order to actively grow<sup>29</sup>. LAB are further classified into two sub-groups determined by the end product(s) formed by the process of carbohydrate fermentation.

##### *1.4.1 Homolactic Fermentation*

Homolactic fermentation produces lactic acid (> 95 % from glucose) as the end product of carbohydrate fermentation. This is due to the presence of the enzyme aldolase, which is the key enzyme required for glycolysis – the metabolic pathway that converts glucose into 2 pyruvates.

Homolactic fermentation is carried out by several genera including *streptococcus*, *pediococcus*, *enterococcus*, *lactococcus* and a number of *lactobacillus* species. A number of these species play active roles in the dairy industry especially in the production of a variety of cheeses. They are also utilised in food preservation, being used in the fermentation of various meat products<sup>30</sup>. The Homolactic fermentation pathway is displayed in Figure 16.

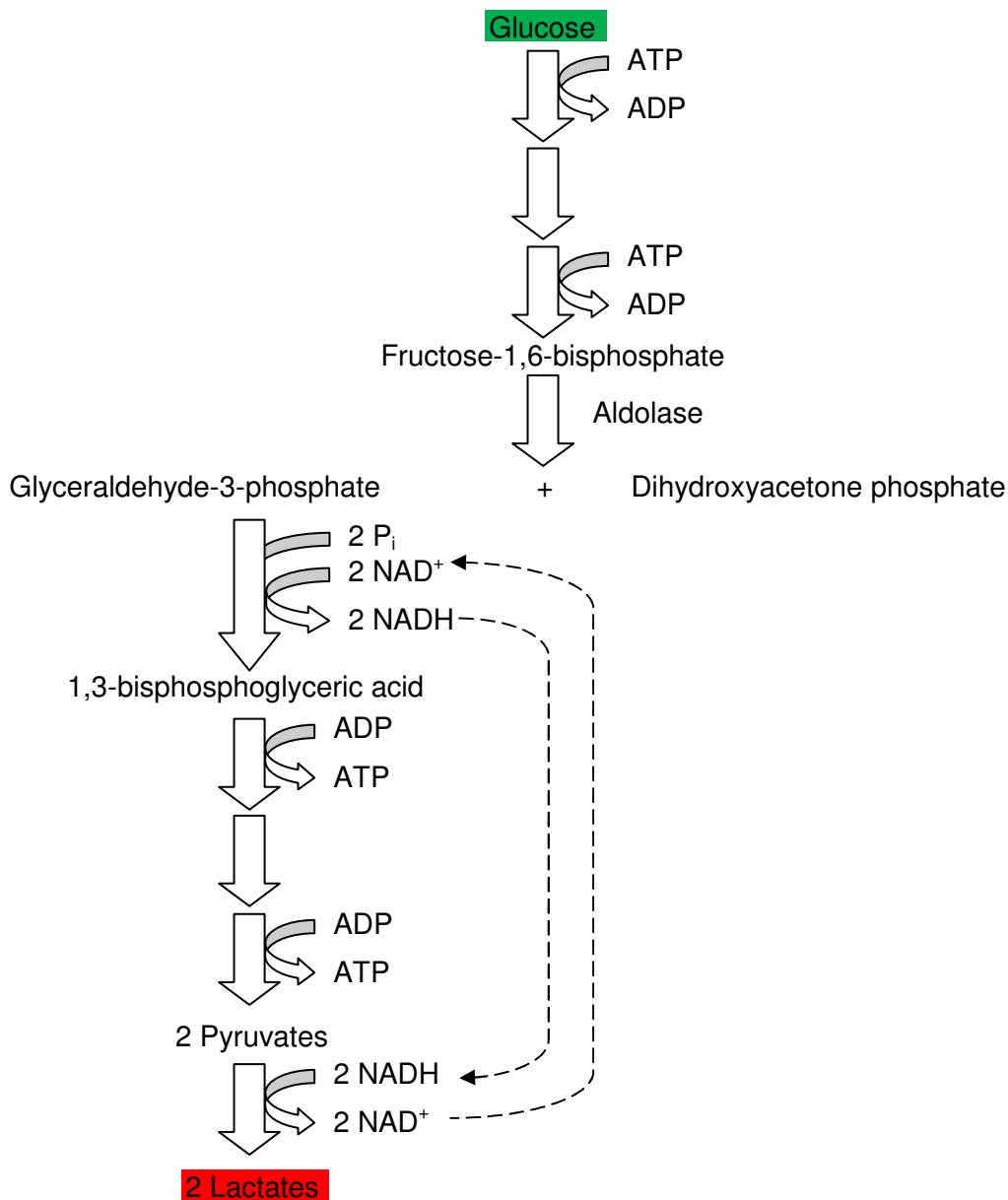
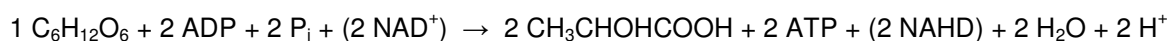


**Figure 16: Homolactic Fermentation Pathway**

As previously mentioned glucose is converted to two moles of pyruvate, this occurs in order to extract the chemical energy in the form of adenosine triphosphate (ATP) from the glucose.

The overall reaction (glycolysis) involves one glucose being broken down into two pyruvates. This process involves two adenosine diphosphates (ADP) being converted to two ATP, the addition of two inorganic phosphates ( $P_i$ ) and the reduction of two molecules of nicotinamide adenine dinucleotide ( $NAD^+$ ) yielding two molecules of NADH. The two molecules of NADH are then oxidised back to  $NAD^+$  in the conversion of two pyruvates into two molecules of lactate (lactic acid). The overall reaction is summarised in Equation 1.



**Equation 1: Overall Reaction of Homolactic Fermentation**

#### 1.4.2 Heterolactic Fermentation

Heterolactic fermentation is carried out by *Leuconostoc* and various *Lactobacillus* species. *Leuconostoc* being of particular importance in both the fermentation of wines<sup>31</sup> and the production of sauerkraut<sup>32</sup>. Some heterolactic strains of *Lactobacillus* are used in the production of the fermented milk drink Kefir<sup>33</sup>.

Heterolactic fermentation produces ethanol and  $\text{CO}_2$  along with lactate (Figure 17). This process proceeds via the phosphoketolase pathway due to the lack of the enzyme aldolase (observed in homolactic fermentation). Glucose is phosphorylated at C6 (via ATP to ADP conversion) to produce glucose-6-phosphate which is oxidised and decarboxylated to yield 6-phosphogluconic acid (via  $NAD^+$  reduction to NADH). Next  $\text{CO}_2$  is produced as 6-phosphogluconic acid is converted to ribulose-5-phosphate (via  $NAD^+$  reduction to NADH). Ribulose-5-phosphate is isomerised to xylulose-5-phosphate which is cleaved (via phosphoketolase and with the addition of  $P_i$ ) to glyceraldehyde-3-phosphate (GAP) and acetyl phosphate. GAP is converted to lactate (via pyruvate) as observed in the homolactic pathway. Acetyl phosphate is reduced to ethanol via successive NADH to  $NAD^+$  oxidations.

The overall reaction is summarised in Equation 2.



**Equation 2: Overall Reaction of Heterolactic Fermentation**



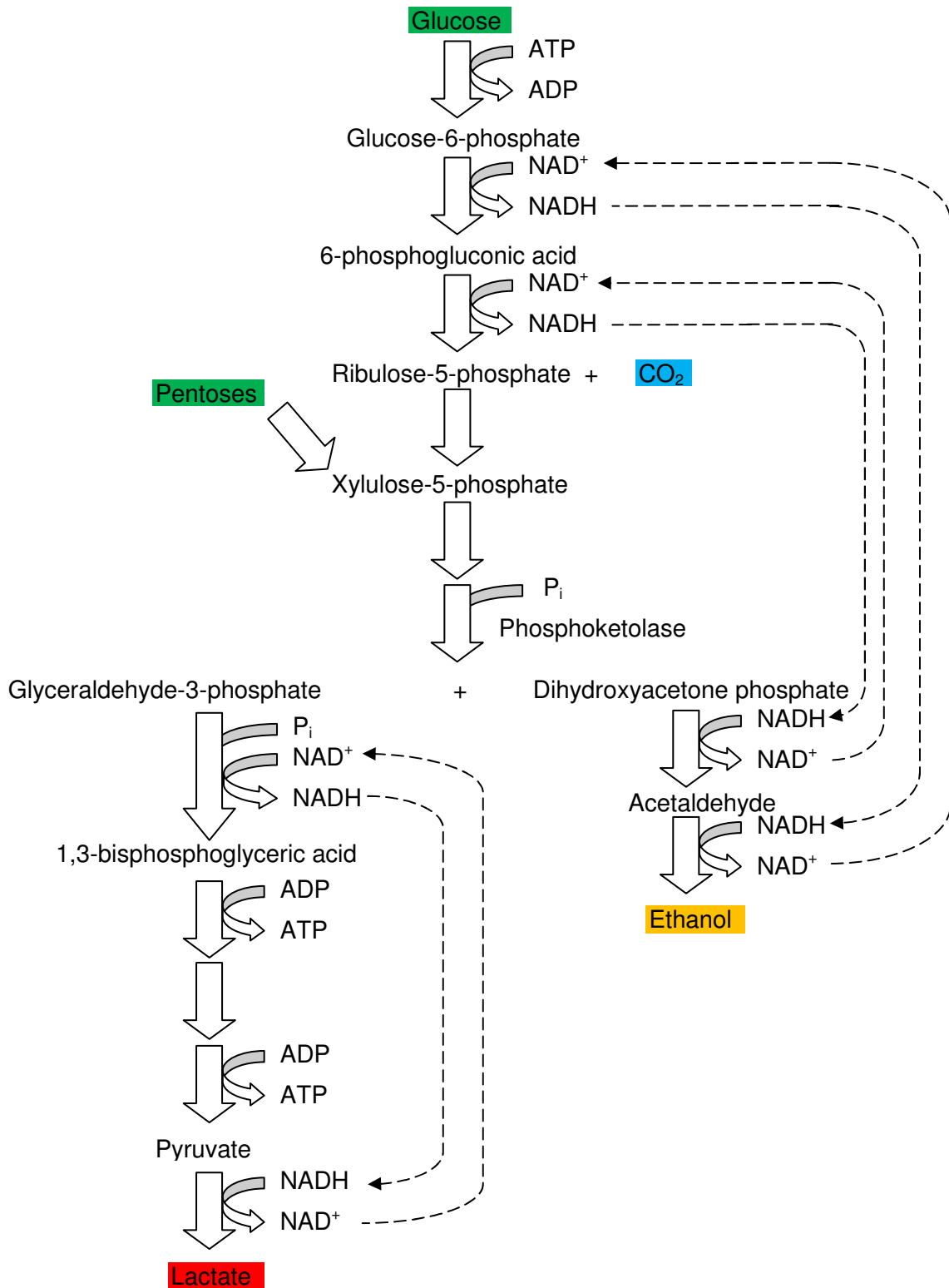


**Figure 17: Heterolactic Fermentation Pathway**

Exopolysaccharides can be divided into two groups: homopolysaccharides or heteropolysaccharides. Homopolysaccharides produced by LAB can be further subdivided into two main categories: those made up entirely of D-glucose (glucans) or those containing only D-fructose (fructans). Glucans can again be further classified depending on whether they are made up of  $\alpha$ -D-glucose or  $\beta$ -D-glucose<sup>34</sup>.

**Table 1: Homopolysaccharides Produced by Lactic Acid Bacteria**

Subgroups	Lactic Acid Bacteria Strain	Polysaccharide Produced
$\alpha$ -D-glucans	<i>Leuconostoc mesenteries</i> subsp. <i>mesenteroides</i> <i>Leuconostoc mesenteroides</i> subsp. <i>dextranicum</i> <b>Dextrans</b>	$\alpha$ -1,6 – linked D-glucose, variable degree's of branching at C3, less frequent at C2 and C4 (strain dependent)
	<i>Streptococcus mutans</i> <i>Streptococcus sobrinus</i> <b>Mutans</b>	$\alpha$ -1,3 – linked and $\alpha$ -1,6 – linked D-glucose
	<i>Leuconostoc mesenteries</i> <b>Alternan</b>	
$\beta$ -D-glucans	<i>Pediococcus</i> spp. <i>Streptococcus</i> spp.	$\beta$ -1,3 – linked D-glucose with $\beta$ -1,2 – branching
Fructans	<i>Streptococcus salivarius</i> <b>Levans</b>	$\beta$ -2,6 – linked D-fructose with some $\beta$ -2,1 – branching
	<i>Streptococcus mutans</i> <b>Inulin-like</b>	$\beta$ -2,1 – linked D-fructose

It should also be noted that the strain *Lactococcus lactis* subsp. *lactis* H414 produces a polygalactan composed of  $\alpha/\beta$ -1,3 and 1,4 – linked D-galactose<sup>35</sup>.

The species of LAB that produce heteropolysaccharides can be split into two groups depending on the temperature at which the bacteria grow best at. Mesophilic strains grow best at moderate temperatures typically ranging from 20 – 40°C, whilst thermophilic strains

grow best at elevated temperatures, generally above 40°C. An example of several mesophilic and thermophilic LAB strains are given in Table 2.

**Table 2: Mesophilic and Thermophilic LAB Strains Producing Heteropolysaccharides**

Subgroups	Lactic Acid Bacteria Strains
Mesophilic	<i>Lactococcus lactis</i> subsp. <i>lactis</i> <i>Lactococcus lactis</i> subsp. <i>cremoris</i> <i>Lactobacillus casei</i> <i>Lactobacillus sake</i> <i>Lactobacillus rhamnosus</i> <i>Lactobacillus paracasei</i>
Thermophilic	<i>Lactobacillus acidophilus</i> <i>Lactobacillus delbrueckii</i> subsp. <i>bulgaricus</i> <i>Lactobacillus helveticus</i> <i>Streptococcus thermophilus</i>

#### 1.4.3 LAB in the Food Industry and Possible Health Affects

As mentioned previously in sections 1.4.1 and 1.4.2, LAB are implemented in a wide range of food related applications. Some LAB are used routinely in the food industry in a variety of areas, the LAB utilised include: *Lactobacillus*, *Lactococcus*, *Streptococcus*, *Pediococcus*, *Leuconostoc*, *Aerococcus*, *Carnobacterium*, *Oenococcus*, *Tetragenococcus* and *Weisella*<sup>36</sup>. A number of LAB secrete EPS into the surrounding media as well as producing lactic acid, these properties are especially utilised in fermented dairy products (consisting of cheeses, yoghurts and milks)<sup>37</sup>. LAB, and consequently the EPS they secrete are 'generally recognised as safe' (GRAS), meaning that they are acceptable for utilisation in food preparations.

Lactate metabolism by LAB (*Lactobacillus*, *Pediococcus*, etc) has implications for cheese flavour, texture, appearance and functionality, especially in relation to low-fat products<sup>38</sup>.

Cheese quality is determined by flavour, rheological properties and visual appearance, however during the production of low-fat cheeses there is a constant challenge to maintain good flavour and textual character as the two products (low-fat and full-fat) differ greatly in composition. LAB are introduced as either starter cultures or they are already present in the original milk or have entered through the manufacturing environment<sup>39</sup>. The introduction of specific starter cultures can help overcome the problems encountered with the change in flavour and texture experienced in low-fat cheese production.

There is a consistent need for the manufacture of good quality dairy based products (particularly milks and yoghurts), that have good texture, 'mouth-feel' and stability<sup>40</sup>. An alternative way to improve yoghurt texture and viscosity is to use slime-producing bacteria in starter cultures. Slime-producing thermophilic strains of LAB have demonstrated an increase in viscosity and a decrease in the susceptibility to syneresis<sup>41</sup>. Production of these milk-based foods depends on LAB fermenting lactose in milk to form mainly lactic acid which imparts a fresh acidic flavour to fermented milks and yoghurts. LAB also assist in curd coagulation, texture formation and the low pH helps to suppress the growth of pathogens and organisms that cause spoilage<sup>42</sup>. In Scandinavian countries slime-producing mesophilic LAB are used regularly in a commercial capacity in the manufacture of many fermented drinks. One such example is the presence of a slime-producing strain of *Lactococcus lactis* subsp. *cremoris* in the Finnish fermented milk "Viili", which is essential for proper consistency<sup>43</sup>.

LAB and the EPS they produce may also be disadvantageous in the food industry by causing spoilage. Food spoilage is any change in the appearance, smell, or taste of food product that makes it unacceptable to the consumer. The EPS from LAB play an important role in *in vivo* biofilm formation and biofouling processes. Biofilms are an aggregate of microorganisms that adhere to a surface, bacterial biofilms are supported by a matrix partly composed of EPS<sup>34</sup>. Biofouling is due to the biofilm formation in the equipment used for the

processing of dairy products<sup>28</sup>, such as cheese<sup>44</sup> and milk<sup>45</sup>. LAB can also cause spoilage in the production of a number of alcohol beverages including beer<sup>46</sup>, wine<sup>47</sup> and cider<sup>48</sup>.

In addition to their roles in the food industry it has been claimed that LAB EPS possess a number of putative health benefits. These include antitumor<sup>49</sup>, antiulcer<sup>50</sup>, immunomodulating<sup>51</sup> and also the lowering of blood cholesterol levels<sup>52</sup>. It can be summarised that there is a great deal of current and potential uses for EPS from LAB with a view to combining their functional food usage with possible health benefits.

Prebiotics are defined as non-digestible food ingredients that beneficially affect the host by selectively stimulating the growth and/or activity of a limited number of bacteria in the colon, and thus improving host health<sup>53</sup>. The most common example of a prebiotic being inulin<sup>54</sup>,  $\beta$ -2,1 – linked D-fructose (with a varying degree of D-glucose branching). To date there have been no reports for EPS produced by LAB as prebiotics. Research is however currently being undertaken (*in vitro*) in the study of the prebiotic properties of exopolysaccharides from *Lactobacillus* strains (2001)<sup>55</sup>. To employ EPS from LAB as potential prebiotics more studies are currently needed. Investigation into the degradation, specifically the breakdown by beneficial colonic bacteria and healthy effect in human hosts are required (2002)<sup>56</sup>. However, recent initial findings have been reported for a strain of *Lb. Plantarum* and its possible use as a prebiotic (2010)<sup>57</sup>.

Probiotics are defined as a live microbial feed supplement which beneficially affects the host animal by improving its intestinal microbial balance<sup>58</sup>. Increasingly interest in recent years has focused around the area of prebiotic yoghurt and milk drinks. Probiotic preparations may consist of single strains or a formulation may contain as many as eight strains. Current strains most commonly used include *Lactobacillus acidophilus*, *Lactobacillus casei*, *Lactobacillus lactis* and a variety of species from the *Bifidobacterium* genus. It is also common to co-culture a *Lactobacillus* species with a strain of *Bifidobacteria*. It should be noted that the *Bifidobacterium* genus is often regarded as a member of the LAB group,

*Bifidobacteria* however are phylogenetically unrelated to LAB and also differ physiologically in that they utilise a sugar fermentation pathway unique to their particular genus<sup>29</sup>.

## **1.5 Bifidobacteria**

*Bifidobacteria* were first discovered in 1900 by Tissier and were originally labelled as *Lactobacillus bifidus*<sup>59</sup>. They are Gram-positive, strictly anaerobic, fermentative and non-motile. They appear either as Y-shaped or clubbed at the ends<sup>60</sup>. Despite being recognised as a separate (from *Lactobacillus*) taxon in 1924<sup>61</sup> it was not until 1986 they were transferred to the genus *Bifidobacterium* (*B.*)<sup>62</sup>.

The *Bifidobacterium* genus is often associated with LAB as they are both present in similar ecosystems such as the intestinal tract of humans and animals. However, they are part of a different taxonomic phyla and do not fit in with the LAB classification as they differ in a number of distinctive ways. Firstly they have a higher GC content (55 – 57 mol %) in their DNA than LAB. Also their phylogenetic relatedness places them in the *Actinomyces* subdivision of Gram-positive bacteria<sup>63</sup>. The fermentation end products differ to those produced by either homolactic or heterolactic LAB fermentations; this will be discussed in more depth in the following section.

The human intestinal microflora consists of hundreds of different species of bacteria. It is thought *Bifidobacteria* may comprise up to 25 % of the cultivatable human gut microflora<sup>64</sup>, hence the reason for the inclusion of the genus in probiotic supplements. At present 30 different species of *Bifidobacteria* have been recorded and identified from various sources including: human faeces, vagina, dental caries, sewage, human and animal intestine as well as the intestine of the honey bee<sup>65</sup>. The strains most commonly found in the human gastrointestinal tract (GIT) are *Bifidobacterium adolescentis*, *B. angulatum*, *B. breve*, *B. catenulatem*, *B. dentium*, *B. longum* and *B. pseudocatenulatem*<sup>66</sup>. *B. Animalis* subsp. *lactis* is also detected but is thought to be from dietary origin as it is frequently isolated from functional dairy products<sup>67</sup>.

### 1.5.1 Heterolactic Fermentation of *Bifidobacterium*

*Bifidobacteria* undergo heterolactic fermentation of carbohydrates, but utilise a unique pathway different to that employed in LAB heterolactic fermentations. The *Bifidobacteria* fermentation pathway employs a different key enzyme in the form of fructose-6-phosphate phosphoketolase that splits fructose phosphate into erythrose-4-phosphate and acetyl phosphate, this is referred to as the 'fructose-6-phosphate'<sup>68</sup> or 'bifid shunt'. The fermentation also subsequently produces markedly different ratios of end products: producing acetic acid and lactate in a 3:2 ratio. There is also no CO<sub>2</sub> produced via this fermentative pathway.

In the first step in the heterolactic fermentation pathway of *Bifidobacteria* (Figure 18) two glucose units are phosphorylated to form two glucose-6-phosphates. The action of glucose-6-phosphate isomerase then yields two fructose-6-phosphates. The key enzyme, fructose-6-phosphate phosphoketolase acts to produce erythrose-4-phosphate and acetyl phosphate – which is converted to acetate (acetic acid). An additional molecule of fructose-6-phosphate and erythrose-4-phosphate are converted to sedoheptulose-7-phosphate and GAP (via transaldolase), xylulose-5-phosphate and ribose-5-phosphate are produced via transketolase. Xylulose-5-phosphate is split into two molecules of GAP which is converted to two units of lactate (via two pyruvates). Ribose-5-phosphate is then isomerised and epimerised to xylulose-5-phosphate which splits to two acetyl phosphates (via xylulose-5-phosphate phosphoketolase), which in turn are converted to two acetates.

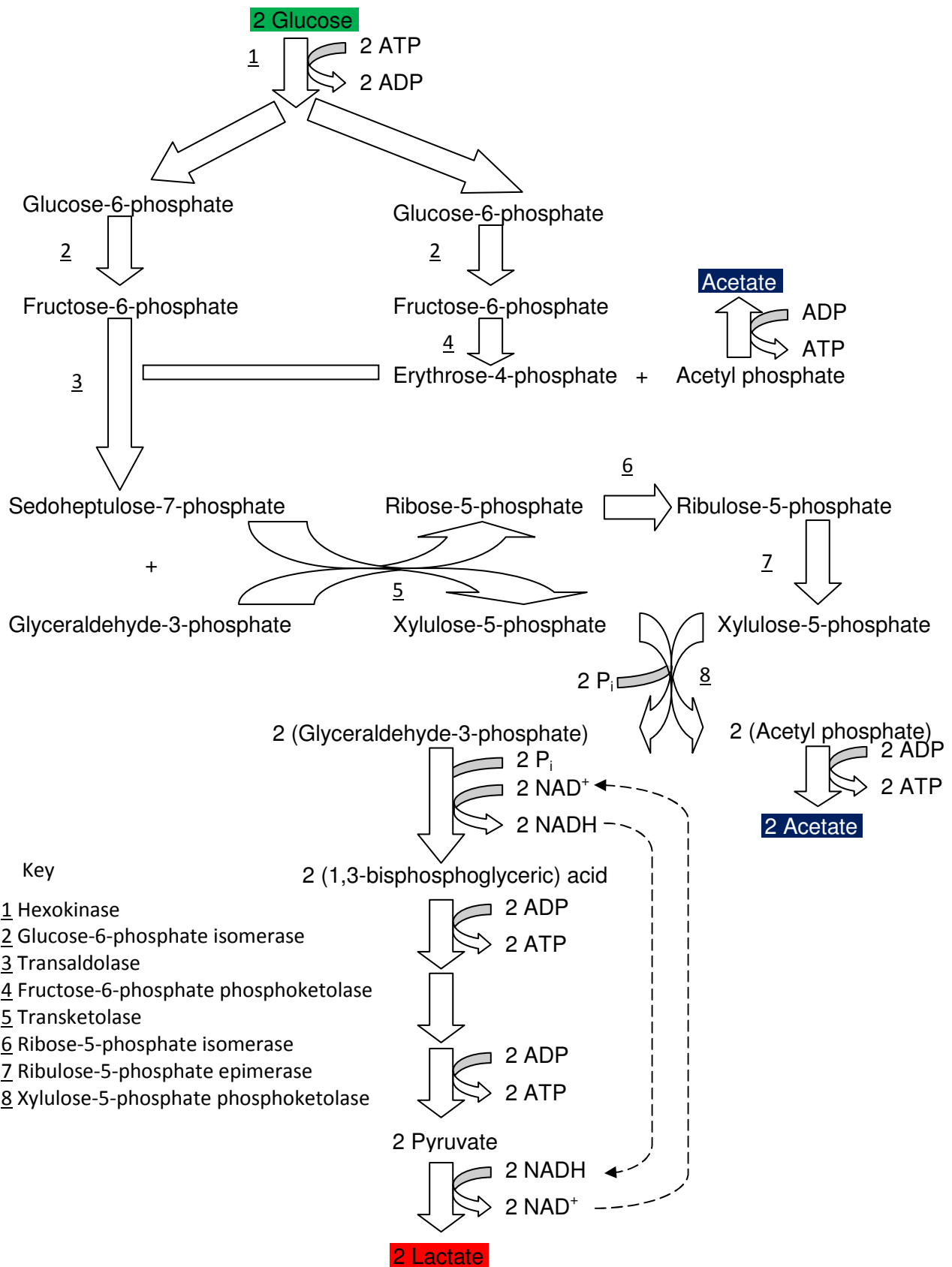


**Figure 18: Heterolactic Fermentation Pathway of *Bifidobacteria***



### 1.5.2 *Bifidobacteria – Uses, Benefits and Problems*

As previously mentioned there has been an exponential rise in the number of probiotic fermented milk and yoghurt products developed. The gut microflora plays an important role in both human health and disease. Resident bacteria within the human gut are considered to represent a crucial line of defence against colonisation by potentially pathogenic microorganisms<sup>69</sup>. The presence of *Bifidobacterium* within the GIT has been associated with a number of health benefits.

*Bifidobacteria* have been proven to provide a protective effect against acute diarrhoeal disease<sup>70</sup>, which can be devastating to children in the developing world. The use of *B. longum* has demonstrated a positive probiotic effect in the relief of lactose intolerance<sup>71</sup>. *Bifidobacteria* have also been deployed in the area of effective resistance to microbial infections: a high intake of *Bifidobacterium* has demonstrated a decrease in numbers of potentially harmful *Clostridium* bacteria whilst other species have demonstrated a protective effect against *Listeria monocytogenes*<sup>72</sup>.

As it is thought that the intestinal microflora play a key role in the onset of Inflammatory Bowel Disease (IBD) it was hypothesised that modifying the composition and activity of the normal microflora may be able to lessen the observed symptoms<sup>73</sup>. Constipation alleviation has been explored recently by the administration of a prebiotic which was observed to enhance bifidobacterial growth<sup>74</sup>. Again, as with LAB, the possible role of *Bifidobacteria* on immune function and its immunomodulating capabilities have also been explored<sup>75</sup>. Probiotic *Bifidobacteria* has also been used in attempting to reduce serum cholesterol levels<sup>76</sup>.

The most commonly employed strains of *Bifidobacteria* include *B. animalis* subsp. *lactis*, *B. bifidum*, *B. breve* and *B. longum* biotypes *infantis* and *longum*. These strains were originally often co-cultured with LAB including *Lactobacillus delbrueckii* subsp. *bulgaricus* and *Streptococcus thermophilus*. In recent years however much focus has surrounded the co-

culturing of *Bifidobacteria* and *Lactobacillus acidophilus* as this LAB is an indigenous inhabitant of the GIT<sup>77</sup>.

*Bifidobacteria* do not grow well or at all in milk<sup>78</sup>. Therefore much better products are produced by combining cultures. The presence of so called 'bifidus factors' can influence how well (if at all) bacteria grow in milk. It is thought that the presence of certain amino sugars, carbohydrates and peptides play a major role in growth of *Bifidobacteria* in milk. Viability is another issue to consider if *Bifidobacterium* species are to function efficiently as probiotics. To produce therapeutic effects, a sufficient number of viable microorganisms must be present throughout the entire shelf-life of the particular product<sup>79</sup>. Viability is affected by a number of factors including pH, temperature, O<sub>2</sub> concentration and the presence of other microorganisms<sup>80</sup>. The main problem however is overcoming the biological barriers in the body, particularly the acid in the stomach and bile in the intestine<sup>81</sup>. Recent work has been undertaken to study and develop bile-resistant strains of *B. animalis* subsp. *lactis*<sup>82,83</sup>. Another problem with using *Bifidobacteria* is due to the taste and texture it can impart on a product. *Bifidobacteria* species follow the heterolactic fermentation pathway and as a result are less efficient (producing more acetic than lactic acid) than most LAB used in fermented milk and yoghurt production. They produce unwanted by-products including undesired amounts of acetic acid which has an 'acid sharp' taste compared to the required 'acid sour' taste of lactic acid<sup>84</sup>, problems with texture and rheology may also arise. The texture and rheology issues may though be overcome with the use of polysaccharide producing strains of LAB and *Bifidobacteria*.

## **1.6 Exopolysaccharides**

Certain strains of LAB and *Bifidobacteria* are able to synthesise EPS that are secreted into their surrounding environments, such as milk in the production of fermented dairy products. The EPS produced have been described as 'ropy' (slime-forming) whereas capsular extracellular polysaccharide producing bacteria are described as 'mucoid'. The incorporation

of ropy cultures in mixed bacterial cultures in the production of fermented milk products is not a new technique having been applied in Scandinavia<sup>85</sup> for many years, as previously mentioned in section 1.4.3. Although it should be considered that due to complex physical-chemical processes involved in the texture generation, the inclusion of a ropy strain of LAB or related bacteria does not guarantee an optimal, creamy and smooth quality in the end product<sup>86</sup>. EPS have increasingly important functions as natural biothickeners and are used to improve rheology, physical stabilizers to bind water and to limit syneresis and also as viscosifying and gelling agents.

Currently polysaccharides from plant and seaweed (e.g. alginates) sources, are employed as biothickeners. One problem with these sources is that a degree of chemical modification (such as cross-linking with Ca or Na ions or derivatised by sulfonation<sup>87</sup>) is usually required to observe the desired effect. Hence, the reason for the current interest towards the use of EPS as 'natural biopolymers', removing the need for chemical modification of the polysaccharide before it can be used. One main problem, and reason as to why EPS are not readily applied, is due to the reliability of their production and variability in the amount generated; meaning the available supplies are not sufficient to match the demand<sup>28</sup>. A very small number of EPS have unique properties which have led to their commercial production. Current industrially important EPSs include dextrans, pullulan (homopolysaccharides) and xanthan (as previously referred to in Section 1.2) and gellan (heteropolysaccharides)<sup>34</sup>.

Xanthan (See Section 1.2), produced by *Xanthomonas campestris*<sup>88</sup> is produced by various companies and is widely applied as a thickening, gelling and stabilising ingredient in the food industry. Even though xanthan is readily used in the food industry *Xanthomonas campestris* is a non-food-grade bacterium<sup>89</sup>, as is *Sphingomonas paucimobilis*<sup>90</sup> which produces gellan. Gellan is also produced commercially and is employed in the pharmaceutical and cosmetic industries as well as in a number of food preparations.

More information on the structure-function relationship of EPS in fermented products is currently required in order to further their technological applications. Since LAB and *Bifidobacteria* have GRAS status and are commonly used as probiotics, their EPS will hopefully provide a safer and healthier option for the replacement of the chemically modified and non-food-grade bacteria presently being employed<sup>66</sup>. This will be of great benefit combined with the current knowledge of their health-promoting properties. EPS producing LAB strains have recently been used in the production of low-fat mozzarella cheese to enhance moisture retention<sup>91</sup>.

Within the natural environment the role of EPS is not a clearly established one. It is suspected that they play a role in protecting the cell against desiccation, phagocytosis and phage attack, providing higher O<sub>2</sub> tension, participating in uptake of metal ions, functioning as adhesive agents, promoting interactions between plants and bacteria, and in development systems such as those occurring in myxobacteria<sup>92</sup>.

### 1.6.1 Exopolysaccharide Biosynthesis

The synthesis of the vast majority of bacterial homopolysaccharides and all of the heteropolysaccharides is a complex intercellular process in which sugar nucleotides (normally nucleoside diphosphate sugars) provide activated forms of the monosaccharides<sup>15</sup>. Heteropolysaccharides are made by the polymerisation of repeating unit precursors formed in the cytoplasm<sup>93</sup>. Heteropolysaccharides are principally composed of glucose, galactose and rhamnose; however *N*-acetylglucosamine (GlcNAc) and *N*-acetylgalactosamine (GalNAc) can also be present, whilst L-fucose has been identified in a limited number of EPSs. In addition a number of non-carbohydrate moieties (e.g. pyruvate) are present in side chains, further contributing to their heterogeneity<sup>66</sup>. The sugar nucleotides provide monosaccharides or, if polysaccharides contain phosphorylated sugars, sugar phosphates for the repeating unit structures. They also provide the bacterial cells with a means of interconversion or synthesis of various monosaccharides. Through epimerisation, dehydrogenation and decarboxylation reactions, respectively, at the sugar nucleotide level,

sugars such as D-glucose or D-mannose can be converted to galactose, uronic acids or pentoses. D-Mannose can also be converted to L-fucose. Acyl linkages such as acetyl and ketal groups also require a form of activated precursor such as acetyl-Coenzyme A (CoA) and phosphoenolpyruvate (PEP), respectively<sup>15</sup>.

EPS synthesis in LAB (assembly of the monosaccharide repeating unit) is achieved by several EPS-specific enzymes, as initially identified in *Streptococcus thermophilus* Sfi6<sup>94</sup> and *Lactococcus lactis* NIZO B40<sup>95</sup> (Figure 19).

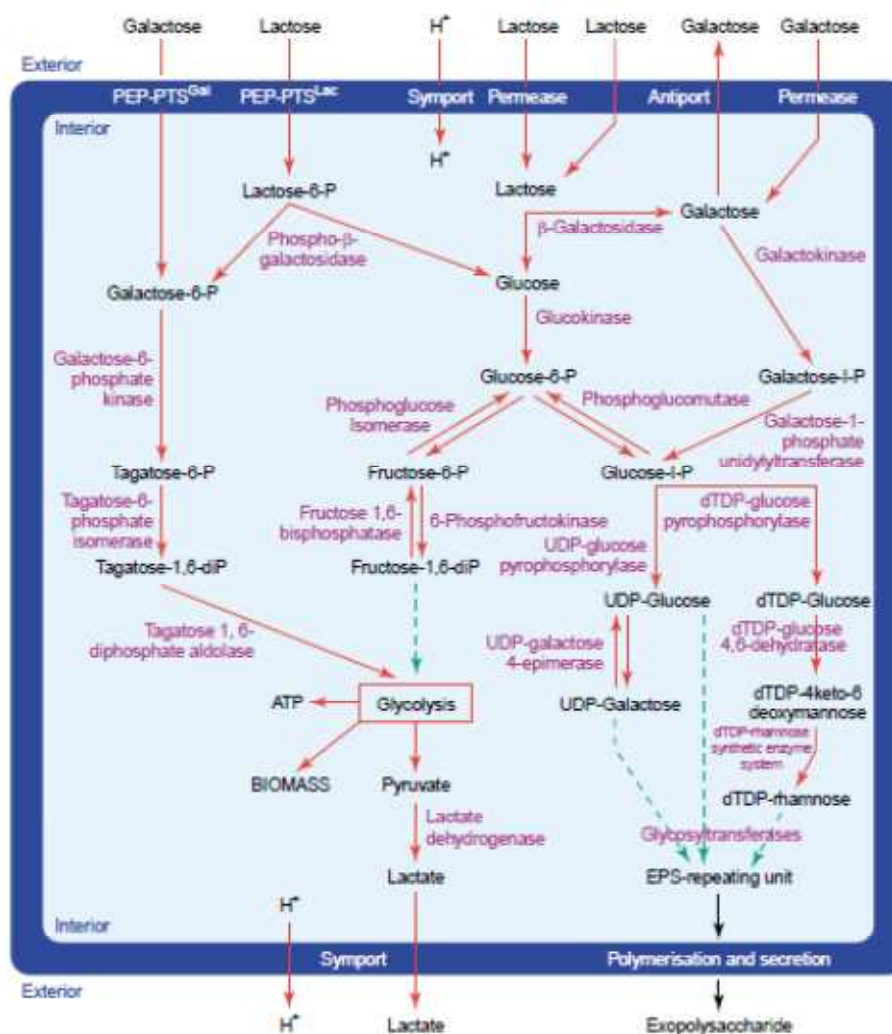


**Figure 19: Generalised diagram of the conversion of lactose, galactose and glucose to EPS and to glycolysis in LAB (Reproduced from Welman and Maddox, 2003<sup>96</sup>)**

The biosynthesis process can be summarised into five distinct steps: (1) Activation of sugars through specific sugar nucleotides; (2) Assembly of the repeating unit on an isoprenoid lipid-

phosphate (bactoprenol, C<sub>55</sub>-isoprenoid lipid) through the sequential addition of monomers to the lipid carrier; (3) Addition of any acyl groups to the oligosaccharide attached to the lipid carrier<sup>97</sup>; (4) Polymerisation of the repeat units; and (5) Excretion of the polysaccharide from the cell membrane into the extracellular environment<sup>15</sup>.

The first step involves transporting the sugar into the cytoplasm. The most frequently encountered system that operates in LAB functions via the PEP transport system (PTS). In this system a phosphate group, released from the conversion of PEP into pyruvate, is transferred to the incoming sugar by two general cytoplasmic phosphocarrier proteins; enzyme I and histidine protein (HPr)<sup>98</sup>. There are other sugar transport systems suggested but this particular method is energetically efficient as the sugar is translocated and phosphorylated in a single step at the expense of one ATP that would otherwise be generated by PEP conversion into pyruvate catalysed by pyruvate-kinase<sup>89</sup>.

Once inside the cytoplasm, the fate of the carbon feed/energy source is determined by the state of the phosphorylation of the sugar: sugar-6-phosphates are consumed in the catabolic pathway (Figures 17 and 18) whilst sugar-1-phosphates can participate in polysaccharide synthesis. It is thought phosphoglucomutases (PGMs) may play a vital role in diverting flux between the two pathways<sup>99</sup>. It is thought  $\alpha$ -PGMs may direct the glucose-6-phosphate to  $\alpha$ -glucose-1-phosphates and consequently into use for EPS synthesis.

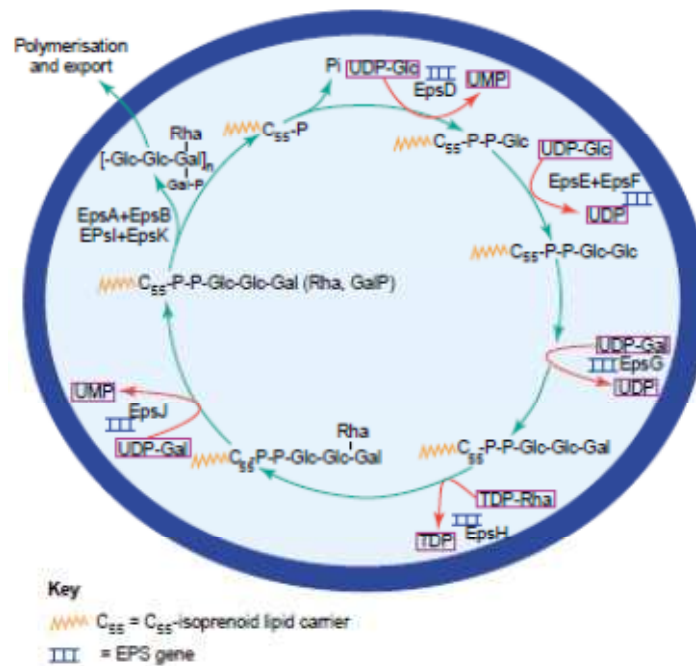


**Figure 20: Model of EPS Biosynthesis in *Lactococcus lactis* NIZO B40 (Reproduced from Welman and Maddox, 2003<sup>96</sup>)**

The sugar nucleotides required for the construction of the majority of EPS structures are UDP-glucose, UDP-galactose and dTDP-rhamnose. The precursors of the repeating unit observed from *Lactococcus lactis* NIZO B40 being a particular example. Polymerisation of thousands of the repeating unit takes place through sequential addition of the sugar residues by specific glycosyl transferases from the nucleotide sugars to a growing repeat unit that is coupled to the isoprenoid glycosyl lipid carrier (C<sub>55</sub>) (Figure 20). The assembly of the repeat unit on the lipid carrier is a process that is used for the synthesis of excreted polysaccharides, for cell wall peptidoglycans and for cell surface oligosaccharides and polysaccharides<sup>28</sup>. There is however only limited evidence of the presence of the lipid carrier in LAB systems<sup>100</sup>.

The final step involves the polymerisation of the EPS and its export into the surrounding medium. This action requires a flippase to translocate the lipid-bound repeating units, a polymerase to catalyse the coupling of repeating units and finally an enzyme to catalyse the detachment of the lipid-bound polymer to control chain length<sup>28</sup>. Both polymerisation and transport may affect both the amount and sugar composition of the EPS generated<sup>34</sup>.

### 1.6.2 Exopolysaccharide Production and Isolation

A growing bacterial strain is initially examined for its possible EPS producing ability by testing the species to determine if it is 'ropy'. The ropy trait is determined by the observation of a long filament which is produced when the strain is extended with an inoculation loop from bacteria cultured on a plate<sup>101</sup>. The ropy characteristic can also be detected in liquid cultures of EPS-producing bacteria that demonstrate a high resistance to flow through serological pipettes, and form viscous strands during free fall from the pipette tip<sup>102</sup>.

#### 1.6.2.1 EPS Production

As previously mentioned the EPS yields for homopolysaccharides and heteropolysaccharides varies greatly. The production of homopolysaccharides polymerised by secreted enzymes e.g. dextran-sucrase, can reach several g L<sup>-1</sup> if enough sucrose (enzyme substrate) is present and optimal growth variables are assured. The recovered concentrations of EPS produced by LAB and related bacteria is often drastically lower, with amounts commonly varying from 20 – 600 mg L<sup>-1</sup>, this is often heavily dependent on the species growth and optimisation of the conditions employed<sup>86</sup>. The bacteria are either grown on solid media, in plates or in liquid media, most commonly in either Erlenmeyer (shake) flasks (for small scale production) or in fermenters (larger scale production).

A large number of factors can affect the growth of bacteria and consequently the production of EPS. It must also be considered that LAB are facultative anaerobes whilst *Bifidobacteria* strict anaerobes. Issues to be considered include: composition of the culture media (C and N sources and other nutrients), growth conditions (pH, temperature and O<sub>2</sub> concentration) and incubation period<sup>103</sup>.

Bacteria are grown in a variety of different media, the most frequently encountered of which include milk, chemically defined media (CDM), semi-defined medium (SDM) or de Man, Rogosa, Sharpe media (MRS). The media are usually supplemented with an assortment of different carbon sources which can include glucose (most regularly used), fructose, sucrose,



galactose and lactose. The choice of an adequate EPS production media is of great importance given that some of the components could potentially interfere with EPS analysis and quantification<sup>101</sup>.

It has frequently been reported that sub-optimal conditions for bacterial growth are often favourable for EPS synthesis<sup>104</sup>. Although evidence suggests that a multitude of combined variables, with strain type being considered as one of the most significant, determines the effect of temperature on EPS production. This is demonstrated by results observed with *Lactobacillus lactis* subsp. *bulgaricus* that indicate the optimal temperature for its synthesis for this species to be very close to the optimal conditions required for bacterial growth<sup>105</sup>.

Determining optimal pH also plays a key role in bacterial growth and EPS synthesis. The pH can either be allowed to fall or be systematically controlled (usually with NaOH) to remain at a constant level throughout the duration of the fermentation. The optimal pH for EPS production was found to be close to the optimal pH for growth (5.8 – 6.5 pH) for a number of EPS producing LAB strains including *Lactobacillus delbrueckii* subsp. *bulgaricus*<sup>105,106</sup> and *Streptococcus thermophilus*<sup>107,108</sup>. It has been proposed that conversion of sugar to EPS is more efficient at pH 5.8, but sugar is more efficiently converted to biomass at pH 6.2<sup>109</sup>. This factor is again heavily dependent on the type of strain encountered.

As previously mentioned mesophilic strains produce the maximum yield of EPS under non-optimal conditions for bacterial growth. It appears though that the production of EPS from thermophilic LAB is growth associated<sup>110</sup>. EPS biosynthesis starts immediately, with the maximum rate of production occurring when a culture is in its exponential growth phase and reaches a maximum yield towards the end of the active growth period<sup>105</sup>. It has also been observed that not only EPS production but also molecular weight (MW) is growth associated<sup>111</sup>.

Increased incubation periods have been found to impart an adverse effect on the yield of EPS, a consequence of EPS degradation. This is thought to be due to a physiologically

changing cell environment and generation of glycosyl-hydrolase activities that reduce molecular mass<sup>112</sup>.

It should also be noted that there is evidence that varying the fermentation conditions for a particular strain can lead to the production of either two (or more) EPS of either differing MW<sup>34</sup> or in fact chemical composition<sup>113</sup>.

#### 1.6.2.2 EPS Isolation

The isolation method employed can also have a highly notable effect on the amount of EPS produced (in the end product). The complexity of the method used for the isolation and purification of EPS is dependent on the composition of the culture media used for its production<sup>101</sup>. A couple of established methods exist for the isolation and subsequent purification of EPS from LAB and related bacterial species.

The first step involves the removal of the milk proteins, caseins. This is performed either using proteinase (Pronase) to hydrolyse the caseins present<sup>114</sup> or by the addition of trichloroacetic acid (TCA) to precipitate caseins<sup>115</sup>. Both methods are followed by centrifugation steps to separate the precipitated biomass. Over recent years several publications have reported working to optimise the concentration of TCA to 14 % (w/v). The resulting mixture is then centrifuged to facilitate the removal of cells and proteins; the EPS is then precipitated by the addition of either acetone<sup>94,116,110</sup> or now more commonly with ethanol<sup>117,10</sup>. The precipitated EPS is then dissolved in deionised water and dialysed to remove any remaining salts, small proteins and remaining free sugars. The dialysed solution is then lyophilised to produce pure solid EPS which is commonly white in appearance with a light, fluffy texture.

Further purification steps can also be undertaken if required. Such techniques as microfiltration<sup>118</sup> and size-exclusion chromatography<sup>35</sup> are currently still readily utilised.

## **1.7 Characterisation of Exopolysaccharides**

The isolation and subsequent characterisation of EPS produced by bacterial species is essential with regards to understanding the potential roles played by this class of molecules in a wide range of functional applications.

As previously explained in Section 1.4, EPS can be present as either homopolysaccharides or heteropolysaccharides. As heteropolysaccharides are constructed from more than one type of monosaccharide they have the ability to produce a wide variety of different repeat unit structures, such structures have been reviewed and catalogued on several occasions in recent years<sup>28,101,103</sup>. Structural variation in heteropolysaccharides is further increased as the monomeric units may be present in either  $\alpha$  or  $\beta$  configuration, in their pyranose (*p*) or furanose (*f*) forms or in either D- or L- absolute configuration.

The way in which the monosaccharide units are connected to each other through their glycosidic bonds to form the repeating unit structure is also required. The molecular mass must also be determined in order to complete the characterisation of the polysaccharide.

The repeating unit structure is the simplest form of the polysaccharide, the first of which was isolated from *St. thermophilus* and characterised by Doco *et al* in 1990<sup>119</sup> (Figure 21). Repeating units generally range from disaccharides up to heptasaccharide structures.

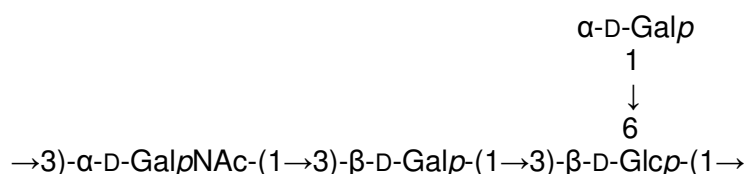


**Figure 21: Tetrasaccharide Repeating Unit Structure of the Isolated EPS from *St. thermophilus***

To identify the primary structure of the EPS repeat unit it is firstly necessary to identify the monomer composition.

### 1.7.1 Monosaccharide Analysis

Cleavage of the glycosidic linkages of the repeating unit structures is required to determine the monosaccharide constituents of the oligosaccharide. The most readily employed method involves the production of alditol acetates which are then analysed by gas chromatography (GC) and where possible by gas chromatography in combination with mass spectrometry (GC-MS).

Although the monomer analysis technique has been continually developed and revised over the years, the most commonly employed method is derived from the methods of Albersheim *et al* (1967)<sup>120</sup> and Blake *et al* (1970)<sup>121</sup>. The current analysis procedure for monosaccharide analysis is detailed in Figure 22.

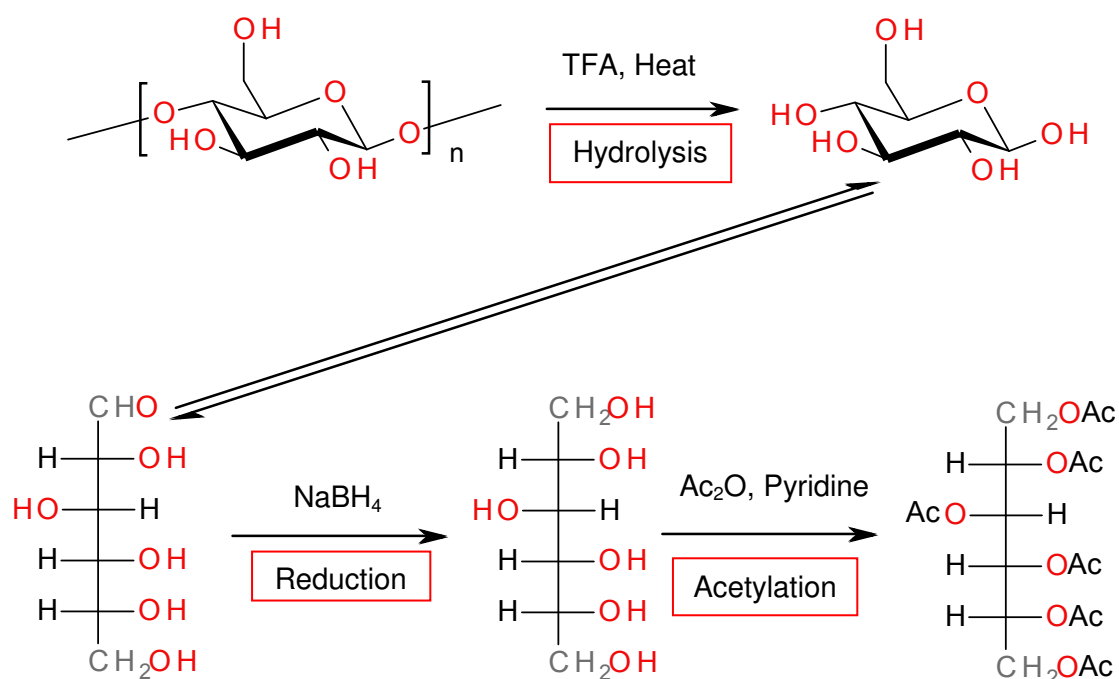


**Figure 22: Alditol Acetate Formation for Monosaccharide Analysis**

The polysaccharide is firstly hydrolysed with the help of an acid catalyst to form sugar monomers. Common catalysts include hydrochloric acid (HCl), sulphuric acid (H<sub>2</sub>SO<sub>4</sub>) and trifluoroacetic acid (TFA), which is now the most frequently used acid<sup>122</sup>. Conditions are chosen such that there is a trade off between incomplete cleavage of glycosidic linkages

under relatively mild conditions and decomposition of the liberated monosaccharides under more severe conditions (4M TFA, 120 °C, 1 hour)<sup>123</sup>. This will be investigated further in Section 3.3.1.2.

The monomers are then reduced to sugar alditols with sodium borohydride (NaBH<sub>4</sub>); extra care should be taken at this stage to ensure the complete removal of borate produced as it inhibits the proceeding acetylation step. The sugar alditols are then converted to alditol acetates by acetylation with acetic anhydride in the presence of pyridine which acts as a catalyst. The derivatised sugars produced are sufficiently volatile to make GC analysis possible. These volatile sugars are then identified by comparison with monosaccharide standards.

There are several issues with the alditol acetates method implemented for the monomer analysis of polysaccharides, the major issue being that the process is a highly time consuming multistep procedure. The presence of amino sugars also causes well documented problems<sup>124</sup> as thermal decomposition occurs leading to under estimation of this particular class of carbohydrates. They also suffer from poor sensitivity, long retention times and chemical changes during the chromatographic analysis<sup>125</sup>.

#### 1.7.1.2 Alternative Methods of Monosaccharide Analysis

In recent years, alternative methods have been developed for monosaccharide analysis. High Performance Anion Exchange Chromatography with Pulsed Amperometric Detection (HPAEC-PAD) in particular has become increasingly more widely employed as it holds a number of advantages over the current methods used with GC analysis. The applications and effectiveness of the technique have been reviewed on a number of occasions<sup>126,127</sup> since the procedure was first brought to the forefront of carbohydrate analysis by Rocklin and Pohl (1983)<sup>128</sup>. The main advantage of this method is that it allows for the determination of intact monosaccharides (acid hydrolysis is initially required for depolymerisation) without pre or post column derivatisation. This therefore greatly decreases analysis times whilst

eliminating the decrease in recovery often observed due to incomplete derivatisation<sup>129</sup>. Although, problems still exist (as with the GC-MS technique) with the analysis of *N*-acetylated amino sugars as they cannot be distinguished from amino sugars once acid hydrolysis has been performed<sup>123</sup>.

#### 1.7.1.3 Absolute Configuration Analysis

As previously expressed, knowledge of the absolute configuration (D or L) of the constituent monomers of the repeating unit structure is also required. Hydrolysed monomers are converted to acetylated glycosides of a chiral secondary alcohol such as 2-butanol<sup>130</sup>. The secondary alcohol is linked at the chiral centre to the glycosidic oxygen of the monosaccharide forming epimers which can then be separated by GC-MS.

#### 1.7.1.4 Monosaccharides of Exopolysaccharides

Whilst a wide range of monosaccharide constituents have been identified in an ever increasing number of EPS oligosaccharide repeating unit structures there are definite common similarities with regard to their monomer compositions<sup>28</sup>. Galactose is the most frequently observed monomer followed closely by glucose, these two monomeric units are almost always identified but in differing ratios. Rhamnose is also a highly prevalent monosaccharide. Glucose and galactose always appear in the D-absolute configuration whilst rhamnose has constantly expressed the L-absolute configuration. It has also been noted that there is a slight preference for the  $\beta$  anomer for both glucose and galactose whilst rhamnose has a distinct preference for the  $\alpha$  anomer. The only sugar to adopt a furanose ring conformation is galactose<sup>116</sup>. The presence of *N*-acetylglucosamine (GlcNAc)<sup>131</sup> and *N*-acetylgalactosamine (GalNAc)<sup>119</sup> along with glucuronic acid (GlcA)<sup>132</sup> and galacturonic acid (GalA) have also been reported in a small number of structures. A number of other non-carbohydrate substituents including phosphor-diester, acetyl esters and pyruvate-acetals have also been recorded<sup>133</sup>.

### 1.7.2 Linkage Analysis

Along with a large number of possible combinations of monosaccharide constituents that can be present in the repeating unit oligosaccharide of the EPS; each monomer can also possess a number of different linkages to other monomeric residues within the structure.

The method used to identify how each of the monomeric units are linked together is very similar to the basic procedure applied for the analysis of monosaccharides. The most widely used method for determining the linkage structure of polysaccharides is methylation analysis and involves GC-MS of partially *O*-methylated alditol acetate (PMAA) derivatives (Figure 23). Initially, the polysaccharide is per-*O*-methylated at all unsubstituted hydroxyl groups. The polysaccharide is then hydrolysed with an acid catalyst (TFA) to form methylated sugar monomers. The methylated monomers are then reduced to sugar alditols with sodium borodeuteride (NaBD<sub>4</sub>). The sugar alditols are then converted to methylated alditol acetates by acetylation with acetic anhydride in the presence of a pyridine catalyst. The location of the methoxy groups identifies sites of free hydroxyls, whilst the acetylated sites identify the location of glycosidic linkages to other monosaccharides. The mass spectral fragmentation patterns of the peaks produced by the methylated alditol acetates are analysed by GC-MS and compared to a series of known standards for identification<sup>123</sup>.

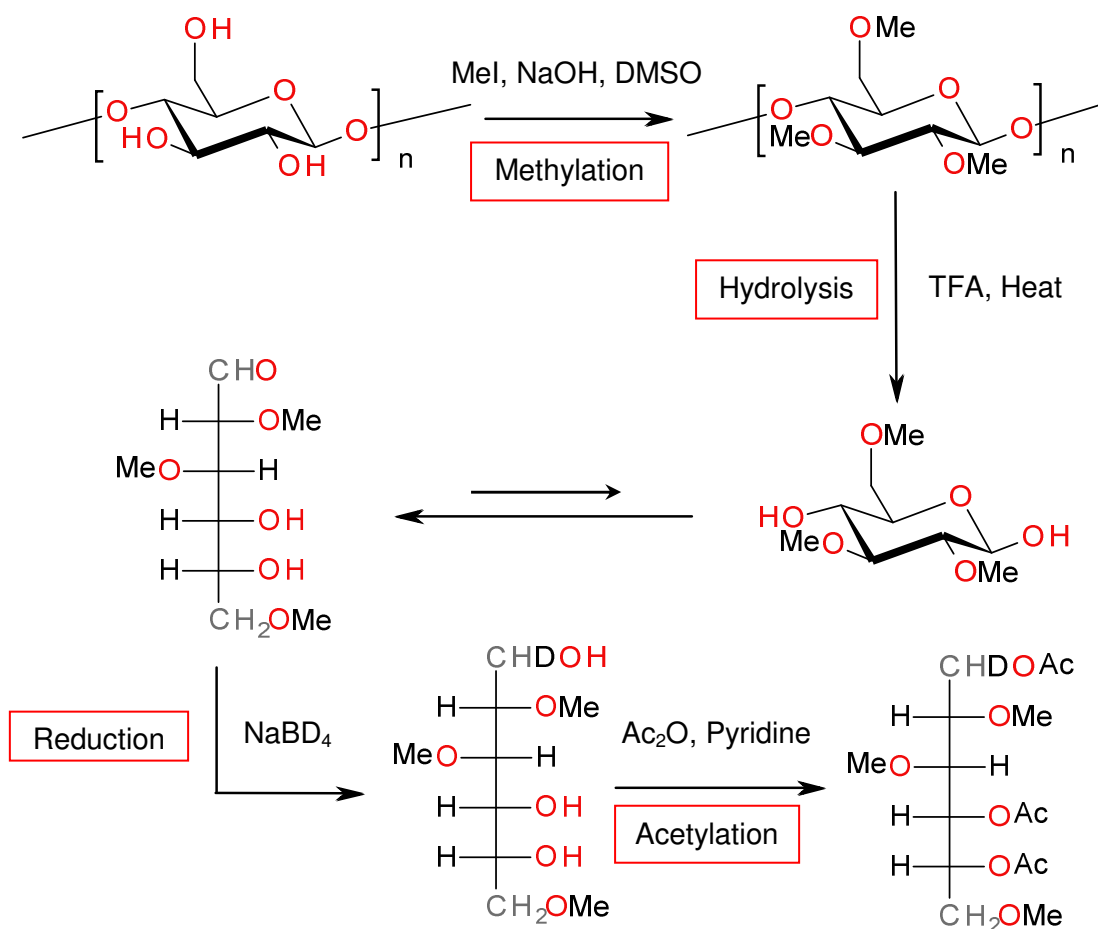


**Figure 23: Methylated Alditol Acetate Formation for Linkage Analysis**

The initial methylation step has undergone many changes, revisions and incarnations. Firstly performed by Purdie in 1903<sup>134</sup> with methyl iodide (MeI) and silver oxide in methanol, this method is still used in some laboratories today. This procedure was further developed by Howarth in 1915<sup>135</sup> when a mixture of methyl sulphate and sodium hydroxide (NaOH) was employed. Both methods were routinely used for preparative and analytical *O*-methylation of carbohydrates for the next 50 years with very little changes to either technique. This was until 1964 when Hakomori<sup>136</sup> developed a new one step method by adding a solution of sodium methylsulphonyl carbanion (Dmsyl ion)<sup>137</sup> and MeI to carbohydrates dissolved in dimethyl sulfoxide (DMSO). The ‘Hakomori’ method provided a better quality of methylation in comparison with the earlier techniques.



However, under methylation of carbohydrates was still an issue. This coupled with the fact that the production of the dimethyl ion can be hazardous, laborious and requires the strict avoidance of air, moisture and CO<sub>2</sub> to minimise the occurrence of side reactions (which can degrade the purity of the final product) led to alternative methods to be developed. The method of methylation currently favoured was developed by Ciucanu and Kerek in 1984<sup>138</sup>, this involves the dissolution of carbohydrates in DMSO and treatment with powdered NaOH and MeI. The per-*O*-methylation is performed in one step and has been found to be not as sensitive to moisture whilst providing very short reaction times with the production of high yields of fully per-*O*-methylated carbohydrates.

Another key step in the linkage analysis and the only other change from the monosaccharide analysis is the reduction step. Reduction of the anomeric carbon to form the corresponding alditol eliminates the asymmetry that would otherwise result in equivocal determination of some derivatives<sup>123</sup>. Reduction with NaBD<sub>4</sub> instead of NaBH<sub>4</sub> however introduces a single deuterium atom onto the C1 position, labelling the former anomeric carbon. The deuterium is used to differentiate between symmetrical derivatives that can often not be fully resolved by chromatography.

#### 1.7.2.1 Linkages in Exopolysaccharides

As with monomer analysis (see Section 1.7.1.4) the frequency at which different particular linkages occur has also been investigated<sup>28</sup>.

A large number of the reviewed structures produced to date have branches (side-chains) that are terminated with a galactose unit whilst rhamnose is frequently observed as a branching point.  $\beta$ -D-galactose is often linked either as a branch terminus or linked to the main backbone chain via its 3-, 4-, or 6-hydroxyl group.  $\beta$ -D-glucose is linked via either its 3-, 4-, or 6-hydroxyl group whilst  $\alpha$ -D-glucose is preferentially attached via either its 3- or 6-hydroxyl group. In bonding with sugars in the main backbone chain of the repeat unit  $\beta$ -L-rhamnose and  $\alpha$ -D-galactose are frequently attached via the 2- or 3-hydroxyl groups.

### 1.7.3 NMR Analysis

Along with the information obtained relating to the linkages present in the oligosaccharide repeating unit from GC-MS analysis, NMR spectroscopy is also used for the elucidation of glycosidic linkages. NMR is applied to determine the overall secondary structure of the EPS by providing information on ring size (pyranose/furanose) and anomeric configuration ( $\alpha/\beta$ ) of the individual monomers whilst also determining the relative orientations of the monomeric units to each other. The importance of NMR spectroscopy as a tool for structural determination of carbohydrates is underlined by the large number of reviews published in recent years<sup>139-142</sup>.

#### 1.7.3.1 <sup>1</sup>H NMR Analysis

When analysing <sup>1</sup>H NMR the spectra observed should be split and viewed as having 'structural reporter signals' (up field and down field) and a 'bulk region'<sup>143</sup>. This approach breaks down the spectra enabling the simpler identification of individual sugars along with their structural features and linkage compositions.

The up field (high field) reporter region contains resonances from structural motifs. These include ring substituents such as acyl, alkyl and acetal, ring substitutions such as *N*-acetylamino groups and H6 signals of 6-deoxy sugars (e.g. rhamnose). The anomeric proton resonances are located in the down field (low field) reporter region of the spectra between 4.4 – 5.5 ppm. These protons are shifted down field from the other ring proton signals due to glycosylation. Integration of the anomeric resonances can be used to estimate the number of different monosaccharide units present in the repeat unit structure. The remaining ring protons are situated in the 'bulk region' located between 4.3 – 3.0 ppm.

The anomeric configuration of the individual monosaccharides can be determined using the <sup>1</sup>H NMR spectra by examining the <sup>3</sup> $J_{1,2}$  (H-H) and from 2D- spectra measuring <sup>1</sup> $J_{H-C}$  coupling constants. For pyranose sugars adopting the <sup>4</sup>C<sub>1</sub> conformation the  $\alpha$ -anomer resonates down field in comparison to the  $\beta$ -anomer. The vicinal coupling (<sup>3</sup> $J_{1,2}$ ) between the anomeric

H1 and H2 protons indicates the relative orientation of the two protons (Figure 24). If both hydrogens in a pyranose structure are in the axial configuration (dihedral angle of  $180^\circ$ ) a large coupling constant of approximately 8 Hz is observed. Whereas if they are in the equatorial – axial configuration (dihedral angle of  $60^\circ$ ) the coupling constant observed is smaller at approximately 4 Hz. The relationship between the dihedral angle and the coupling constant is known as the Karplus relationship which is derived from the Karplus curve<sup>144</sup>. It must be noted however that the Karplus curve can only be applied to sugars when the proton on the C2 is in the axial position e.g. glucose and galactose.

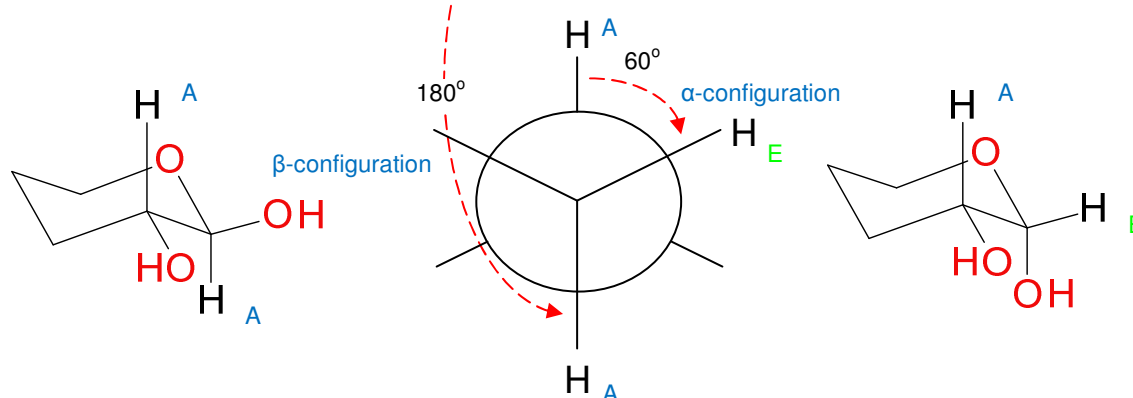


**Figure 24: Demonstration of the Dihedral Angle - Coupling Constant Relationship**

One bond heteronuclear coupling constants ( $^1J_{H-C}$ ) in pyranoses can also be determined in order to identify the anomeric configuration. For D-sugars in the  ${}^4C_1$  conformation a sugar with an  $\alpha$ -anomeric configuration demonstrates a coupling constant of  $\sim 170$  Hz whilst a  $\beta$ -anomeric configuration exhibits a coupling constant of  $\sim 160$  Hz<sup>145</sup>. These values however are reversed for L-sugars.

### 1.7.3.2 DEPT 135 ${}^{13}C$ NMR Analysis

DEPT (Distortionless Enhancement by Polarization Transfer) 135  ${}^{13}C$  NMR provides information on the carbon atoms that are connected to hydrogens atoms in the molecule (attached protons). The  $-CH_3$  and  $-CH$  groups both generate positive signals in the spectra whilst  $-CH_2$  groups display a negative signal.

As with  ${}^1H$  NMR spectra, specific regions of interest relating to carbohydrates can also be identified in the DEPT 135  ${}^{13}C$  NMR. The  $-CH$  emanating from the ring carbons (C2 – C5)

are located between 65 – 85 ppm, whilst carbons substituted with either an amino or methyl group are shifted up field. The anomeric carbons (C1) are shifted down field between 95 – 105 ppm due to glycosylation. The signals for the C6 atoms appear as – CH<sub>2</sub>'s and are therefore represented as negative signals between 60 – 70 ppm.

### 1.7.3.3 Two-dimensional NMR Analysis

In combination with the 1D-NMR analysis, selective 2D- experiments can be applied to determine the structure of the oligosaccharide unit by establishing how the monosaccharide units are linked together.

Combinations of the following 2D- experiments are often required for unequivocal structural determination of the repeating unit structure:

COSY	-	Correlation Spectroscopy
TOCSY	-	Total Correlation Spectroscopy
HMBC	-	Heteronuclear Multiple Bond Correlation
HMQC/HSQC	-	Heteronuclear Multiple Quantum Coherence/Single Quantum Coherence
ROESY/NOESY	-	Rotating frame/Nuclear Overhauser Enhancement Spectroscopy

### 1.7.3.4 Choice of Solvent

EPS are analysed in deuterium oxide (D<sub>2</sub>O) as they suffer from poor solubility in the majority of other common NMR solvents. Samples are commonly analysed at elevated temperatures (~ 70°C). The elevated temperature acts to shift the HOD signal observed from the D<sub>2</sub>O to an up field position and into a clear region of the spectrum so it no longer interferes with possible important signals. The temperature increase also helps to aid in heightening spectral resolution due to the reduction in sample viscosity. It should also be noted that before analysis takes place EPS samples should be exchanged in D<sub>2</sub>O, a procedure often repeated numerous times and combined with intermittent lyophilisation<sup>101</sup>.

#### 1.7.4 *Weight-average Molecular Weight Determination*

EPS from LAB and related bacterial species generally possess molecular masses that range from  $4.0 \times 10^4$  to  $6.0 \times 10^6 \text{ g mol}^{-1}$ <sup>34</sup>. Molecular mass is commonly recognised as one of the contributing factors in EPS functionality<sup>34</sup>. In general terms, the size of a polysaccharide is expressed by the number of monosaccharide units it contains; this is termed the degree of polymerisation (DP).

Determination of molecular weight (MW) has often until recent times been a highly tedious and inaccurate procedure due to EPS polydispersity. Previously, gel permeation chromatography (GPC) has been used to indicate a range of MW by comparison with controlled standards of a particular MW. This method however relies on the comparison with standards and often requires a large quantity of sample. The technique is now more often adopted as a purification method in the process of EPS isolation and purification.

The current method used to determine MW and sizes of polysaccharides is high performance size exclusion chromatography with multi-angle laser light scattering (HP-SEC-MALLS)<sup>146</sup>. HP-SEC-MALLS works initially on the similar principle of weight and size separation as used with GPC but instead of preparative columns the sample is run through smaller analytical scale columns. The sample is then, generally, passed through an online ultraviolet (UV) light detector which provides information on the presence of any residual proteins or nucleic acids which may be present in the sample. The system is then coupled with both a MALLS and differential refractive index (RI) detectors which allow for the determination of the accurate molecular mass of the EPS without the requirement of reference materials<sup>147</sup>.

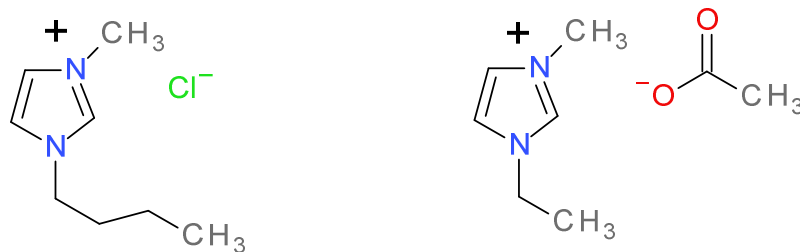
## **1.8    Dissolution of Polysaccharides**

Solubility varies considerably amongst polysaccharides; this is mainly caused by a large DP and/or a strong crystalline structure (e.g. cellulose). Even neutral carbohydrates of a low molecular weight are soluble in relatively limited number of polar and hydrogen bonding solvents. This prevents their use in various applications and complicates their structural determination, thus making it difficult to elucidate the structure-activity relationship<sup>148</sup> not only of EPS but of carbohydrates in general. For example, as previously mentioned, this causes issues with NMR analysis as EPS are generally insoluble (without chemical modification such as derivatisation) in the majority of common deuterated solvents used in NMR studies.

Some improvement in solubility is often recorded using techniques such as dry milling (prior to dissolution), sonication or gentle heating. Even if a slight improvement in solubility is achieved there is still the concern surrounding the application of volatile organic solvents (VOCs) due to the environmental impact of their constant usage. As more environmentally friendly alternatives for VOCs have been sought in recent years one group of 'solvents' in particular that have garnered considerable interest are ionic liquids.

### *1.8.1 Ionic Liquids*

Ionic liquids are often referred to as 'designer solvents'. They have been continually developed over the past decade and applied to a wide variety of applications. They are seen as potential 'green solvents' and a possible replacement for traditional VOCs. They are composed of an organic cation and an inorganic anion (Figure 25).



1-butyl-3-methylimidazolium chloride (BMIMCl)

1-ethyl-3-methylimidazolium acetate (EMIMAc)

### **Figure 25: Examples of Ionic Liquids**

Ionic liquids possess a number of properties which make them highly desirable. They have almost no vapour pressure resulting in low volatility. Ionic liquids are non-flammable, odourless and thermally stable reagents. They are also recyclable, a property which means they are viewed as being extremely favourable to work with in contrast with VOCs.

These properties can be 'tuned' through modification of their cation and anion moieties, allowing them to dissolve both polar and non-polar solutes. Ionic liquids are solid, poorly coordinated salts with a melting point (mpt.) below 100°C whilst some are liquid at room temperature (room temperature ionic liquids, RTILs). They do not crystallise and remain liquid through a wide range of temperatures.

#### *1.8.2 Ionic Liquids and Carbohydrates*

These designer solvents also offer a unique opportunity to study carbohydrate structures and their properties using a variety of modern spectroscopic and analytical methods<sup>148</sup>. There is a current push to use carbohydrates as readily available, relatively inexpensive and renewable fuel feedstocks for the chemical and related industries<sup>149</sup>. The dissolution and chemical modification of cellulose in particular has undergone a vast amount of study in recent years<sup>150,151</sup>. This work prompted the investigation into the (bio)catalytic transformation of mono-, di- and other polysaccharides in an ionic liquid reaction media, into industrially relevant carbohydrates<sup>149</sup>.

With the current knowledge and expanding interest in the utilization of ionic liquids as solvents for the dissolution of carbohydrates, especially with regards to polysaccharides

such as cellulose, it would seem a sensible step to explore the possible dissolution of EPS in ionic liquids.

## **1.9 Research Aims**

The research aims for this project are divided into three distinct areas and are as follows:

The first aim of the study will focus on reviewing and developing the current EPS characterisation protocols utilised in conjunction with the established chromatographic techniques (GC-MS and HPAEC-PAD), as detailed in section 1.7. This will be achieved by analysing the current monomer and linkage methods used and further developing these to achieve a more efficient and reliable procedure for the structural characterisation of EPS.

The second aim of the study will be concerned with employing chromatographic and NMR techniques in order to characterise the repeating unit oligosaccharide structures of two EPSs generated by the bacterial strains *Lactobacillus helveticus* subsp. Rosyjski and *Bifidobacterium animalis* subsp. *lactis* A1dOxR. HP-SEC-MALLS will also be used to determine the molecular weights of the resulting EPSs.

The third aim of this study will focus on investigating the use of ionic liquids, to prepare derivatives of carbohydrates, leading to the possible application of the technique to be used for: analytical structural determinations of exopolysaccharides; for the derivatisation of polysaccharides and finally, as a medium for performing their chemical derivatisation.



## 2. Experimental

### **2.1 General Reagents**

The general materials described throughout the experimental section were all obtained from Sigma-Aldrich Co. Ltd (Gillingham, Dorset, UK), Fisher Scientific UK (Loughborough, Leicestershire, UK) or Avocado Research Chemicals Ltd (Heysham, Lancashire, UK) unless otherwise stated.

### **2.2 Fermentation of *Lactobacillus helveticus* Rosyjski**

This section will be concerned with the fermentation of the bacterial culture *Lactobacillus helveticus* Rosyjski and the procedures and techniques utilised for the subsequent production and isolation of the exopolysaccharide generated.

#### *2.2.1. Bacterial Cultures*

The bacterial culture *Lactobacillus helveticus* Rosyjski was obtained from an industrial partner (Rhodia Food Biolacta, Poland) on slants (MRS).

##### 2.2.1.1 Conservation and Storage of Bacterial Cultures

Cultures were revived in skimmed milk (10% w/v, provided by St. Ivel Ltd. Swindon, UK) and streaked onto an MRS-C agar plate. After incubation at 42°C for 24 h, a single isolated colony was removed from the plate and grown in skimmed milk. The skimmed milk media was maintained as a frozen stock, a primary working culture (1 mL), in a cryoprotectant (10% glycerol) on a plastic bead at -80°C according to methods described by Jones *et al* (1984)<sup>152</sup>.

##### 2.2.1.2 Preparation of Fermentation Inoculum

Prior to inoculation into skimmed milk for batch fermentation, a master culture was produced first. A (1 mL) sample of primary working culture was inoculated into skimmed milk (20 mL, 10% w/v) supplemented with D-glucose (0.166M, 3% w/v), the resulting media was shaken

and subsequently incubated at 42 °C for 24 h to create a master culture. The master culture was then used as a 1% (v/v) inoculum for the two litre batch fermentation.

## 2.2.2 Media

### 2.2.2.1 Preparation of Skimmed Milk

Skimmed milk (10% w/v, provided by St. Ivel Ltd. Swindon, UK) was used as the culture media in both the preparation of the inoculum and as the media for the batch fermentation. Skimmed milk powder (10% w/v) was added to deionised water, typically 20 mL for the preparation of a master culture and two litres for batch fermentation. The media was agitated at 70 °C for 20 mins to form a homogeneous suspension. The milk was then left to stand at room temperature for 24 h before being transferred into a fermentation vessel; the vessel was then autoclaved at 121 °C for 5 mins.

### 2.2.2.2 Preparation of D-Glucose Supplement

Supplementing the skimmed milk media with D-glucose has previously been reported to increase the yield of EPS produced from batch fermentations<sup>131</sup>. A solution of D-glucose (0.166M, 3%) was prepared using deionised water (100 mL). The solution was autoclaved at 121 °C for 5 mins, after this time the supplement was added (aseptically) to the fermentation vessel via vacuum pressure, prior to inoculation with the master culture.

### 2.2.2.3 Preparation of MRS-C Agar

MRS (Oxiod Ltd, Basingstoke, UK) agar was prepared by adding of MRS powder (62.0 g) into a 1 litre Schott bottle. The MRS agar was supplemented with L-cysteine (0.05%), the addition of which supports optimum bacterial growth under anaerobic conditions<sup>153</sup>. The contents of the Schott bottle were diluted with one litre of deionised water; the media was then autoclaved at 121 °C for 15 minutes and stored in a water bath at 50 °C until required.

### 2.2.3 Batch Fermentation of *Lactobacillus helveticus* Rosyjski

#### 2.2.3.1 Fermentation Conditions

*Lactobacillus helveticus* Rosyjski was grown in a two litre fermentation vessel with all of the conditions controlled and continually maintained using a BioFlo 110 fermentor (New Brunswick Scientific Co. Edison, NJ, USA). The temperature was maintained at 42°C using a thermostatically controlled heating jacket. The batch was continually agitated at 100 rpm whilst the pH was set to 5.82 and maintained by the addition of sodium hydroxide (NaOH) (4 M) via a peristaltic pump (BioFlo 110 liquid addition, New Brunswick Scientific Co. Edison, NJ, USA).

#### 2.2.3.2 Fermentation

The fermentation vessel was allowed to equilibrate to the set conditions as detailed in section 2.2.3.1. The batch was inoculated with the working culture (20 mL) which was added (aseptically) to the fermenter using a peristaltic pump (BioFlo 110 liquid addition, New Brunswick Scientific Co. Edison, NJ, USA). The consumption of NaOH (4 M) was continually monitored throughout the entirety of the fermentation as the up-take of NaOH provides a crude indication of EPS growth. After 48 h the media was harvested, and initially heated to 80°C and then left to cool to room temperature.

### 2.2.4 Isolation of *Lactobacillus helveticus* Rosyjski

The procedure employed for the extraction of EPS from the milk media was developed in the laboratories at the University of Huddersfield<sup>115</sup>.

To the harvested media an 80% (w/v) solution of trichloroacetic acid (TCA) was added to produce a final concentration of 14% (v/v) of TCA, the resulting solution was stored overnight at 4°C. The solution was then centrifuged at 25,000 g (Avanti J-26 XPI centrifuge, Beckman Coulter Ltd UK, High Wycombe, UK) for 35 mins at 4°C in order to remove cells and proteins. The solution was then filtered through a grade 4 filter paper (Whatman UK Ltd, Kent, UK). The crude EPS was precipitated by the addition of an equal volume of chilled

absolute ethanol to the supernatant liquid; this was stored overnight at 4°C. The sample was then centrifuged at 25,000 g for 35 mins at 4°C. After decanting off the ethanol solution the recovered pellet was re-dissolved in deionised water (~50 mL). Gentle heating in a water bath at 50°C was required for complete dissolution of the pellet. The dissolved crude EPS was subjected to another precipitation step with chilled absolute ethanol, followed by subsequent centrifugation and decantation of ethanol as described above. The pellet obtained was then re-dissolved in a minimum of deionised water (~10 mL); again gentle heating in a water bath at 50°C was required for complete dissolution of the pellet. Small neutral sugars were then removed from the solution by dialysis, for 72 h at 4°C, against three changes of deionised water per day. After three days the contents of the dialysis tubing was collected in a round-bottom flask and subjected to lyophilisation (freeze-drying) using an Edwards freeze-drier (Northern Scientific, York, UK). The dry weight of the EPS produced was then determined.

#### 2.2.4.1 Preparation of Dialysis Tubing

Dialysis tubing (Cellulose membrane, 12,400 M.W. Cut-off) was prepared by adding lengths of tubing to boiling water (500 mL) containing ethylenediaminetetraacetic acid (EDTA) (0.186 g) and sodium hydrogen carbonate (10 g) and stirring for 10 mins. The tubing was then rinsed before boiling again in deionised water for a further 10 mins. The tubing was then rinsed once more with deionised water and stored at 4°C in deionised water.

#### 2.2.5 Isolation of HMW EPS from Crude *Bifidobacterium animalis* subsp. *lactis* A1dOxR

The crude EPS produced by *Bifidobacterium animalis* subsp. *lactis* A1dOxR was sourced from a collaborative partner (Instituto de Productos Lácteos de Asturias, Consejo Superior de Investigaciones Científicas (IPLA-CSIC), Carretera de Infiesto s/n, 33300 Villaviciosa, Asturias, Spain).

Two methods of dialysis were used to separate and isolate the desired HMW material from the crude *Bifidobacterium animalis* subsp. *lactis* A1dOxR.

### 2.2.5.1 Dialysis using Vivaspin 20 Centrifugal Concentrators

Firstly a sample of crude EPS (20 mg) was dissolved in D<sub>2</sub>O (20 mL). The solution was then added to a Vivaspin 20 centrifugal concentrator (Sartorius Mechatronics, Goettingen, Germany) using a Pasteur pipette. The solution was then centrifuged at 3000 rpm (Centaur 2, MSE (UK) Ltd, London, UK) for 30 mins at room temperature. The filtrate was added to a round bottom flask whilst the retentate was dissolved into a small amount of D<sub>2</sub>O and added to a separate round bottom flask. Both samples were then freeze-dried as detailed in section 2.2.4.

### 2.2.5.2 Dialysis using Spectra/Por<sup>®</sup> Float-A-Lyzer<sup>®</sup>

Firstly the Spectra/Por<sup>®</sup> Float-A-Lyzer<sup>®</sup> (Spectrum Laboratories Inc., Breda, The Netherlands) was washed with an amount of deionised water (10 mL). A sample of crude EPS (45 mg) was dissolved in D<sub>2</sub>O (10 mL), the solution was then transferred to the float-alyzer using a Pasteur pipette. The solution was then dialysed, for 72 h at 25 °C, against two changes of deionised water per day. The retentate was dissolved into a small amount of D<sub>2</sub>O and added to a round bottom flask. The sample was then freeze-dried as detailed in section 2.2.4.

## **2.3 Structural Characterisation of Exopolysaccharides**

This section will focus on the chromatographic and NMR techniques employed for the structural characterisation of exopolysaccharides.

### *2.3.1 NMR Analysis*

All NMR spectra of exopolysaccharides were run on either a Bruker Avance DPX400 400.13MHz or a Bruker Avance DPX500 500.13MHz by Dr. Neil McLay.

All samples of EPS were prepared in deuterium dioxide (D<sub>2</sub>O) (GOSS Scientific Instruments Ltd, Nantwich, UK) and spectra were acquired using Bruker pulse sequences at a

temperature of 70°C unless otherwise stated. Chemical shifts were expressed in ppm relative to an internal standard of acetone.

Mild acid hydrolysis of *Bifidobacterium animalis* subsp. *lactis* A1dOxR was carried out using a procedure adapted from Yamamoto *et al* (1995)<sup>154</sup>. <sup>1</sup>H NMR spectrum of EPS prepared in D<sub>2</sub>O was recorded prior to the addition of trifluoroacetic acid (TFA) (1% v/v). Following this, spectra were recorded every hour for 9 h with an additional spectra being recorded after 24 h.

### 2.3.2 Molecular Weight Determination

The weight-average molecular weight ( $M_w$ ) and polydispersity ( $M_w/M_n$ ) of the pullulan standard and the exopolysaccharides produced by *Lactobacillus helveticus* Rosyjski and *Bifidobacterium animalis* subsp. *lactis* A1dOxR were determined by HP-SEC-MALLS analysis. It should be noted that  $dn/dc$  values for all samples have previously been determined at the University of Huddersfield and by industrial partners.

Solutions of 1 mg mL<sup>-1</sup> were prepared in deionised water. Upon complete dissolution samples were filtered through 0.2 µm PTFE Puradisc syringe filters (Whatman UK Ltd). Filtered samples (200 µl) were injected (using a 7125i injection port, Rheodyne LLC, California, USA) onto an analytical size exclusion column (Polymer Labs Aquagel-OH-Mixed-H 8µm particle size, 300 x 7.5mm, Polymer Laboratories, UK). Ultra pure water delivered by a HPLC pump (Prominence LC-20AD, Shimadzu, Milton Keynes, UK) at 1 mL min<sup>-1</sup>, the neutral analytes were eluted and passed through a series of detectors. The samples pass first through a UV detector (Prominence SPD-20A, Shimadzu) with a wavelength set to 260 nm; this identifies the presence of any residual DNA present in the samples. The concentration of the samples is then determined by a refractive index (RI) detector (Optilab rEX, Wyatt Technology, Santa Barbara, USA) and finally the weight-average molecular weight is measured using a multi-angle laser light scattering (MALLS)

photometer with the laser set to 690nm (Dawn OES, Wyatt Technology, Santa Barbara, USA).

### Chromatographic Conditions

Pump	-	Prominence LC-20AD
Flow Rate	-	1 mL min <sup>-1</sup>
Mobile Phase	-	Ultra pure water
Injection Volume	-	200 µL
Column	-	Plaquagel-OH-Mixed-H 8µm, 300 x 7.5mm
Detector Calibration Constant	-	2.000x10 <sup>-5</sup> (V <sup>-1</sup> )
Detectors	-	UV, RI and MALLS
Run Time	-	45 mins

### 2.3.3 Monomer Analysis

This section is concerned with the analysis of the monosaccharide compositions of exopolysaccharides by hyphenated chromatographic techniques (HPAEC-PAD and GC-MS).

#### 2.3.3.1 Monomer Analysis Using HPAEC-PAD

The analysis of hydrolysis products, generated by utilising different acid catalysts, to examine the release of neutral and amino sugars from *Lactobacillus acidophilus* 5e2 was studied using HPAEC-PAD. For all hydrolysis reactions 2 mg of EPS sample was utilised.

##### 2.3.3.1.1 Hydrolysis Reaction – Variation of Acid Type and Reaction Duration

A sample of EPS was added to a pressure tube containing TFA (1 mL of 2 M); the tube was heated to 120°C for 1 h. After 1 h the solution was evaporated to dryness under a stream of nitrogen gas at 50°C. This procedure was repeated with 2 M TFA for 2 h and with 4 M TFA for 1 h and 2 h.

In a separate series of experiments a sample of EPS was added to a pressure tube containing H<sub>2</sub>SO<sub>4</sub> (1 mL of 0.5 M), the tube was heated to 100°C for 1 h. After this time an amount of barium carbonate was used to neutralise the acid and precipitate the sulphate, the solution was then filtered and evaporated to dryness under a stream of nitrogen gas at 50°C. This procedure was repeated with 0.5 M H<sub>2</sub>SO<sub>4</sub> for 2 h and with 1 M H<sub>2</sub>SO<sub>4</sub> for 1 h and 2 h.

In a separate series of experiments a sample of EPS was added to a pressure tube containing HCl (1 mL of 1 M); the tube was heated to 100°C for 1 h. After 1 h the solution was freeze-dried over night. This procedure was repeated with 1 M HCl for 2 h and with 2 M HCl for 1 h and 2 h.

In a separate series of experiments a sample of EPS was added to a pressure tube containing formic acid (1 mL of 90% (v/v)) and heated to 100°C for 2 h. After 2 h the solution was evaporated to dryness under a stream of nitrogen gas at 50°C. The residue was then dissolved in H<sub>2</sub>SO<sub>4</sub> (0.5 mL 0.25 M) and heated at 100°C for 12 h. After 12 h the solution was cooled and neutralised with an amount of barium carbonate, subsequently filtered and then concentrated by evaporation to dryness under a stream of nitrogen gas at 50°C.

Monomer analysis for the EPS produced by both *Lactobacillus helveticus* Rosyjski and *Bifidobacterium animalis* subsp. *lactis* A1dOxR (HMW) was performed using 2 mg of sample in a solution of TFA (1 mL 4 M), heated to 120°C for 1 h as previously described.

#### 2.3.3.1.2 HPAEC-PAD Analysis

In each case, the dry residue obtained after the hydrolysis reactions was dissolved in deionised water (1 mL) in preparation for HPAEC-PAD analysis. The reconstituted hydrolysed EPS samples were injected (AS50 Autosampler, Dionex BioLC, Dionex Co. Sunnyvale, CA, USA) onto an anion-exchange column (CarboPac PA20 3 x 150 mm, Dionex Co.). Sodium hydroxide (8 mM, Isocratic) delivered by a gradient pump (GS50 Gradient pump, Dionex Co.) at 0.5 mL min<sup>-1</sup> was used to elute the monosaccharides and the eluent was passed through a pulsed amperometric detector (PAD) (ED50 Electrochemical detector,



Dionex Co.). The monosaccharide standards used to obtain the linear calibration data were prepared to the specific concentrations in deionised water and were run using the chromatographic conditions listed.

### Chromatographic Conditions

Pump	-	GS50 Gradient Pump
Flow Rate	-	0.5 mL min <sup>-1</sup>
Mobile Phase	-	8 mM Sodium Hydroxide
Injection Volume	-	20 µL
Column	-	CarboPac PA20 3 x 150mm
Detector	-	PAD
Run Time	-	20 mins

#### 2.3.3.2 Monomer Analysis Using GC-MS

As well as HPAEC-PAD, monomer analysis was also performed by GC-MS for the EPS produced by both *Lactobacillus helveticus* Rosyjski and *Bifidobacterium animalis* subsp. *lactis* A1dOxR (HMW).

##### 2.3.3.2.1 Alditol Acetate Method

The monosaccharides composition analysis was determined by following the modified procedures as developed by Albersheim *et al* (1967)<sup>120</sup> and Blake *et al* (1970)<sup>121</sup>. A structural representation of the current method can be observed in Figure 22.

A sample of EPS (2 mg) was added to a pressure tube containing TFA (1 mL of 4 M); the tube was heated to 120°C for 1 h. After 1 h the solution was evaporated to dryness under a stream of nitrogen gas at 50 °C.

The dried residue (hydrolysed monomers) was dissolved in deionised water (1 mL). Sodium borohydride (40 mg) was then added in order to reduce the sugar monomers; the tube was sealed and heated at 40 °C for 2 h. After 2 h the solution was evaporated as previously

detailed. Glacial acetic acid (1 mL) was then added to destroy any excess borohydride present; the solution was then evaporated to dryness. Methanol (3 x 1 mL) was added and repeatedly evaporated to remove the borate complex (the methanol 'mops' up the borate to form B(OMe)<sub>3</sub>, which is then subsequently evaporated).

Pyridine (1 mL) and acetic anhydride (1 mL) were then added to the dry residue (sugar alditols) in the pressure tube; the sample was heated at 100 °C for 2 h. After 2 h the resulting solution was evaporated as previously detailed. The dried acetylated monomers (alditol acetates) were suspended in deionised water (1 mL) and extracted with chloroform (3 x 3 mL); the total organic layer was then washed with deionised water (2 mL). The solution was then dried over anhydrous sodium sulphate for 30 mins before being filtered and the resulting solution evaporated as previously described. The dried residue was reconstituted by dissolution in acetone (1.5 mL) in preparation for GC-MS analysis.

#### 2.3.3.1.2 GC-MS Analysis of Alditol Acetates

GC-MS analysis was performed on an Agilent 7890A GC (Agilent Technologies UK Ltd. Cheshire, UK) equipped with an Agilent 5975B inert XL EI/CI MSD (Agilent Technologies UK Ltd.). Samples were eluted from an Agilent HP5-MS (30m x 250µm-id, 0.25 µm) column (Agilent Technologies UK Ltd.) eluting with helium (1 mL min<sup>-1</sup>). The conditions for monomer analysis by GC-MS are listed:

#### Chromatographic Conditions

Flow Rate	-	1 mL min <sup>-1</sup>
Mobile Phase	-	Helium
Injection Volume	-	1 µL
Column	-	Agilent HP5-MS
Ionisation	-	Electron Impact (EI)
Detector	-	MSD
Rosyjski Method Program	-	160 °C for 1 min, 3 °C/min to 240 °C, hold

Column Oven Temperature		240 °C for 5 mins
Run Time	-	32.667 mins
A1dOxR Method Program	-	175 °C for 1 min, 0.75 °C/min to 190 °C,
Column Oven Temperature		hold at 190 °C for 5 mins
Run Time	-	26 mins

### 2.3.4 Linkage Analysis

This section is concerned with the conversion of a series of disaccharide compounds (into model compounds for use as linkage standards) and exopolysaccharides (from *Lactobacillus helveticus* Rosyjski and *Bifidobacterium animalis* subsp. *lactis* A1dOxR (HMW)) into per-*O*-methylated alditol acetates (PMAAs), followed by analysis by GC-MS.

#### 2.3.4.1 Methylated Alditol Acetate Method

The method employed for sugar linkage analysis is a modified technique adapted from the previously developed method of by Ciucanu and Kerek (1984)<sup>138</sup> and later by Ciucanu and Caprita (2007)<sup>155</sup>.

A sample of EPS (or disaccharide) was added to a pressure tube containing anhydrous dimethyl sulfoxide (DMSO) (0.7 mL) and stirred at room temperature until the formation of a slurry was observed. Dried and crushed NaOH (70 mg) was added with stirring along with methyl iodide (60 µL). After 20 mins the resulting solution was suspended in deionised water (1 mL) and extracted with dichloromethane (1 mL), the organic layer was then washed with deionised water (3 x 5 mL). The resulting liquid was then evaporated to dryness under a stream of nitrogen gas at 50 °C.

The dried residue (methylated polysaccharide/disaccharide) was then subjected to the same procedure as previously described for GC-MS monomer analysis (Section 2.3.3.2.1), with the only alteration to the method being the substitution of sodium borohydride with sodium borodeuteride (20 mg) in the reduction reaction.

## 2.3.4.1.2 GC-MS Analysis of PMAAs

GC-MS analysis of the generated PMAAs was performed as detailed in Section 2.2.3.1.2, the chromatographic conditions for the EPS and disaccharide samples analysis are listed as follows:

Chromatographic Conditions for PMMAs of A1dOxR and Disaccharides

Flow Rate	-	1 mL min <sup>-1</sup>
Mobile Phase	-	Helium
Injection Volume	-	1 µL
Column	-	Agilent HP5-MS
Ionisation	-	EI
Detector	-	MSD
A1dOxR Method Program	-	155°C for 1 min, 0.75°C/min to 175°C,
Column Oven Temperature		hold at 175°C for 5 mins
Run Time	-	32.667 mins
Disaccharides		
Method Program	-	160°C for 1 min, 1.5°C/min to 200°C,
Column Oven Temperature		hold at 200°C for 5 mins
Run Time	-	32.667 mins

Chromatographic Conditions for PMMAs of Rosyjski

Flow Rate	-	1.2 mL min <sup>-1</sup>
Mobile Phase	-	Helium
Injection Volume	-	1 µL
Column	-	SGE BPX-70 (30 m x 250 µm – id, 0.25 µm) (SGE Analytical Science Ltd. Milton Keynes, UK)
Ionisation	-	EI

Detector	-	MSD
Rosyjski Method Program	-	160 °C for 1 min, 0.75 °C/min to 200 °C,
Column Oven Temperature		200 °C for 5 mins
Run Time	-	59.333 mins

### 2.3.5 Absolute Configuration

The absolute configuration of the substituent monomers in the repeating unit structure of an EPS is determined by the GC-MS analysis of the acetylated butyl glycosides present, the method employed is adapted from the technique previously developed by Gerwig *et al* (1978)<sup>130</sup>.

#### 2.3.5.1 Preparation of Acetylated Butyl Glycosides

A sample of EPS (0.5 mg) was added to a pressure tube containing TFA (0.5 mL 4 M). After 1 h at 120 °C the solution was evaporated to dryness under a stream of nitrogen gas at 50 °C. Methanol (2 x 0.5 mL) was added to the dried residue and was removed by evaporation as previously described. (S)-(+)-2-Butanol (0.5 mL) and acetyl chloride (30 µL) were added to the tube which was then purged with nitrogen gas, sealed and subsequently heated at 80 °C for 12 h. After 12 h the resulting solution was cooled and evaporated as previously detailed.

Pyridine (0.5 mL) and acetic anhydride (0.5 mL) were then added to the dry residue (butyl glycosides) in the pressure tube; the sample was heated at 100 °C for 2 h. After 2 h the resulting solution was evaporated as previously detailed. The dried acetylated butyl glycosides were suspended in deionised water (0.5 mL) and extracted with ethyl acetate (3 x 0.5 mL), the total organic layer was then washed with deionised water (1 mL). The resulting solution was then evaporated. The dried residue was reconstituted by dissolution in acetone (0.5 mL) in preparation for GC-MS analysis.

This procedure was repeated for the butyl glycoside monomer standards (D-glucose, D-galactose and L-rhamnose), the only alteration to the method occurring with the initial sample size used for the monomer standards (0.15 mg).

Chromatographic Conditions

Flow Rate	-	1 mL min <sup>-1</sup>
Mobile Phase	-	Helium
Injection Volume	-	1 µL
Column	-	Agilent HP5-MS
Ionisation	-	EI
Detector	-	MSD
Rosyjski Method Program	-	175°C for 1 min, 1°C/min to
Column Oven Temperature		180°C, hold at 180°C for 1 min, 0.5°C/min to 185°C, hold at 185°C for 2 mins
Run Time	-	19 mins

**2.4 Analysis of Carbohydrates in Ionic Liquids**

The experimental details along with the analytical procedures utilised for the analysis of carbohydrates in ionic liquids will be detailed in the following section.

***2.4.1 Dissolution of Carbohydrates***

A sample (typically 5 g) of ionic liquid (either 1-methyl-3-butylimidazolium chloride or 1-ethyl-3-methylimidazolium acetate) was added to a round bottom flask containing a magnetic flea under an atmosphere of nitrogen gas. The ionic liquid was heated to 100°C in an oil bath with continual stirring until the crystalline solid (BMIMCl) or viscous liquid (EMIMAc) became visibly fluid. A sample of carbohydrate (typically 10% w/w, 500 mg) was added to the flask; the solution was then continually monitored by visual examination until complete dissolution of the carbohydrate was observed (typically ~30 mins).

#### 2.4.2 *Acetylation of Carbohydrates in Ionic Liquids*

Once samples had dissolved acetylation was initiated by the addition of acetic anhydride and one of three acetylation catalysts (pyridine/sodium acetate/zinc chloride).

Acetic anhydride (2 mL) and pyridine (2 mL)/sodium acetate (230 mg)/zinc chloride (140 mg) were added to the carbohydrate-ionic liquid solution (10% w/w) whilst stirring. After 2 h the stirring was ceased and the solution cooled to room temperature.

#### 2.4.3 *Extraction of Carbohydrates from Ionic Liquids*

Carbohydrates, both native and acetylated were extracted from ionic liquid solutions by liquid-liquid extraction. A sample (typically 2 mL) of the reaction product (dissolution and acetylation) was removed from the round bottom flask using a Pasteur pipette. The reaction product was suspended in deionised water (5 mL) and extracted with chloroform (2 x 10 mL); the total organic layer was then washed with deionised water (5 mL). The solution was then dried over anhydrous sodium sulphate for 30 mins before being filtered and the resulting solution evaporated to dryness under a stream of nitrogen gas at 50 °C.

#### 2.4.4 *NMR Analysis*

Again all NMR spectra of carbohydrates were run on either a Bruker Avance DPX400 400.13MHz or a Bruker Avance DPX500 500.13MHz by Dr. Neil McLay. All spectra were acquired at either room temperature or at 70 °C.

Extracted samples were prepared in deuterated chloroform ( $\text{CDCl}_3$ ) whilst un-extracted samples were subjected to NMR analysis by the addition of either 15% v/v of deuterated dimethyl sulfoxide ( $\text{DMSO-d}_6$ ) or by using a  $\text{D}_2\text{O}$  capillary insert to achieve field-frequency lock.

#### 2.4.5 *GC-MS Analysis of Acetylated Carbohydrates*

The dried residue obtained from the extraction procedure detailed in section 2.4.3 was dissolved in acetone (2 mL) in preparation for GC-MS analysis.

GC-MS analysis of the acetylated carbohydrates was performed as detailed in Section 2.3.3.1.2, the chromatographic conditions for this group of samples are listed as follows:

#### Chromatographic Conditions

Flow Rate	-	1 mL min <sup>-1</sup>
Mobile Phase	-	Helium
Injection Volume	-	1 µL
Column	-	Agilent HP5-MS
Ionisation	-	EI
Detector	-	MSD
Column Oven	-	140°C for 1 min, 2.5°C/min to 240°C,
Temperature Program		hold at 240°C for 5 mins, 2.5°C/min to 300°C, hold at 300°C for 5 mins
Run Time	-	75 mins

#### *2.4.6 MS with MS/MS Analysis*

Extracted acetylated samples, along with acetylated compound standards, were dissolved in acetone in preparation for MS analysis.

The samples were injected directly into the nebuliser of the MS via a syringe pump (180 µL/hour) and data was acquired for 60 seconds to allow the spectra produced to be averaged. The MS and MS/MS conditions are as follows:

#### Mass Spectrometry Conditions

Instrument	-	MicrOTOF-q with ESI interface, (Bruker Daltonics, Billerica, USA)
Capillary Voltage	-	-4500 V
Dry Gas	-	4.0 L min <sup>-1</sup>
Nebulizer	-	0.4 bar



Mass Range	-	50-3000 m/z
Collision Energy	-	4.0 eV
Collision RF	-	200 Vpp
PrePulse Storage	-	6.0 $\mu$ s

#### Mass Spectrometry/Mass Spectrometry Conditions

Isolation Width	-	1 m/z
Collision Energy	-	30 eV
Isolation Mass	-	[M + Na] <sup>+</sup>

#### *2.4.7 Recycling of Ionic Liquids*

The aqueous portions obtained from the liquid-liquid extraction procedure detailed in section 2.4.3 were pooled and added to a round bottom flask (separate flasks for reactions utilising BMIMCl and EMIMAc). The contents of the flask were firstly frozen and then freeze dried overnight. The resulting viscous solution was prepared for NMR analysis by dissolution in CDCl<sub>3</sub>.

# Results and Discussion Sections

3. Structural Characterisation of the Novel  
EPS from *Lactobacillus helveticus* Rosyjski

4. Structural Characterisation of the Novel  
EPS from *Bifidobacterium animalis* subsp.  
*lactis* IPLA-R1 (A1dOxR)

5. Ionic Liquids and Carbohydrates

### 3. Structural Characterisation of the Novel EPS from *Lactobacillus helveticus* Rosyjski

#### **3.1 Introduction**

The exopolysaccharide produced by *Lactobacillus helveticus* Rosyjski was first isolated at the University of Huddersfield in the year 2000. Since that time there have been numerous fermentations undertaken along with previous attempts to identify the monomeric constituents and how they are connected together to form the repeating unit structure of the EPS. The chapter will discuss the structural characterisation of the EPS produced by *Lactobacillus helveticus* Rosyjski undertaken as part of this research programme.

The chromatographic techniques currently employed for structural analysis and elucidation will also be examined.

#### **3.2 Production and Isolation of Rosyjski**

This section will be concerned with the production and isolation of the resulting EPS material produced by the fermentation of the isolated bacterial strain *Lactobacillus helveticus* Rosyjski.

##### *3.2.1 Production and Isolation of EPS*

The fermentation of the bacterial species and the procedure employed for the isolation of the solid material produced (EPS) are described in Chapter 2. The solid material recovered and subsequently isolated from the fermentation was recorded as 194.0 mg L<sup>-1</sup>. The batch was numbered XN361, in accordance with the current protocol in operation at the University of Huddersfield. The EPS yield obtained from batch XN361 is in accordance with those previously attained from prior fermentations of *Lactobacillus helveticus* Rosyjski with 237.0 mg L<sup>-1</sup> being recorded by Chadha (2009)<sup>156</sup> and 32.0 mg L<sup>-1</sup> (obtained before optimisation of fermentation conditions) being recorded by Dunn (2002)<sup>157</sup>. It should be noted that there is a

degree of fluctuation between batches. The general variation between EPS yields can partly be rationalised by taking into consideration the complexity of the isolation procedure employed combined with the fact that the EPS producing ability of LAB is often regarded as being unstable<sup>28</sup>.

### 3.2.2 Initial Observations

<sup>1</sup>H NMR analysis along with weight-average molecular weight determinations using HP-SEC-MALLS were carried out as initial observations on the isolated EPS sample.

#### 3.2.2.1 <sup>1</sup>H NMR Interpretation

As was the case in previous batches of the EPS isolated from the *Lactobacillus helveticus* Rosyjski, from the analysis of the <sup>1</sup>H NMR integration identified that there were six protons in the low field region. These have previously been shown to be five anomeric protons (arbitrarily designated **A-E** from left to right) and one ring proton (**B2**). In older batches (such as XN286) the three signals at the highest chemical shift appear as isolated singlets, these are followed by two overlapping doublets at ~ 4.7 ppm and finally, immediately adjacent to this is the ring proton (Figure 26).

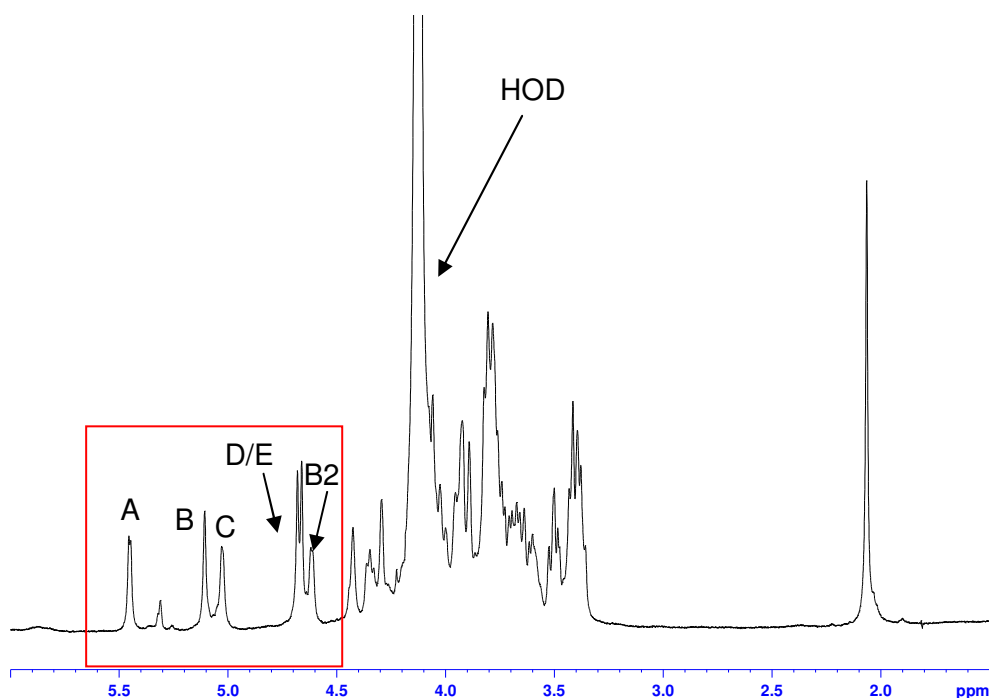


**Figure 26: <sup>1</sup>H NMR Spectrum of EPS from *Lactobacillus helveticus* Rosyjski in D<sub>2</sub>O at 70°C (Batch XN286)**

Interestingly, in later batches of the EPS (such as XN361), a shift in the position of the **B2** proton was observed, this placed **B2** directly beneath the anomeric doublets (see Figure 27). With this in mind, it was decided that all NMR analysis would be carried out on spectra from an older batch of the EPS (XN286). It is also worth pointing out that the spectra provided evidence for the presence of an amino sugar in the repeating unit with an *N*-acetyl methyl being present at 2.06 ppm.

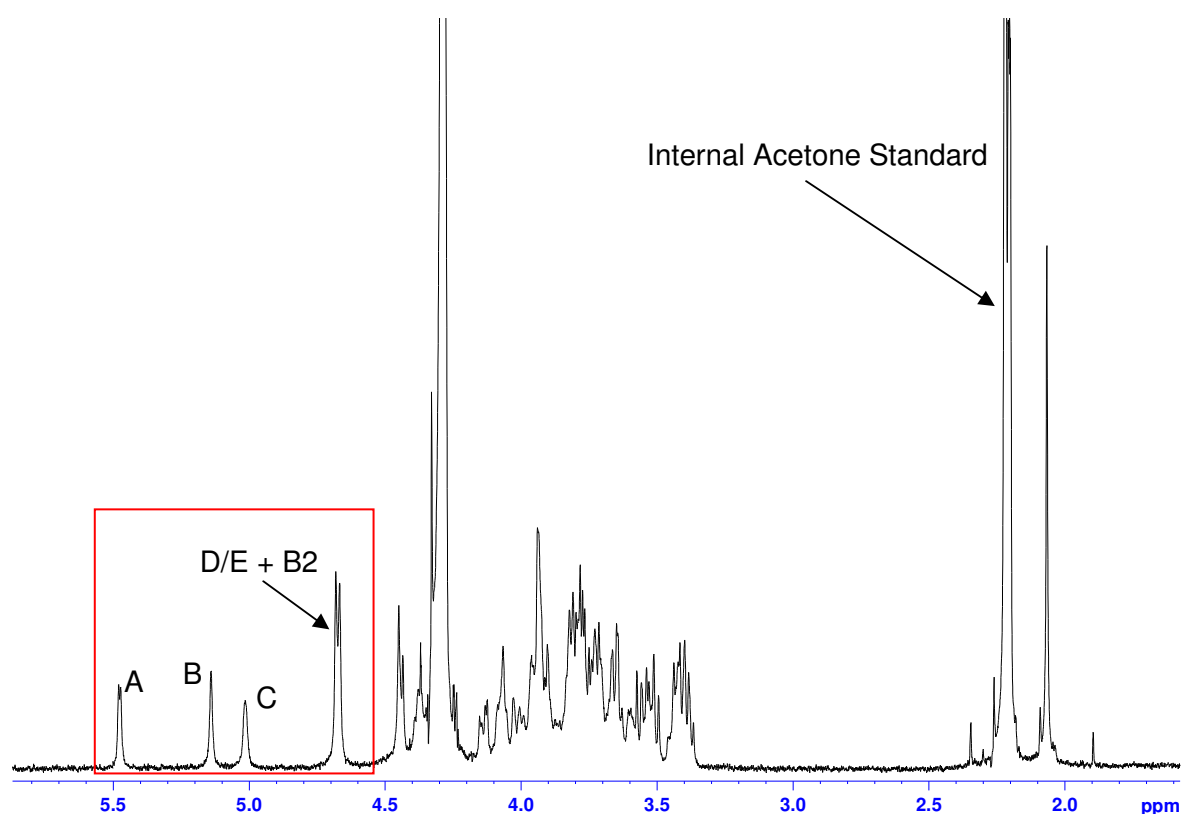


**Figure 27:  $^1\text{H}$  NMR Spectrum of EPS from *Lactobacillus helveticus* Rosyjski in  $\text{D}_2\text{O}$  at  $70^\circ\text{C}$  (Batch XN361)**

The  $^1\text{H}$  NMR spectrum, along with other 1D- and 2D- spectra will be discussed and interpreted in section 3.3.1.

### 3.2.2.2 Weight-Average Molecular Weight Determination

Firstly, a standard material of known molecular weight and low polydispersity was chosen to check to ensure the accuracy of the instrumentation. Pullulan (as previously referred to in section 1.6) is a linear homopolysaccharide consisting solely of glucose units. The  $M_w$  of the

pullulan standard is reported in the literature<sup>158</sup> as 800,000 g mol<sup>-1</sup> with a polydispersity ( $M_w/M_n$ ) of 1.23 and a  $dn/dc$  value of 0.148 mL g<sup>-1</sup>.

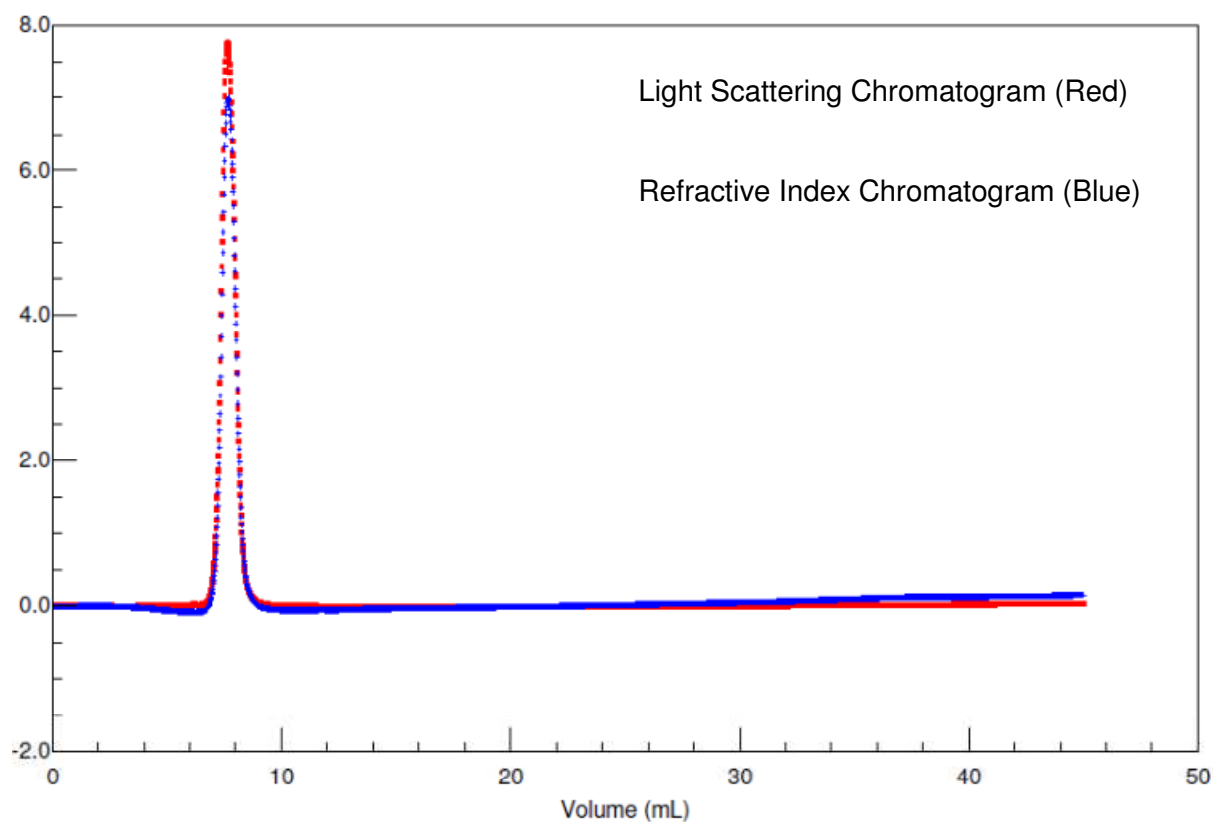


**Figure 28: A Chromatogram of the Pullulan Standard (800,000  $M_w$ )**

The experimental values obtained for the pullulan standard (Figure 28) confirmed the good accuracy of the instrumentation with  $M_w$  recorded as 806,200 and the  $M_w/M_n$  as 1.177.

With the pullulan standard confirming the accuracy of the HP-SEC-MALLS a sample of Rosyjski EPS from batch XN361 was analysed. A  $dn/dc$  value of 0.1980 mL g<sup>-1</sup> was used for the analysis, this value was previously determined from prior fermentations of Rosyjski<sup>156</sup>.

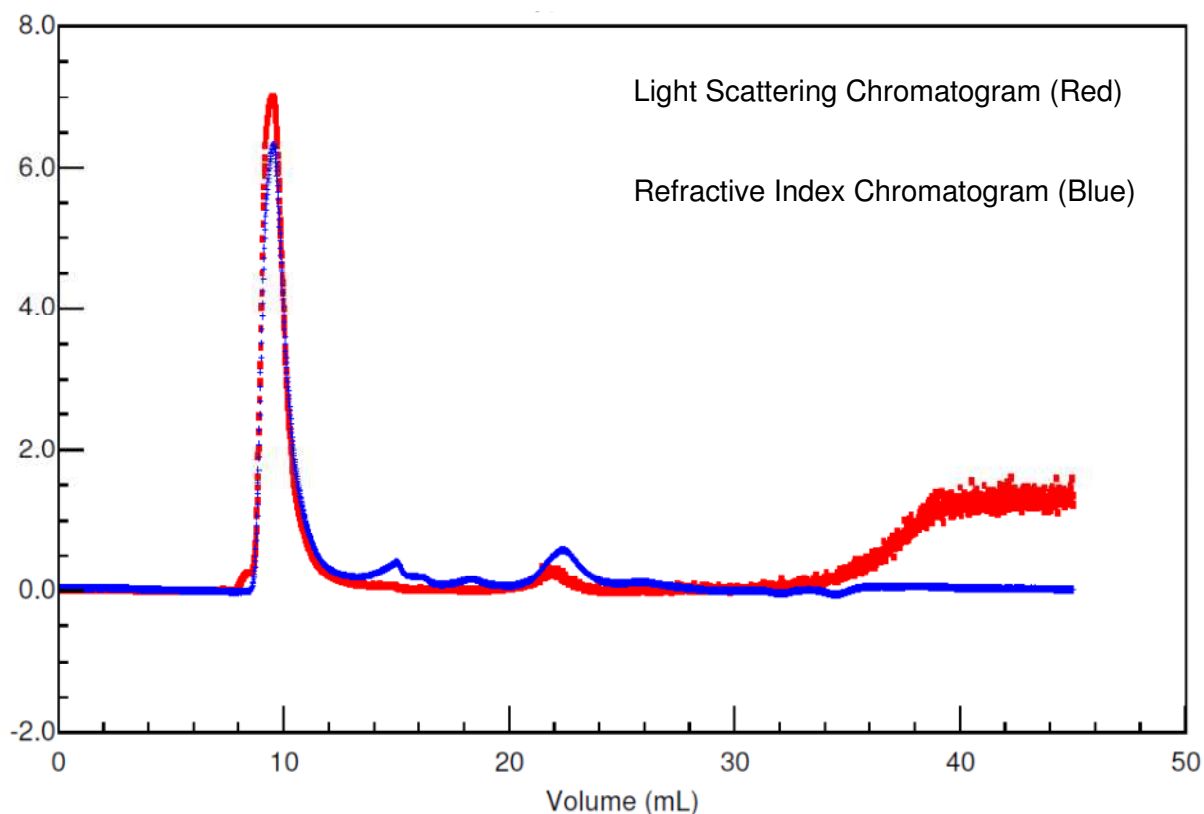


**Figure 29: A Chromatogram of EPS Produced By Fermentation of Rosyjski Batch XN361**

The results obtained from the HP-SEC-MALLS (Figure 29) study produced an  $M_w$  of 1,349,000 whilst the polydispersity ( $M_w/M_n$ ) was recorded as 1.151. The values observed for both weight-average molecular weight and polydispersity demonstrate a discernible difference between those previously documented for Rosyjski fermentations<sup>156</sup>. The  $M_w$  was found to be higher whilst the  $M_w/M_n$  was found to be lower than the value previously recorded by Chadha ( $M_w$  – 997,300 and  $M_w/M_n$  – 1.445). As previously explained with regard to isolated yields of EPS, the instability of EPS production from LAB can go some way to explaining the fluctuations observed from one batch to another. The length of time the fermentation is conducted for can also have considerable influence on these values<sup>111</sup>.

### **3.3 Monomer and Linkage Analysis for Rosyjski**

This section will discuss the current procedures utilised for the monomer and linkage analysis, namely the use of gas chromatography mass spectrometry (GC-MS) and high

performance anion exchange chromatography with pulsed amperometric detection (HPAEC-PAD) for both monomer and linkage analysis. An overview of these techniques and their applications in carbohydrate analysis has previously been provided in section 1.7.1 and 1.7.2.

Monomer analysis for Rosyjski has previously been undertaken by a number of researchers at the University of Huddersfield (Dr. Marcus Chadha and Mr. Mohammed Maqsood (unpublished results) and by De Vuyst *et al* (2000) at the University of Brussels (private correspondence). Using standard techniques (GC-MS – University of Huddersfield and HPAEC-PAD – University of Brussels), the only monomers observed were glucose and galactose. However, as previously stated, it is clear from the NMR studies that the EPS from Rosyjski contains an *N*-acetyl amino sugar which is not being detected. All of the *N*-acetyl amino sugars that have been previously been identified in EPS are either *N*-acetylglucosamine or *N*-acetylgalactosamine. Previous studies could not detect either of the two *N*-acetyl amino sugars in the EPS from *Lactobacillus helveticus* Rosyjski.

In order to try to understand why it was not possible to detect the amino sugar using HPAEC-PAD it was decided to review the methods that are employed for monomer analysis and to study the analysis of monomer compositions, including amino sugars.

### 3.3.1 Monomer Analysis Techniques

As explained in section 1.7.1 monomer composition determination is still a problematic area of analysis in carbohydrate (EPS) characterisation, mainly due to the difficulty in detecting and quantifying amino sugars. Amino sugars, though, are relatively commonly observed monomers in EPS, with *N*-acetylglucosamine and *N*-acetylgalactosamine being reported in a number of EPS from LAB.

The difficulties in the analysis of amino sugars has been overcome to an extent in recent years with the advent of HPAEC-PAD technology, which is now a regularly adopted



technique for monomer analysis, often replacing the laborious and often inaccurate GC-MS technique. Problems still also arise however as sugars are notoriously unstable when heated at high temperatures in the presence of strong acids<sup>123</sup>. The degradation that often occurs due to this procedure frequently leads to the erroneous reporting of the monomeric constituents of EPS. During acid hydrolysis *N*-acetyl amino sugars are deacetylated and subsequently converted to amino sugars, whilst neutral sugars are degraded and converted to aromatic compounds and small acids.

### 3.3.1.2 Acid Catalysts for Hydrolysis

Three main acid catalysts have been commonly employed for the hydrolysis of polysaccharides over the years; these include HCl<sup>159</sup>, H<sub>2</sub>SO<sub>4</sub><sup>160</sup> and TFA<sup>120</sup> (listed in decreasing acidity), also formic acid (formolysis)<sup>161</sup>, has been utilised to a much lesser extent for specific carbohydrates. All of the acids employed for hydrolysis have associated problems. HCl is often considered too harsh for hydrolysis and degrades the liberated monosaccharides<sup>162</sup>. Also this method requires HCl to be removed by lyophilisation, a technique which is particularly time consuming. Great care must also be taken to exclude oxygen from the reaction as its presence can increase monomer decomposition. H<sub>2</sub>SO<sub>4</sub> catalysed hydrolysis, when performed on a micro scale can also present issues as the reaction requires neutralisation (with either barium carbonate or silver carbonate) and then subsequent filtration, techniques which can incur sample losses. TFA is the most commonly used acid for hydrolysis as it is milder in comparison<sup>163</sup> and can be easily removed from the reaction by evaporation under a dry stream of nitrogen. Again, though, as with HCl, care must be taken to purge the reaction vessel of oxygen in order to avoid/reduce possible losses through degradation. Also, as glycosidic links to amino sugars are more difficult to hydrolyse than neutral sugars, TFA analysis can lead to an under-estimation of the quantity of this particular group of sugars<sup>123</sup>. Formolysis, a much less frequently encountered hydrolysis technique, employing dilute formic acid (~90% v/v) has been observed to produce reasonable hydrolysis with minimal degradation. The main problem that arises from

formolysis is that the time for this reaction to occur has been found to be much longer than with any of the other acids. This method is more frequently utilised with methylated polysaccharides, rather than EPS, and can be employed as a pre-hydrolysis technique before further hydrolysis with H<sub>2</sub>SO<sub>4</sub><sup>161</sup>.

### 3.3.1.3 Monomer Analysis Utilising Differing Hydrolysis Techniques

To investigate the monomer composition analysis utilising a variety of acid catalysts a previously characterised EPS with a known composition of monomeric constituents was examined.

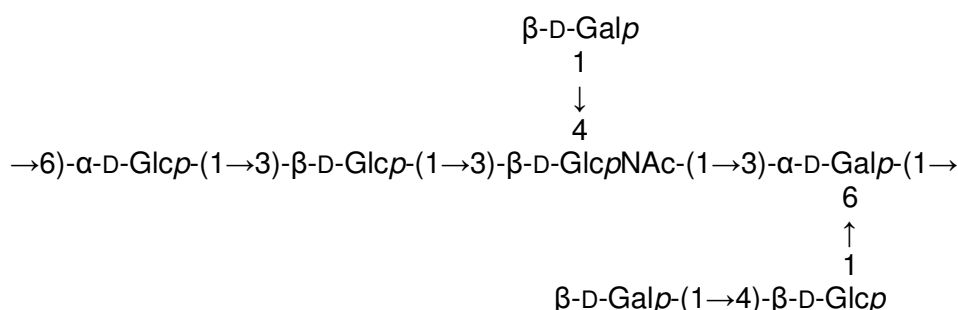


**Figure 30: Line Drawing Structure of EPS produced by *Lactobacillus acidophilus* 5e2**

The EPS produced by *Lactobacillus acidophilus* 5e2 (Figure 30) has previously been fully structurally characterised<sup>131</sup>, the monomer composition analysis provided ratios of 3.1:2.9:0.7 (a whole number ratio of 3:3:1) of D-glucose, D-galactose and *N*-acetyl-D-glucosamine respectively for the heptasaccharide repeating unit. It should be noted that the original analysis utilised the GC-MS detection method employing TFA (2M, 2 Hr).

Each acid hydrolysis reaction was performed as detailed in Chapter 2 (Section 2.3.3.1.1), the resulting peak areas (in  $\mu\text{C}$ ) of the monomers present from the chromatograms were converted to their corrected molar ratios (see Appendix for Standard Curve Data) (Table 3). It should be noted that upon hydrolysis the *N*-acetyl-D-glucosamine moiety liberated from the repeat unit of the EPS is de-*N*-acetylated to produce the monomer glucosamine.

**Table 3: Monomer Ratio Analysis Utilising Differing Hydrolysis Techniques**

Hydrolysis Conditions	Monomer Ratios		
	Glucose	Galactose	<i>N</i> -acetyl-glucosamine*
H <sub>2</sub> SO <sub>4</sub> 0.5M 1Hr	2.60	3.00	1.30
H <sub>2</sub> SO <sub>4</sub> 0.5M 2Hr	2.76	3.00	1.33
H <sub>2</sub> SO <sub>4</sub> 1M 1Hr	2.94	3.00	1.47
H <sub>2</sub> SO <sub>4</sub> 1M 2Hr	3.00	2.98	1.28
HCl 1M 1Hr	1.75	3.00	0.13
HCl 1M 2Hr	3.00	1.58	2.95
HCl 2M 1Hr	3.00	1.74	1.31
HCl 2M 2Hr	2.61	1.77	3.00
TFA 2M 1Hr	3.00	2.82	0.79
TFA 2M 2Hr	3.00	2.46	1.11
TFA 4M 1Hr	3.00	2.86	1.15
TFA 4M 2Hr	3.00	2.38	1.13
Formolysis	2.99	3.00	1.25

\*As glucosamine

Firstly it should be pointed out that glucose and particularly galactose are not being reported at the correct levels in almost all of the hydrolysis conditions analysed. Consequently this will have a bearing on the accuracy of the ratios observed, even when corrected with the standard curve data obtained for the response factors for each monomer.

The second point to be identified from Table 3 is that HCl, as expected, is (at the concentrations examined) too harsh to be utilised as an acid hydrolysis catalyst for glycosidic bond cleavage. The monomer ratios observed reflected the harshness of the procedure and were greatly distorted from those expected (3:3:1), extra peaks, attributed to monomer degradation were also detected in the chromatograms.

Results obtained from the H<sub>2</sub>SO<sub>4</sub> and formolysis analysis, however, established a very comparable collection of results to those obtained previously, especially for the neutral sugars (glucose and galactose). Despite these techniques portraying comparable results for the neutral sugars the data collected for the amino sugar (glucosamine) demonstrated a high monomeric proportion. Although, as previously explained, this may be due to the degradation of the glucose and galactose monomers.

The results attained for the reactions with TFA also produced monomer ratios which were similar to the actual, previously documented values. Additionally the amount of amino sugar was determined to be more in accordance with the actual corrected whole number ratio of total monomers than with any of the other acid catalyst techniques employed.

The monomeric ratio data determined here provides reasoning as to why TFA, in combination with HPAEC-PAD analysis is now the most commonly applied method for carbohydrate (polysaccharide) monomer qualification and quantification. HCl is too harsh and the removal of the acid is time consuming. Whilst H<sub>2</sub>SO<sub>4</sub> and formolysis demonstrated highly comparable monomer ratios, consequent issues with micro-scale analysis and long reaction times respectively, signify they are a less favourable option to that of TFA analysis. Importantly, it should be recognised that for the EPS studied here, which contains *N*-acetylglucosamine, there are no problems observing the amino sugar present.

It should be noted that at the University of Huddersfield, Mr. Mohammed Maqsood had previously provided GC-MS results that supported the presence of *N*-acetylmannosamine in the EPS from *Lactobacillus helveticus* Rosyjski. Further work was then undertaken to see if, under the preferred monomer hydrolysis conditions, *N*-acetylmannosamine could be observed (see later discussion).

### 3.3.2 Linkage Analysis Techniques

As explained in section 1.7.2 the way in which one monomer of an EPS repeating unit structure is linked to another is determined by comparing the mass spectra fragmentation

'fingerprint' pattern obtained from partially *O*-methylated alditol acetates (PMAAs) to a collection of literature standards<sup>123</sup>. The mass spectral data alone however can only offer a certain degree of elucidation as the fragmentation pattern cannot differentiate between epimeric monomers such as glucose, galactose and mannose. A further indication of the hexose present can be obtained from the time taken for them to elute from the GC column, but for this to be feasible it is necessary to generate linkage standards.

### 3.3.2.1 Development of Linkage Standards

Generally compounds employed as standards for linkage analysis of EPS are created from free sugars or methyl glycosides<sup>164</sup> that are sequentially per-*O*-methylated and subsequently converted to their alditol acetate form for GC-MS analysis<sup>165,166</sup>. Developing standards from free sugars can be unpredictable though, mainly due to the limited control over the methylation procedure employed in the first step of the method. This can cause a wide range of products which are methylated to differing degrees (mono-, di-, tri- or tetra-methyl).

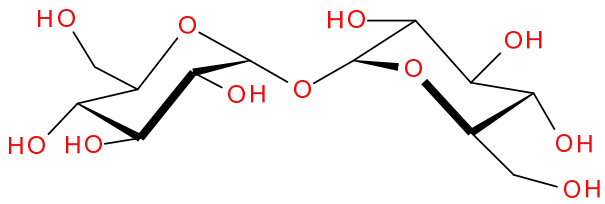
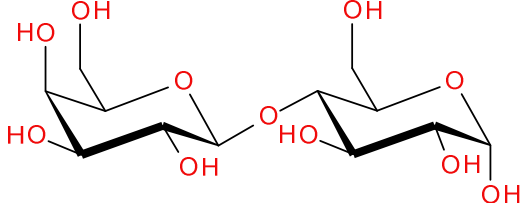
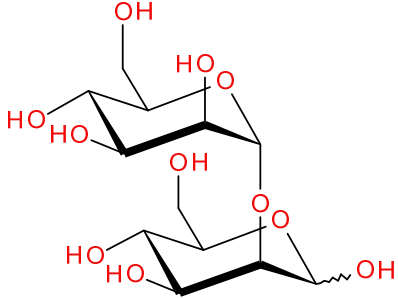
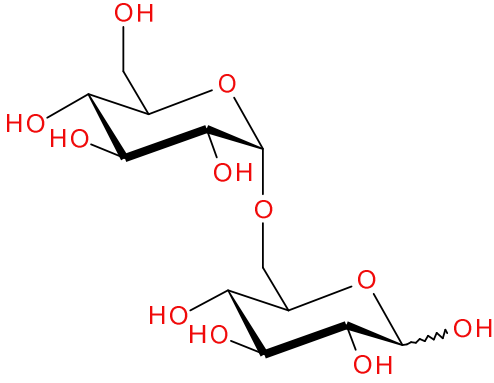
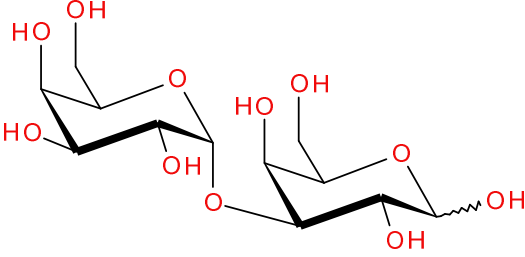
It is also possible however to create a number of useful linkage standards from common disaccharide sugars. Depending on the monomeric composition and linkage present between the monosaccharide constituents, either one or two model compounds are created by the conversion of disaccharides to their corresponding PMAAs.

### 3.3.2.2 Disaccharide Derived PMAA Linkage Compounds

Five disaccharides were chosen to be studied for the development of model linkage standard compounds, the structure of the native disaccharides along with their names are given in Table 4.

The PMAA analysis was performed using the method described in Chapter 2. The resulting reaction products were subjected to GC-MS analysis following the column oven temperature program detailed in Chapter 2. The linkage standards created were identified from data provided in recognised literature<sup>123</sup>, taking into consideration not only the ions present in the MS fragmentation spectra but also the abundance ratios of the fragments observed.

**Table 4: Disaccharide Sugars studied for Model Compounds for Linkage Analysis**

Structural Name	Structure
<p>Trehalose</p> <p><math>\alpha</math>-D-Glucopyranosyl-(1<math>\rightarrow</math>1)-<math>\alpha</math>-D-glucopyranoside</p>	
<p>Lactose</p> <p><math>\beta</math>-D-Galactopyranosyl-(1<math>\rightarrow</math>4)-<math>\alpha</math>-D-glucopyranose</p>	
<p>2-<math>\alpha</math>-Mannobiose</p> <p><math>\alpha</math>-D-Mannopyranosyl-(1<math>\rightarrow</math>2)-D-mannopyranose</p>	
<p>Gentiobiose</p> <p><math>\alpha</math>-D-Glucopyranosyl-(1<math>\rightarrow</math>6)-D-glucopyranose</p>	
<p>3-<math>\alpha</math>-Galactobiose</p> <p><math>\alpha</math>-D-Galactopyranosyl-(1<math>\rightarrow</math>3)-D-galactopyranose</p>	

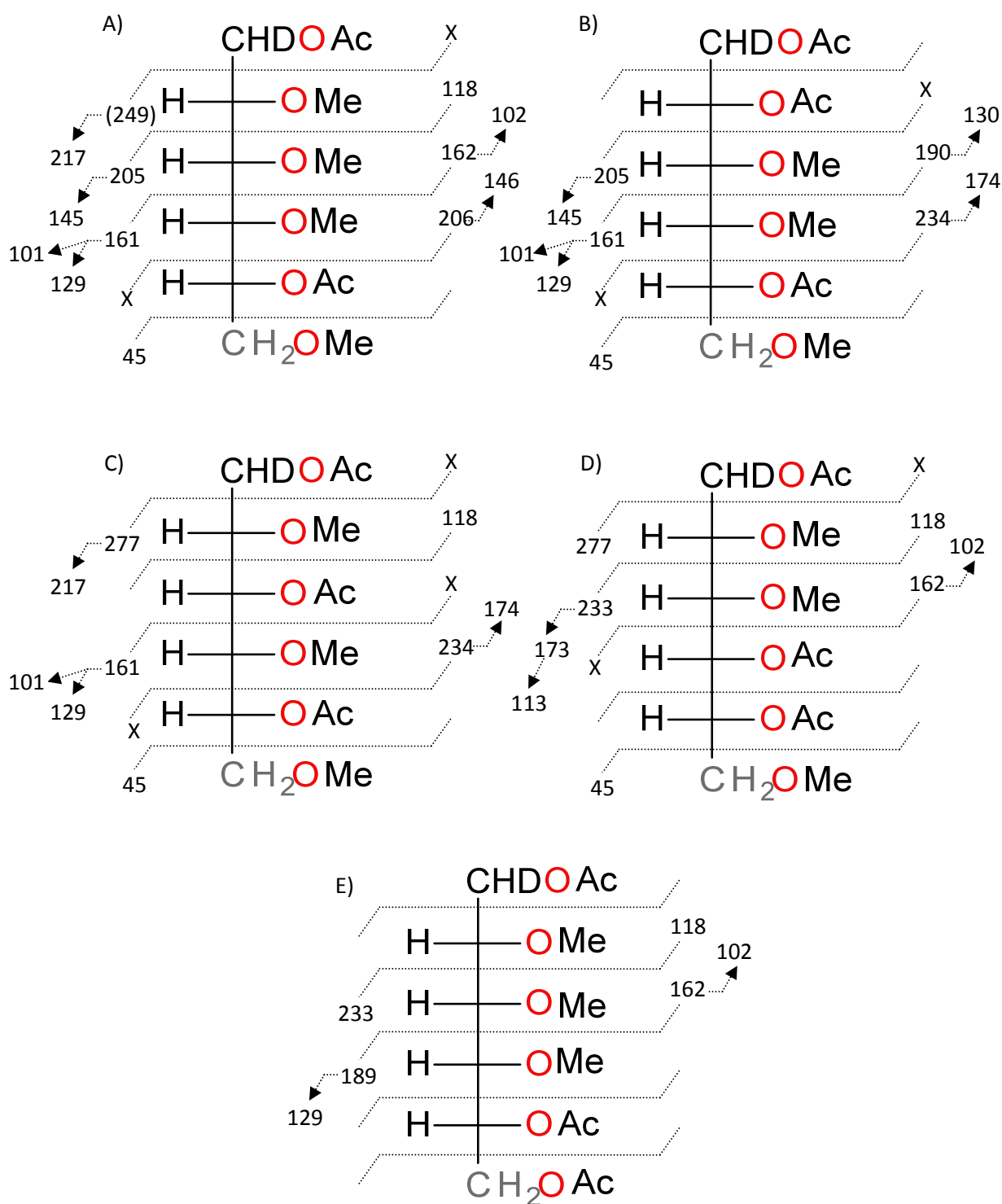


**Figure 31: MS Fragmentation for PMAA Linkage Standards – A) Terminal Glucose/Galactose/Mannose; B) 1-2 Linked Mannose; C) 1-3 Linked Galactose; D) 1-4 Linked Glucose; E) 1-6 Linked Glucose**

### 3.2.2.3 Analysis of Model Linkage Standards

As trehalose is a non-reducing sugar, and as a result of its symmetry, its PMAA synthesis resulted in one peak being observed in the GC-MS chromatogram at 8.627 minutes. Upon interpretation of the mass spectrometry data for the fragmentation linkage standards (Figure 31) it was determined that the compound produced was 1,5-di-*O*-acetyl-(1-deuterio)-2,3,4,6-tetra-*O*-methyl glucitol, alternatively known as a terminally linked glucose moiety (T-Glucose).

The reaction of lactose generated two peaks in the GC-MS chromatogram at 9.216 and 11.875 minutes. Peak one was identified as 1,5-di-*O*-acetyl-(1-deuterio)-2,3,4,6-tetra-*O*-methyl galactitol (T-Galactose) whilst peak two was determined to be 1,4,5-tri-*O*-acetyl-(1-deuterio)-2,3,6-tri-*O*-methyl glucitol, alternatively denoted as a 1→4 linked glucose moiety (1-4 Glucose).

The preparation of linkage standards from the disaccharide 2- $\alpha$ -mannobiose produced two peaks in the GC-MS chromatogram at 8.515 and 11.190 minutes. Peak one was identified as 1,5-di-*O*-acetyl-(1-deuterio)-2,3,4,6-tetra-*O*-methyl mannitol (T-Mannose) whilst peak two was determined to be 1,2,5-tri-*O*-acetyl-(1-deuterio)-3,4,6-tri-*O*-methyl mannitol, also labelled as a 1→2 linked mannose moiety (1-2 Mannose).

The synthesis of gentiobiose generated two peaks in the GC-MS chromatogram at 8.483 and 12.272 minutes. Peak one was identified as 1,5-di-*O*-acetyl-(1-deuterio)-2,3,4,6-tetra-*O*-methyl glucitol (T-Glucose) whilst peak two was determined to be 1,5,6-tri-*O*-acetyl-(1-deuterio)-2,3,4-tri-*O*-methyl glucitol, alternatively denoted as a 1→6 linked glucose moiety (1-6 Glucose).

The preparation of linkage standards from the disaccharide 3- $\alpha$ -galactobiose produced two peaks in the GC-MS chromatogram at 9.060 and 11.193 minutes. Peak one was identified as 1,5-di-*O*-acetyl-(1-deuterio)-2,3,4,6-tetra-*O*-methyl galactitol (T-Galactose) whilst peak



two was determined to be 1,3,5-tri-*O*-acetyl-(1-deuterio)-2,4,6-tri-*O*-methyl galactitol, also labelled as a 1→3 linked galactose moiety (1-3 Galactose).

The standard linkage model compounds synthesised provide an assortment of terminally linked and doubly linked monomers and allowed for the retention times in gas chromatography of these specific hexoses to be determined. The compounds generated can be utilised as comparative models for the structural characterisation of EPS (see discussion that follows).

### **3.3 Structural Characterisation**

This section will focus on the structural characterisation of the EPS isolated from the fermentation of *Lactobacillus helveticus* Rosyjski through the use of NMR along with monomer and linkage analysis using both GC-MS and HPAEC-PAD.

#### *3.3.1 Structural Analysis Using NMR*

In order to determine the structure of the oligosaccharide repeating unit of the EPS produced by *Lactobacillus helveticus* Rosyjski a series of 1D- and 2D- NMR experiments were carried out.

From the initial observation (see Section 3.2.2.1) of the  $^1\text{H}$  NMR spectra (Figure 26) five anomeric proton signals have been identified and labelled **A-E**. Signal **A** appears as a resolved doublet whilst anomeric protons **B** and **C** are single peaks, with **D** and **E** appearing as overlapping doublets. From the chemical shift and the  $^3J_{1,2}$  coupling constant the anomeric configuration of signal **A** can be labelled as possessing  $\alpha$ -anomeric configuration as the coupling constant is below 7 Hz<sup>167</sup> (see Appendix). The anomeric configurations for signals **B-E** were determined using a coupled HMQC experiment. As the values for signals **B**, **D** and **E** were all observed to be over lower than 170 Hz<sup>145</sup> it was determined that the monomers were all of  $\beta$ -anomeric configuration, whilst monosaccharide **C** was observed to be present in the  $\alpha$ -anomeric configuration (see Appendix).

**Table 5: Anomeric Proton Chemical Shifts and  $^3J_{1,2}$  and  $^1J_{H-C}$  Coupling Constants**

Monosaccharide	Chemical Shift (ppm)	$^1J_{H-C}$ and $^3J_{1,2}$ * Coupling Constants (Hz)	Configuration
<b>A</b>	5.45	172 , 3.65*	$\alpha$
<b>B</b>	5.11	166	$\beta$
<b>C</b>	5.03	177	$\alpha$
<b>D</b>	4.67	157	$\beta$
<b>E</b>	4.67	164	$\beta$

Along with the anomeric signals, the spectra also contains peaks corresponding to the ring protons which are located between 3.3 – 4.5 ppm, whilst examination of the higher field region of the  $^1H$  NMR spectrum resulted in the identification of a signal at 2.06 ppm. The position of this signal is commonly associated with the presence of a  $CH_3$  moiety and can normally be attributed to the occurrence of an *N*-acetyl sugar monomer.

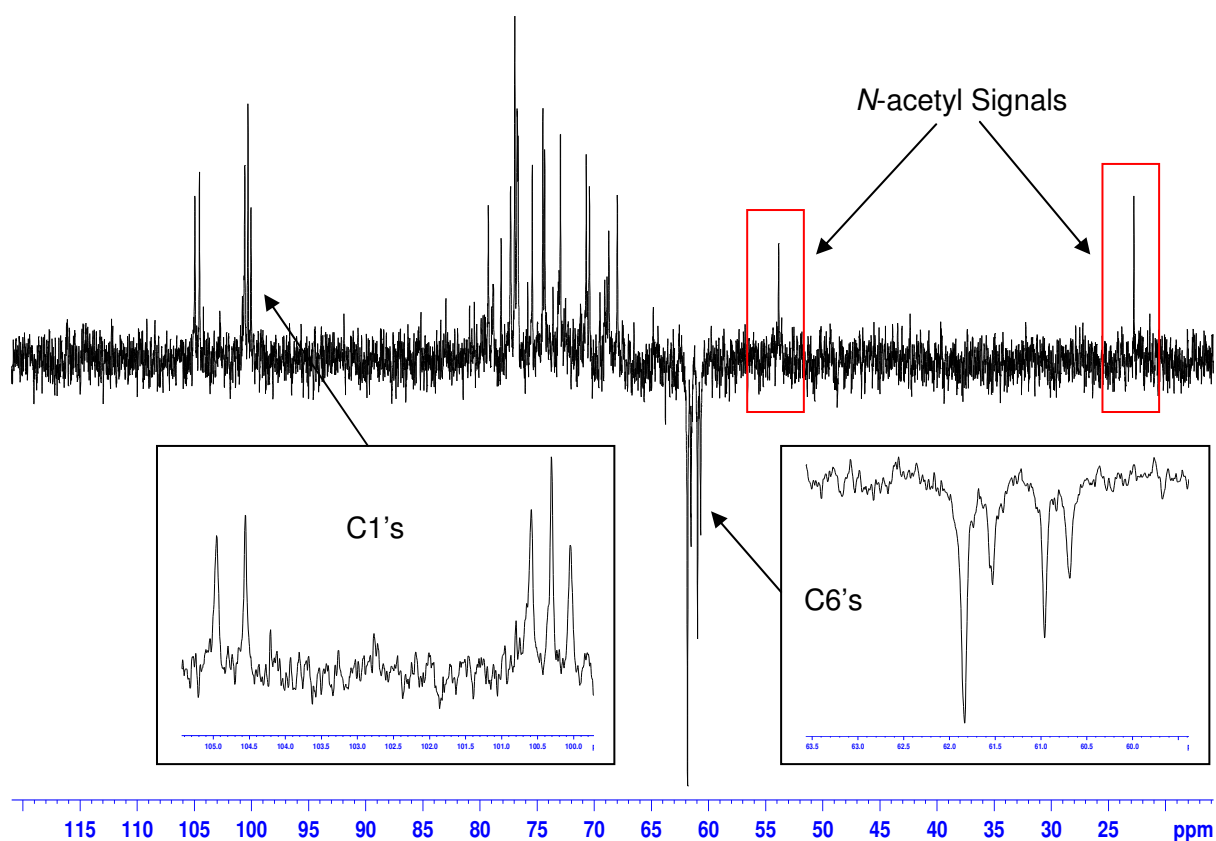


**Figure 32: DEPT 135  $^{13}\text{C}$  NMR Spectrum of *Lactobacillus helveticus* Rosvijski (Main) Magnified Region showing Anomeric C1's (Inset Bottom Left) Magnified Region showing C6's (Inset Bottom Right)**

The DEPT 135  $^{13}\text{C}$  spectrum (Figure 32) shows positive peaks for CHs and  $\text{CH}_3$ s and negative peaks for  $\text{CH}_2$ s. Upon observing the spectrum several areas of interest can be immediately identified: anomeric carbon signals are located above 90 ppm as they appear shifted downfield compared to the ring proton signals (65 – 80 ppm), due to the presence of their neighbouring oxygen atom; there are 4 peaks located between 60 – 65 ppm that can be identified as  $\text{CH}_2$ s (from C6s). It should be stated that 5 peaks are expected to be observed (in accordance with the 5 anomeric signals previously identified) in this region of the spectrum. It is therefore suspected that the largest peak, located furthest up field of the C6s, consists of 2 overlapping signals. As previously eluded to in the interpretation of the  $^1\text{H}$  NMR spectrum, the identification of the presence of an *N*-acetyl sugar monomer is further confirmed by the 135 DEPT  $^{13}\text{C}$  spectrum. The signal located at 22.78 ppm is characteristic of the presence of a  $\text{CH}_3$  moiety (from an *N*-acetyl) whilst the signal at 53.86 ppm is also

associated with the existence of an *N*-acetyl monomer representing the carbon atom (C2) of the sugar<sup>131,168</sup>.

It should be noted that, in later batches, there is some evidence for the presence of an additional sugar; some EPS have reported labile monomers (linked via ester or pyruvate moieties) which can be lost during the isolation procedure<sup>169</sup>. This may account for the movement of the signal for **B2** (See Figures 26 and 27).

Structural elucidation of the oligosaccharide repeating unit of the EPS was performed by a series of 2D-NMR experiments. Initially the COSY (H, H) experiment was performed, this experiment showed protons attached to the adjacent carbon (linked by scalar coupling), the <sup>1</sup>H chemical shifts along both frequency axes are therefore correlated with each other.

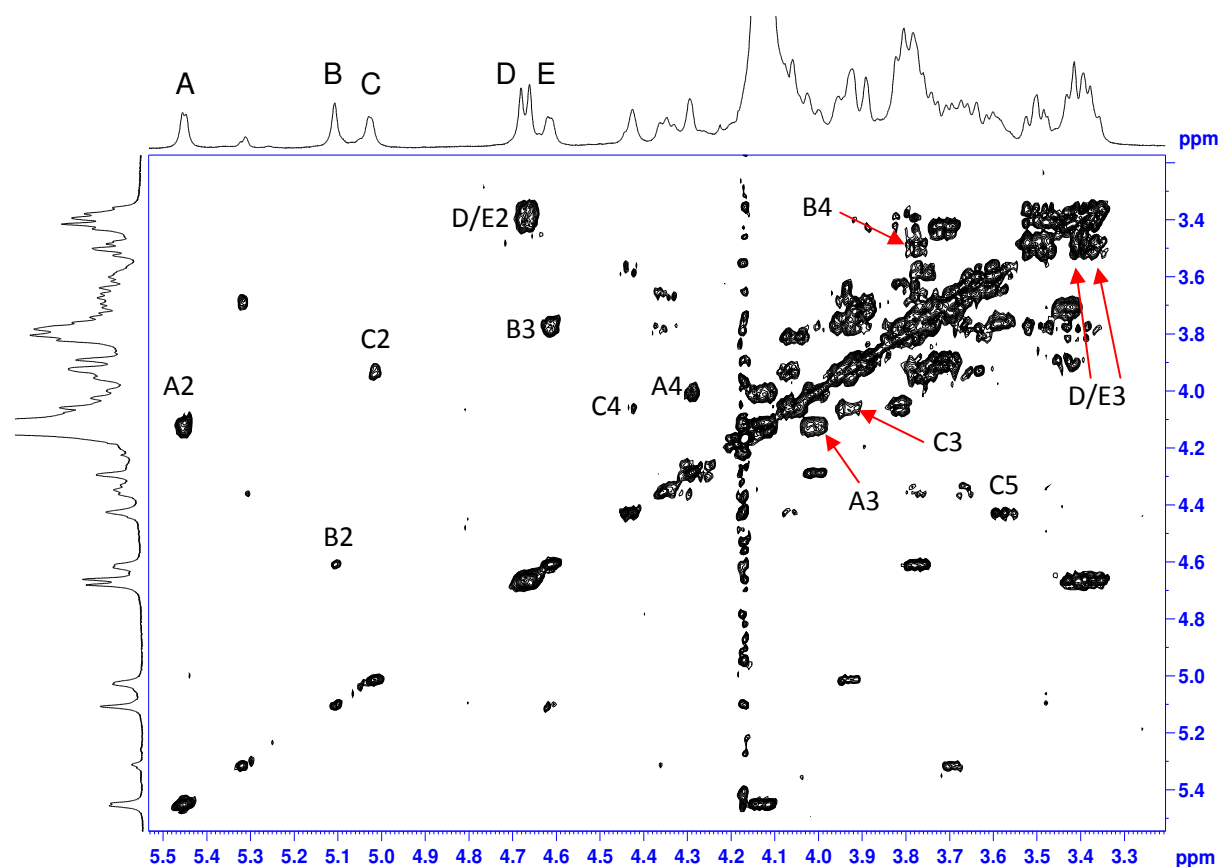


**Figure 33: COSY Spectrum of EPS from *Lactobacillus helveticus* Rosyjski**

Initially beginning with the knowledge of the anomeric protons, the COSY spectrum (Figure 33) firstly allows for the H2 signals on the adjacent carbon to be established. Following the

interconnected diagonal cross peaks a number of protons around the ring can be determined. Protons H2 – H4 can be identified for monosaccharides **A** and **B**, whilst for monosaccharide **C** protons H2 – H5 can be assigned and for monomers **D** and **E**, due to the presence of overlapping protons, only H2 – H3 signals can be confidently identified.

Another important spectrum to be examined for identifying which protons belong to which monosaccharide ring is the TOCSY spectrum (Figure 34). By selectively exciting the resonance of a single proton in the sample this experiment allows for the detection of all of the protons in the same coupled spin system. The “range” within the molecule for detecting a correlation is critically dependent on the length of the mixing time during which the spin-lock is applied<sup>170</sup>.

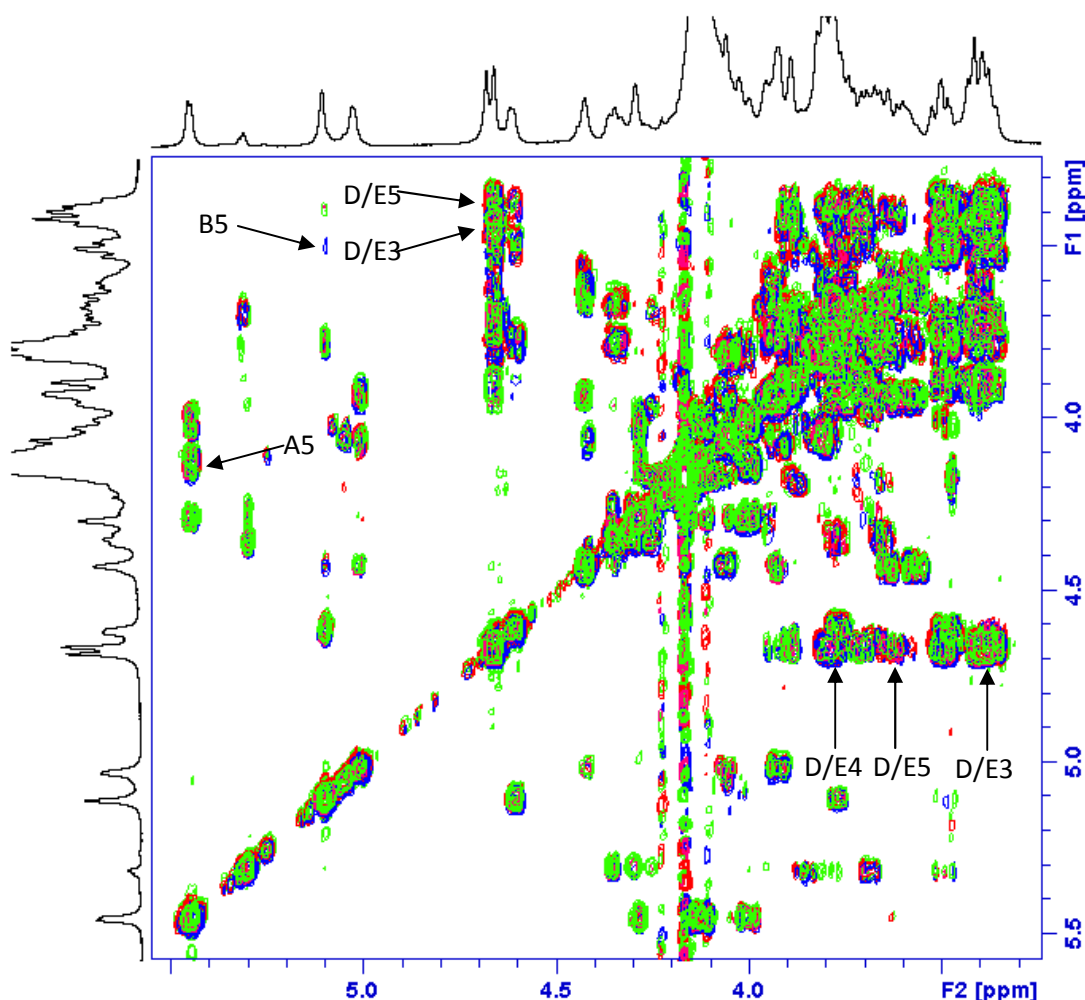


**Figure 34: TOCSY Spectra of EPS from *Lactobacillus helveticus* Rosyiski**

By overlaying spectra from TOCSY experiments subjected to different mixing times (30 – 210 ms) it is possible to view not only the short range coupling (usually due to the proton on the adjacent carbon), but also peaks of lesser intensities become visible; which are usually due to the protons on the next but one carbon.

The H2 – H5 protons can be identified for all monosaccharides **A** – **E**. Again, due to the appearance of several overlapping peaks, primarily for **D** and **E**, identification of the remaining ring protons was achieved in conjunction with the analysis and comparison of several spectra including a  $^1\text{H}$ – $^{13}\text{C}$  HMBC spectrum (Figure 37), a  $^1\text{H}$ – $^{13}\text{C}$  HSQC (Figures 35 and 36) spectrum and a HSQC–TOCSY spectrum (Figure 34).

**Table 6:  $^1\text{H}$  NMR Chemical Shifts of EPS Recorded in  $\text{D}_2\text{O}$  at 70 °C**

Monosaccharide	$^1\text{H}$ Chemical Shift (ppm)						
	H1	H2	H3	H4	H5	H6	H6'
<b>A</b>	5.45	4.18	4.01	4.30	4.07	3.81*	3.81*
<b>B</b>	5.11	4.62	3.77	3.51	3.90	3.79*	3.79*
<b>C</b>	5.03	3.93	4.07	4.43	3.50	3.73*	3.93*
<b>D</b>	4.67	3.36	3.59	3.78	3.62	3.73*	3.93*
<b>E</b>	4.67	3.40	3.41	3.41	4.35	3.73*	3.93*

\*Represents partially overlapping H6 and H6' resonances

Analysing the values assigned to the H4 chemical shifts of each of the monosaccharides, the designation of whether each sugar is a D-glucose or a D-galactose monomer can be achieved. The H4 resonance for D-galactose, regardless of either anomeric configuration or the presence of any linkages to the molecule, is downshifted in comparison to that of a D-glucose monomer. Generally H4 resonances for D-glucose occur between 3.75 – 3.46 ppm whilst H4 resonances for D-galactose occur between 4.26 – 3.83 ppm<sup>171</sup>. **D** and **E** can therefore be designated as D-glucose monomers whilst monomers **A** and **C** can be

confirmed as D-galactose. The identification of monosaccharide **B** will be determined in Section 3.3.2 using a combination of these results and chromatographic methods.

With the complete assignment of the proton signals for monosaccharides **A** – **E** (Table 6) the correlating carbons are designated by inspection of the  $^1\text{H}$ - $^{13}\text{C}$  HSQC experiment (Figures 35 and 36). This spectrum contains a cross peak for each unique proton attached to the coupled  $^{13}\text{C}$ .

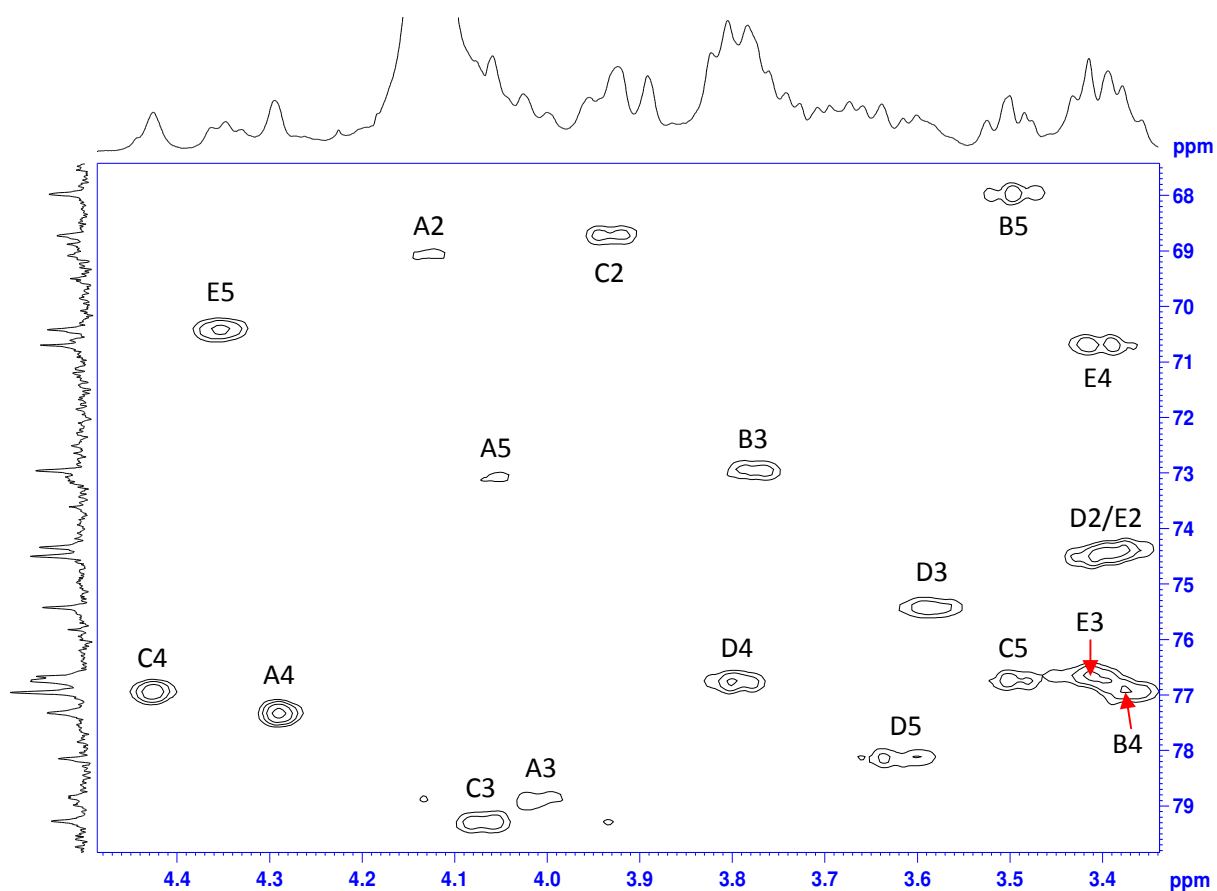


**Figure 35:  $^1\text{H}$ - $^{13}\text{C}$  HSQC Spectrum of EPS from *Lactobacillus helveticus* Rosyjski**

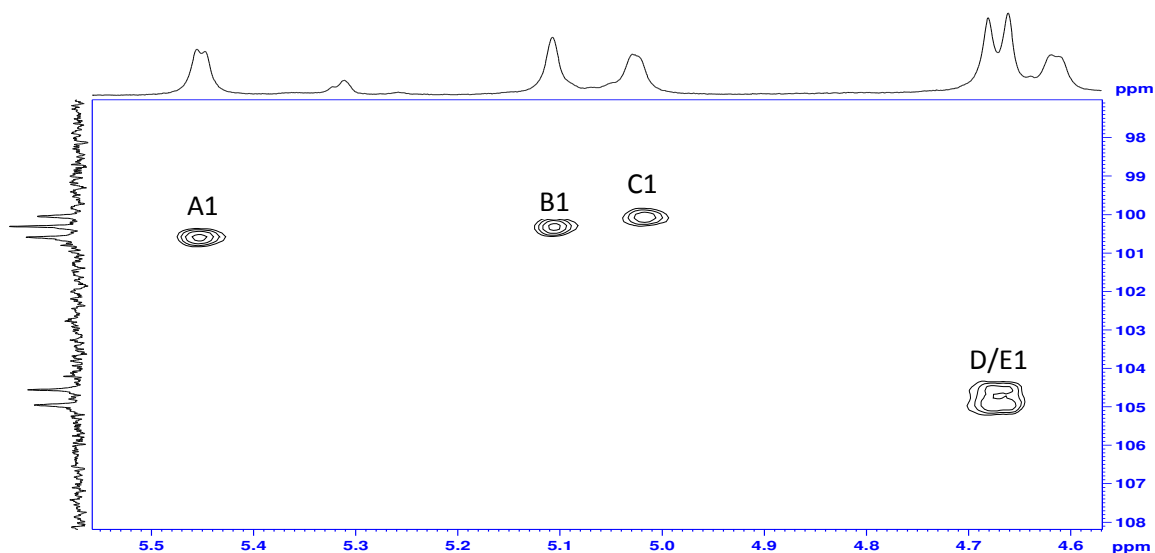


**Figure 36:  $^1\text{H}$ - $^{13}\text{C}$  HSQC Spectrum Anomeric Region of EPS from *Lactobacillus helveticus* Rosyjski**

As can be observed from both figures 35 and 36, all the anomeric and ring carbons have been assigned. As was stated earlier, C2 for sugar **B** (highlighted in Figure 32) is shifted to 53.86 ppm and is therefore not observed in Figure 35. The  $^{13}\text{C}$  chemical shifts are given in Table 7.

**Table 7:  $^{13}\text{C}$  NMR Chemical Shifts of EPS Recorded in  $\text{D}_2\text{O}$  at 70  $^\circ\text{C}$**

Monosaccharide	$^{13}\text{C}$ Chemical Shift (ppm)					
	C1	C2	C3	C4	C5	C6
<b>A</b>	100.62	69.03	78.86	77.32	73.08	60.97
<b>B</b>	100.32	53.86	72.95	76.95	67.96	61.52
<b>C</b>	100.07	68.73	79.27	76.95	75.42	61.84
<b>D</b>	104.56	74.34	76.71	76.75	78.15	61.84
<b>E</b>	104.97	74.50	76.71	70.67	70.67	61.84

\*Highlighted values indicate linkages

The position of the C4 atom is used as an indicator for the determination of whether sugar residues are present in either the furanose (5-membered ring) – C4 above 81 ppm or



pyranose (6-membered ring) form – C4 below 81 ppm<sup>172</sup>. The chemical shifts indicate that all the monosaccharides are present in the pyranose form.

In order to establish the way in which the sugar residues are connected to form the 5 monomer repeating unit, a combination of  $^1\text{H}$ - $^{13}\text{C}$  HMBC and 2D- $^1\text{H}$ - $^1\text{H}$  ROESY are used for sequence determination. The  $^1\text{H}$ - $^{13}\text{C}$  HMBC experiment focuses on long range coupling between protons and carbons two or three bonds away, allowing for the observation of both intra and inter-molecular coupling through the glycosidic bond (from one sugar residue to another).

The  $^1\text{H}$ - $^{13}\text{C}$  HMBC spectra (Figure 37) shows the intra-residue couplings highlighted in red with the inter-residue couplings highlighted in yellow.

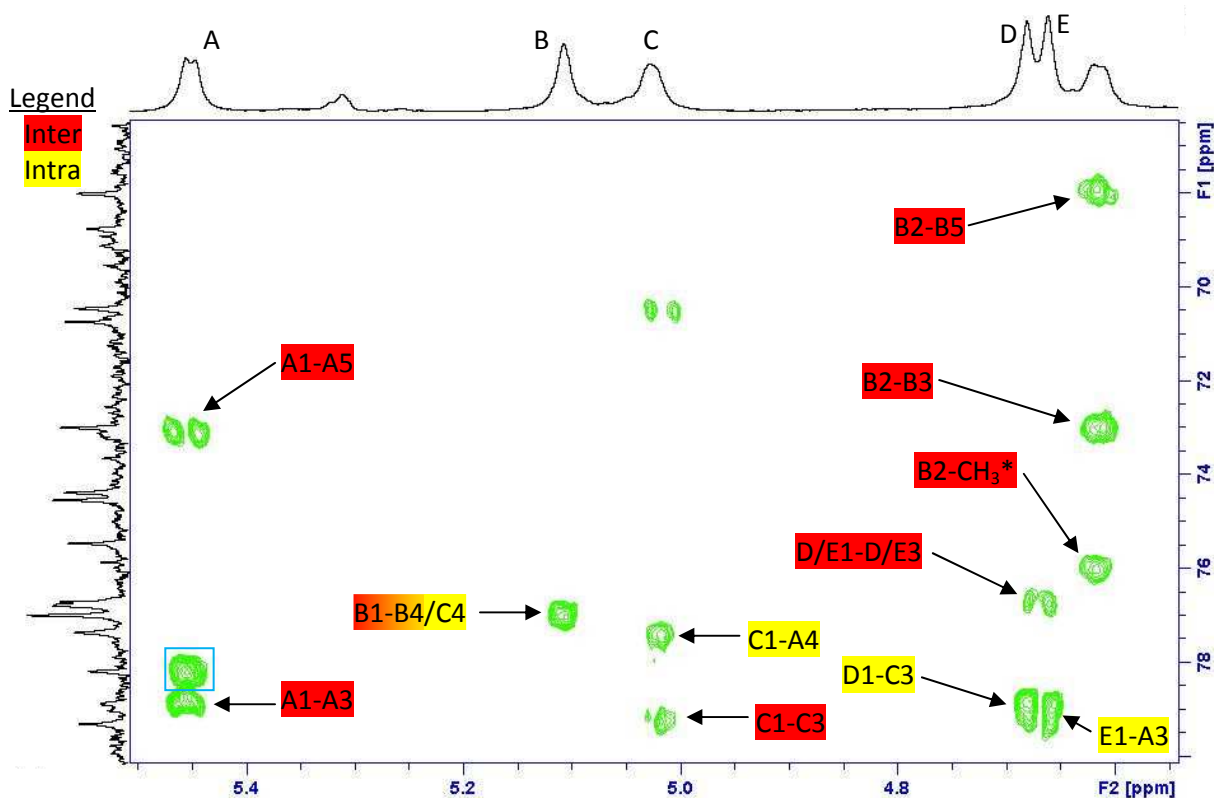


**Figure 37:  $^1\text{H}$ - $^{13}\text{C}$  HMBC Spectra of EPS from *Lactobacillus helveticus* Rosyjski**

The spectra identifies inter-residue cross peaks from coupling between **C** H1 and **A** C4 confirming an **A (1→4) C** linkage; **D** H1 and **C** C3 confirming a **D (1→3) C** linkage and lastly

an inter-residue cross peak is observed between **E** H1 and **A** C3 confirming a **E (1→3) A** linkage. Possibly, also observed is an inter-residue cross peak indicating a linkage between **B (1→4) C**, although this cannot be confidently confirmed as C4 of both monomers **B** and **C** are overlapping. A number of intra-residue couplings are also visible.

To complete the structural conformation, leading to the elucidation of the sequence in which the monosaccharides are linked to form the repeating unit oligosaccharide, a final 2D-NMR experiment was consulted, a  $^1\text{H}$ - $^1\text{H}$  ROESY spectrum. The  $^1\text{H}$ - $^1\text{H}$  ROESY experiment again provides information on both the intra-residue and inter-residue coupling in the molecule. This experiment however provides information on the coupling of proton nuclei in close spatial proximity (distance smaller than 5Å) rather than coupling through bonds<sup>7</sup>.

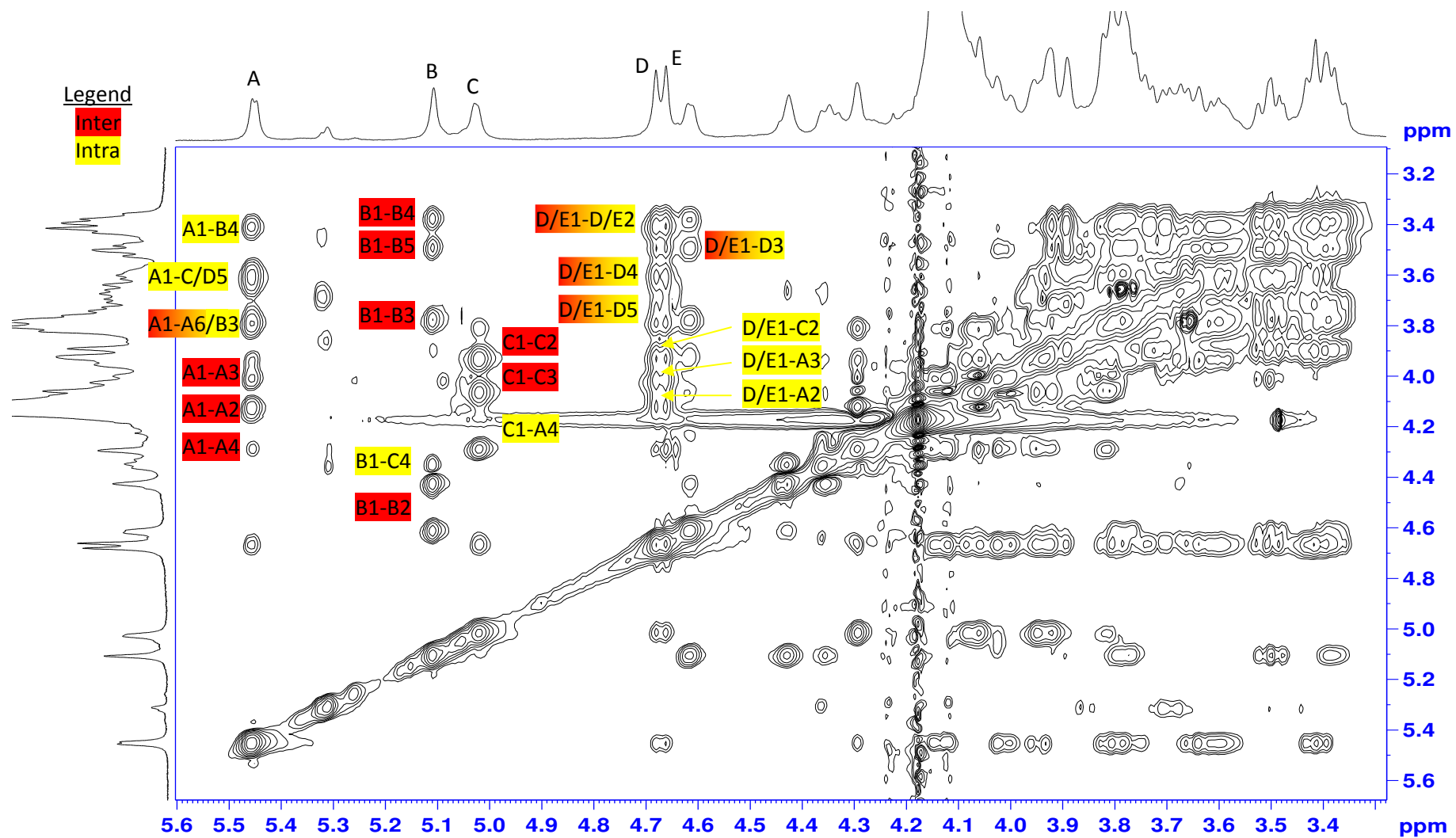


**Figure 38:  $2D\text{-}^1\text{H}\text{-}^1\text{H}$  ROESY Spectrum of EPS from *Lactobacillus helveticus* Rosvjski**

The  $^1\text{H}$ - $^1\text{H}$  ROESY spectra (Figure 38) shows the intra-residue NOEs highlighted in red with the inter-residue NOEs highlighted in yellow. NOE cross peaks are observed between **A** H1 and **B** H4 confirming the **A** (1→4) **B** linkage previously inferred from the  $^1\text{H}$ - $^{13}\text{C}$  HMBC interpretation. Inter-residue cross peaks are also observed between **B** H1 and **C** H4 and between **C** H1 and **A** H4 confirming the linkages **B** (1→4) **C** and **C** (1→4) **A** respectively. Again, as with the  $^1\text{H}$ - $^{13}\text{C}$  HMBC spectra a number of intra-residue couplings are also visible.

### 3.3.2 Structural Analysis using GC-MS and HPAEC-PAD

In order to corroborate the compositional and structural information obtained about the oligosaccharide repeating unit structure from the NMR interpretation, monomer and linkage analysis were performed.

#### 3.3.2.1 Monomer Analysis

Firstly, the identification of the monomers comprising the repeating unit of the EPS was performed by the conversion of the monomer components to alditol acetates using the methods<sup>120,121</sup> described in Chapter 2. The resulting reaction products were then subjected to GC-MS analysis using the column oven temperature program listed in Chapter 2.

The chromatogram obtained (see Appendix) displayed three distinct peaks at 12.796, 13.088 and 20.757 minutes, as has previously been reported by Mr. Mohammed Maqsood *et al* (unpublished results) (2007). The mass spectrometry fragmentation patterns generated by each peak were subsequently analysed. The fragmentation observed for peaks 1 and 2 (12.796 and 13.088 minutes) displayed near identical MS fragmentation, characteristic with the presence of aldohexoses such as glucose (Figure 39A), galactose or mannose in the sugar alditol acetate form. The fragmentation of peak 3 (20.757 minutes) was found to be characteristic of belonging to an amino sugar such as glucosamine, galactosamine or mannosamine (Figure 39B) in the sugar alditol acetate form. A series of alditol acetate standards (see earlier discussion) with known retention times were run in order to determine

which sugar monomer gave rise to which particular peak in the chromatogram. It was resolved that peak 1 at 12.796 minutes was confirmed as glucose whilst peak 2 at 13.088 minutes was confirmed as galactose. Peak 3 at 20.757 minutes was denoted as arising from the presence of mannosamine.

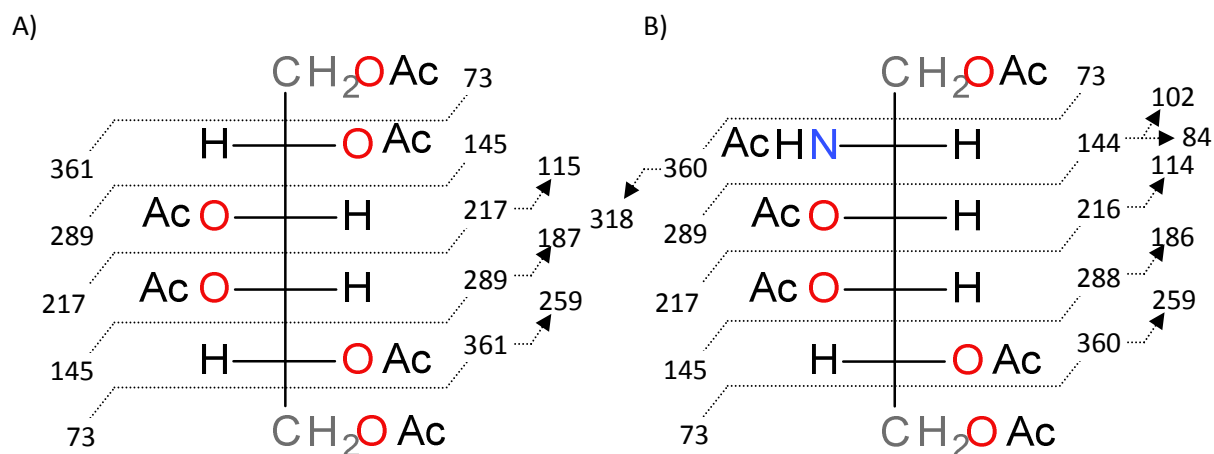


**Figure 39: MS Fragmentation for Sugar Alditol Acetate Monomers of A) Glucose and B) Mannosamine**

Unfortunately, the ratios of monomers observed by GC-MS analysis (Glu 3, Gal 2.98, Mann 0.23) were not as anticipated. As previously stated, amino sugars are difficult to quantify when analysed by GC-MS analysis.

Monomer analysis using HPAEC-PAD is frequently utilised as an alternative option to the GC-MS method of detection. HPAEC-PAD is often used as it involves a simple, quick and efficient one step acid hydrolysis procedure as described previously in this chapter.

As the monomers give different responses upon their interaction with the PAD in the HPAEC system (dependent of the pK<sub>a</sub> of the sugars), standard curves were obtained for the three sugars present in order to correct the overall ratios of sugar monomers present in the EPS (see Appendix).

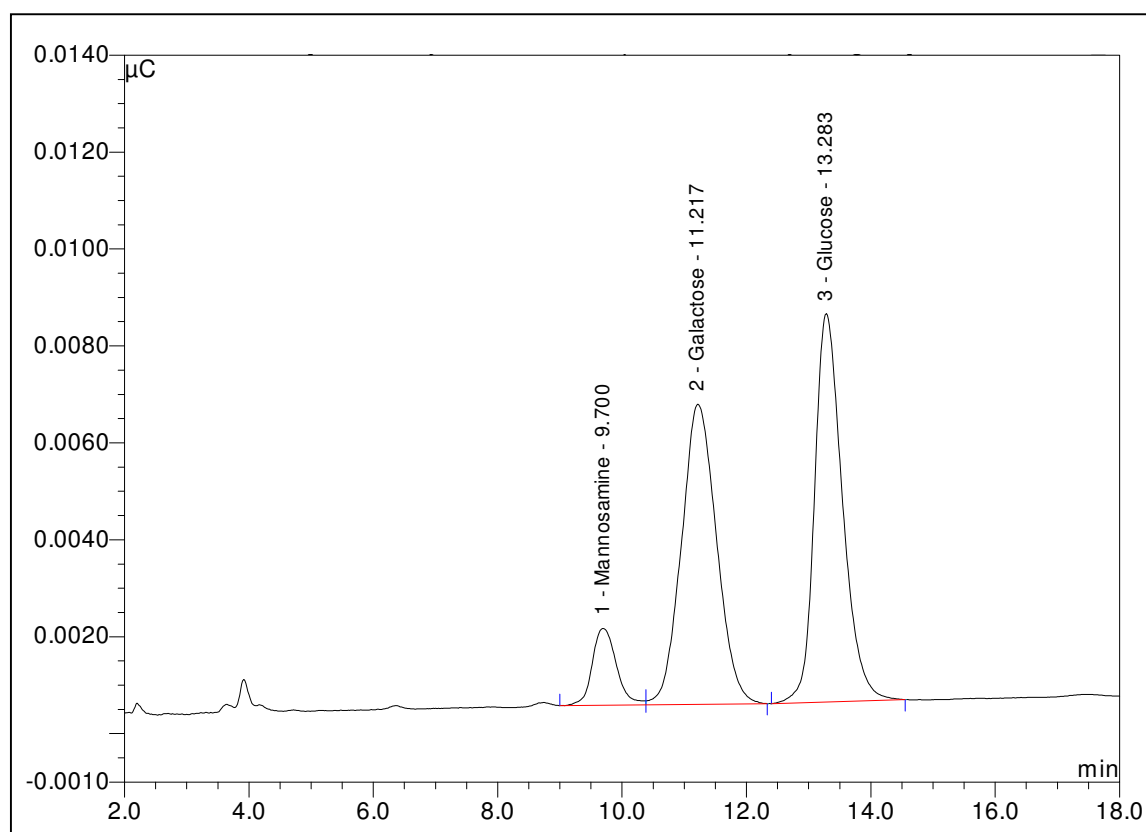


**Figure 40: HPAEC-PAD Chromatogram of EPS from *Lactobacillus helveticus* Rosyjski Monomers**

The identities of the 3 peaks observed in the HPAEC-PAD chromatogram (Figure 40) were determined by spiking of the sample with standard compounds. Peak one was identified as mannosamine, whilst peaks 2 and 3 were identified as galactose and glucose respectively. The corrected molar ratio of the sugars monomer was found to be 2.19:2:1.45 for galactose, glucose and mannosamine respectively. It should be noted that mannosamine is over represented. However, it is not clear why this should be the case; one possible explanation is that the sodium hydroxide concentration used for the development of the standard curves was not identical to that employed in the analysis of the Rosyjski monomers.

### 3.3.2.2 Linkage Analysis

The results of the  $^1\text{H}$ - $^1\text{H}$  ROESY spectrum coupled with the information gained from the  $^1\text{H}$ - $^{13}\text{C}$  HMBC spectrum indicated a number of linked sugar residues. In order to further confirm the presence of the previously identified linkages between monomers and determine the

structure of the oligosaccharide repeat unit structure, linkage analysis (of alditol acetates) was performed by GC-MS<sup>138</sup>.

Analysis of the linkage data (see Appendix) identified several peaks which, when coupled with the corresponding mass spectra (Figure 41 A – D), were confirmed as matching the linkages previously recognized by NMR interpretation.

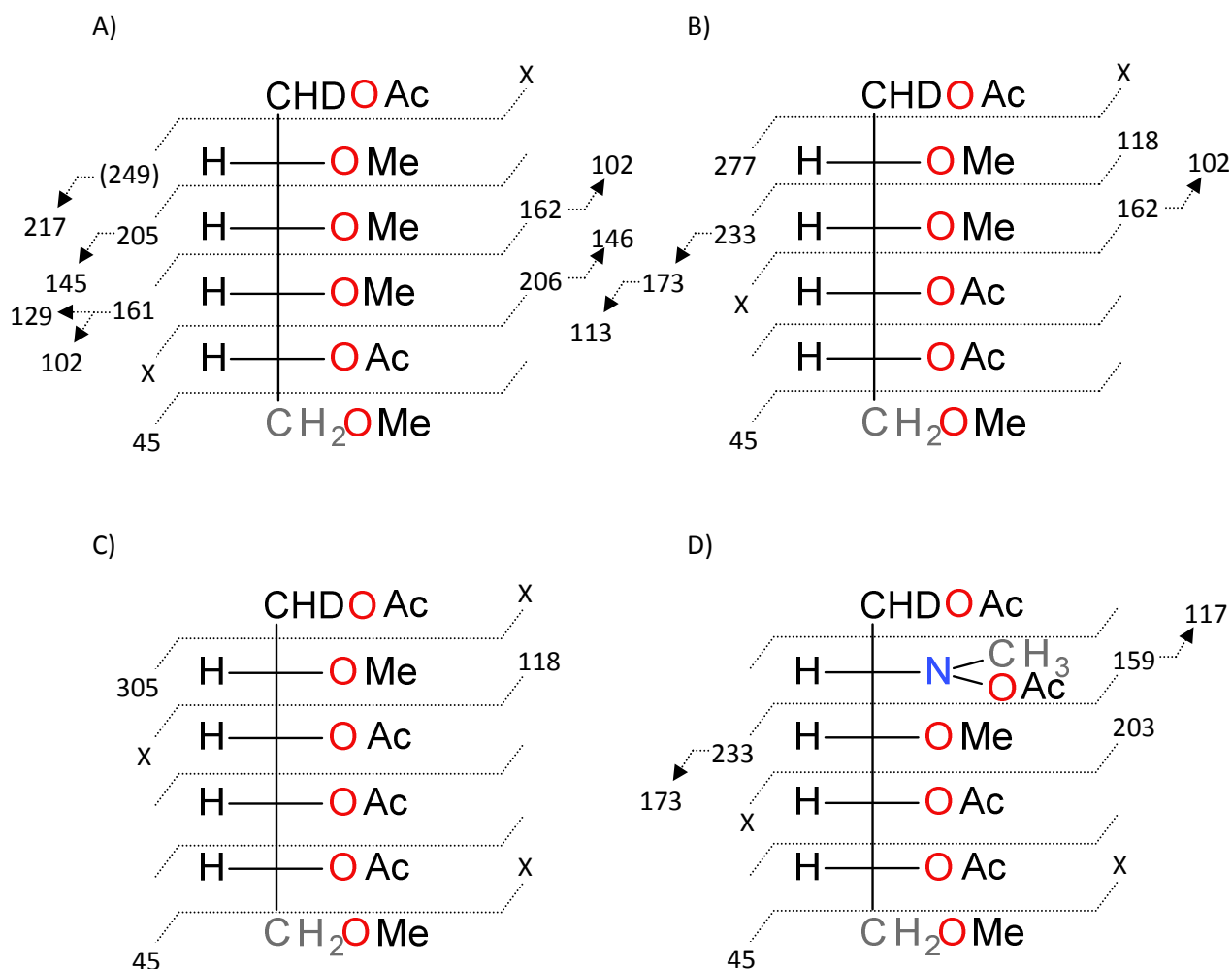


**Figure 41: Mass Spectra Fragmentation A) Terminal Glucose/Galactose; B) 1-4 Linked Glucose/Galactose; C) 1, 3, 4 Linked Glucose/Galactose; D) 1-4 Linked *N*-acetylmannosamine**

The linked monomers were identified from data provided in the literature<sup>123</sup>, taking into consideration not only the ions present in the MS fragmentation spectra but also the abundance ratios of the fragments observed.

Peaks 1 and 2 was identified as 1, 5-di-*O*-acetyl-(1-deuterio)-2, 3, 4, 6-tetra-*O*-methyl hexitol (terminally linked glucose/galactose); this was confirmed by the presence of the characteristic *m/z* peaks 102, 118, 129, 145, 161, 162 and 205. Peak 3 was identified as 1, 4, 5-tri-*O*-acetyl-(1-deuterio)-2, 3, 6-tri-*O*-methyl hexitol (1-4 linked glucose/galactose); this was confirmed by the presence of *m/z* peaks 102, 113, 118, 162, 173, 203 and 233. Peak 4 was identified as 1, 3, 4, 5-tetra-*O*-acetyl-(1-deuterio)-2, 6-*O*-methyl hexitol (1, 3, 4 linked glucose/galactose); this was confirmed by the presence of *m/z* peaks 118 and 205. Peak 5 was identified as 1, 4, 5-tri-*O*-acetyl-(1-deuterio)-(2-*N*-methylacetamide)-3, 6-di-*O*-methyl hexitol (1-4 linked *N*-acetylmannosamine); this was confirmed by the presence of *m/z* peaks 117, 159, 173, 203 and 233.

The specific identities of peaks 1, 2 and 3 were confirmed by the spiking of the linkage sample with disaccharide standards prepared in Section 3.3.2.2, the sample was firstly spiked with lactose ( $\beta$ -D-Galactopyranosyl-(1 $\rightarrow$ 4)- $\alpha$ -D-glucopyranose) and then secondly with trehalose ( $\alpha$ -D-Glucopyranosyl-(1 $\rightarrow$ 1)- $\alpha$ -D-glucopyranoside). Upon the addition of the acetylated lactose standard a distinct increase was observed in the abundance of peaks 2 and 3. This evidence therefore enabled peak 2 to be assigned as a terminally linked galactose whilst peak 3 was confirmed as emanating from the presence of a 1-4 linked glucose monomer. When spiked with trehalose the Rosyjski linkage sample demonstrated an increased abundance for peak 1, therefore confirming the presence of a terminally linked glucose monomer.

### 3.3.3 Absolute Configuration

Absolute configuration analysis was performed by Mr. Yucheng Gu at the University of Huddersfield. Galactose and glucose were both confirmed as having D- absolute configuration. No standard was available for comparison of the *N*-acetylmannosamine moiety.





The anomeric proton on each sugar residue is highlighted in blue. The backbone of the pentasaccharide repeating unit structure consists of three monosaccharides; two D-galactoses and one *N*-acetylmannosamine. The main chain contains two branched side chains comprised of two glucose units, each 1→3 linked to the backbone. It should be noted that the sugar *N*-acetylmannosamine has never before been identified as being present in an LAB exopolysaccharide. The proposed structure presented is a novel EPS.

### **3.4 Future Work**

Future work could potentially include the synthesis of a wider range of standard alditol acetate compounds from di- and possibly trisaccharides to be utilised for GC-MS linkage analysis. Creating an extensive library of partially-*O*-methylated alditol acetates would allow for the rapid, efficient and reliable identification of the way in which monomers of an EPS repeating unit are linked together.

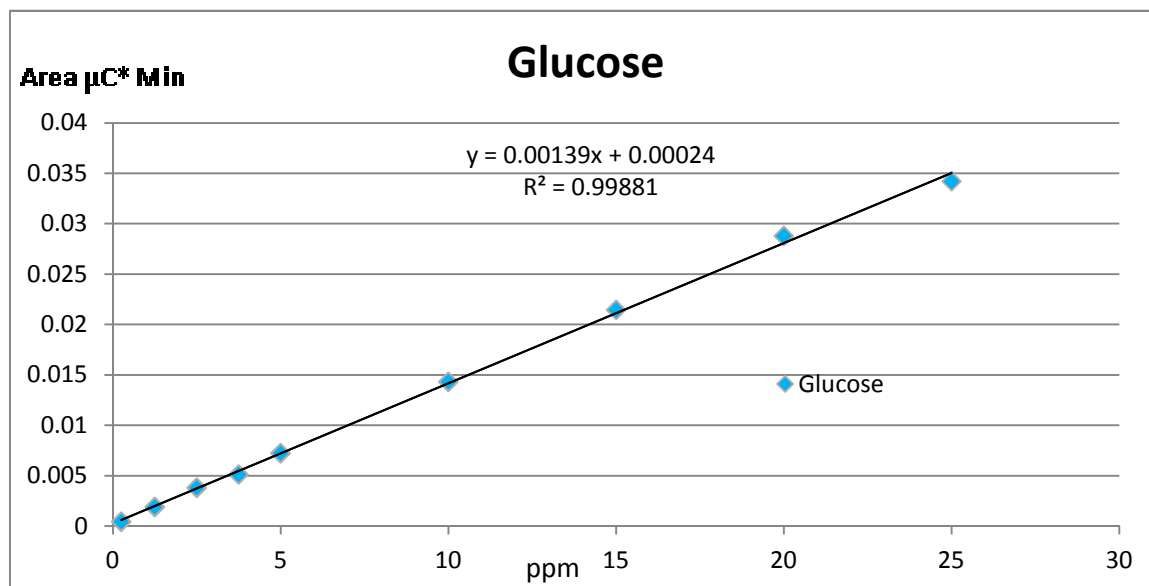
Further work could be carried out with the EPS produced by *Lactobacillus helveticus* Rosyjski to address the discrepancies observed in the NMRs between some batches of the EPS (as discussed in sections 3.2.2.1 and 3.3.1). This may be investigated in a number of different ways.

The fermentation procedure could potentially be extensively explored, examining the protocol of the initial fermentation along with the EPS extraction technique. The fermentation could also be strictly monitored over a set period of time, with portions of the media being removed at regular intervals to analyse whether there is a change in either the molecular weight of the EPS or in the composition of the repeating unit structure over time. This process has previously been explored by Laws *et al* with the EPS produced by *Lactobacillus acidophilus* 5e2<sup>11</sup>. Scrutinising the EPS production and isolation could possibly identify the cause of the inconsistency constantly observed from one isolated batch of EPS to another. Using alternative techniques in the isolation procedure, such as incorporating the use of Pronase and DNase instead of using TCA could also be investigated.

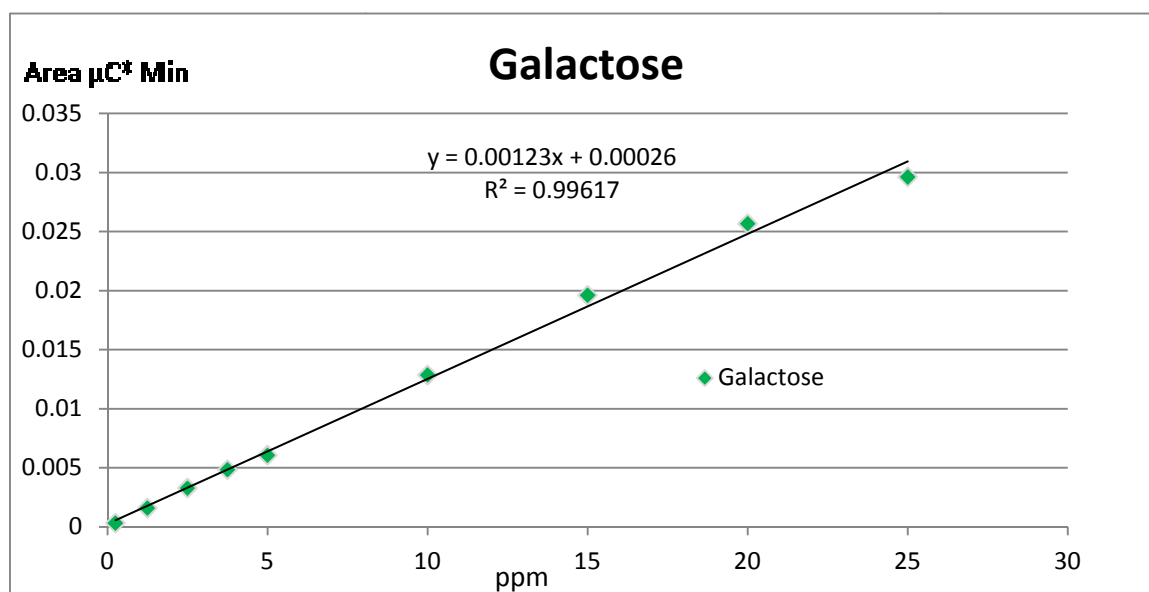
### 3.5 Appendices

#### 3.5.1 HPAEC-PAD Monomer Standard Curves

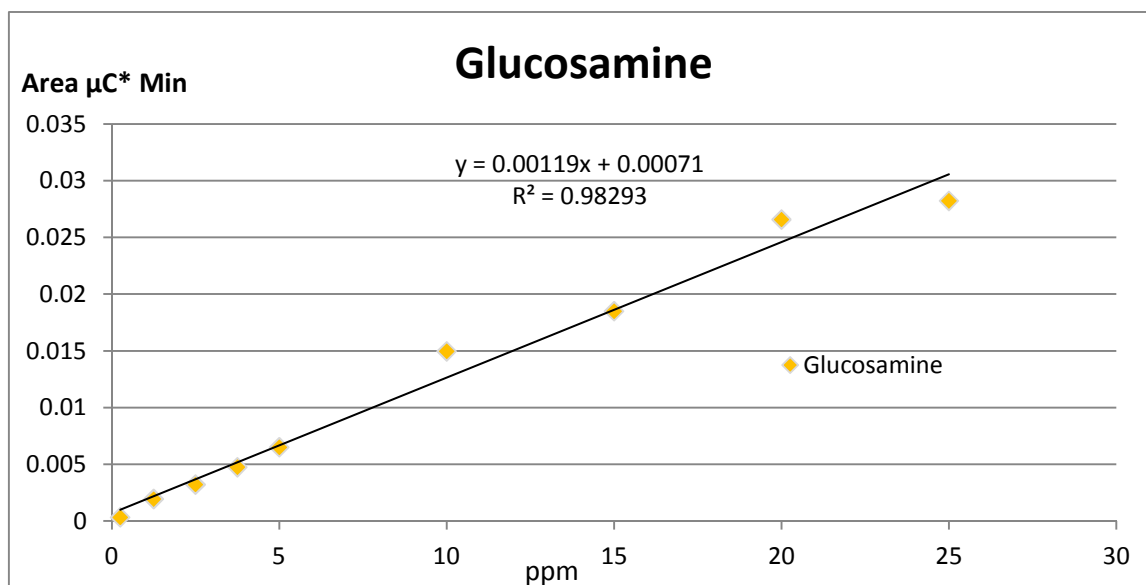
##### 3.5.1.1 Glucose



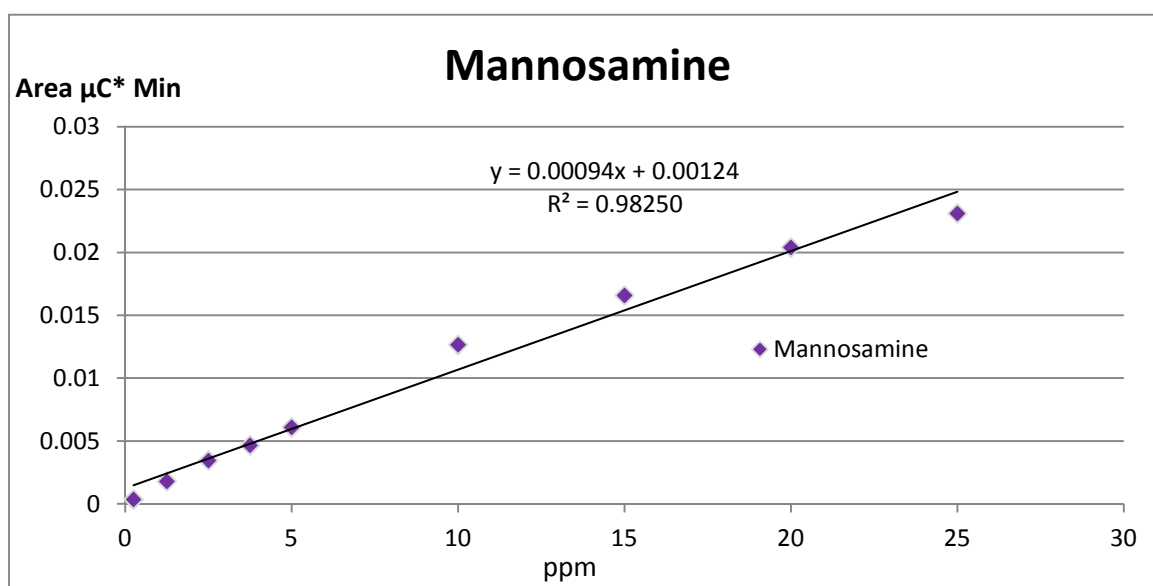
##### 3.5.1.2 Galactose



## 3.5.1.3 Glucosamine

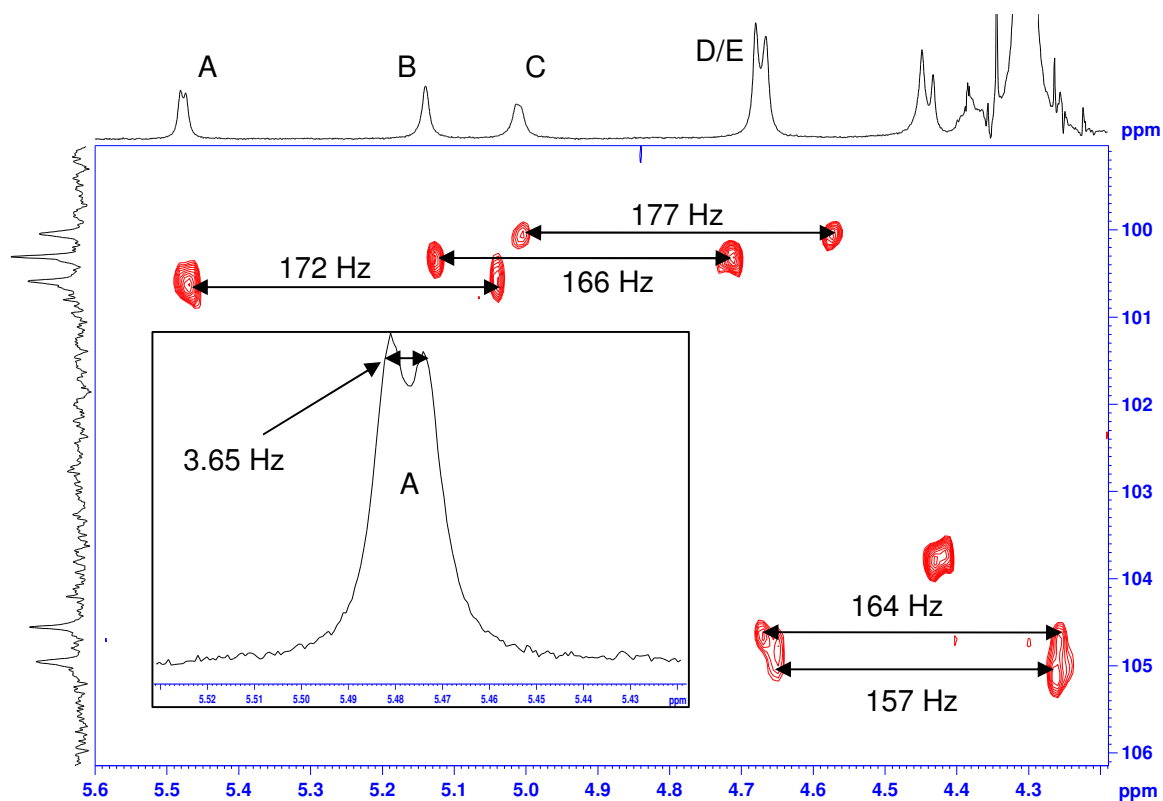


## 3.5.1.4 Mannosamine



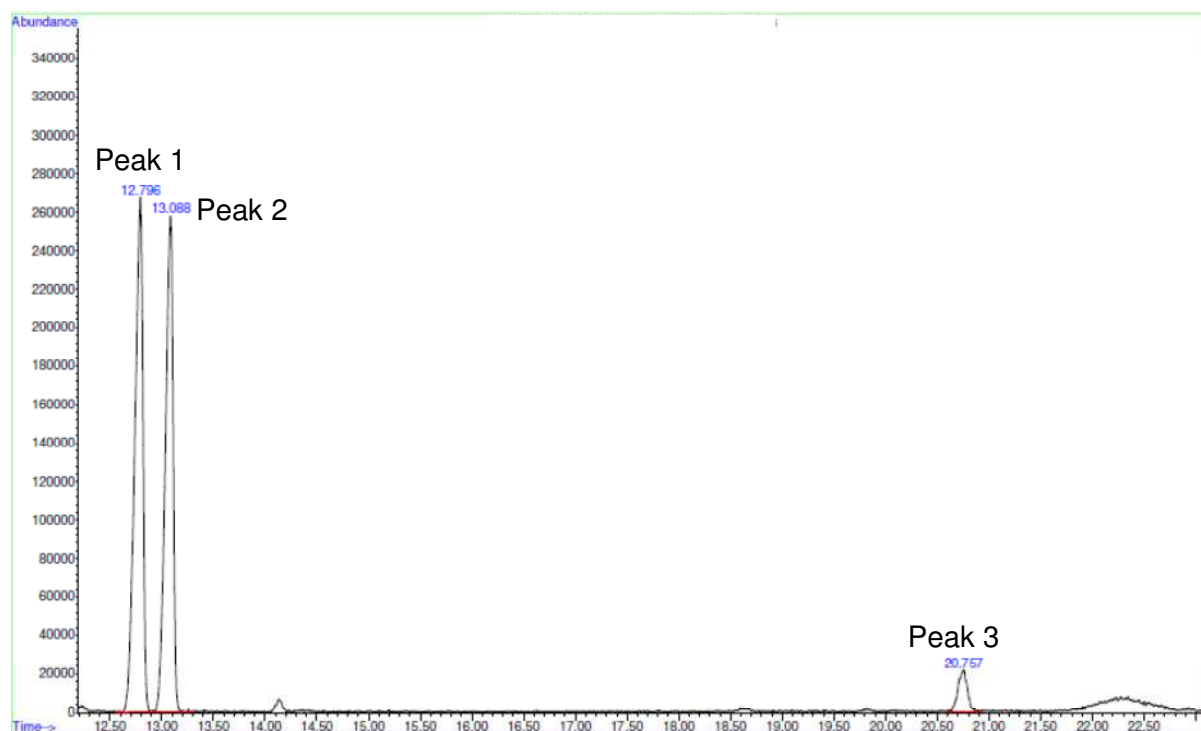
### 3.5.2 Anomeric Configuration Determination

#### 3.5.2.1 Coupled HMQC NMR Spectrum of EPS from *Lactobacillus helveticus* Rosyjski; Inset – Expanded $^1\text{H}$ NMR spectrum showing Anomeric Proton A



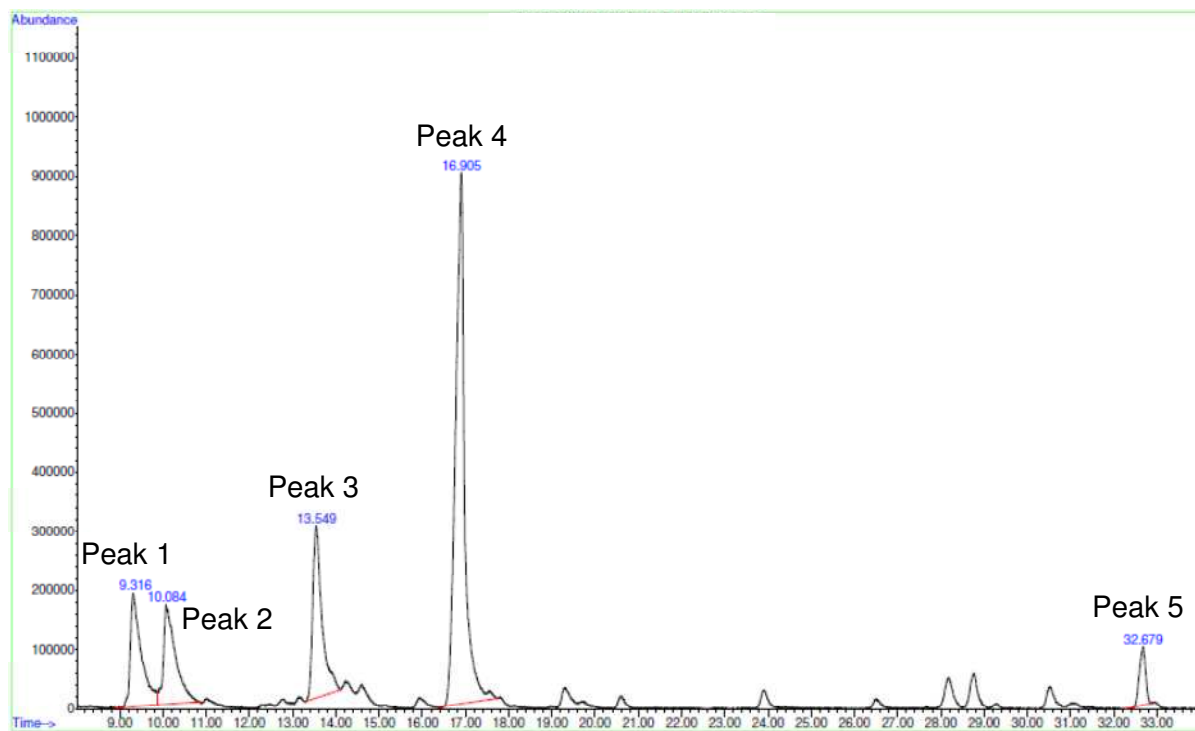
### 3.5.3 GC-MS Monomer Analysis

#### 3.5.3.1 GC-MS Chromatogram of Rosyjski Monomers



### 3.5.4 GC-MS Linkage Analysis

#### 3.5.4.1 GC-MS Chromatogram of Rosyjski EPS Linkages



## 4. Structural Characterisation of the Novel EPS from *Bifidobacterium animalis* subsp. *lactis* IPLA-R1 (A1dOxR)

### 4.1 Introduction

This chapter will discuss the characterisation of an exopolysaccharide produced by the bacteria *Bifidobacterium animalis* subsp. *lactis*. More specifically the bile-adapted derivative A1dOxR strain; created by the progressive adaption of the parental A1 strain of the bacteria to increasing concentrations of bile salts<sup>173</sup>. Another bile-adapted derivative strain was also isolated (A1dOx) from the parental A1 strain but neither of these two strains conferred the ropy phenotype as seen with A1dOxR<sup>174</sup>.

### 4.2 Isolation and Preparation of A1dOxR

This section will be concerned with the isolation and preparation of EPS from the crude fermentation broth of *Bifidobacterium animalis* subsp. *lactis* A1dOxR through the use of two differing dialysis techniques. The EPS was characterised using 1D-NMR experiments along with weight-average molecular weight determinations using MALLS.

#### 4.2.1 *Analysis of Crude Sample*

Initially, the crude A1dOxR polysaccharide was subjected to 1D-<sup>1</sup>H NMR analysis. This spectrum showed signals for all of the protons present in the repeating unit of the EPS (Figure 44).

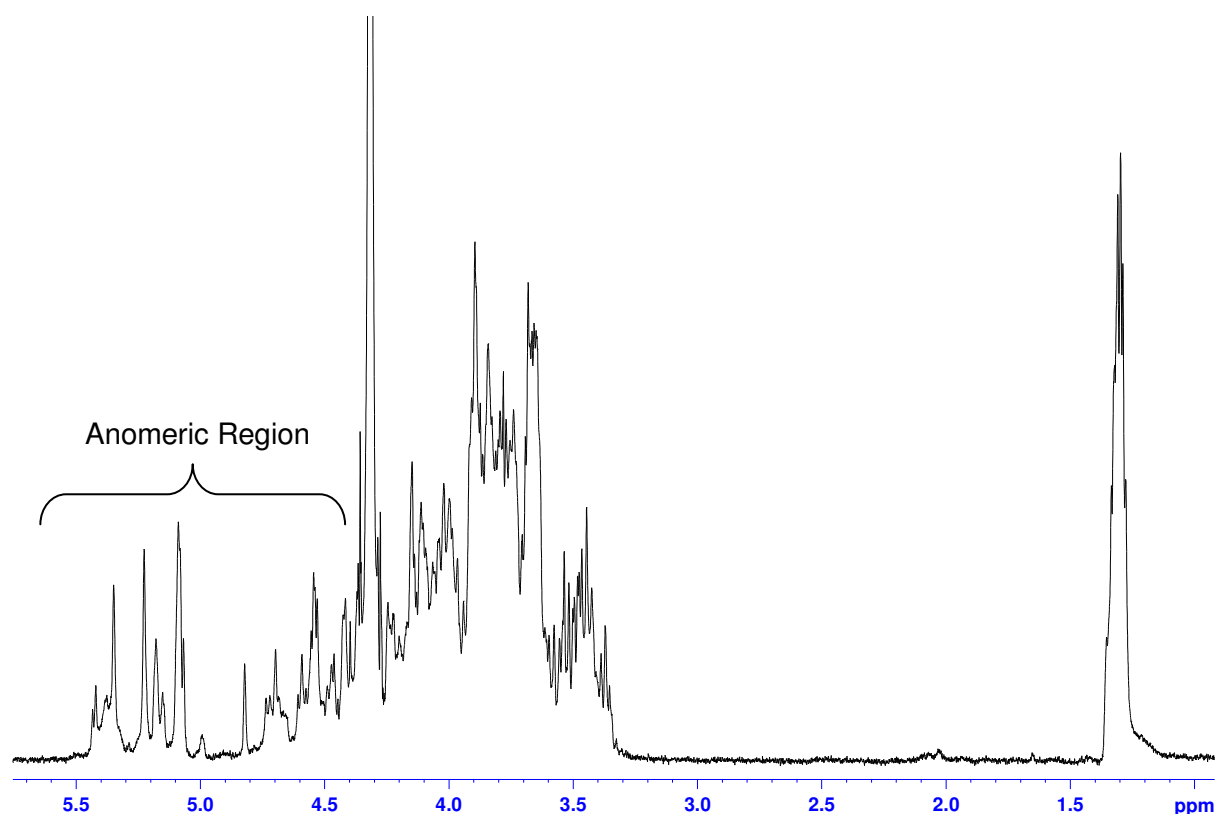


**Figure 44: <sup>1</sup>H NMR Spectrum of Crude EPS from *Bifidobacterium animalis* subsp. *lactis* A1dOxR in D<sub>2</sub>O at 70°C**

Although, when the anomeric region (4.7 – 5.6 ppm) was more closely inspected it could be observed that a number of the proton signals were both highly complex and overlapping. After inspection of the integrals for the anomeric protons it became clear that the crude sample was comprised of more than one regular repeating unit structure (Figure 45), with different integral heights being observed for different protons.

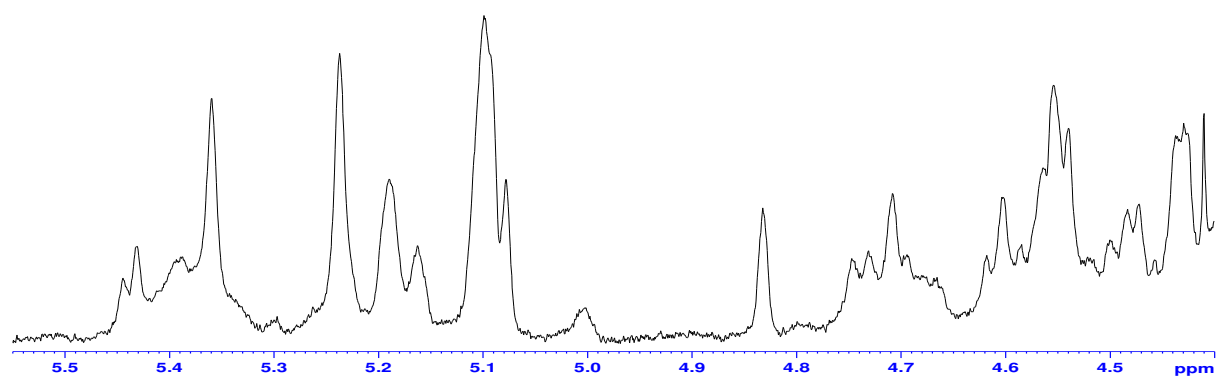


**Figure 45: Expanded Anomeric Region <sup>1</sup>H NMR Spectrum of EPS Crude EPS from *Bifidobacterium animalis* subsp. *lactis* A1dOxR**



The identification of the presence of more than one regular repeating unit from the EPS was further confirmed by the detection of more than one peak when the sample was analysed by size exclusion chromatography (SEC) (Figure 46).

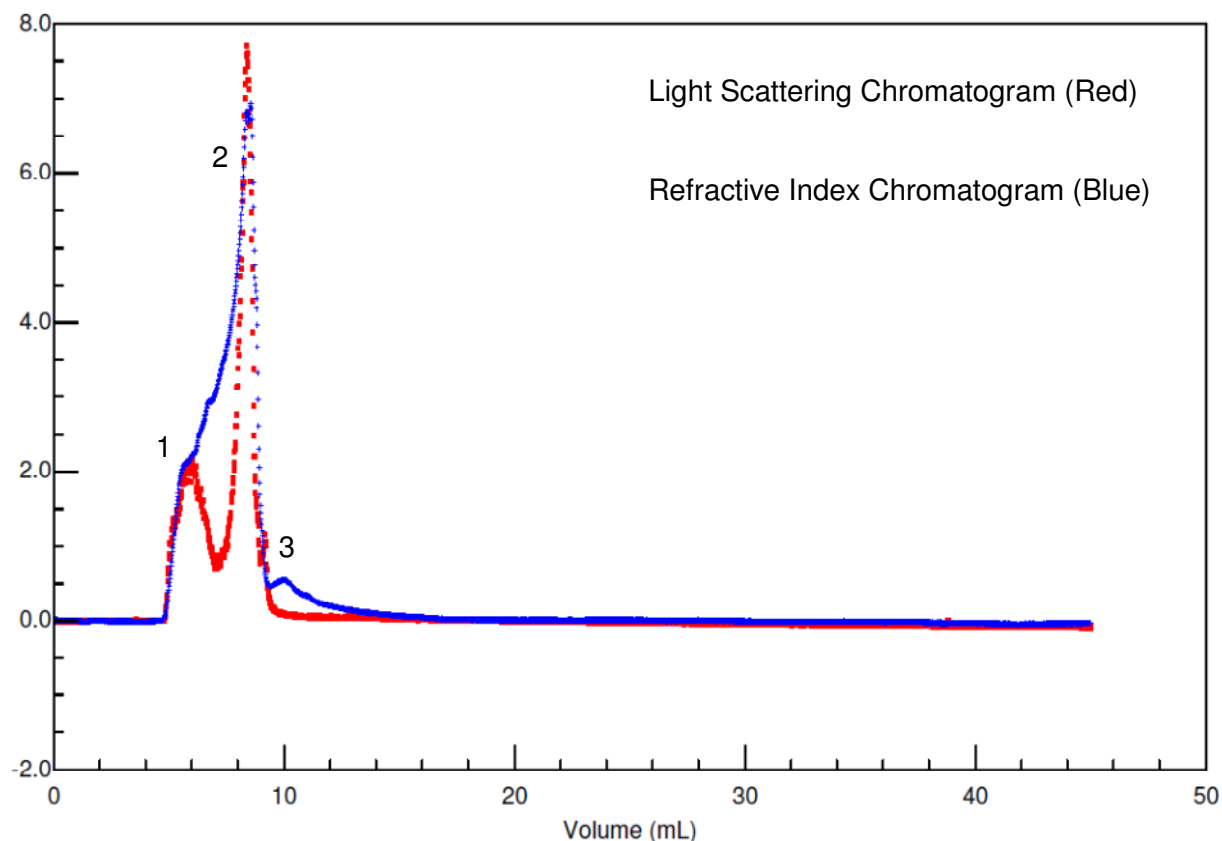


**Figure 46: A Chromatogram of Crude EPS from *Bifidobacterium animalis subsp. lactis* A1dOxR**

Three closely eluting peaks were visible in the chromatogram. The high molecular weight (HMW) peak produced a weight-average molecular weight ( $M_w$ ) of  $3.527 \times 10^6$  Da, whilst the two lower molecular weight peaks demonstrated  $M_w$  of  $2.586 \times 10^6$  and  $4.430 \times 10^5$  respectively. The HMW peak was observed to be comparable to the SEC-MALLS results previously reported by Ruas-Madiedo *et al* in 2010. The lower molecular weight peaks identified however were found to be largely over estimated (Ruas-Madiedo *et al* 2010). This is due to the presence of phosphate, which gives the lower molecular weight material a negative charge, thereby affecting the  $M_w$  interpretation of the chromatogram on a system

operated with water as the eluent as appose to sodium nitrate, which is used for the detection of negatively charged materials<sup>131</sup>.

#### 4.2.2 Isolation of High Molecular Weight material from Crude A1dOxR

In order to separate the larger polysaccharide (high molecular weight – above 100,000 Da) from the other material in the crude A1dOxR sample a separation technique was required.

##### 4.2.2.1 Ultrafiltration using Vivaspin 20 Centrifugal Concentrators

The first method that was used in an attempt to separate the different components from A1dOxR was ultrafiltration. Initially a Vivaspin 20 cartridge was loaded with a solution of EPS in D<sub>2</sub>O with a concentration of 1 mg mL<sup>-1</sup>. The cartridge was then subjected to the procedure detailed in Chapter 2 section 2.2.5.1. Upon recovery of the retentate (material above 100,000 Da) a <sup>1</sup>H NMR spectrum was obtained (Figure 47).

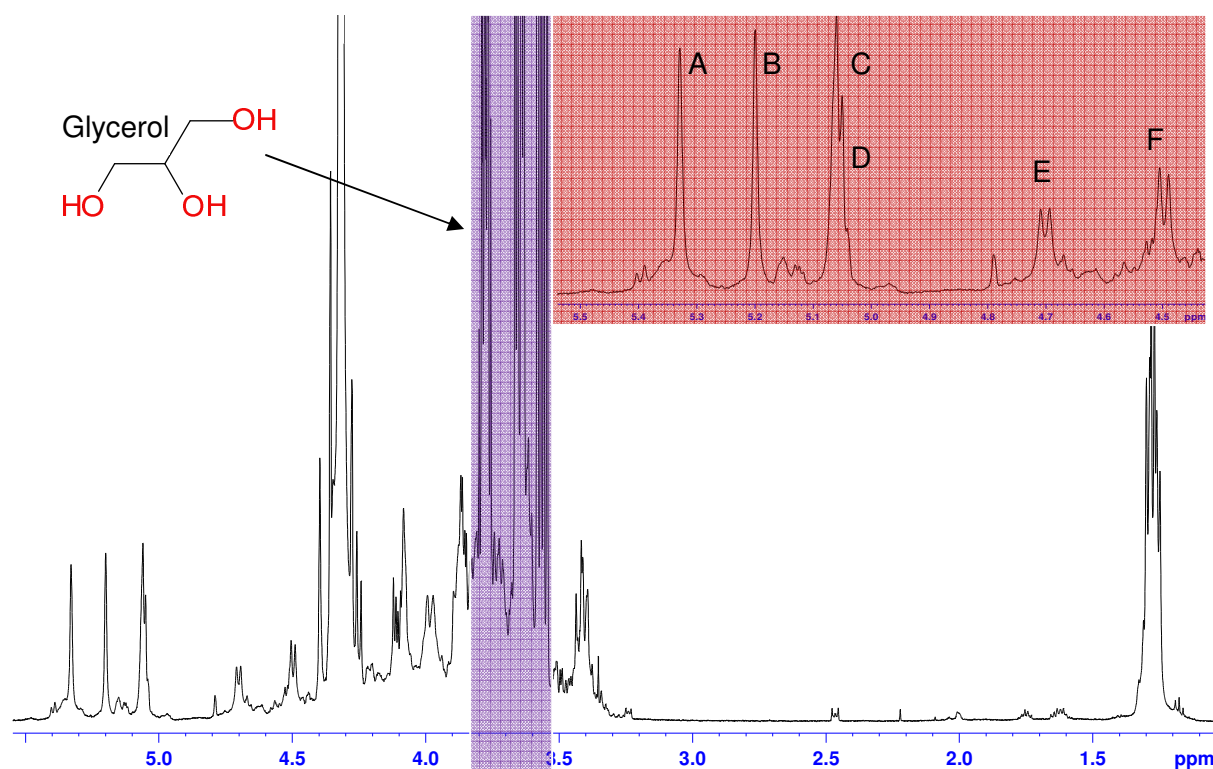


**Figure 47: <sup>1</sup>H NMR Spectrum of High Molecular Weight Material Recovered from Vivaspin 20 (Main) Magnified Anomeric region (Inset)**

The <sup>1</sup>H NMR spectrum of the retentate illustrates the isolation of the high molecular weight material from the original crude sample as a single polysaccharide: this is demonstrated by

the less complex pattern of peaks displayed in the anomeric region of the spectrum (shaded red) and the whole number ratio of the peak integrals observed. The peaks correspond to six anomeric protons labelled **A**, **B**, **C**, **D**, **E** and **F** respectively in order from high chemical shift to low chemical shift – these are identified as the monomer units that comprise the regular repeating unit structure of the high molecular weight material.

This method of separation however introduced a series of extraneous peaks (shaded purple), that were not visible in the original A1dOxR sample. After investigation, involving subjecting blank samples of D<sub>2</sub>O to the Vivaspin 20 separation procedure followed by <sup>1</sup>H NMR it was concluded that the peaks had arisen from contamination introduced from the filters in the Vivaspin concentrators, glycerol, which is used as a humectant.

#### 4.2.2.2 Dialysis using Spectra/Por Float-A-Lyzer

To overcome the issue of contamination experienced when using the centrifugal concentrators a second dialysis technique was applied to the crude sample: dialysis using a float-a-lyzer. The float-a-lyzer was loaded with a solution of EPS in D<sub>2</sub>O with a concentration of 4.5 mg mL<sup>-1</sup>. The cartridge was then subjected to the procedure detailed in Chapter 2 section 2.2.5.2. Upon recovery of the retentate, including the high molecular weight material, a <sup>1</sup>H NMR spectrum was obtained (Figure 48).

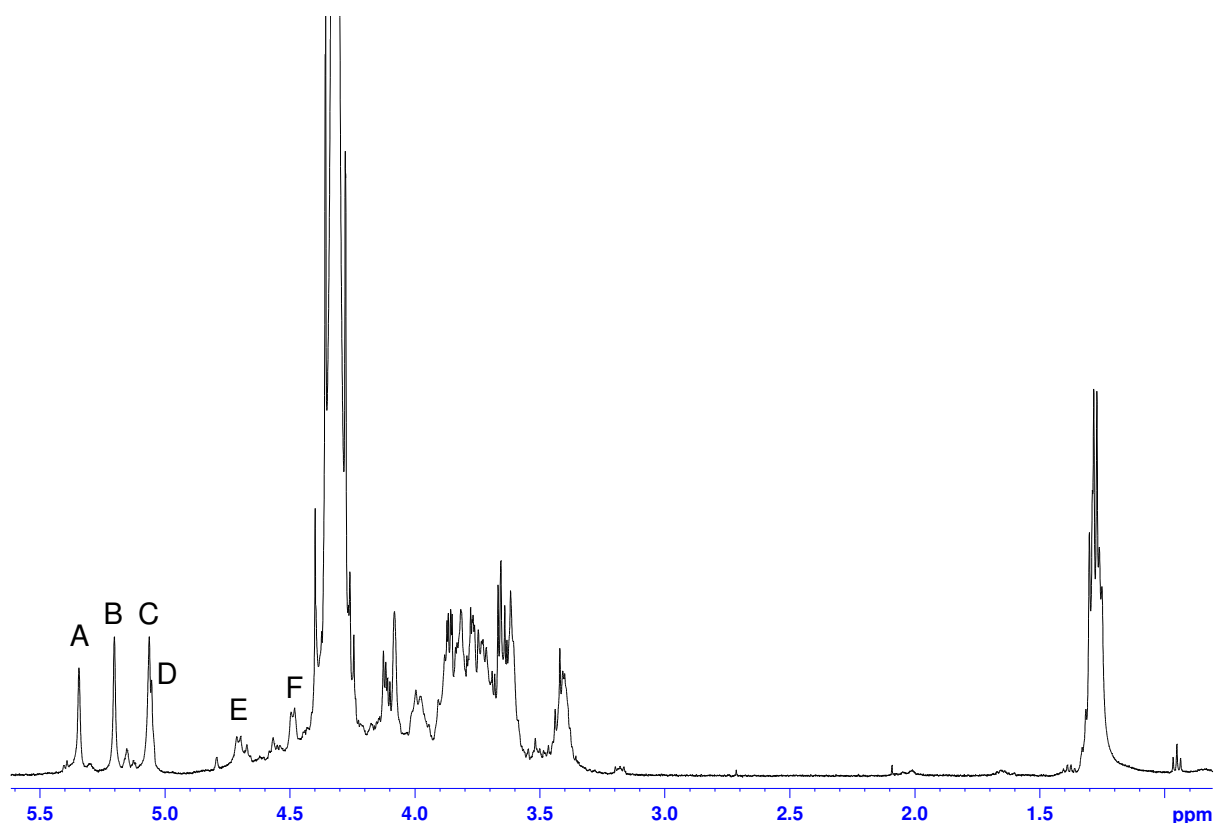


**Figure 48:  $^1\text{H}$  NMR Spectrum of High Molecular Weight Material Recovered from Spectra/Por Float-A-Lyzer**

From inspection of the spectrum it can be clearly seen that separation of the high molecular weight material from the crude has again been successful; more importantly, the area of the spectrum that had previously displayed peaks corresponding to glycerol contamination (3.9 – 4.25 ppm) is much cleaner as the signals present now correspond only to that of the high molecular weight regular repeating unit being studied.

The isolation of the high molecular weight material was further confirmed by subjecting the sample to HP-SEC-MALLs analysis (Figure 49).

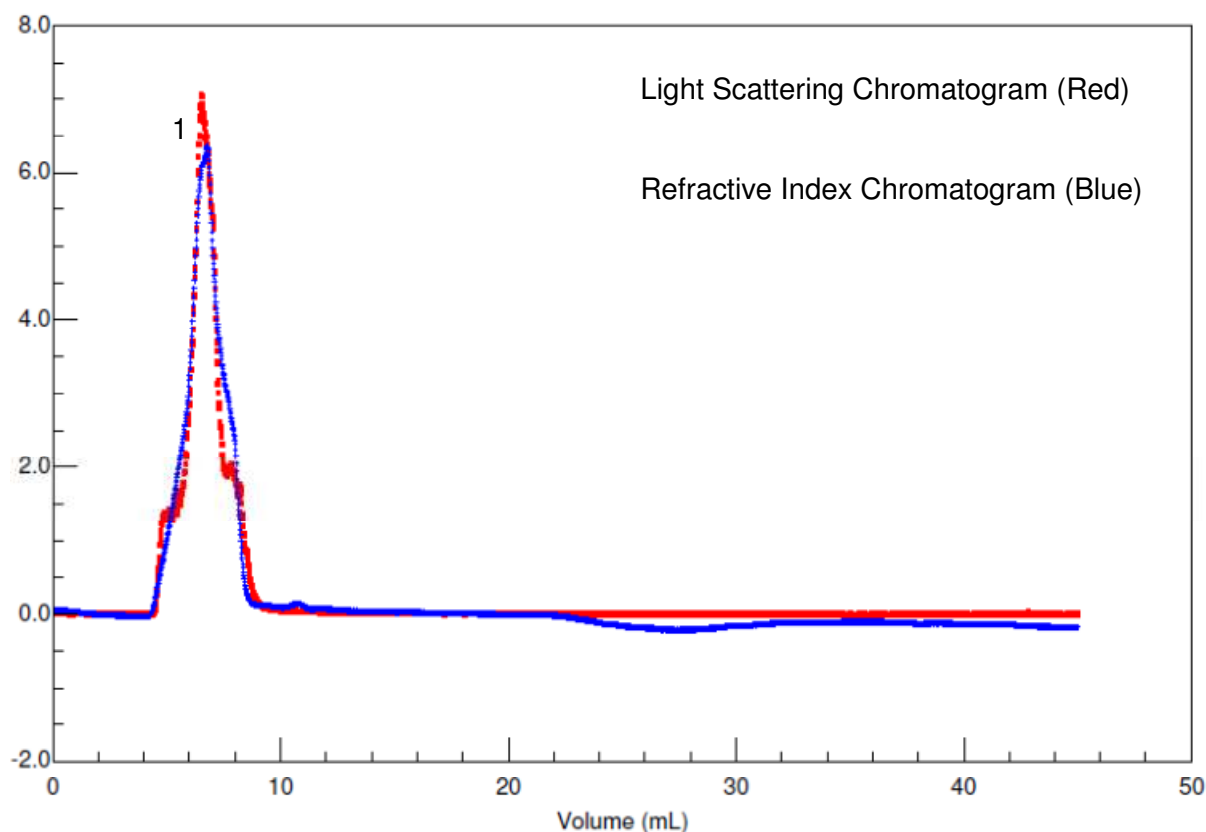


**Figure 49: A Chromatogram of High Molecular Weight material isolated from Crude A1dOxR using Spectra/Por Float-A-Lyzer**

The chromatogram, when compared to that previously obtained for the crude sample now shows predominantly a single peak, relating to the HMW species. The  $M_w$  was determined to be  $3.539 \times 10^6$  Da. It must be noted however that the peak identified did not contain purely the HMW material. Small traces of the lower molecular weight material, previously identified in the crude sample were also detected.

### **4.3 Structural Characterisation**

This section will focus on the structural characterisation of the high molecular weight material isolated from the crude A1dOxR EPS through the use of NMR, GC-MS and HPAEC-PAD.

### 4.3.1 Structural Analysis using NMR

In order to determine the structure of the oligosaccharide repeating unit structure of the EPS produced by *Bifidobacterium animalis subsp. lactis* A1dOxR a series of 1D- and 2D-NMR experiments were carried out.

The first experiment performed was a  $^1\text{H}$  NMR (Figure 48); this spectrum can be used to determine the number of monomer units in the oligosaccharide repeating unit structure. As can be seen, there are 6 proton signals in the anomeric region labelled **A – F** (from left to right). **A – D** appear as single peaks or unresolved doublets whilst **E** and **F** are clearly resolved doublets. From the chemical shifts and  $^3J_{1,2}$  coupling constants the anomeric configuration of signals **E** and **F** can be labelled as possessing  $\beta$ -anomeric configuration as they have coupling constants greater 7 Hz<sup>167</sup> (see Appendix). The anomeric configurations for signals **A – D** were determined using a coupled HMQC experiment. As the values for signals **A – D** were all observed to be over 170 Hz it was determined that the monomers were all of  $\alpha$ -anomeric configuration<sup>145</sup> (see Appendix).

**Table 8: Anomeric Proton Chemical Shifts and  $^3J_{1,2}$  and  $^1J_{\text{H-C}}$  Coupling Constants**

Monosaccharide	Chemical Shift (ppm)	$^1J_{\text{H-C}}$ and $^3J_{1,2}$ * Coupling Constants (Hz)	Configuration
<b>A</b>	5.33	173	$\alpha$
<b>B</b>	5.20	175	$\alpha$
<b>C</b>	5.06	174	$\alpha$
<b>D</b>	5.05	173	$\alpha$
<b>E</b>	4.70	7.78*	$\beta$
<b>F</b>	4.50	7.60*	$\beta$

Upon examining the high field (low frequency) region of the spectrum, the presence of proton signals characteristic of  $\text{CH}_3$  moieties was noted. After integrating the peaks it was determined that there were 9 proton signals; subsequently corresponding to the presence of

three methyl groups. The identification of methyl groups at ~ 1.5 ppm is generally recognised as an indication of the presence of methyl pentoses such as rhamnose or fucose or other commonly encountered EPS moieties such as pyruvate.

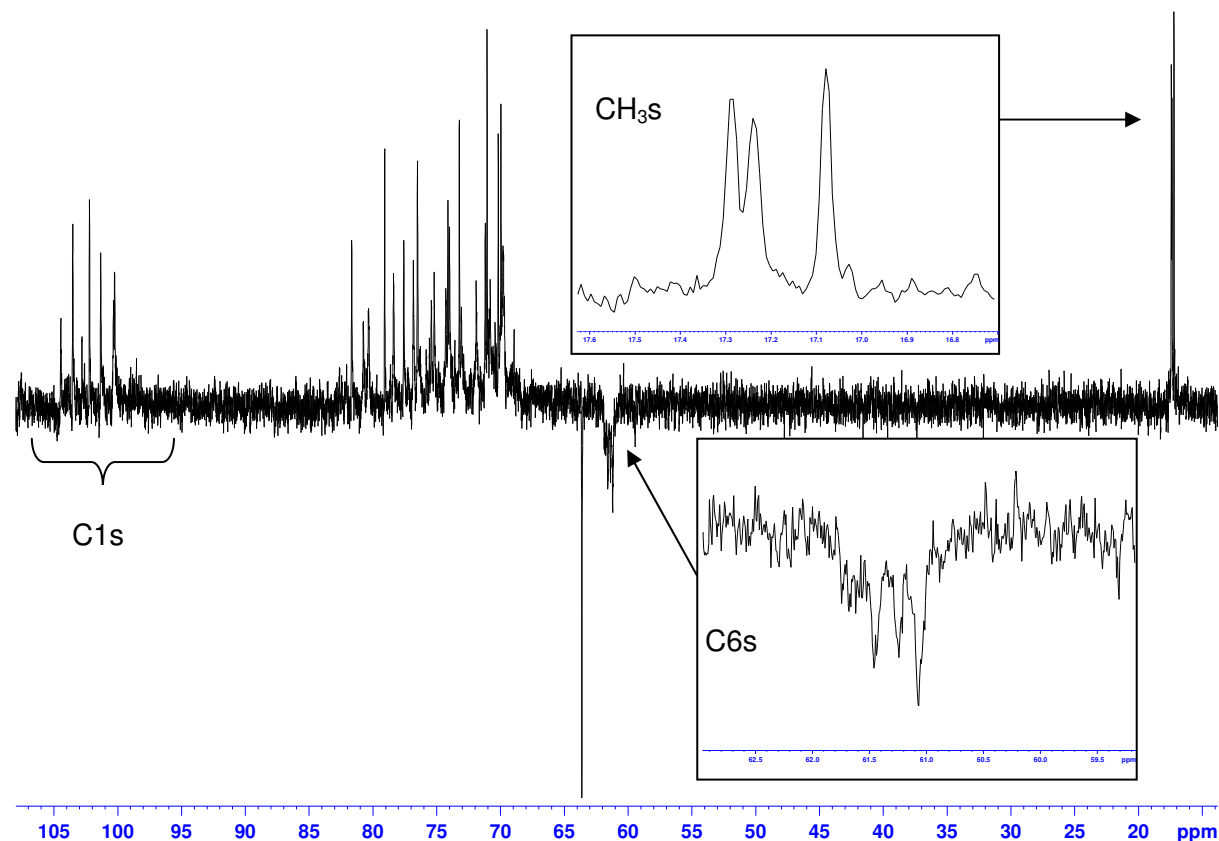


**Figure 50: DEPT 135  $^{13}\text{C}$  NMR Spectrum of High Molecular Weight EPS from *Bifidobacterium animalis* subsp. *lactis* A1dOxR (Main) Magnified Region showing CH<sub>3</sub>s (Inset Top) Magnified Region showing C6s (Inset Bottom)**

The DEPT 135  $^{13}\text{C}$  Spectrum (Figure 50) shows positive peaks for CHs and CH<sub>3</sub>s and negative peaks for CH<sub>2</sub>s. The anomeric carbons (C1s) appear downfield (above 90 ppm) due to the presence of the neighbouring ring oxygen atom and as expected 6 unique signals were observed. There are 3 peaks that can be identified as CH<sub>2</sub>s (from the C6s); these are located between 60 – 65 ppm and three CH<sub>3</sub>s (characteristic of the presence of a methyl pentose) signals appear between 10 – 20 ppm; again confirming the presence of 6 hexoses.

In order to fully characterise the structure of the oligosaccharide repeating unit of the EPS a series of 2D-NMR experiments were performed. Initially the COSY ( $^1\text{H}$ ,  $^1\text{H}$ ) experiment was

performed, this experiment showed protons attached to the adjacent carbon (linked by scalar coupling), and the  $^1\text{H}$  chemical shifts along both frequency axes are therefore correlated with each other.

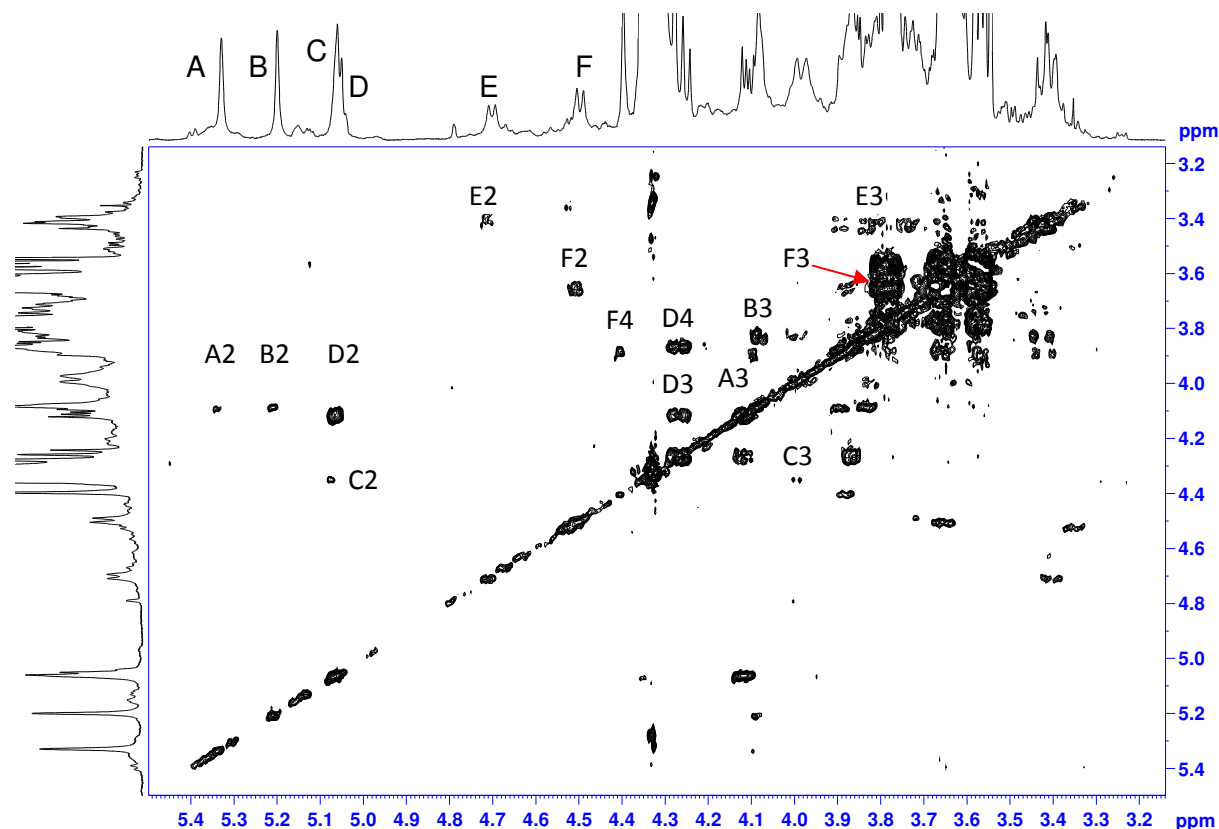


**Figure 51: COSY Spectrum of High Molecular Weight EPS from *Bifidobacterium animalis* subsp. *lactis* A1dOxR**

Starting with the knowledge of the positions of the anomeric protons the COSY spectrum firstly allows the identification of the H2 signals on the adjacent carbon. Following the interconnected diagonal cross peaks a number of other ring protons can be determined. The spectrum in Figure 51 permits the naming of H2 and H3 for **A**, **B**, **C** and **E**. Whilst H2 – H4 can be identified for monosaccharides **D** and **F**.

Another important spectrum to be examined for identifying which protons belong to which monosaccharide ring is achieved are TOCSY spectra (Figure 52). By selectively exciting the resonance of a single proton in the sample this experiment allows for the detection of all of the protons in the same coupled spin system. The “range” within the molecule for detecting



a correlation is critically dependent on the length of the mixing time during which the spin-lock is applied<sup>170</sup>.

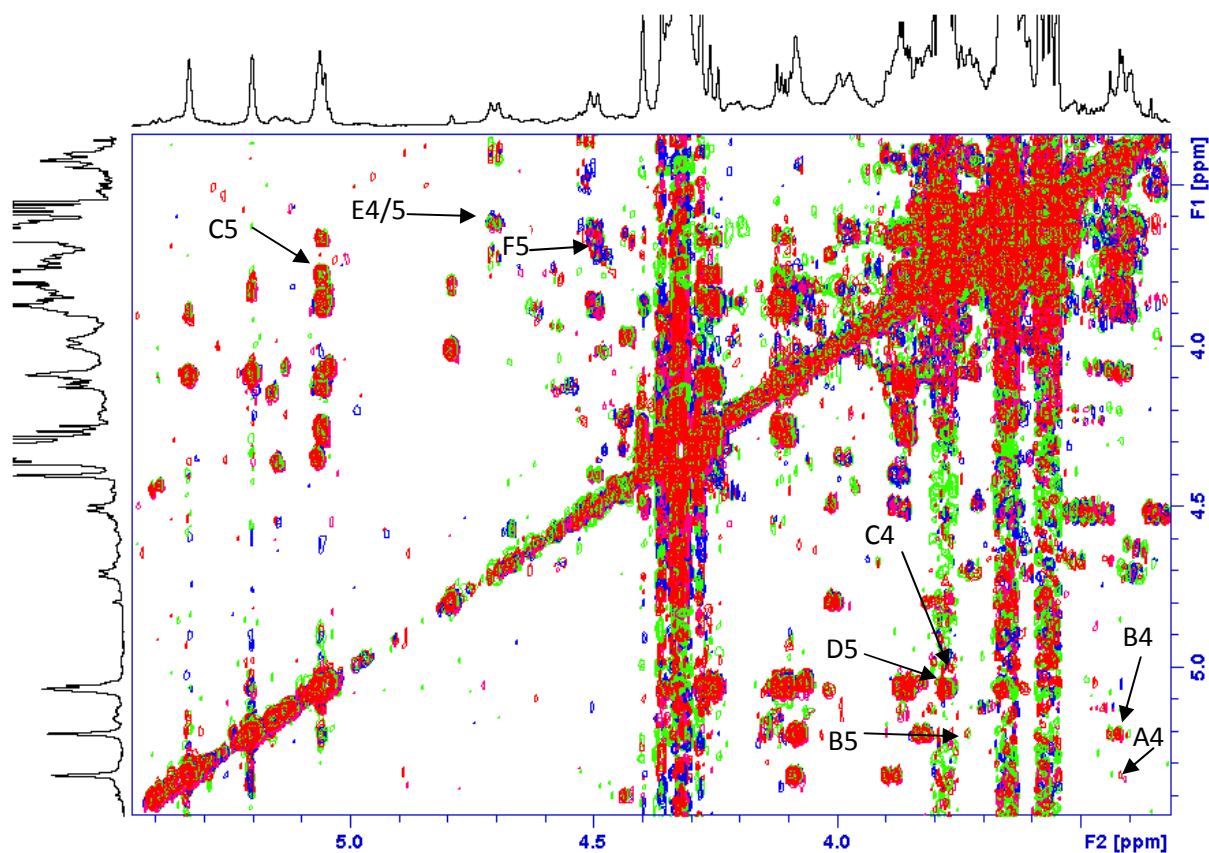


**Figure 52: Overlaid TOCSY Spectra of High Molecular Weight EPS from *Bifidobacterium animalis* subsp. *lactis* A1dOxR**

By overlaying spectra from TOCSY experiments run at different mixing times (30 – 210 ms) it is possible to view not only the short range coupling (usually due to the proton on the adjacent carbon), but also peaks of lesser intensities become visible; which are usually due to the protons on the next but one carbon. The H2 – H5 protons can be identified for monosaccharides **B** – **F**. Only H5 for **A** is not observed in either the COSY or TOCSY experiments.

Overlaying the COSY spectrum with that of the TOCSY spectrum (Mixing Time – 150 ms) enables the H6s for **B** and **C** to be individually assigned (Figure 53). The overlay allows for the identification of H6s by the overlap of the H5 COSY peaks with the corresponding peaks present in the TOCSY spectrum. The identification of the H6s for monosaccharides **B** and **C**

allowed for the position of the H5 proton for **A** to be determined. This was achieved using the information of the positions of the H5 protons for **B** and **C** in conjunction with the knowledge of the **A** H6 proton.

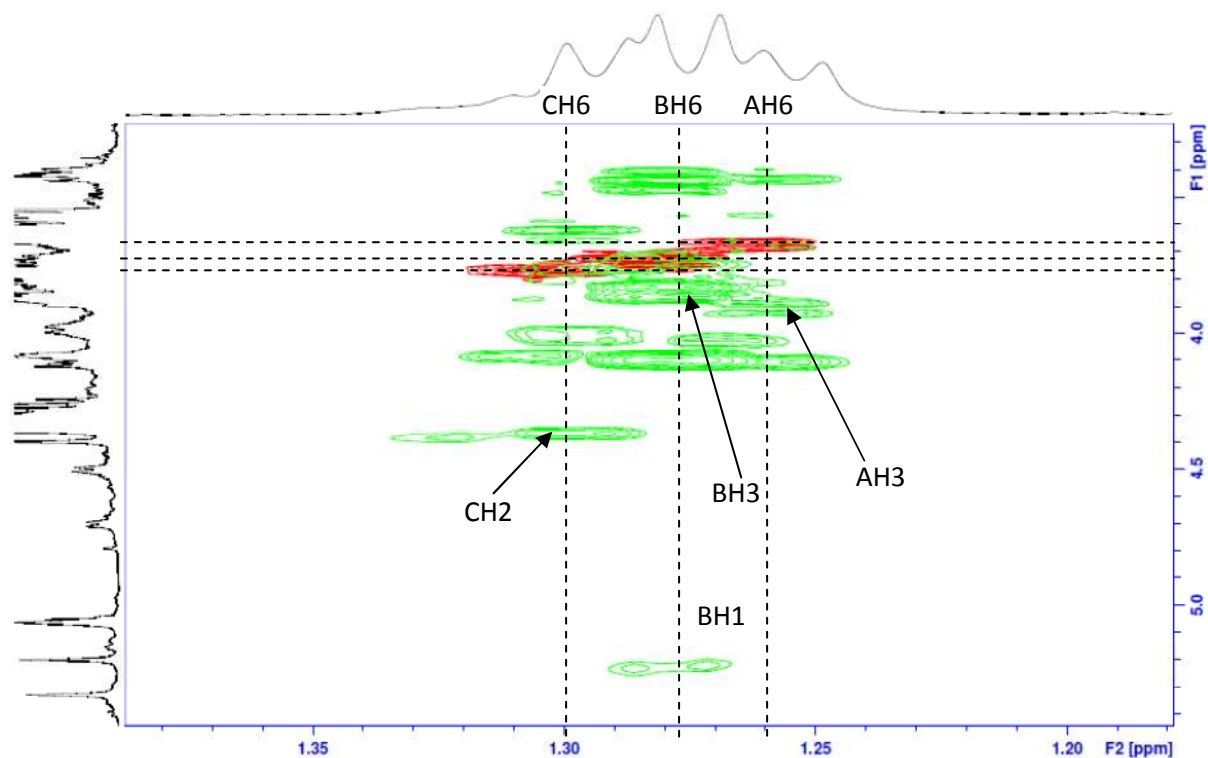


**Figure 53: TOCSY (150 ms) Spectrum with COSY Spectrum Overlaid of High Molecular Weight EPS from *Bifidobacterium animalis* subsp. *lactis* A1dOxR**

With the assignment of the complete proton signals for monosaccharides **A** – **F** (Table 9) the correlating carbons are designated by inspection of the  $^1\text{H}$ – $^{13}\text{C}$  HSQC spectrum (Figures 54 and 55). This spectrum contains a peak for each unique proton attached to the coupled  $^{13}\text{C}$  considered. The  $^{13}\text{C}$  chemical shifts are given in Table 10.

**Table 9:  $^1\text{H}$  NMR Chemical Shifts of EPS Recorded in  $\text{D}_2\text{O}$  at  $70\text{ }^\circ\text{C}$** 

Monosaccharide	$^1\text{H}$ Chemical Shift (ppm)						
	H1	H2	H3	H4	H5	H6	H6'
<b>A</b>	5.35	4.08	3.89	3.40	3.67	1.25	-
<b>B</b>	5.21	4.08	3.83	3.42	3.72	1.29	-
<b>C</b>	5.07	4.35	3.98	3.60	3.77	1.31	-
<b>D</b>	5.06	4.11	4.25	3.86	3.78	3.68*	3.90*
<b>E</b>	4.71	3.40	3.73	3.60	3.60	3.68*	3.90*
<b>F</b>	4.50	3.65	3.86	4.39	3.61	3.68*	3.90*

\*Represents partially overlapping H6 and H6' resonances

From the determination of the H4 position of the remaining unassigned sugar residues (**D**, **E** and **F**), the designation of whether each sugar is a D-glucose or a D-galactose monomer can be identified. The H4 resonance for D-galactose, regardless of either anomeric configuration or the presence of any linkages to the molecule, is shifted downfield in comparison to that of a D-glucose monomer. Generally H4 resonances for D-glucose occur between 3.75 – 3.46 ppm whilst H4 resonances for D-galactose occur between 4.26 – 3.83 ppm<sup>171</sup>. **D** and **F** can therefore be designated D-galactose and **E** as D-glucose.

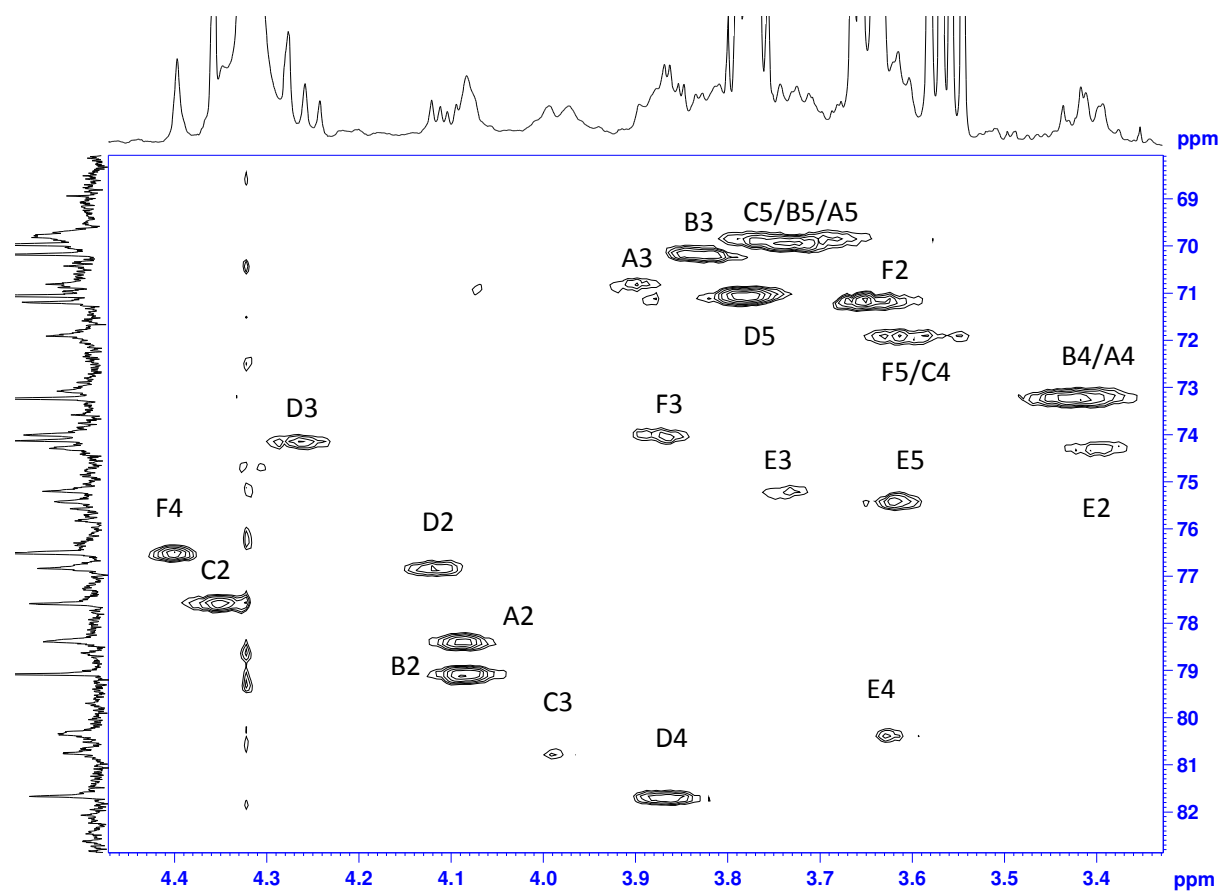


**Figure 54:  $^1\text{H}$ - $^{13}\text{C}$  HSQC Spectrum of High Molecular Weight EPS from *Bifidobacterium animalis* subsp. *lactis* A1dOxR**

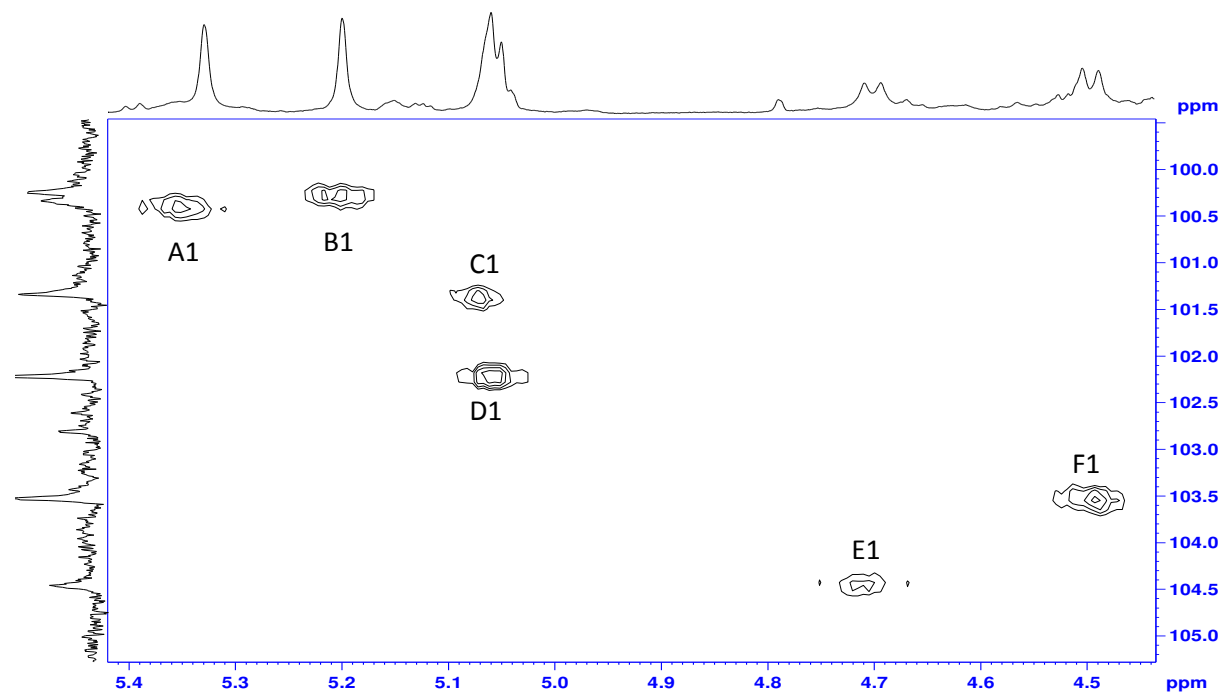


**Figure 55:  $^1\text{H}$ - $^{13}\text{C}$  HSQC Spectrum – Anomeric Region of High Molecular Weight EPS from *Bifidobacterium animalis* subsp. *lactis* A1dOxR**

**Table 10:  $^{13}\text{C}$  NMR Chemical Shifts of EPS Recorded in  $\text{D}_2\text{O}$  at  $70\text{ }^\circ\text{C}$** 

Monosaccharide	$^{13}\text{C}$ Chemical Shift (ppm)					
	C1	C2	C3	C4	C5	C6
<b>A</b>	100.35	78.28	70.84	73.09	69.80	17.40
<b>B</b>	100.25	79.02	70.17	73.25	69.80	17.23
<b>C</b>	101.33	77.49	80.74	71.86	69.81	17.44
<b>D</b>	102.12	76.78	74.13	<u>81.50</u>	71.09	61.61
<b>E</b>	104.37	74.17	75.22	80.37	75.30	61.41
<b>F</b>	103.45	71.06	73.88	76.47	71.92	61.22

\*Highlighted values indicate linkages; Underlined value indicates presence of a furanose

As previously referred to in Chapter 3 the position of the C4 atom is used as an indicator for the determination of whether sugar residues are present in either the furanose (5-membered ring) or pyranose (6-membered ring) ring structures. The chemical shifts indicate that all the monosaccharides are present in the pyranose form with the exception of **D**, which is either present in the furanose form or participates in a C4 glycosidic linkage.

In order to establish the way in which the sugar residues are connected to form the 6 monomer repeating unit, a combination of  $^1\text{H}$ - $^{13}\text{C}$  HMBC and 2D- $^1\text{H}$ - $^1\text{H}$  NOESY spectra are used for sequence determination. The  $^1\text{H}$ - $^{13}\text{C}$  HMBC spectra (Figure 56) shows the intra-residue couplings highlighted in red with the inter-residue couplings highlighted in yellow. The spectra identifies inter-residue cross peaks from coupling between **A** H1 and **F** C4 confirming an **A (1→4) F** linkage; **B** H1 and **C** C2 confirming a **B (1→2) C** linkage; **D** H1 and **B** C2 confirming a **D (1→2) B** linkage and lastly an inter-residue cross peak is observed between **C** H1 and **A** C2 confirming a **C (1→2) A** linkage. A number of intra-residue couplings are also visible.

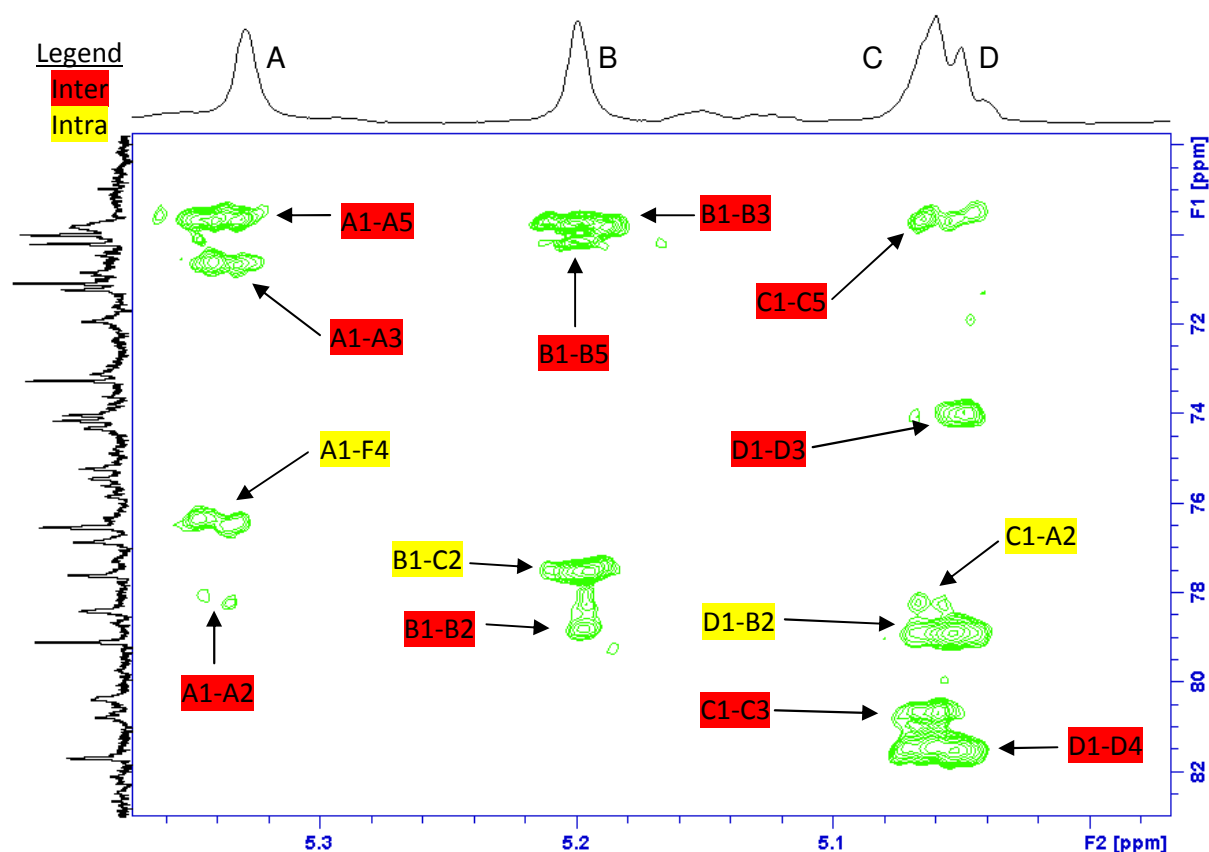


**Figure 56:  $^1\text{H}$ - $^{13}\text{C}$  HMBC Spectrum of High Molecular Weight EPS from *Bifidobacterium animalis* subsp. *lactis* A1dOxR**

To complete the structural conformation leading to the elucidation of the sequence in which the monosaccharides are linked to form the repeating unit oligosaccharide a final 2D-NMR spectrum is required. As with the  $^1\text{H}$ - $^1\text{H}$  ROESY experiment (Chapter 3) the  $^1\text{H}$ - $^1\text{H}$  NOESY experiment provides information on both the intra-residue and inter-residue coupling in the molecule. Again providing information on the coupling of proton nuclei in close spatial proximity (distance smaller than  $5\text{\AA}$ ) rather than coupling through bonds.

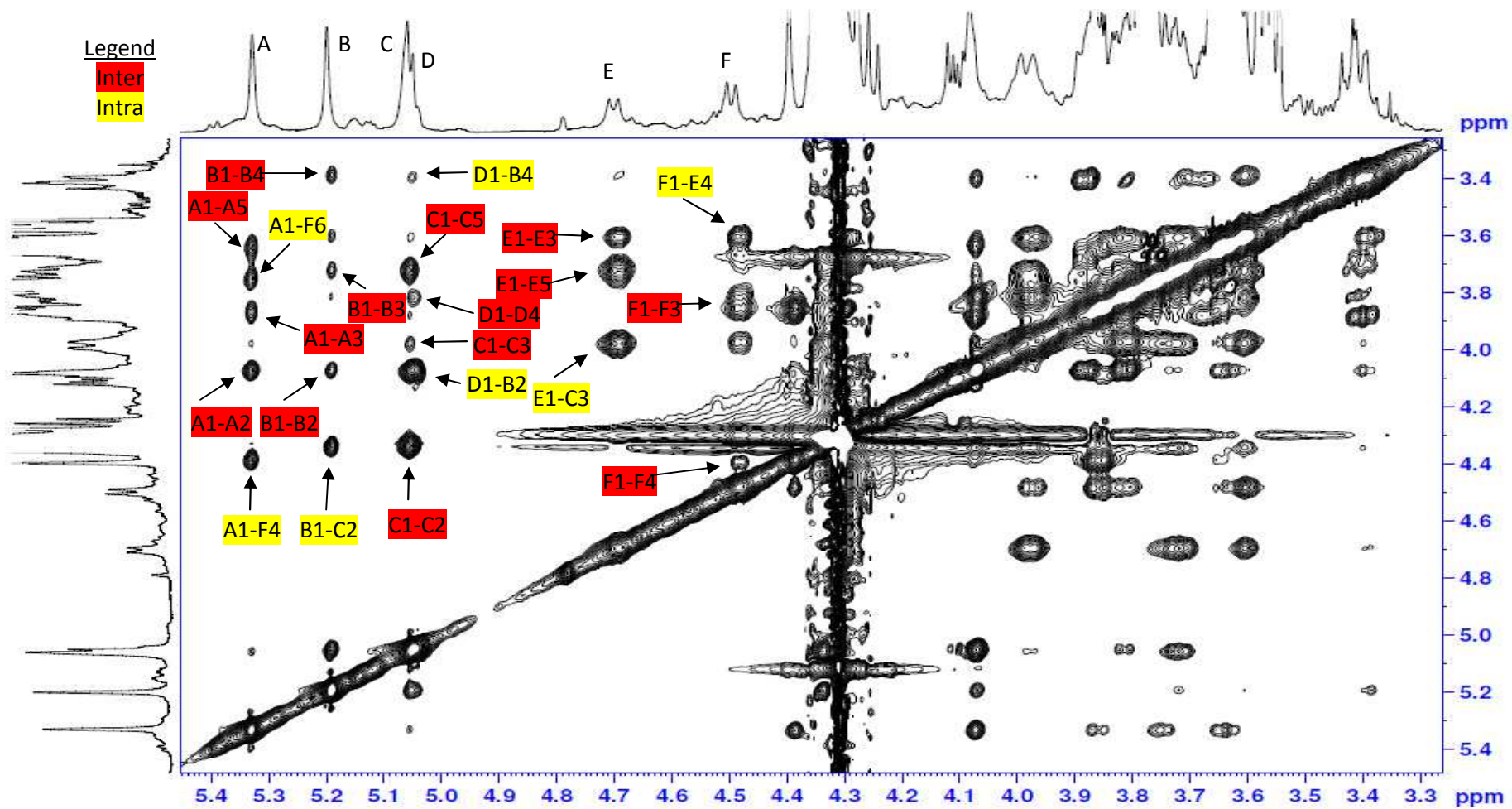


Figure 57:  $2D$ - $^1H$ - $^1H$  NOESY Spectrum of High Molecular Weight EPS from *Bifidobacterium animalis* subsp. *lactis* A1dOxR

The  $^1\text{H}$ - $^1\text{H}$  NOESY spectrum (Figure 57) shows the intra-residue NOEs highlighted in red with the inter-residue NOEs highlighted in yellow. Strong NOE cross peaks are observed between **A** H1 and **F** H4 and between **B** H1 and **C** H2 further confirming the **A (1→4) F** and **B (1→2) C** linkages identified by the  $^1\text{H}$ - $^{13}\text{C}$  HMBC spectrum. Strong NOE cross peaks are also observed between **D** H1 and **B** H2 confirming a **D (1→2) B** linkage and between **E** H1 and **C** H3 confirming an **E (1→3) C** linkage and finally **F** H1 and **E** H4 confirming a **F (1→4) E** linkage. Medium and weak NOE cross peaks are observed between **A** H1 and **F** H6 and **D** H1 and **B** H4. These cross peaks occur due to the NOE coupling through space between monosaccharides present in close proximity. Again, as with the  $^1\text{H}$ - $^{13}\text{C}$  HMBC spectrum a number of intra-residue couplings are also visible.

#### 4.3.1.1 Mild Acid Hydrolysis of the Oligosaccharide Unit

From the  $^1\text{H}$ - $^{13}\text{C}$  HMBC and  $^1\text{H}$ - $^1\text{H}$  NOESY interpretation, coupled with the prior knowledge gained from previously characterised EPS structures<sup>85</sup> it can be determined that a side-chain is present in the oligosaccharide repeat unit.

Mild acid hydrolysis was performed *in situ* in an NMR tube following the method<sup>154</sup> detailed in Chapter 2 section 2.3.1. A  $^1\text{H}$  NMR spectrum (Figure 58) was recorded prior to the addition of acid, following this spectra were recorded every hour for 9 hours with an additional spectra being record after 24 hours.



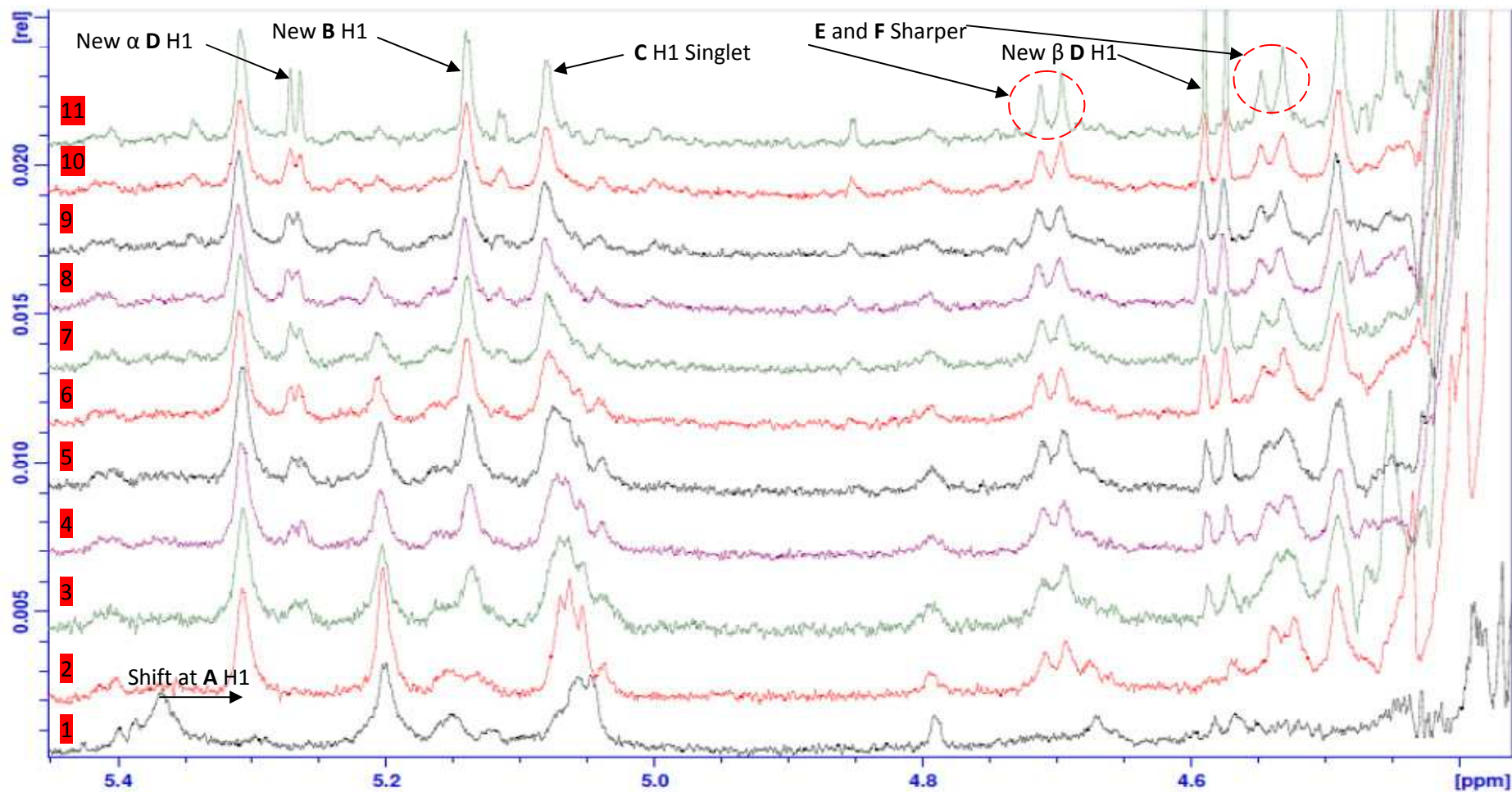


**Figure 58:  $^1\text{H}$  NMR Spectra of Acid Hydrolysed High Molecular Weight EPS from *Bifidobacterium animalis* subsp. *lactis* A1dOxR (Spectra 1) Pre-hydrolysis (Spectra 2-10) Post-hydrolysis 1 – 9 hours (Spectra 11) Post-hydrolysis 24 hours**

The first change to be observed is a shift in the position of **A** H1, the signal shifts up field by 0.06 ppm, this occurs rapidly upon addition of the acid. This is thought to be due to a slight change in hydrogen bonding in the molecule. Secondly, the shape of the overlapping anomeric signals assigned to **C** H1 and **D** H1 begins to change. This is attributed to the cleavage of monosaccharide **D** from the oligosaccharide repeating unit. The change is observed in accordance with the appearance of two new doublet signals at 5.25 ppm and 4.56 ppm. This occurs as monosaccharide **D** is now free in solution and therefore present in both the alpha (4.56 ppm) and beta (5.25 ppm) anomeric forms (Figure 59). This in turn reveals signal **C** H1 as a singlet peak.

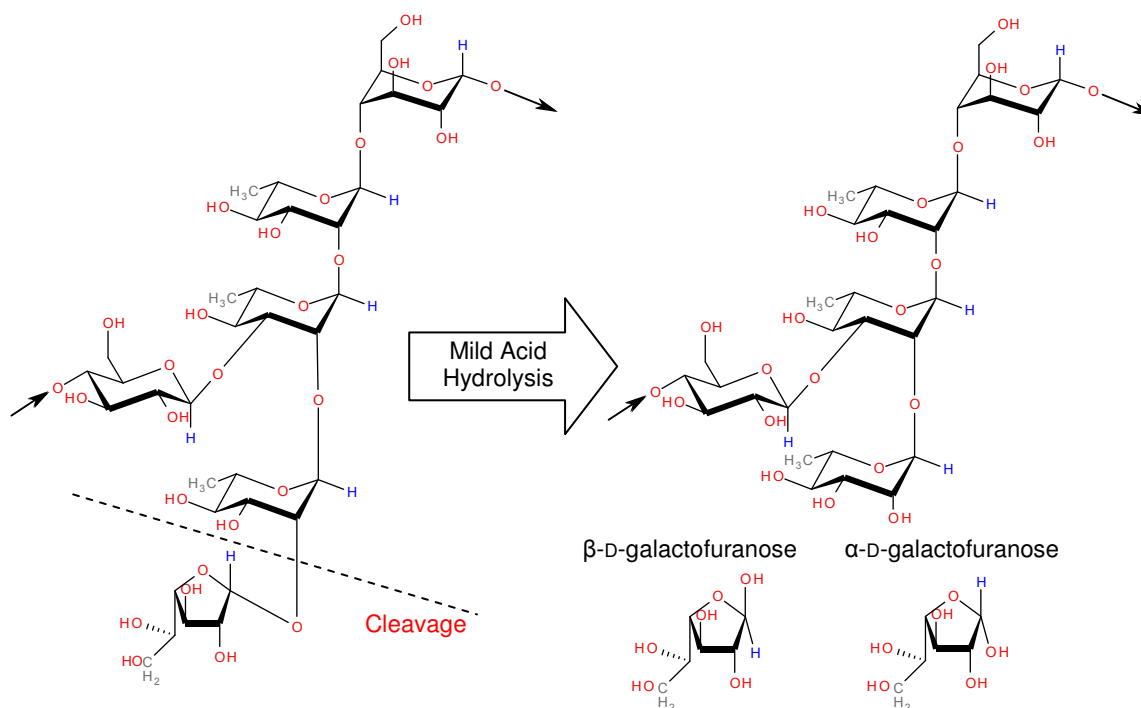


**Figure 59: Mild Acid Hydrolysis Effect on EPS Repeat Unit Structure**

Further examination of the spectra reveals a shifting in the position of the anomeric signal for residue **B** to 5.16 ppm. This shift is a consequence of the cleavage of the connected monosaccharide **D** (**D** (1 $\rightarrow$ 2) **B** linkage as indicated by the  $^1\text{H}$ - $^1\text{H}$  NOESY experiment). As the glycosidic bond to **D** is hydrolysed over time, the environment of the anomeric proton of monosaccharide **B** is affected. This is due to the short distance (3 bonds) between the

anomeric proton at **B** H1 and the point on the monosaccharide at which residue **D** was previously attached, **B** C2. Finally it can be noted that as the oligosaccharide unit becomes smaller over time (due to the loss of residue **D**) the anomeric signals for monosaccharides **E** and **F** become increasingly sharper.

#### 4.3.2 Structural Analysis using GC-MS and HPAEC-PAD

To characterise the EPS oligosaccharide repeating unit structure, established chromatographic techniques were implemented for determining its monomer composition and the linkages of the sugars.

##### 4.3.2.1 Monomer Analysis

Initially the monomer identification was performed by GC-MS analysis (Alditol Acetates) using the methods<sup>120,121</sup> described in Chapter 2 section 2.3.3.2. The resulting reaction product was then subjected to GC-MS analysis following the temperature program as detailed in Chapter 2 section 2.3.3.1.2.



**Figure 60: GC-MS Chromatogram of HMW EPS Monomers**

The chromatogram obtained displayed three distinct peaks (Figure 60) at 7.568, 16.940 and 17.384 minutes. The mass spectrometry fragmentation patterns generated by each peak were then analysed. The fragmentation observed for Peak 1 (7.568 minutes) was characteristic of belonging to a 6-deoxy hexose (methyl pentose) in the sugar alditol acetate form; either rhamnose (Figure 61A) or fucose. Peaks 2 and 3 (16.940 and 17.384 minutes) displayed almost identical MS fragmentation, characteristic of belonging to aldohexoses such as glucose (Figure 61B), galactose or mannose etc in the sugar alditol acetate form. A series of alditol acetate standards with known retention times were run in order to determine which sugar monomer arose from which particular peak in the chromatogram. It was resolved that peak one at 7.568 minutes was denoted as arising from the presence of rhamnose. Peak two at 16.940 minutes was confirmed as glucose whilst peak three at 17.384 minutes was confirmed as galactose.

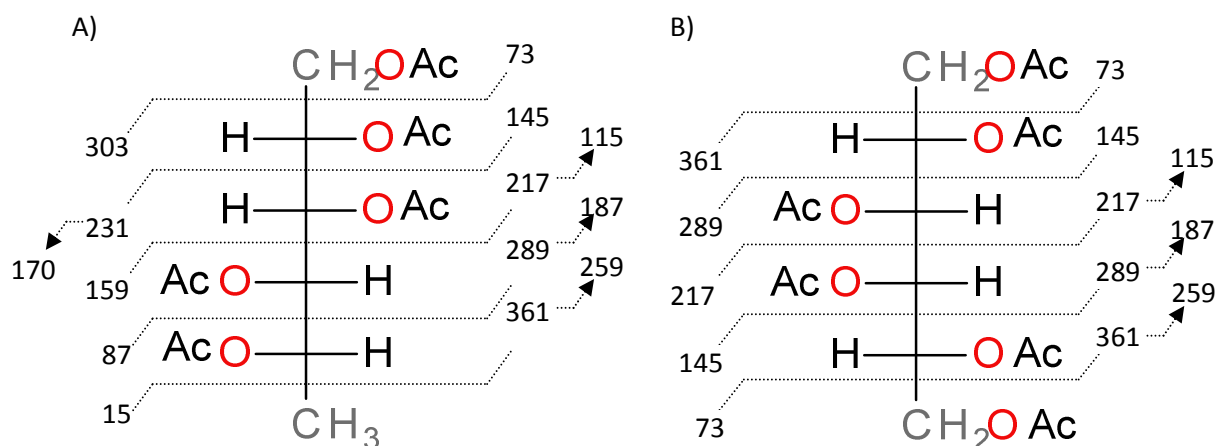


**Figure 61: MS Fragmentation for Sugar Alditol Acetate Monomers of A) Rhamnose and B) Glucose**

Unfortunately, the ratios of monomers observed by GC-MS analysis were not as anticipated. Under estimation of sugar residues when analysis is carried out by GC-MS is often observed due to the under derivatisation (pre column) of the constituent monomers; therefore an alternative method of quantification is often sought<sup>175</sup>.

Monomer analysis using HPAEC-PAD is frequently utilised as an alternative option to the method involving GC-MS detection. HPAEC-PAD is often employed instead of GC-MS methods due to the simple, quick and efficient one step acid hydrolysis procedure<sup>128,129</sup> as described in Chapters 2 and 3. Initially however, again the sugar monomers ratio was not as expected from the NMR analysis. This was credited to a problem with the online mixing of the mobile phase eluent used in the HPAEC (sodium hydroxide and water) to form the required concentration of dilute sodium hydroxide essential to accurately perform the analysis. Subsequent work undertaken at the University of Huddersfield by Mr. Glenn Robinson however gave the expected and correct results for the monomer ratios (Figure 62). As the monomers give different responses upon their interaction with the PAD in the HPAEC system, standard curves were obtained for the three sugars present in order to correct the overall ratios of sugar monomers present in the HMW EPS (see Appendix).

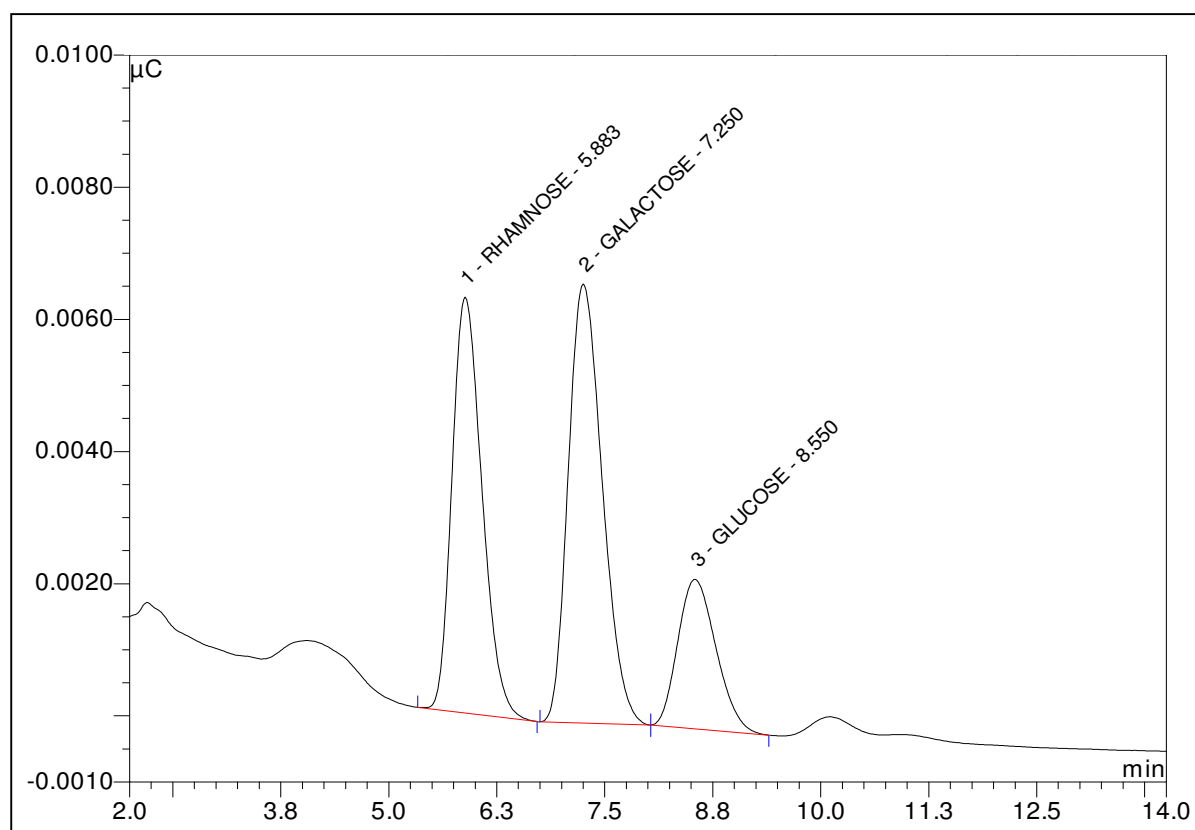


**Figure 62: HPAEC-PAD Chromatogram of HMW EPS Monomers**

The response factor for each monomer was corrected in accordance with the standard curve data obtained, from the monomer analysis it was determined that the HMW EPS repeating unit was composed of rhamnose, galactose and glucose in a molar ratio of 3:2.07:0.84. It is noted that the glucose residue is still very slightly under determined.

#### 4.3.2.2 Linkage Analysis

The results of the  $^1\text{H}$ - $^1\text{H}$  NOESY spectrum coupled with the information gained from the  $^1\text{H}$ - $^{13}\text{C}$  HMBC spectrum indicated a number of linked sugar residues. In order to further confirm the presence of the previously identified linkages between monomers and determine the structure of the oligosaccharide repeat unit structure, linkage analysis (of alditol acetates) was performed by GC-MS<sup>138</sup>.

It must be noted that, as the HMW EPS could not be separated entirely from the lower molecular material originally present in the crude sample other peaks not corresponding to the structure of the HMW EPS do appear in the chromatogram for the linkage data. It is estimated that ~ 10% of the lower molecular weight material was still present in the HMW EPS sample.

The linkage data (see Appendix) identified several peaks which, when coupled with the corresponding mass spectra (Figure 63 A – D) were confirmed as matching the linkages as previously indicated by NMR interpretation.

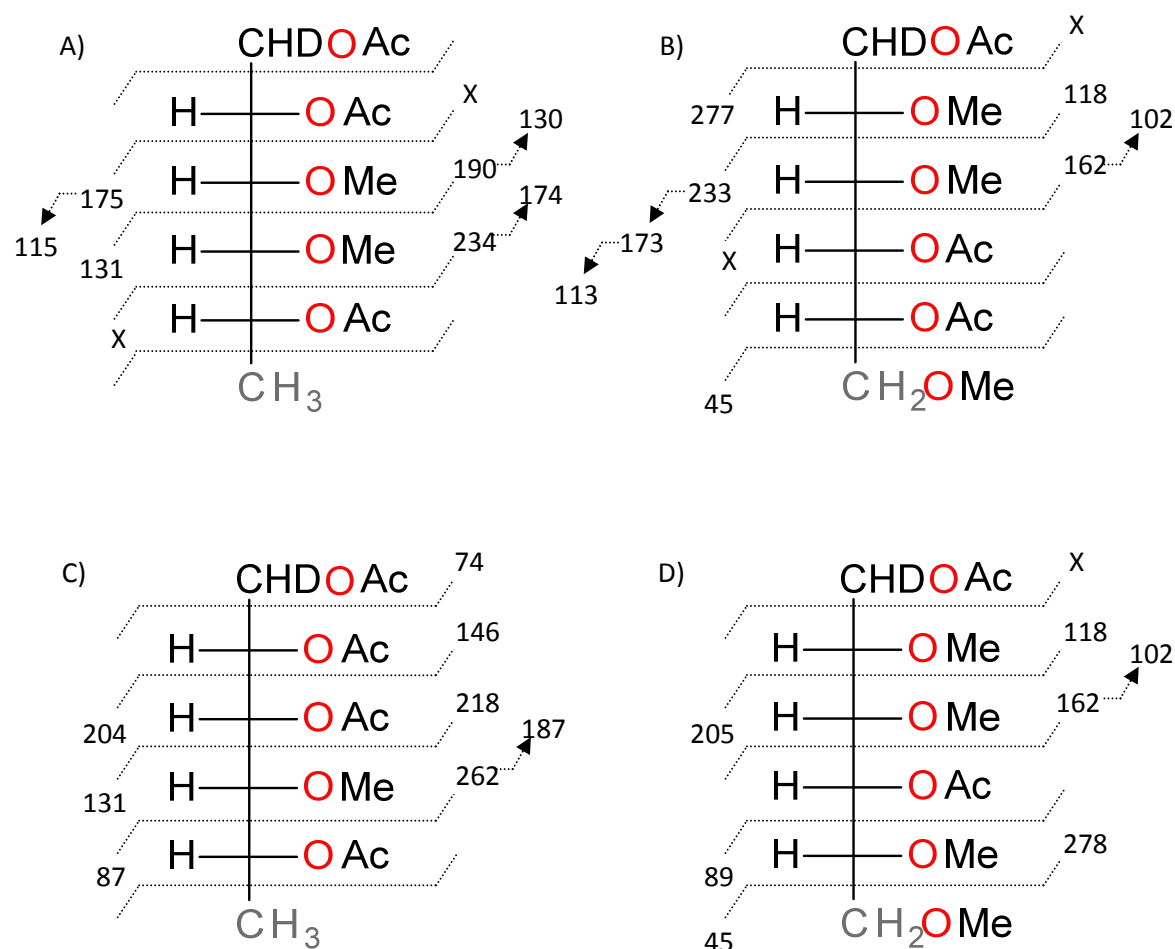


**Figure 63: Mass Spectra Fragmentation A) 1-2 Linked deoxy hexose; B) 1-4 Linked hexose; C) 1, 2, 3 Linked deoxy hexose; D) Terminal hexose (f)**

The linked monomers were identified from data provided in the literature<sup>123</sup>, taking into consideration not only the ions present in the MS fragmentation spectra but also the abundance ratios of the fragments observed.

Peak 1 was identified as 1, 2, 5-tri-*O*-acetyl-(1-deuterio)-3, 4-di-*O*-methyl-6-deoxy hexitol (1-2 linked deoxy hexose); this was confirmed by the presence of *m/z* peaks 131, 190 and 234.

Peak 2 was identified as 1, 4-di-*O*-acetyl-(1-deuterio)-2, 3, 5, 6-tetra-*O*-methyl hexitol (terminally linked hexofuranose); this was confirmed by the presence of *m/z* peaks 89, 102, 118, 162, 205 and 278. Peak 3 was identified as 1, 2, 3, 5-tetra-*O*-acetyl-(1-deuterio)-4-*O*-methyl-6-deoxy hexitol (1, 2, 3 deoxy hexose); this was confirmed by the presence of *m/z*

peaks 131 and 262. Peak 4 was identified as 1, 4, 5-tri-*O*-acetyl-(1-deuterio)-2, 3, 6-tri-*O*-methyl hexitol (1-4 linked hexose); this was confirmed by the presence of *m/z* peaks 102, 113, 118, 162, 173 and 233. Peak 5 was identified as 1, 4, 5-tri-*O*-acetyl-(1-deuterio)-2, 3, 6-tri-*O*-methyl hexitol (1-4 linked hexose); this was confirmed by the presence of *m/z* peaks 102, 113, 118, 162, 173 and 233.

Peak 4 was further analysed and confirmed as 1-4 linked glucose by spiking the linkage sample with the disaccharide lactose ( $\beta$ -D-Galactopyranosyl-(1 $\rightarrow$ 4)- $\alpha$ -D-glucopyranose) in its per-*O*-methylated alditol acetate form as described in Chapters 2 and 3. As well as producing an increased response for peak 4 (indicating the presence of 1-4 linked glucose), a new peak (attributed to terminally linked galactopyranose) was also observed between peaks 2 and 3 further confirming the lack of this particular monomer residue in the hexasaccharide repeating unit.

#### 4.3.3 Absolute Configuration

Finally, to complete the characterisation of the hexasaccharide repeat unit structure the absolute configurations (D- or L-) of the substituent monomers are required to be determined. The absolute configuration is determined by the preparation of acetylated butyl ((S)-(+)-2-butanol) glycosides<sup>130</sup>, using the method described in Chapter 2 section 2.3.5.2. Although all of the EPS structures identified to date express rhamnose in the L- configuration with glucose and galactose in their D- configurations it is still important to determine the absolute configurations of the constituent monomers in order to fully communicate and validate the structure of the oligosaccharide repeating unit structure.

The chromatogram obtained (see Appendix) contained five distinct peaks. The identity of these peaks was determined by comparison with standards of acetylated butyl ((S)-(+)-2-butanol) D-glucose, D-galactose and L-rhamnose (Figure 64).



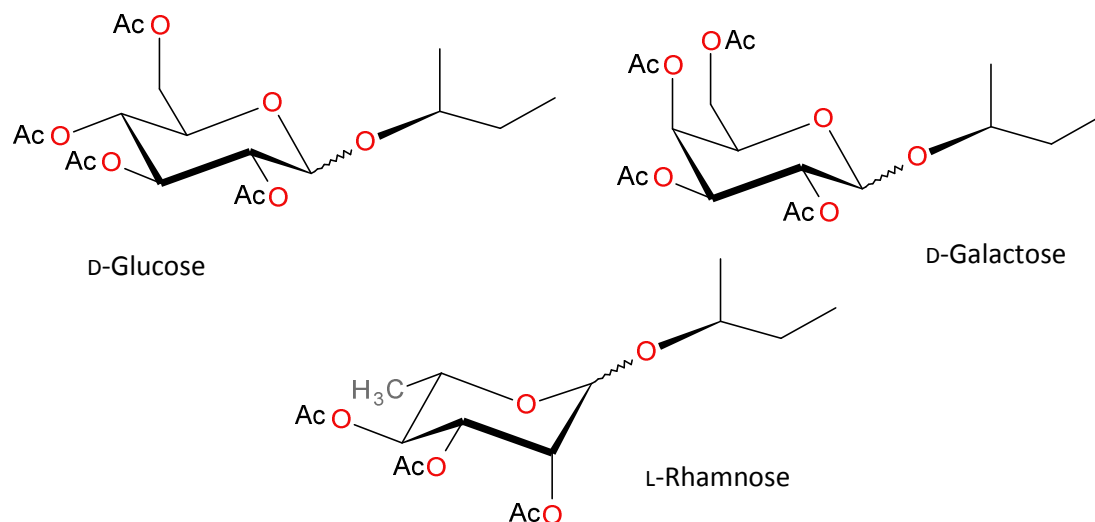


**Figure 64: Acetylated Butyl ((S)-(+)-2-butanol) Glycosides**

Each monomer should generate two peaks due to the (S)-(+)-2-butanol bonding to both the  $\alpha$  and  $\beta$  anomers of the respective monomers. Peak 1 was determined to originate from L-rhamnose; the retention time and mass spectra data were compared to the standard for confirmation. It should be noted that the epimers of L-rhamnose were not able to be separated by the GC-MS column temperature program utilised. Peaks 2 and 5 were confirmed as D-galactose; the retention time and mass spectra data were compared to the standard for confirmation. Peaks 3 and 4 were confirmed as D-glucose; the retention time and mass spectra data were compared to the standard for confirmation.

4.3.4 Proposed Structure of the HMW EPS produced by *Bifidobacterium animalis* subsp. *lactis* IPLA-R1 (A1dOxR)

Using the information provided from NMR and GC-MS interpretation the following structure for the EPS is proposed:

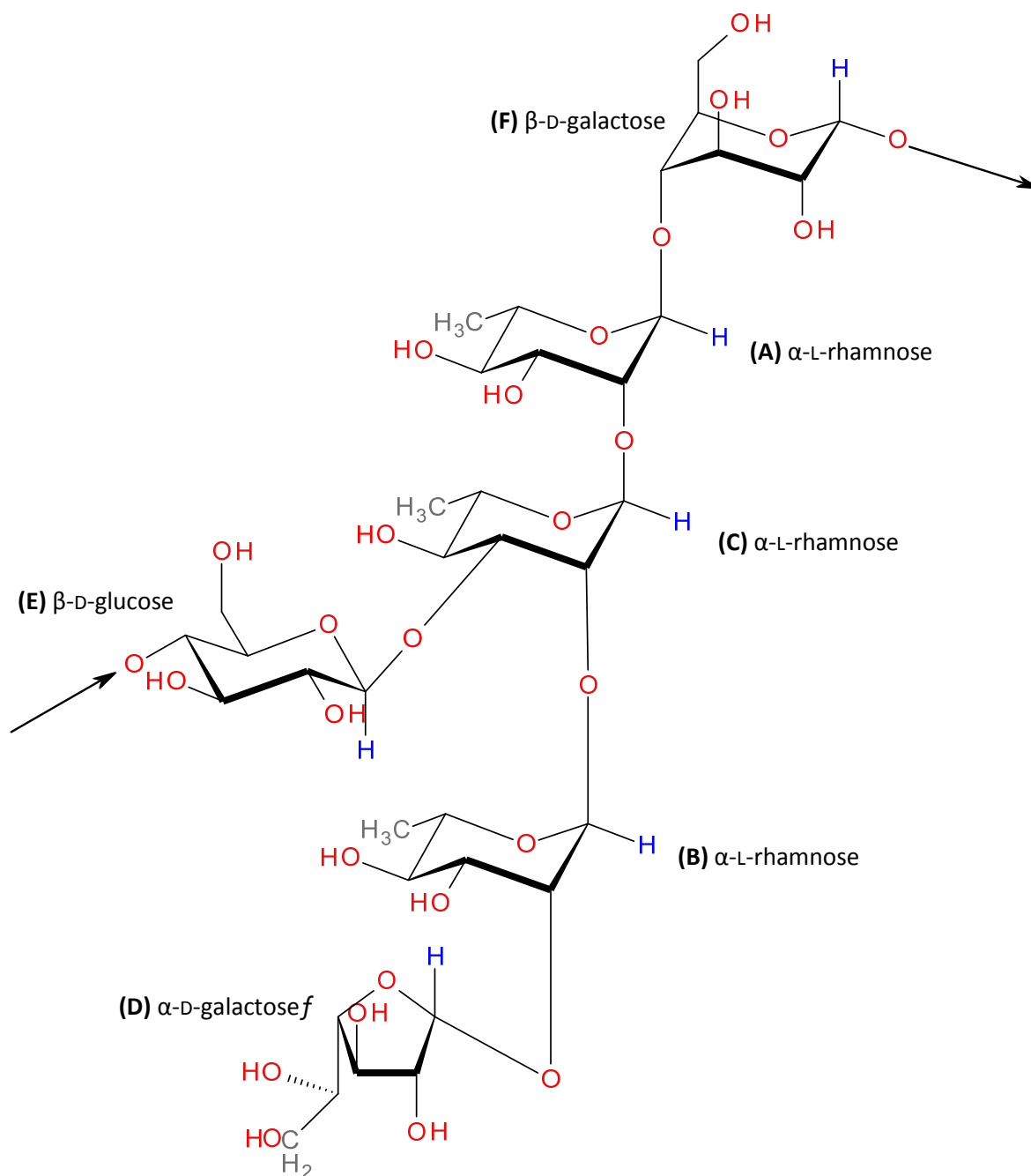


**Figure 65: Structure of HMW EPS produced by *Bifidobacterium animalis* subsp. *lactis* A1dOxR**

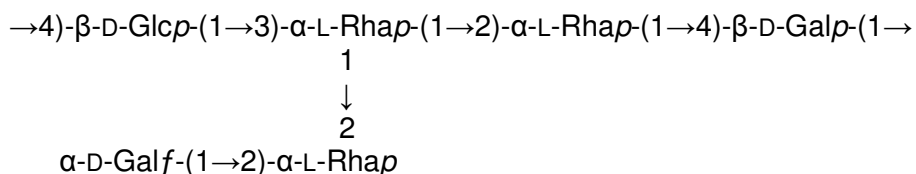


**Figure 66: Line Drawing Structure of HMW EPS produced by *Bifidobacterium animalis* subsp. *lactis* A1dOxR**

The anomeric proton on each sugar residue is highlighted in blue. Rhamnose is the most abundant sugar monomer present. The backbone of the hexasaccharide structure consists of four monomers: two L-rhamnoses and one each of D-glucose and D-galactose. The main chain has a branched side chain attached at a rhamnose unit; the side chain section consists of a 1→2 linked rhamnose connected to a terminal galactofuranose monomer. It should also be noted that the galactofuranose moiety is an infrequently encountered sugar in documented characterised EPS structures<sup>116,176</sup>; with galactose usually occurring in its more commonly observed and preferred pyranose form. This is a novel EPS and its proposed structure is currently awaiting publication.

#### **4.4 Initial Analysis of LMW Fraction of Crude Material from *Bifidobacterium animalis* subsp. *lactis* A1dOxR**

As discussed previously in this chapter the original crude sample material of A1dOxR contained not only the isolated and characterised HMW EPS but other material believed to possibly be EPS. The material obtained from the supernatant recovered from the dialysis of the crude sample was retained and designated low molecular weight (LMW) EPS material.

##### *4.4.1 Comparison and Examination of LMW, HMW and the Original Crude EPS Sample*

Upon examination of the <sup>1</sup>H proton NMR spectra for the HMW, LMW and crude (neither dialysed nor ultra filtrated) samples (Figure 67) it can be observed which signals in the crude are present in either the LMW, HMW or in fact appear in both samples.

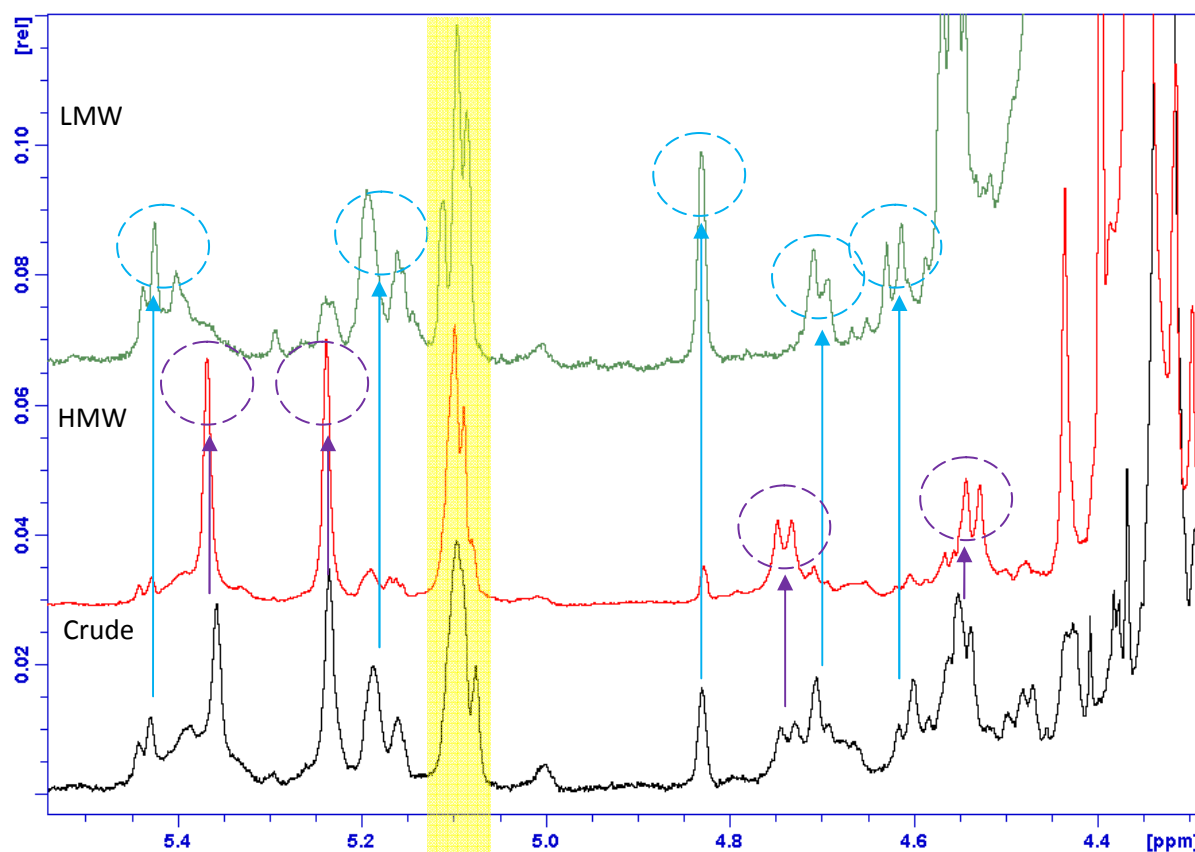


**Figure 67: Anomeric Region  $^1\text{H}$  NMR Spectra of Crude (Black), HMW (Red) and LMW (Green) material from *Bifidobacterium animalis* subsp. *lactis* A1dOxR**

Observation of the anomeric region of the LMW spectrum revealed several peaks. Amongst these peaks it is noted that monomers **C** (and possibly **D**) appear in both the HMW and LMW EPS material (shaded yellow band in Figure 67). This is further supported by the existence of peaks corresponding to methyl groups; indicating the presence of at least one rhamnose monomer.

The anomeric region however is highly complex, indicating the presence of an even lower molecular weight species not corresponding to an EPS. As with the isolation of the HMW EPS from the original crude sample it is necessary to employ a further dialysis or ultra filtration step in order to interpret and characterise the EPS present in the LMW fraction. This work is currently on going and will form the research program for another PhD student.

#### 4.4.2 Comparison and Examination of A1, A1dOx and A1dOxR

Along with the bile adapted A1dOxR strain of *Bifidobacterium animalis* subsp. *lactis*, two other strains also exist; the parental A1 strain and the minimally bile adapted strain A1dOx.

As with A1dOxR strain, the isolated material from these strains was supplied for initial NMR analysis. The  $^1\text{H}$  proton NMR spectra for each sample were compared along with the isolated LMW material from the original crude A1dOxR strain (Figure 68).

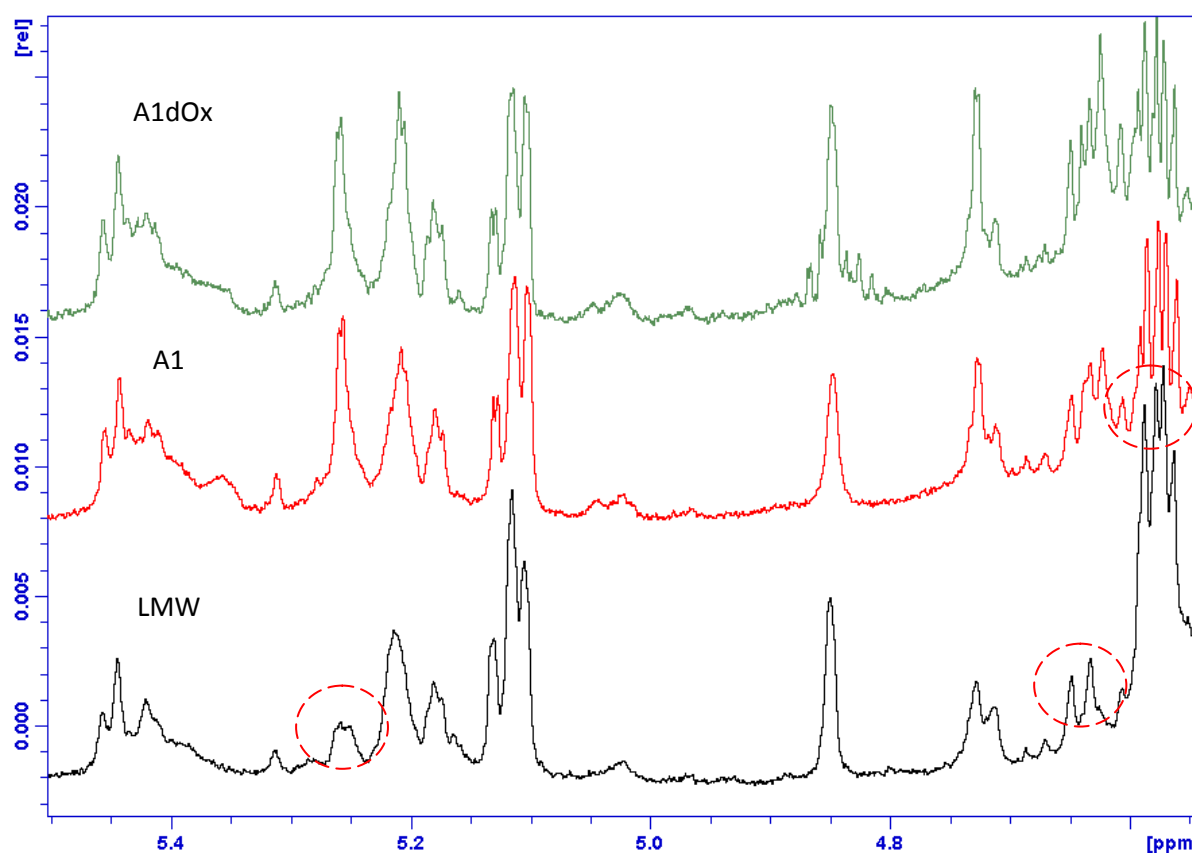


**Figure 68: Anomeric Region  $^1\text{H}$  NMR Spectra of LMW material isolated from Crude A1dOxR (Black), A1 (Red) and A1dOx (Green)**

Firstly it is immediately apparent that the spectra for all 3 samples are similar. This indicates that the LMW material produced by all 3 strains (A1, A1dOx and A1dOxR) is of a similar composition. There are however minor differences in the spectra as represented by the red dashed circles in Figure 67. However this may be due to the occurrence of a minor amount of HMW EPS still present in the sample. As previously eluded to regarding the LMW (isolated from crude A1dOxR) it will be necessary to also perform a dialysis or ultra filtration

procedure on both the A1 and A1dOx samples in order to remove the obvious impurities in order to characterise the EPS material present.

#### **4.5 Future Work**

Future work could potentially include further analysis of the LMW EPS material isolated from the crude EPS from *Bifidobacterium animalis* subsp. *lactis* A1dOxR. This could involve further purification of the sample to remove the remaining traces of the HMW EPS by using preparative size exclusion chromatography. Upon the isolation of a pure sample of LMW EPS, characterisation of the material could be performed by the same methods (NMR analysis coupled with the employment chromatographic techniques) as utilised in the structural elucidation of the HMW EPS repeating unit structure as observed throughout this chapter.

The *eps* cluster for *Bifidobacterium animalis* subsp. *lactis* A1dOxR has been successfully sequenced by Ruas Madiedo *et al* (awaiting publication). The cluster includes the genes involved in EPS formation, including the presence of genes coding for rhamnose precursors. The *eps* cluster however contains two priming-glycosyl transferase (p-GTF) genes, responsible for EPS synthesis activation. This is an unusual observation as *eps* clusters only require one p-GTF for EPS synthesis. This, however, could explain the presence of the LMW EPS material isolated from *Bifidobacterium animalis* subsp. *lactis* A1dOxR.

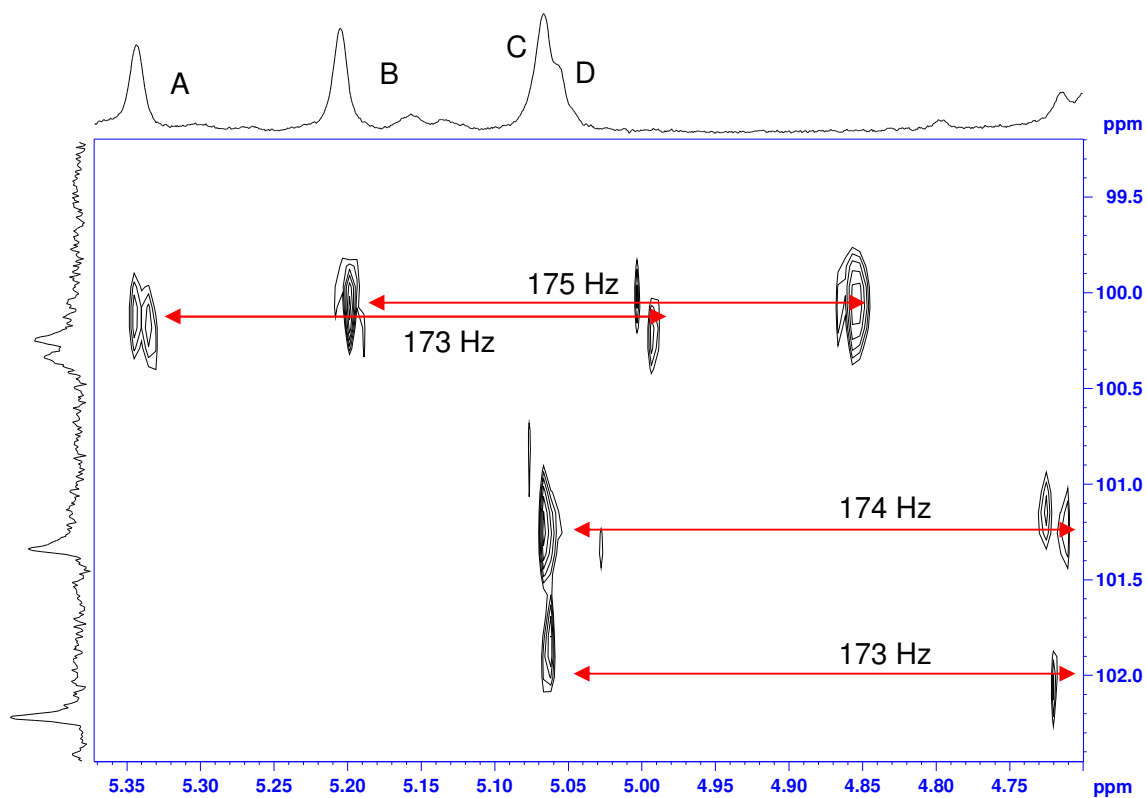
Many of the beneficial health effects attributed to probiotics rely on the ability of the probiotic strains to adhere to the intestinal mucosa<sup>173</sup>. The tolerance of such bacteria to biological barriers such as gastric acidity and high bile salt concentrations in the intestine is also an important criteria to consider when selecting probiotic strains<sup>83</sup>. It has been suggested that the production of an EPS may enhance a probiotics ability to resist degradation by biological barriers and aid in the adherence for the probiotic helping it to colonise the intestinal mucosa<sup>66</sup>. For this reason it is essential to characterise the identity of the EPS produced by

*Bifidobacterium animalis* subsp. *lactis* A1dOxR to greater understand the relationship between EPS structure and bacterial adherence.

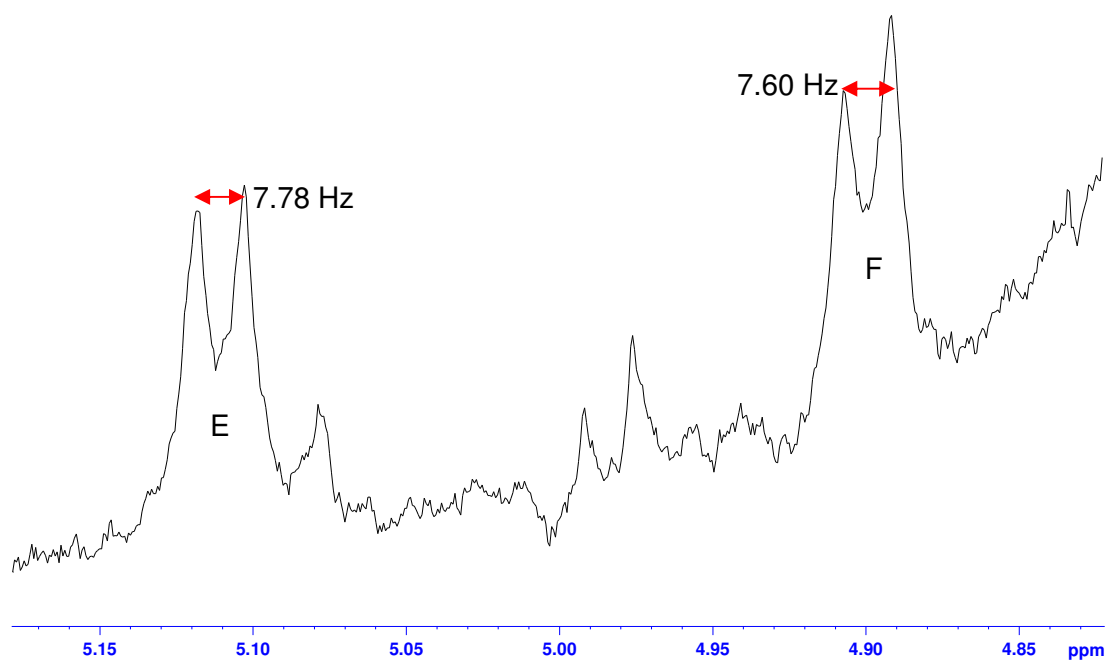
## 4.6 Appendices

### 4.6.1 Anomeric Configuration Determination

#### 4.6.1.1 Coupled HMQC NMR Spectrum of High Molecular Weight EPS from *Bifidobacterium animalis* subsp. *lactis* A1dOxR



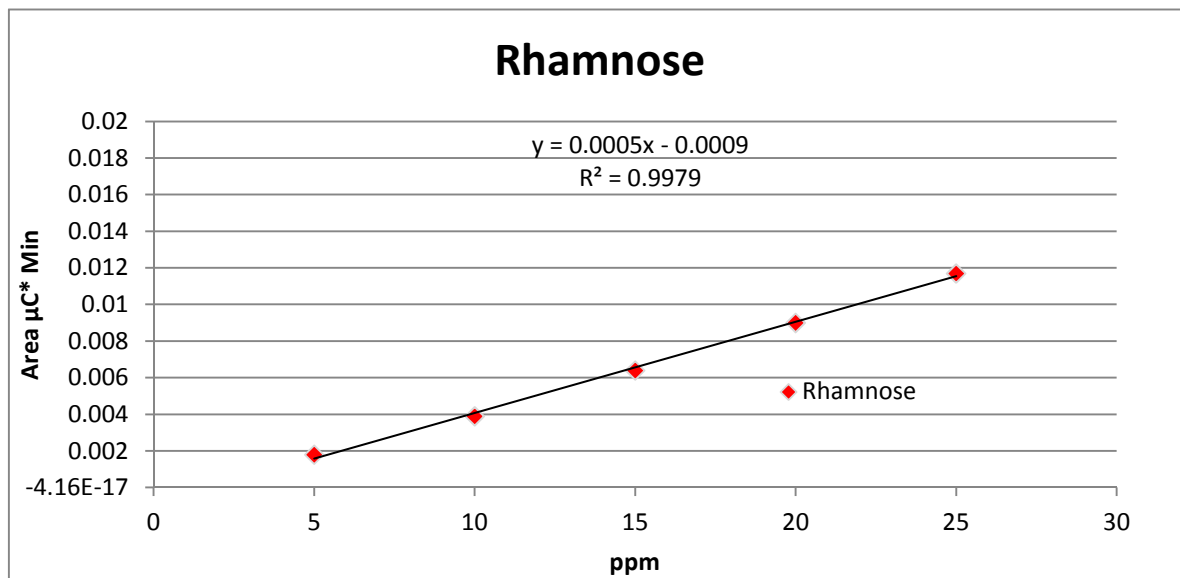
#### 4.6.1.1 Expanded <sup>1</sup>H NMR Spectrum of High Molecular Weight EPS from *Bifidobacterium animalis* subsp. *lactis* A1dOxR



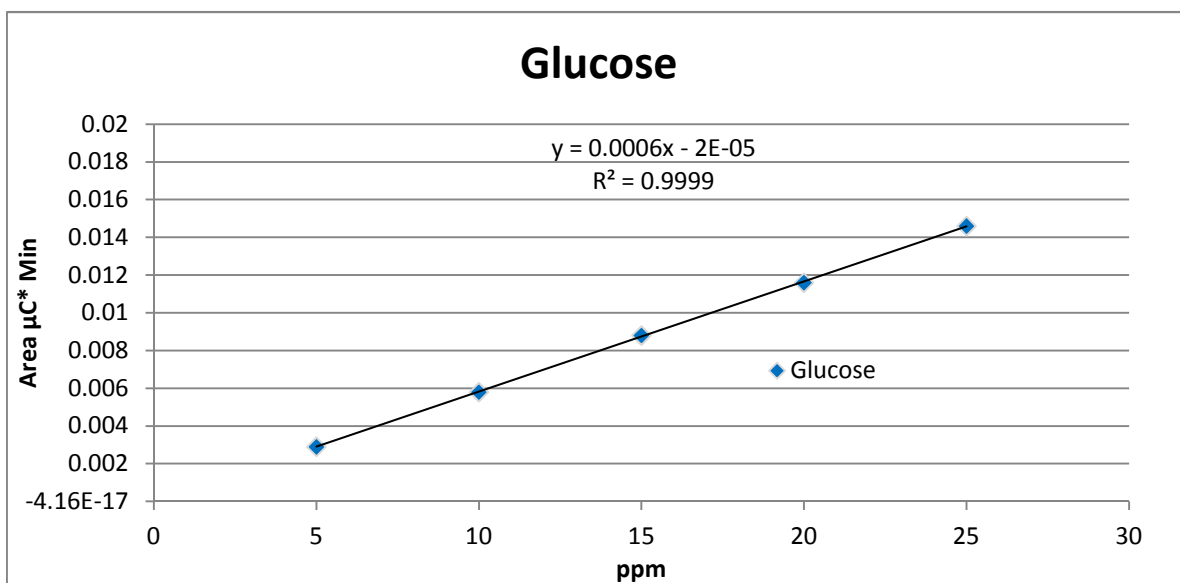


## 4.6.2 HPAEC-PAD Monomer Standard Curves

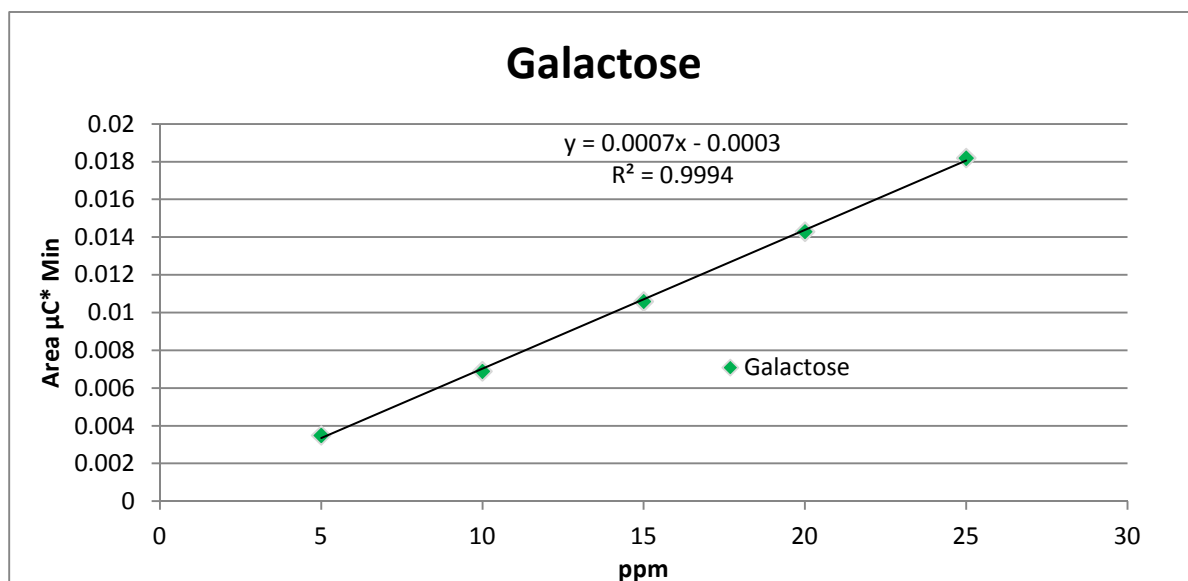
## 4.6.2.1 Rhamnose



## 4.6.2.2 Glucose

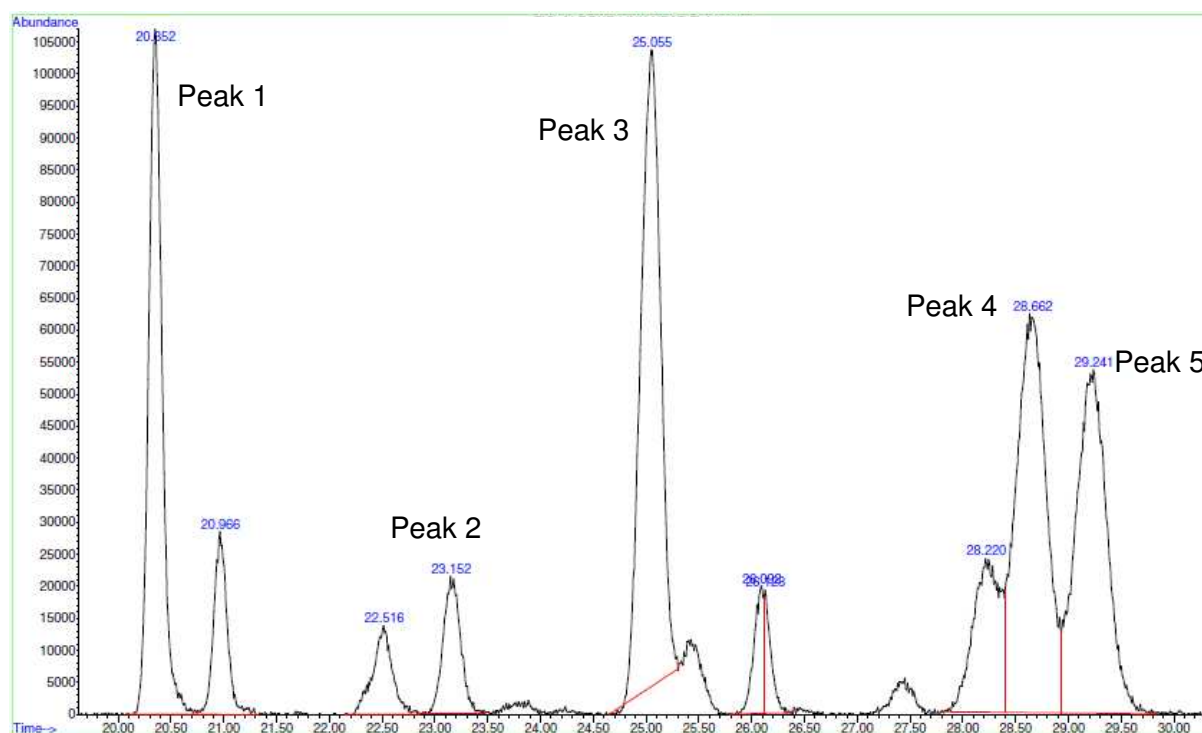


4.6.2.3 Galactose



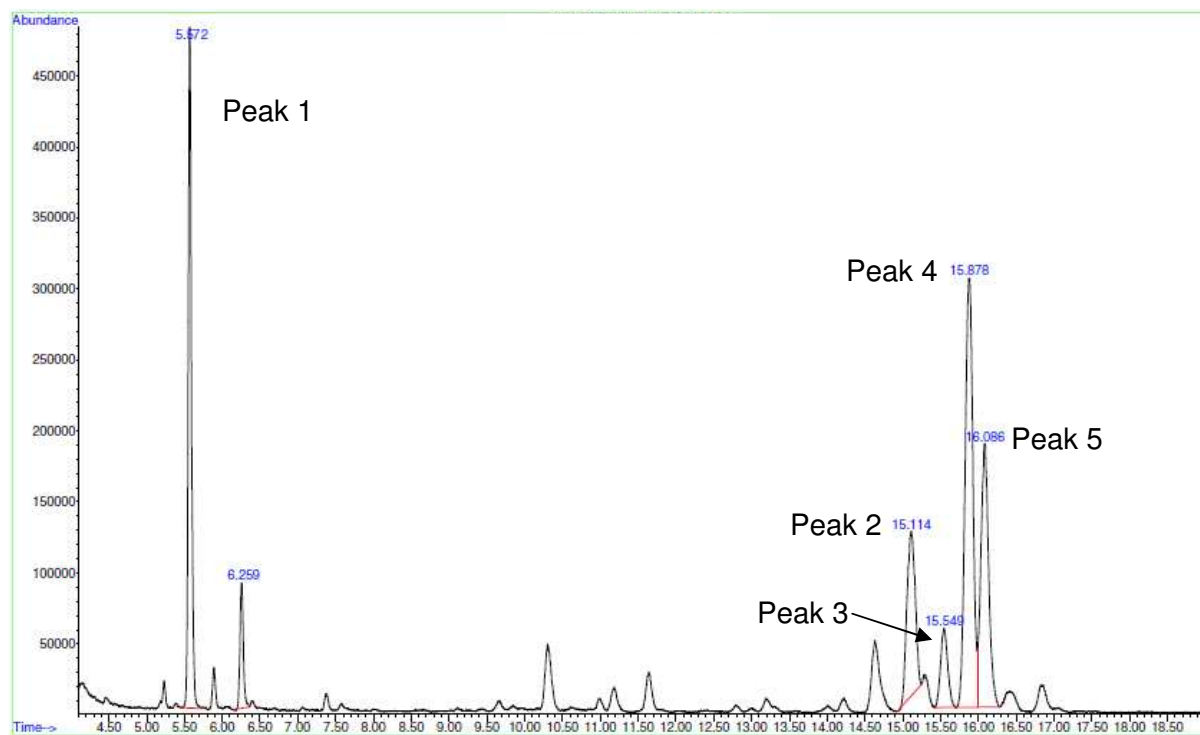
4.6.3 GC-MS Linkage Analysis

4.6.3.1 GC-MS Chromatogram of HMW EPS Linkages



#### 4.6.4 Absolute Configuration Analysis

##### 4.6.4.1 GC-MS Chromatogram of Absolute Configuration of HMW EPS Monomers



## 5. Ionic Liquids and Carbohydrates

### 5.1 Introduction

This chapter will discuss the dissolution and reactions of carbohydrates in two different ionic liquids: 1-butyl-3-methylimidazolium chloride (BMIMCl) and 1-ethyl-3-methylimidazolium acetate (EMIMAc). Firstly, cellulose will be examined as it has been widely studied in a variety of ionic liquids mediums. Following this the dissolution and chemical modification of a series of mono- and disaccharides in ionic liquids will also be examined.

#### 5.1.1 *EPS and Ionic Liquids*

The initial aim of this work was to study the dissolution of EPS in ionic liquids with the intention of analysing their structures and performing derivatisation on the sample *in situ*. Initially two previously characterised EPS samples were selected for analysis, these were derived from the strains *Lactobacillus acidophilus* 5e2<sup>131</sup> and *Lactobacillus delbrueckii* subsp. *bulgaricus* NCFB2074<sup>171</sup>.

Firstly <sup>1</sup>H and <sup>13</sup>C NMR spectra were obtained for each of the two ionic liquids (Figures 69 – 72). The samples of EPS (10% w/w) in the ionic liquids were prepared via the general dissolution method (see Chapter 2) and were subjected to <sup>1</sup>H and <sup>13</sup>C NMR analysis with D<sub>2</sub>O as the deuterated solvent present in the form of a glass insert inside the NMR tube. Analysis of the spectra revealed no signals corresponding to the presence of either of the two EPS structures. An attempt to increase the amount of EPS solubilised in the ionic liquids to greater than 10% w/w proved unsuccessful, dry milling of the samples prior to dissolution also did not result in an increase in solubility.

After extensive attempts to employ ionic liquids as alternative solvents for the dissolution and study of the native EPS structures it was determined that the technique would not be a viable venture. Very poor spectra were obtained that could not be used for structural characterisation. It is likely that a combination of factors including low sample solubility,

potential degradation of the EPS during dissolution and the preparation of solutions with high viscosity is responsible for the poor spectra.

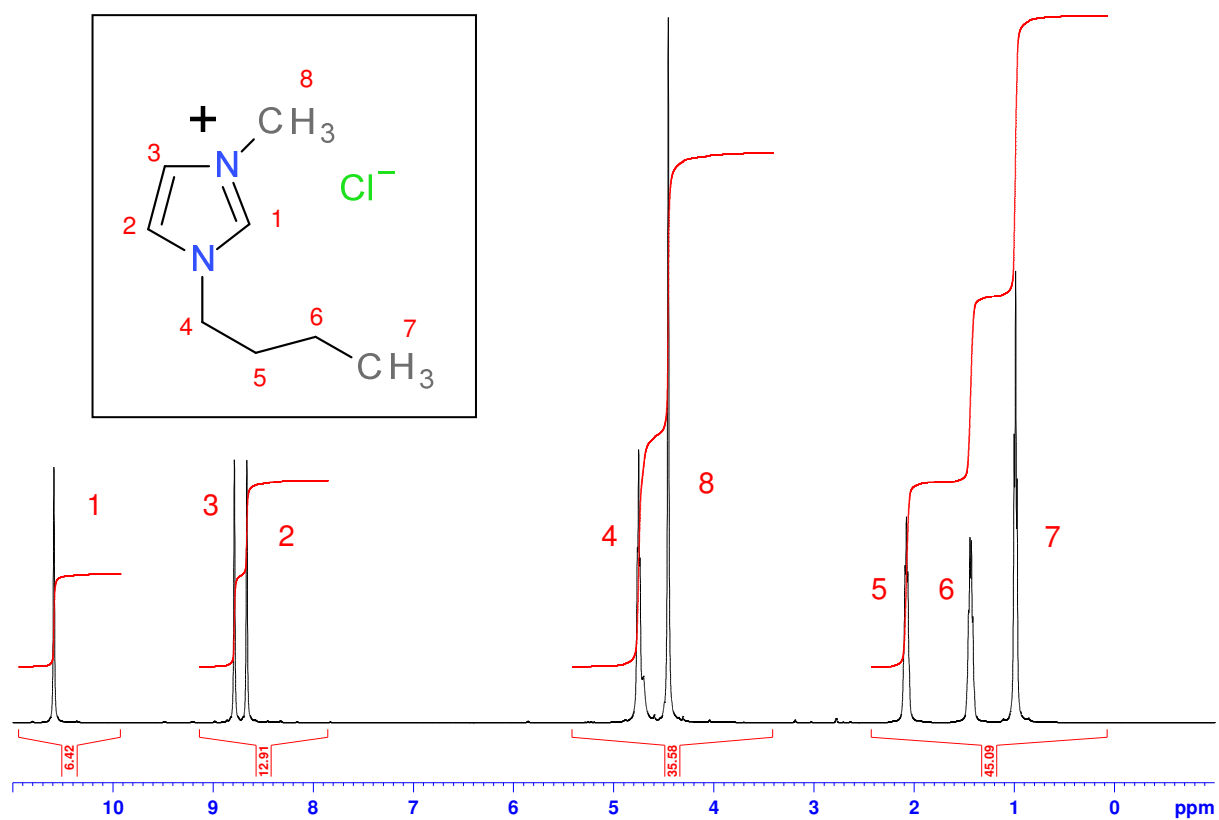


**Figure 69:  $^1\text{H}$  NMR Spectrum of BMIMCl with  $\text{D}_2\text{O}$  Insert at  $70^\circ\text{C}$**

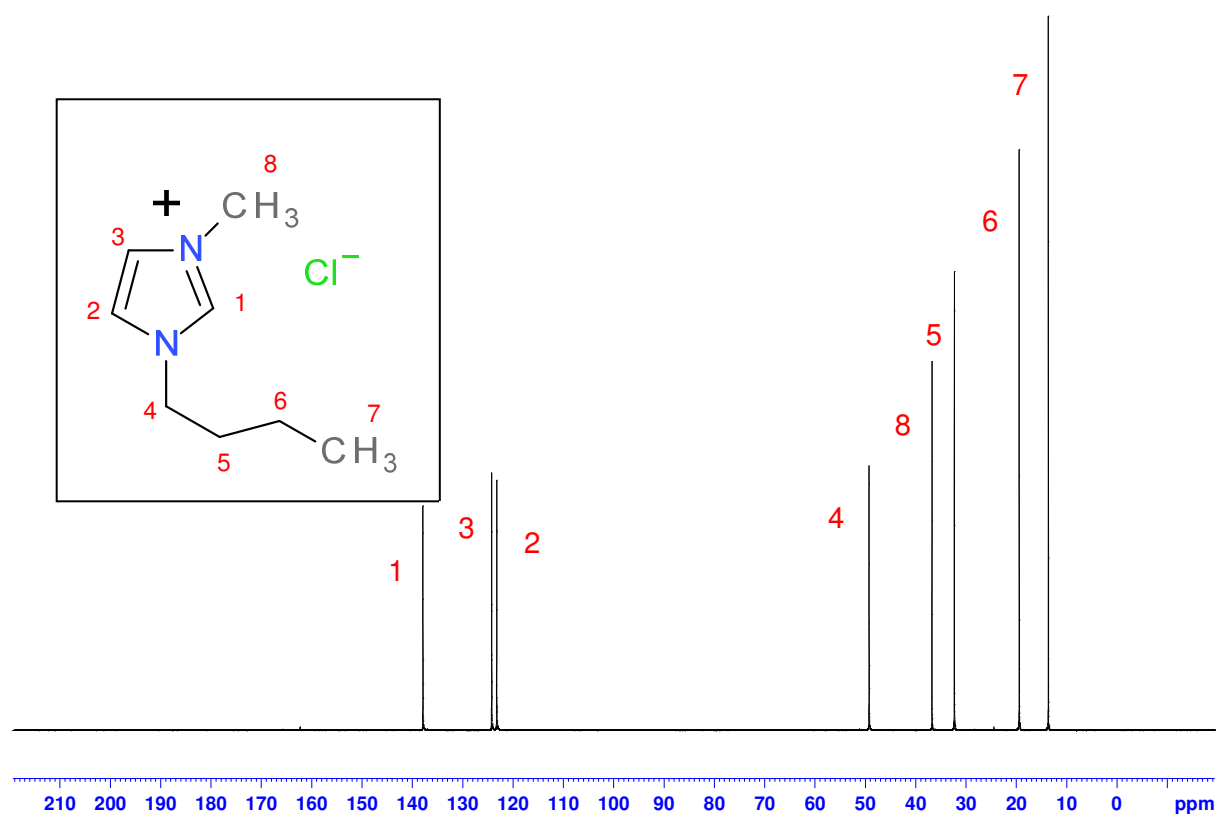


**Figure 70:  $^{13}\text{C}$  NMR Spectrum of BMIMCl with  $\text{D}_2\text{O}$  Insert at  $70^\circ\text{C}$**

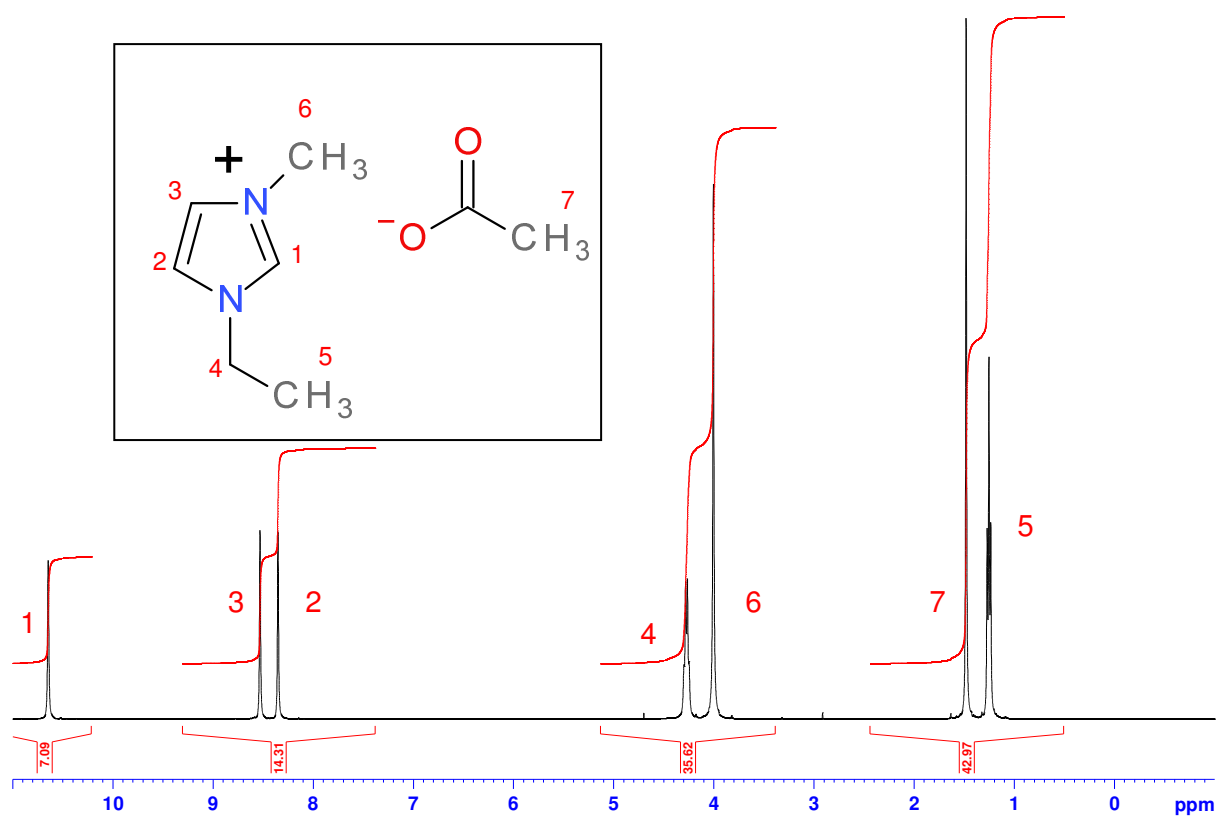


**Figure 71:  $^1\text{H}$  NMR Spectrum of EMIMAc with  $\text{D}_2\text{O}$  Insert at  $25^\circ\text{C}$**

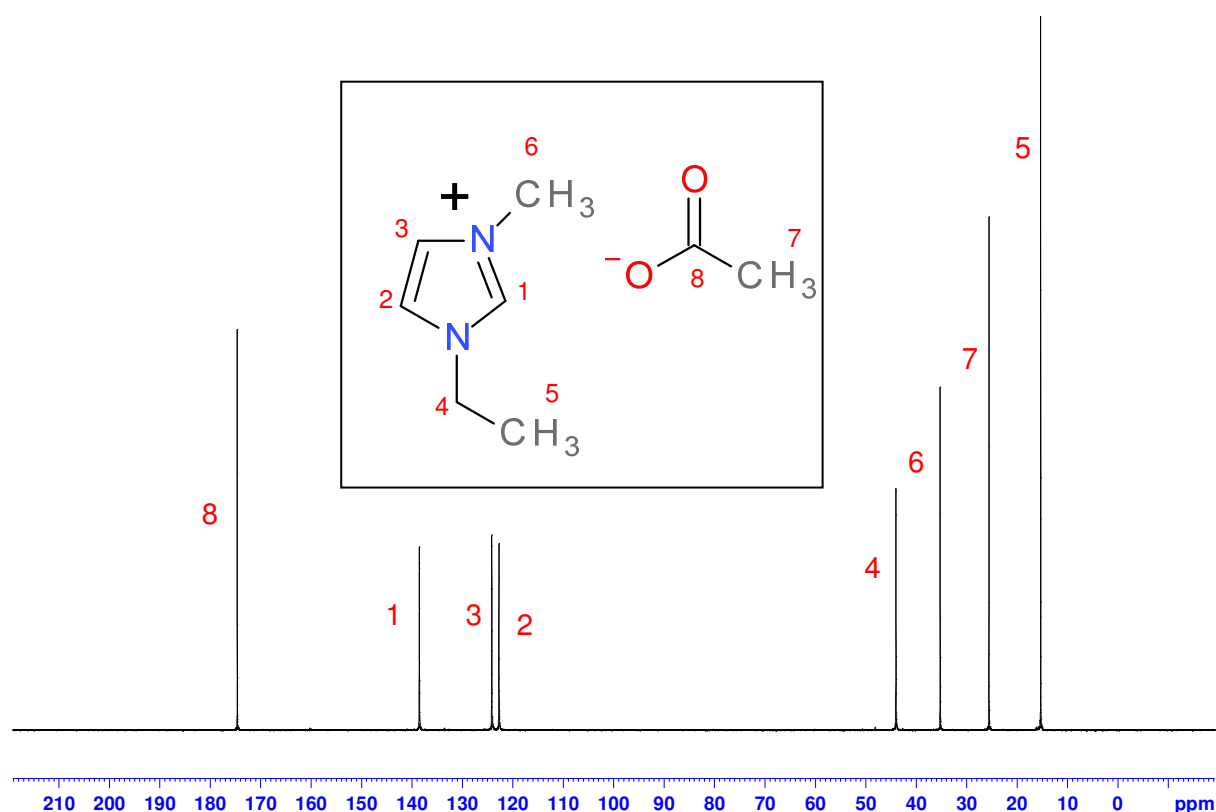


**Figure 72:  $^{13}\text{C}$  NMR Spectrum of EMIMAc with  $\text{D}_2\text{O}$  Insert at  $25^\circ\text{C}$**

## **5.2 Cellulose Dissolution and Modification in Ionic Liquids**

As previously discussed, cellulose has undergone numerous studies in ionic liquids in recent times<sup>177</sup>. Cellulose dissolution and modification has been widely studied as it is the most abundant biorenewable material on earth and there is an ongoing demand for the development of new cellulosic materials. Current technologies and methods involving cellulose however are seen to be of a non-environmentally friendly nature, hence the reason for the development of a new, 'greener' media for the processing and derivatisation of cellulose.

### *5.2.1 Cellulose Dissolution*

Cellulose (Figure 1) consists of polydisperse linear D-glucose polymer chains ( $n = 400 - 1000$ ) which form H-bonded supramolecular structures (Figure 73). Cellulose is insoluble in water as well as most common organic solvents, hence making its study in solution and

subsequent modification a challenging issue. Solubility is related to the molecular weight of the cellulose to be analysed, which in turn is controlled by the DP<sup>178</sup>.

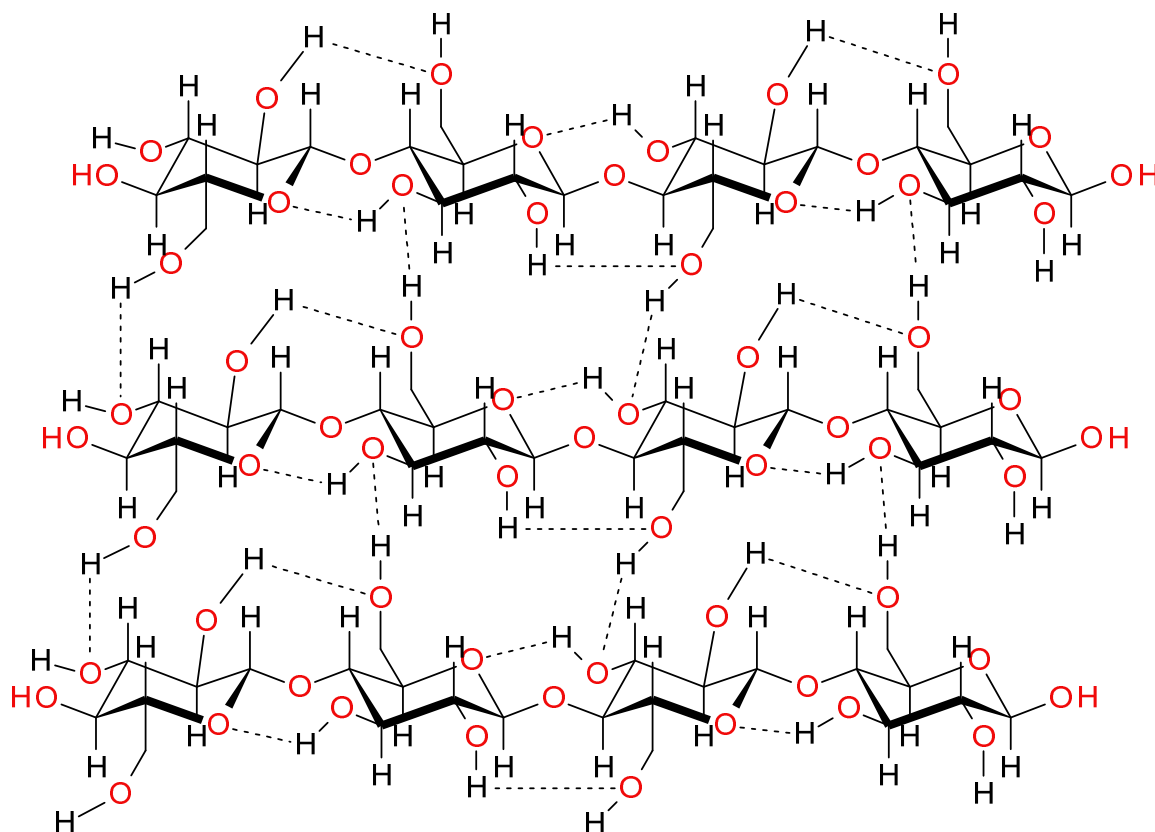


**Figure 73: Cellulose Supramolecular Structure**

It was decided that the initial ionic liquid work with cellulose and cellulose related materials undertaken by Swatloski *et al* in 2002<sup>150</sup> and continued with NMR studies by Moulthrop *et al* in 2005<sup>151</sup> would be examined. Minor changes were made to the referenced methodology as the concentration of cellulose was increased to 10% w/w (from 5%) whilst the spectra were recorded at the lower temperature of 70°C (instead of 90°C). The samples of cellulose were prepared via the general dissolution method (see Chapter 2) using both BMIMCl and EMIMAc; the resulting media were subjected to <sup>13</sup>C NMR analysis with DMSO-d<sub>6</sub> as the deuterated solvent in each case (Figure 74). Precautions were taken to exclude any presence of H<sub>2</sub>O from the reaction media as its presence can significantly decrease cellulose solubility due to competitive hydrogen bonding to the cellulose<sup>150</sup>.



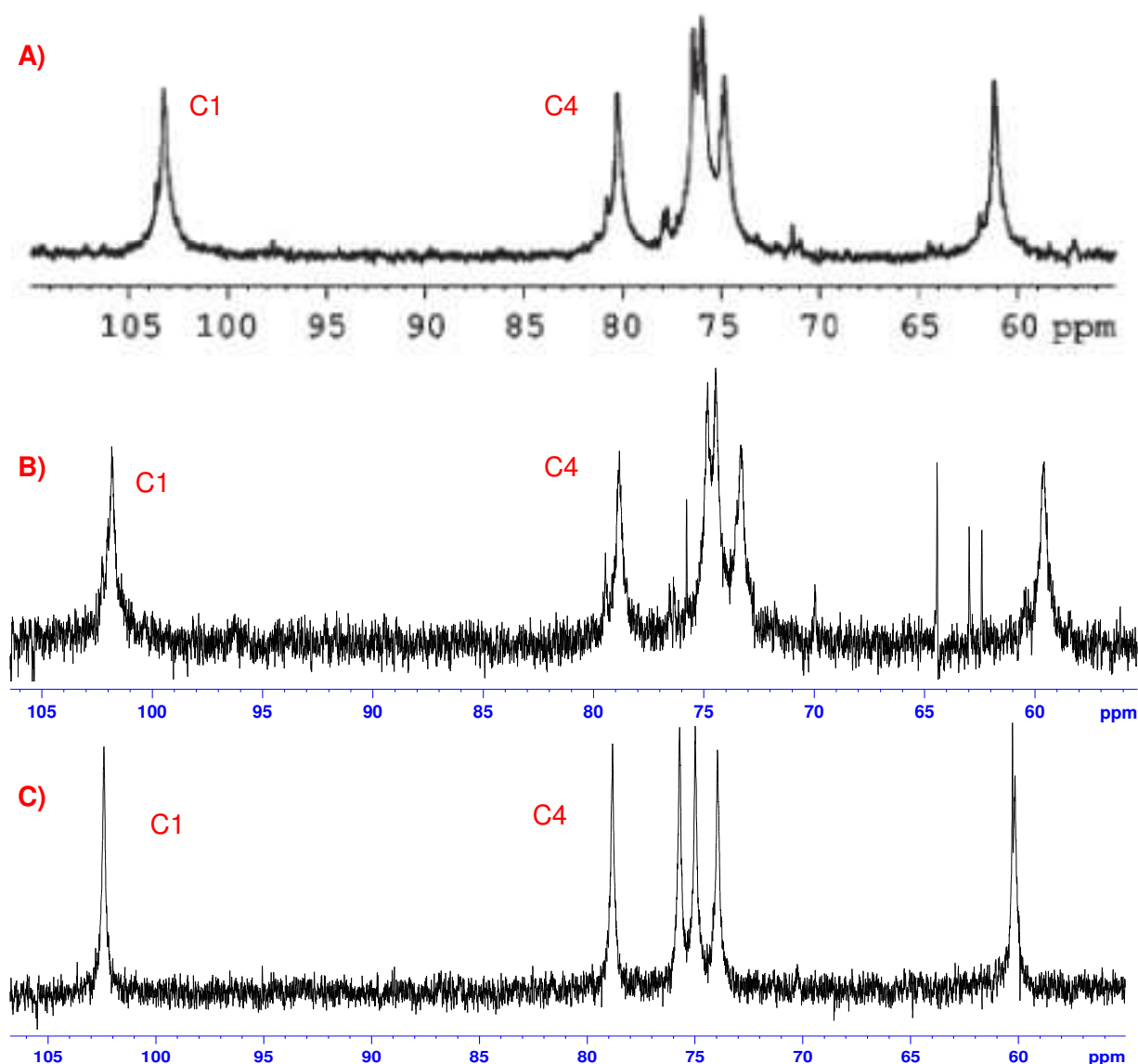


**Figure 74:  $^{13}\text{C}$  NMR Spectra of Cellulose in Solution BMIMCl/DMSO- $\text{d}_6$  5% w/w at  $90^\circ\text{C}$  – adapted from Moulthrop *et al* 2005<sup>151</sup>; B) BMIMCl/DMSO- $\text{d}_6$  10% w/w at  $70^\circ\text{C}$ ; C) EMIMAc/DMSO- $\text{d}_6$  10% w/w at  $70^\circ\text{C}$**

It should firstly be noted that the small amount of DMSO- $\text{d}_6$  was selected as the lock solvent as it does not interfere with potential areas of interest in the spectra. From the initial inspection of all three spectra it can be observed that they share the same main peaks. The C1 and C4 signals can be identified in both spectra B) and C) and demonstrate similar chemical shifts when contrasted to those previously obtained by Moulthrop *et al*<sup>151</sup> (spectra A)) (Table 11). Direct comparison of the BMIMCl/10% with the EMIMAc/10% spectra indicates that the peaks in the latter are more resolved.

**Table 11: Recorded  $^{13}\text{C}$  Chemical Shift Values for C1 and C4 for Samples A), B) and C)**

Cellulose Sample	$^{13}\text{C}$ Chemical Shift (ppm)	
	C1	C4
A)	103.2	80.2
B)	101.9	79.0
C)	103.3	79.7

Also visible in the BMIMCl spectrum were a number of small impurity peaks, indicating a degree of cellulose degradation. The implications of possible polymer degradation will be further explored in the following sections with the dissolution and chemical modification of a series of disaccharides.

EMIMAc was chosen to be studied along with BMIMCl as they both possess a similar general structural motif but confer differing properties. For example, the decrease in chain length of the alkyl moiety (from butyl to ethyl) on the cation portion of the ionic liquid decreases hydrophobicity therefore reducing the viscosity of the solution<sup>148</sup>. This difference in viscosity could account for the greater resolution of the signals observed in the EMIMAc spectrum. Another difference to be noted is that EMIMAc is a room temperature ionic liquid (RTIL) (mpt.  $< 20^\circ\text{C}$ ), whilst BMIMCl has an mpt. of  $\sim 70^\circ\text{C}$ , traditionally RTILs are easier to work with for obvious reasons. The potential effects due to the properties of the anion must also be considered. The  $\text{Cl}^-$  ion in the BMIMCl complex has been proven to be highly effective in breaking the strong hydrogen bonding present in cellulose. Hydrogen bonding between carbohydrate hydroxyl protons and  $\text{Cl}^-$  ions of the ionic liquid has demonstrated the presence of a 1:1 stoichiometry<sup>179</sup> (Figure 75).

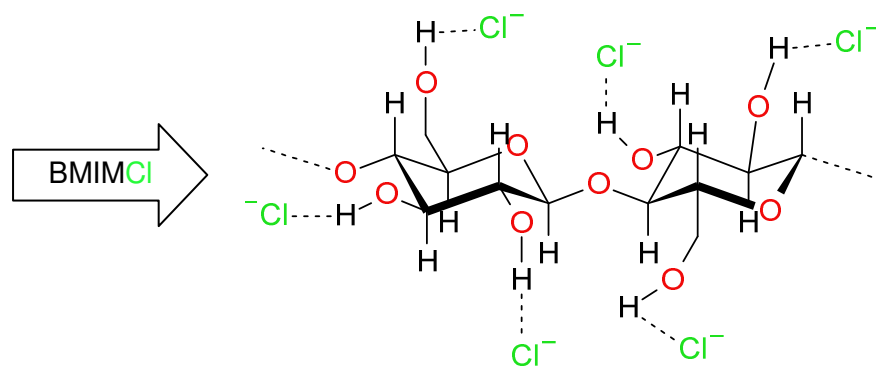


**Figure 75: Cellulose Hydrogen Bonding Disruption by BMIMCl**

### 5.2.2 Cellulose Modification to Improve Dissolution

As previously mentioned due to the vast availability combined with its highly renewable nature, cellulose is a common target for the development of new cellulosic based polymers. However along with this development of new functionalised cellulose polymers, alternative methodologies for established and currently commercially produced functionalised forms of cellulose, including acetates, nitrates and carboxymethyls are also being continually developed<sup>180</sup>. An alternative method for preparing EPS samples suitable for analysis would be to form derivatives that were soluble in ionic solvents. Laws *et al* (2005)<sup>171</sup> have previously achieved solubility of EPS samples by per-methylation.

The acetylation of cellulose to form cellulose acetate is a well documented reaction with cellulose acetate being produced on a commercial scale for a variety of uses. Cellulose acetate is conventionally made by treatment with acetic anhydride in the presence of sulphuric acid (acting as a catalyst)<sup>181</sup>. With the advent of ionic liquids and the current drive towards their use as an alternative reaction media for carbohydrate dissolutions and functionalisations, many common methods including cellulose acetylation have previously been reported<sup>177</sup>. In an attempt to observe if EPS could potentially be per-acetylated in ionic liquids an initial investigation was performed to determine the best conditions for acetylating cellulose.

In this study, the acetylation of cellulose employing conventional reagents (pyridine and acetic anhydride) in both BMIMCl and EMIMAc was explored. The samples of cellulose (5% w/w) were prepared via the general dissolution method using both BMIMCl and EMIMAc, and acetylated following the general acetylation protocol (see Chapter 2 section 2.4.1 and 2.4.2). The samples were then extracted using the liquid – liquid extraction procedure (see Chapter 2 section 2.4.3). Both samples were subjected to a series of 1D- and 2D-NMR experiments with all spectra recorded at 70°C in deuterated chloroform ( $\text{CDCl}_3$ ).

The first spectra recorded (in  $\text{CDCl}_3$ ) were 1D- $^1\text{H}$  NMR (Figures 76) and 1D- $^{13}\text{C}$  spectra; from this, the regions of interest can initially be identified. The methyl hydrogens of the acetyl can be identified occurring between 1.75 – 2.2 ppm whilst the ring protons of the glucose monomer can be observed between 3.5 – 5.2 ppm. The carbonyl carbons of the acetyl can be observed between 169 – 171 ppm whilst the methyl carbons of the acetyl can be identified between 20 – 21 ppm (Figure 77). The ring carbons of the glucose monomer can be observed between 60 – 105 ppm. The NMR data observed is in accordance with previously reported literature values<sup>182</sup>. Only BMIMCl data shown.

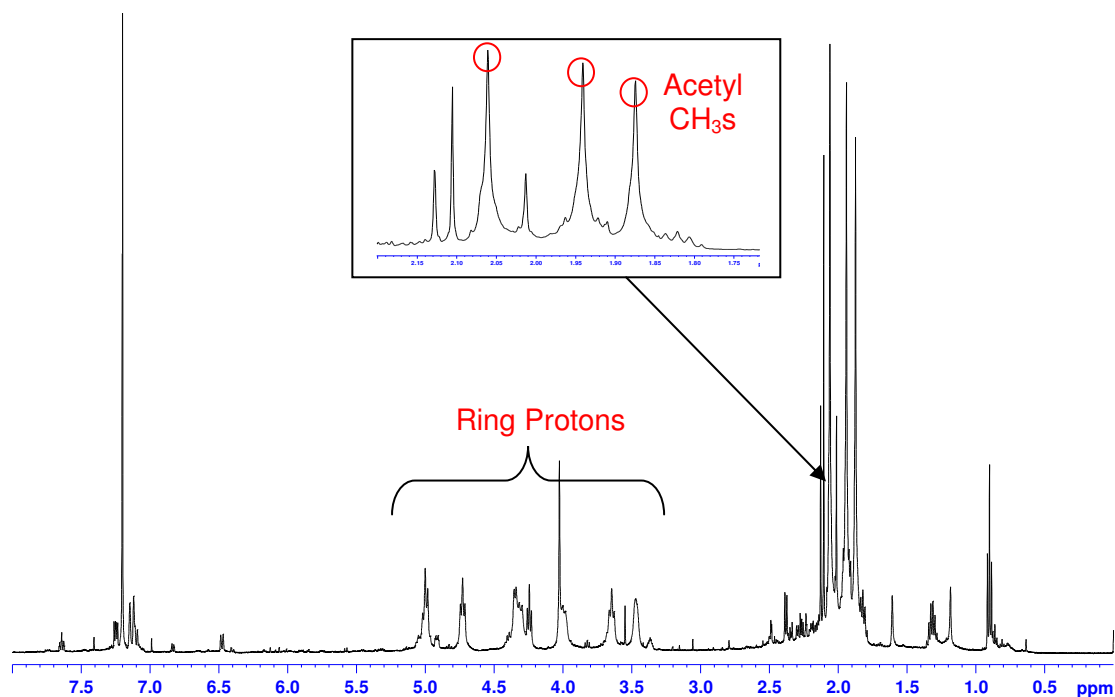


**Figure 76:  $^1\text{H}$  NMR Spectrum of Cellulose Acetylated in BMIMCl at 70°C in  $\text{CDCl}_3$**

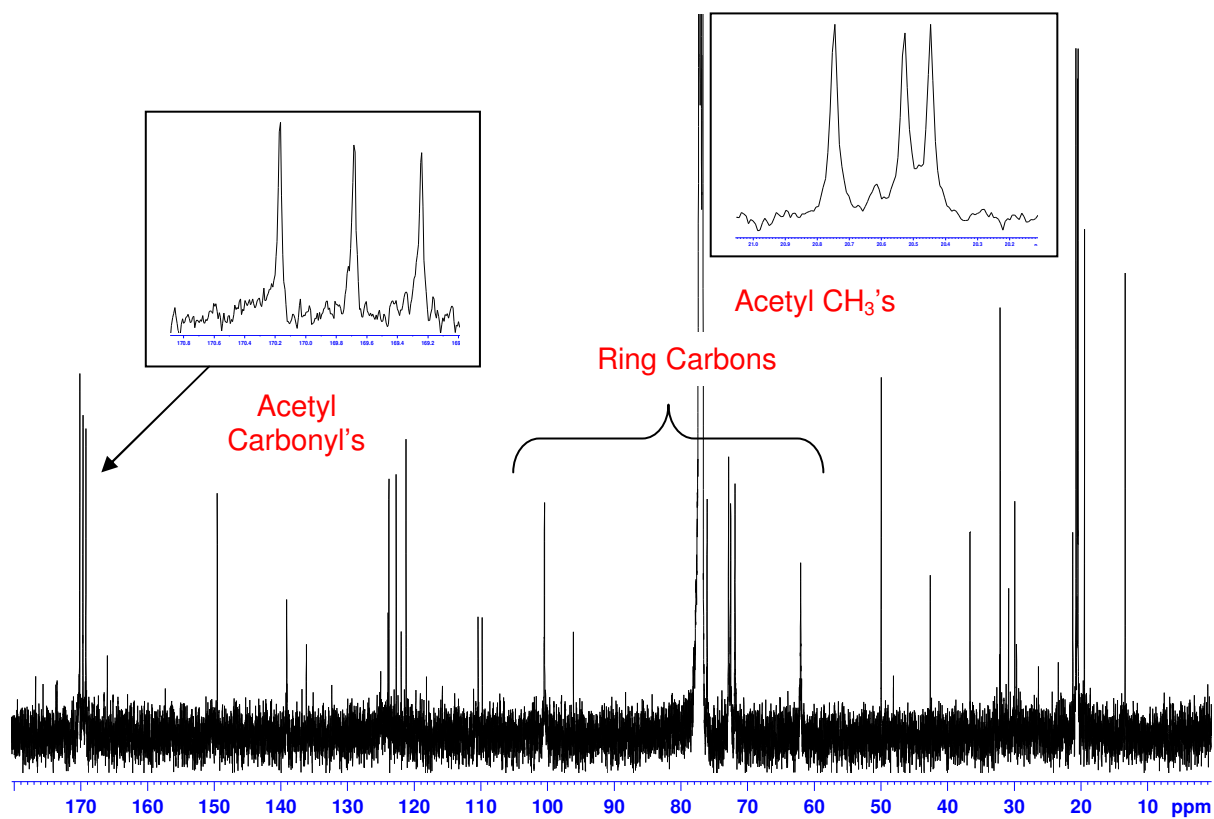


**Figure 77:**  $^{13}\text{C}$  NMR Spectrum of Cellulose Acetylated in BMIMCl at 70°C in  $\text{CDCl}_3$

In order to assign the identity of the position of each of the protons present in the monomer ring a COSY (H, H) experiment was performed (Figure 78). Starting with the knowledge of the position of the anomeric proton at 4.34 ppm (See Figure 79), all of the remaining ring protons could be successfully elucidated.

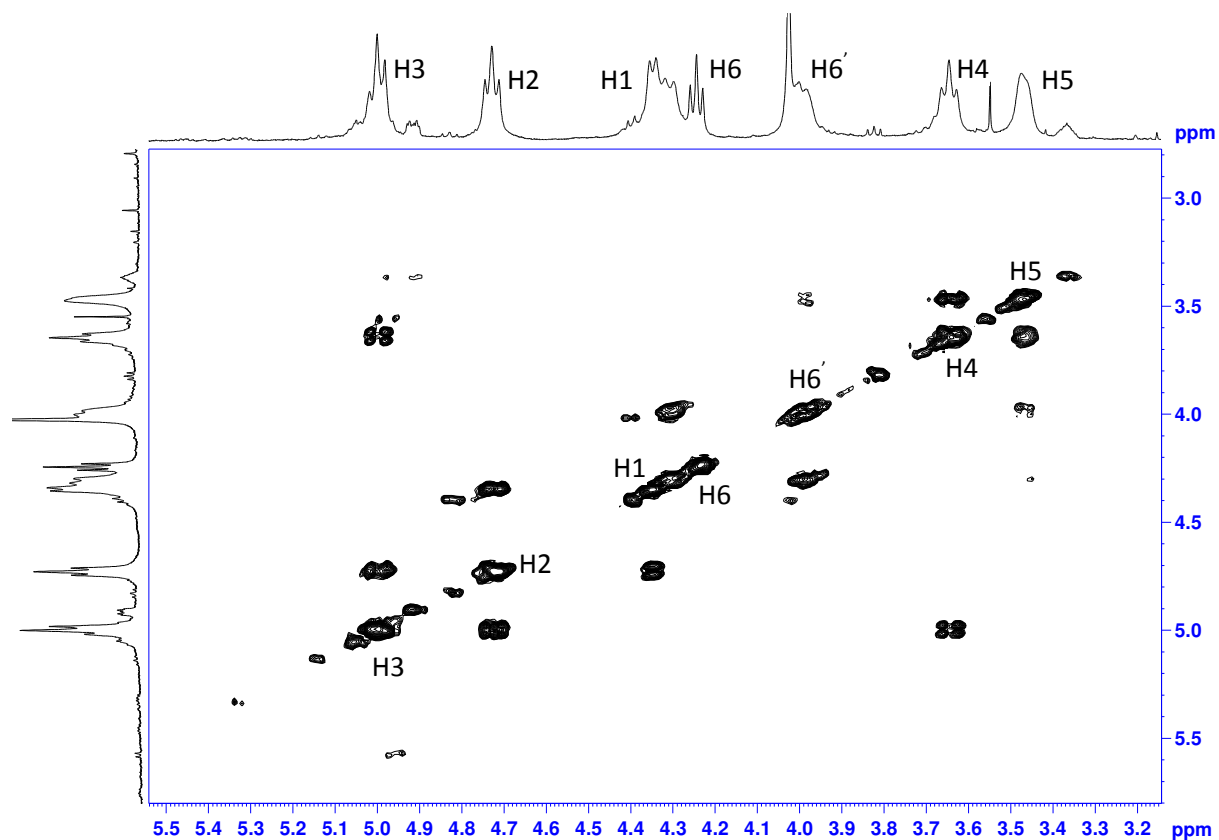


**Figure 78: COSY Spectrum of Ring Proton Region of Cellulose Acetylated in BMIMCl at 70°C in  $\text{CDCl}_3$**

With the assignment of the complete proton signals for the acetylated cellulose monomer the correlating carbons can be identified on the  $^1\text{H}$ - $^{13}\text{C}$  HSQC experiment (Figure 79).

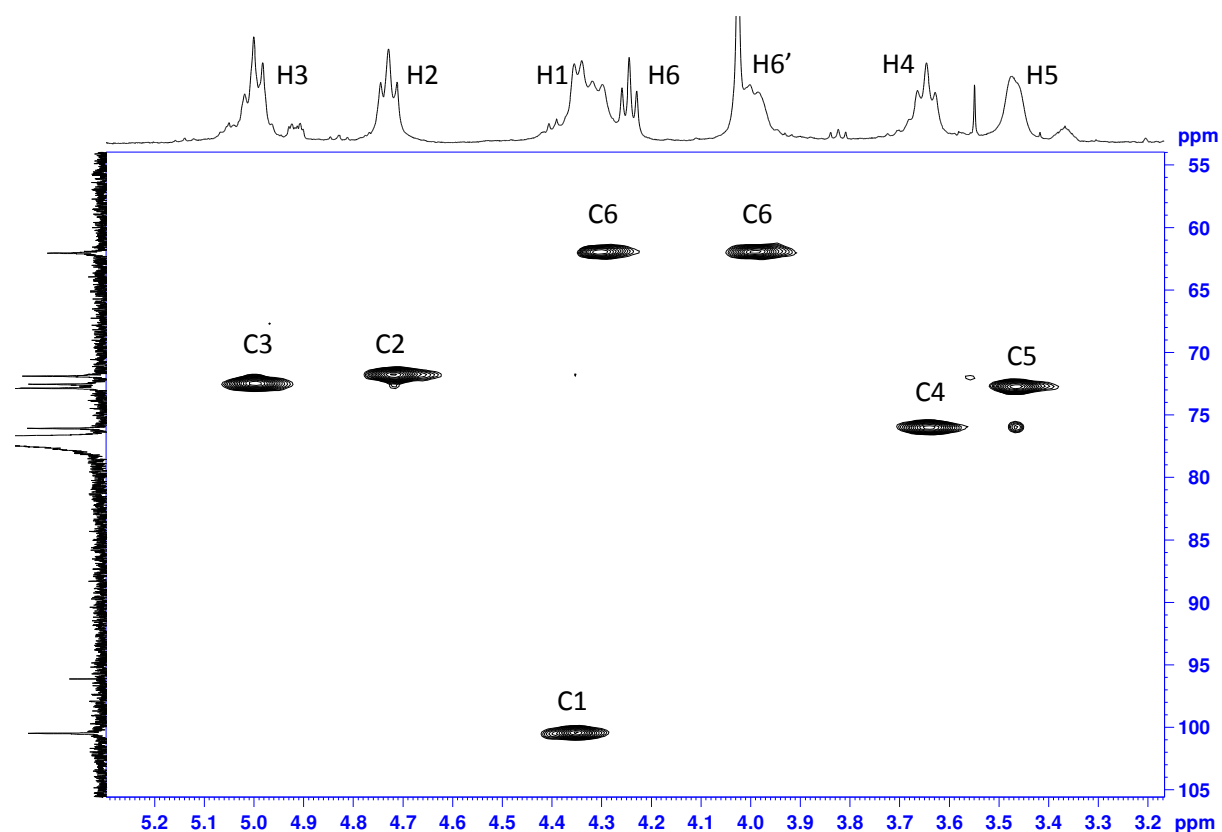


**Figure 79:  $^1\text{H}$ - $^{13}\text{C}$  HSQC Spectrum of Ring Proton Region of Cellulose Acetylated in BMIMCl at 70°C in  $\text{CDCl}_3$**

The  $^1\text{H}$  and  $^{13}\text{C}$  chemical shifts are detailed in Table 12.

**Table 12:  $^1\text{H}$  and  $^{13}\text{C}$  NMR Shifts of Cellulose Acetate in  $\text{CDCl}_3$  at 70 °C**

	Chemical Shift (ppm)						
	H1	H2	H3	H4	H5	H6	H6'
<b>Cellulose</b>							
<b>Acetate</b>	4.34	4.72	5.00	3.64	3.46	4.39	3.99
<b>(BMIMCl)</b>							
	C1	C2	C3	C4	C5	C6	
	100.47	71.92	72.58	76.09	72.88	62.05	

It can be observed from the examination of the NMR spectra that the cellulose sample is fully acetylated (at positions C2, C3 and C6)<sup>183</sup>. The degree of substitution (DS) of the cellulose acetate generated (by both reactions – BMIMCl and EMIMAc) was also determined by  $^1\text{H}$  NMR.

The DS of acetyl cellulose was determined by using the ratio of 1/3 three methyl protons integration between 1.75 – 2.2 ppm divided by 1/7 of the total cellulose ring proton CH areas observed between 3.5 – 5.2 ppm. The DS for cellulose acetylated in BMIMCl was determined to be approximately 2.15 whilst the DS for cellulose acetylated in EMIMAc was determined to be approximately 1.91<sup>184</sup>. These results are comparable with data obtained by Wu *et al* in 2004<sup>181</sup> using another ionic liquid, 1-allyl-3-methylimidazolium chloride (AMIMCl). It should be noted that ideally, for NMR analysis a DS of 3 is usually required. It should be noted that, the other acetyl peaks in the spectrum occur as a result of free glucose residues which have been fully acetylated.

Again, as with the initial dissolution of cellulose, possible polymer degradation products, this time acetylated, were identified from the NMR spectra.

### 5.2.2 Ionic Liquid Recycling

A desirable feature often attached to ionic liquids is their ability to be recycled and subsequently used again. This attribute has been repeatedly demonstrated with a variety of ionic liquids in a variety of reactions<sup>177</sup>.

The two ionic liquids employed in this section were successfully recycled on more than one occasion. As the ionic liquids are miscible in water the aqueous portion obtained from the liquid – liquid extraction procedure (used to isolate the synthesised products) was retained. The aqueous sample was then dried via either rotary evaporation at a heightened temperature or by lyophilisation overnight. A sample was then subjected to <sup>1</sup>H NMR analysis (D<sub>2</sub>O insert at 70°C) for examination of its purity. Whilst the recycled BMIMCl was slightly contaminated with acetic anhydride the EMIMAc sample was observed to be free of any starting materials or reaction end products (see Appendix).



### **5.3 Disaccharide Dissolution and Modification**

As well as cellulose, many other carbohydrates have undergone dissolution and modifications in a variety of ionic liquids. Moulthrop *et al* (2005) also studied the dissolution of cellulosic oligomers<sup>151</sup> whilst Liu *et al* (2005) examined the solubility of sucrose and lactose<sup>149</sup>, (amongst other compounds) and their behaviour in ionic liquids.

#### *5.3.1 Analysis of Cellobiose in Ionic Liquid Systems – A Simplified Model for Derivatisation Reactions*

Following on from the dissolution and acetylation of cellulose in BMIMCl and EMIMAc it is a logical step to examine the properties of cellobiose (see Table 4, Chapter 3) in solution. Cellobiose was used as a model system; the aim of the reactions was to see if degradation could be reduced whilst producing fully acetylated derivatives. Cellobiose is the smallest repeating unit ( $n = 1$ ) of cellulose (Figure 1), comprised of two  $\beta$ -(1 $\rightarrow$ 4) linked glucose monomers.

##### 5.3.1.2 Dissolution of Cellobiose in BMIMCl

Initially a 10 % w/w sample of cellobiose was prepared via the general dissolution method (see Chapter 2) using BMIMCl; the resulting solution was subjected to <sup>13</sup>C NMR analysis with DMSO-d<sub>6</sub> as the lock solvent (Figure 80).

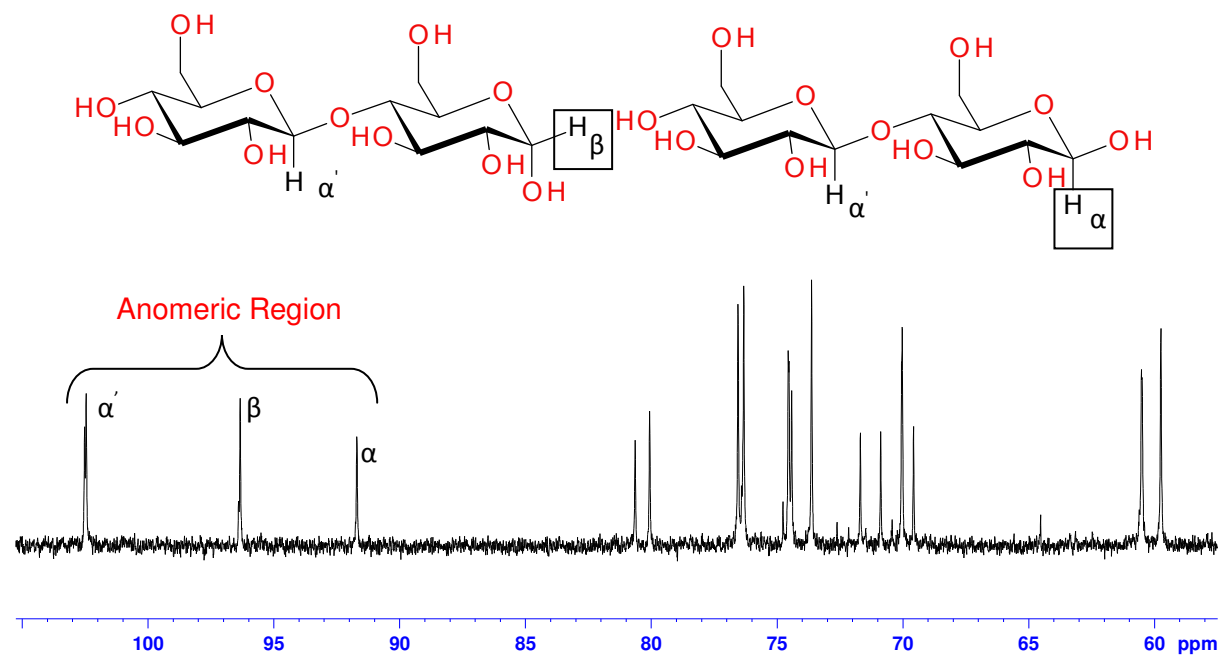


**Figure 80: Cellobiose Displayed in Both Reducing End Conformations (Above)  $^{13}\text{C}$  NMR Spectra of Cellobiose in Solution BMIMCl/DMSO- $d_6$  10% w/w at 70°C (Below)**

From the spectra it can be observed that cellobiose is readily soluble in the ionic liquid. The anomeric carbons can immediately be identified ( $\alpha'$  – 102.49 ppm,  $\beta$  – 96.36 ppm and  $\alpha$  – 91.70 ppm) and these values are comparable to literature values<sup>185</sup>.

### 5.3.1.3 Acetylation Catalysts

The following section will focus on the acetylation of cellobiose in ionic liquids; this will be documented and analysed through the use of NMR, GC-MS and MS with MS/MS. A number of other, alternative acetylation techniques will also be explored.

As previously referred to, acetylation is a technique applied in carbohydrate chemistry not only for hydroxyl group protection but also for purification and structural elucidation purposes<sup>186</sup>. Pyridine is the most frequently employed acetylation catalyst and also can be used as the reaction solvent, whilst sodium acetate is also commonly utilised, however a number of other alternative catalytic reagents have also been explored. Such alternative catalysts include: - Lewis acids e.g. zinc chloride<sup>187</sup>; phase-transfer catalysts e.g. tetra-*n*-butylammonium bromide-sodium hydroxide<sup>188</sup>; heterogeneous catalysts e.g. inorganic solid

acids such as Montmorillonite K-10<sup>189</sup>; enzymatic catalysts e.g. lipases<sup>190</sup>. Ionic liquids have also been applied in the acetylation process as either solely in the capacity as a solvent or as a catalytic solvent<sup>191,186</sup>.

The three classical and most frequently encountered catalytic reagents were selected to be studied as they provide differing degrees of anomeric specificity. In acetylation of monosaccharides, pyridine produces a mixture of  $\alpha$  and  $\beta$  anomers as acetylation occurs faster than mutarotation about the anomeric carbon (caused by the electrophile catalysing the epimerisation of the anomeric centre); therefore producing a ratio of anomers that corresponds to the anomeric mixture in the free sugar starting material. Sodium acetate is a weak base and consequently the reaction is required to be performed at an elevated temperature (100°C). This allows for mutarotation to occur faster than the acetylation, thereby allowing the more nucleophilic  $\beta$ -hydroxyl preference in the reaction permitting the selective formation of the  $\beta$ -product. The addition of zinc chloride as a catalyst however confers a preference for the  $\alpha$  anomer. This occurs as the  $\alpha$  anomer is thermodynamically favoured by the anomeric effect which takes prominence in the reaction as the zinc chloride catalyses the equilibration of the final product<sup>6</sup>.

#### 5.3.1.4 Acetylation of Cellobiose in BMIMCl

In this study, the acetylation of cellobiose was achieved initially by employing conventional reagents (pyridine/acetic anhydride, zinc chloride/acetic anhydride and sodium acetate/acetic anhydride) in BMIMCl. The samples of cellobiose (10% w/w in BMIMCl) were prepared via the general dissolution method and acetylated following the general acetylation protocol (see Chapter 2). The products were then extracted using the liquid – liquid extraction procedure (see Chapter 2). Firstly the samples were subjected to <sup>1</sup>H proton NMR with all spectra being recorded at 70°C in CDCl<sub>3</sub>.

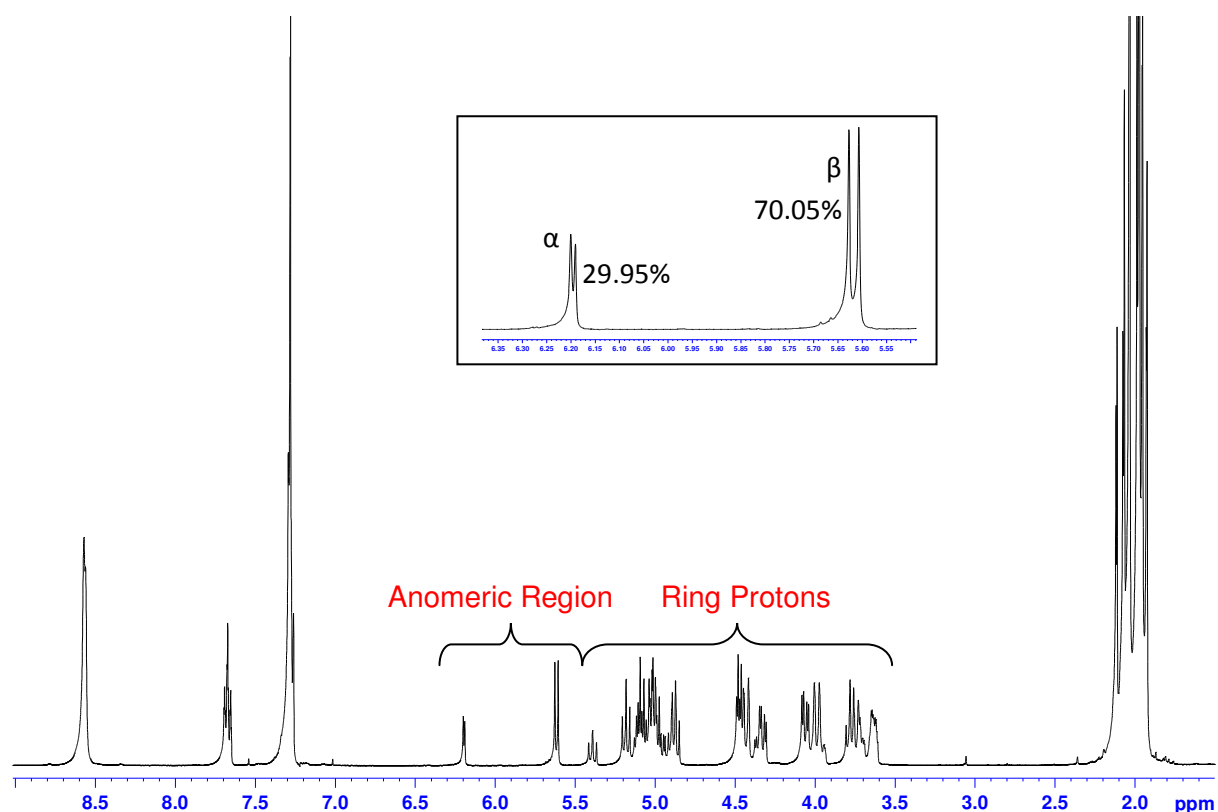


**Figure 81:  $^1\text{H}$  NMR Spectrum of Cellobiose Acetylated in BMIMCl with Pyridine at  $70^\circ\text{C}$  in  $\text{CDCl}_3$ ; Inset - Magnified Region showing Reducing End anomeric Signals**

The acetylation of cellobiose with pyridine led to the generation of the fully acetylated octaacetate product (Figure 81). The expected ratio of  $\alpha/\beta$  anomers (for the reducing end of the cellobiose molecule) was also observed as 29.95 % and 70.05 % for  $\alpha$  and  $\beta$  respectively, this was determined by the analysis of the signal heights in the NMR spectra. As further confirmation, the product was also subjected to GC-MS and MS with MS/MS analysis.

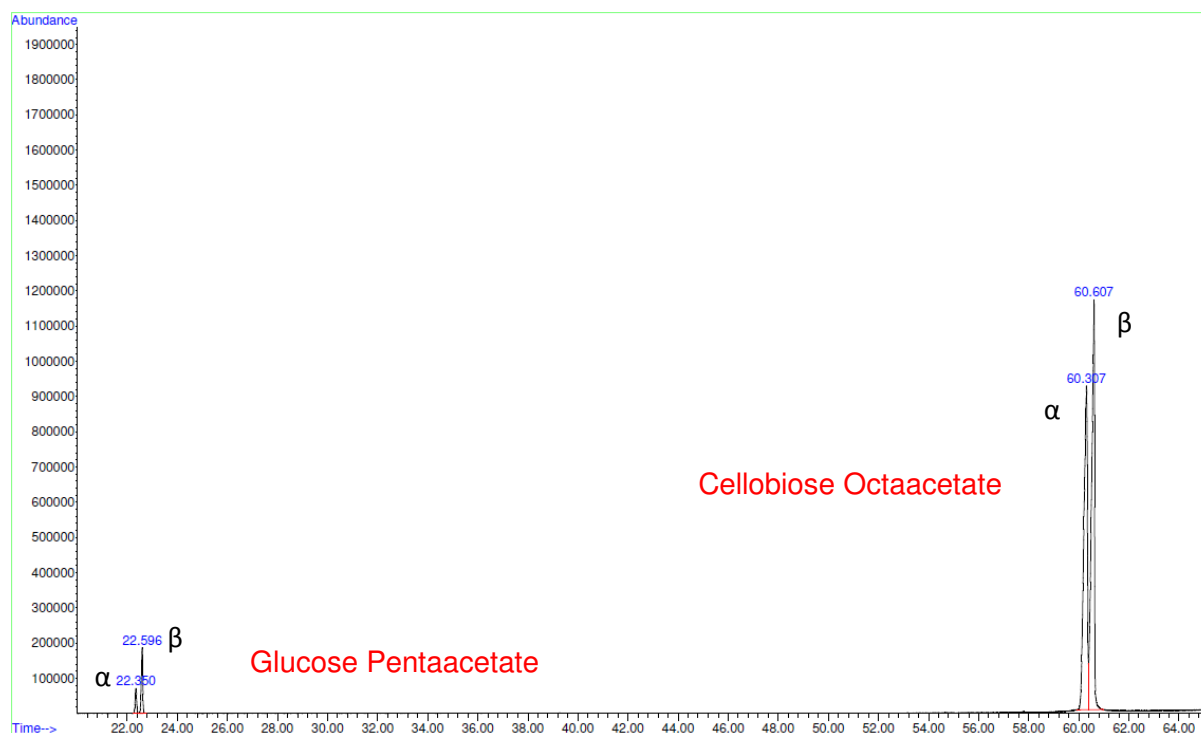


**Figure 82: GC-MS Chromatogram of Cellobiose Acetylated in BMIMCl with Pyridine**

In GC-MS analysis the product produced four distinct peaks in the GC-MS chromatogram (Figure 82). The two most abundant peaks (at 60.309 and 60.610 minutes) were identified as arising from each of the  $\alpha$  and  $\beta$  cellobiose octaacetate anomers, this was confirmed by comparison with a standard of  $\alpha$ -cellobiose octaacetate (see Appendix). The two smaller peaks (at 22.350 and 22.596 minutes) were identified as  $\alpha$  and  $\beta$  glucose pentaacetate. It was not clear however whether the degradation products ( $\alpha/\beta$  glucose pentaacetate) were generated during the acetylation reaction or as a result of the GC-MS analysis.

The MS (Figure 83) with MS/MS (see Appendix) data also provided further confirmation of successful acetylation of the cellobiose.

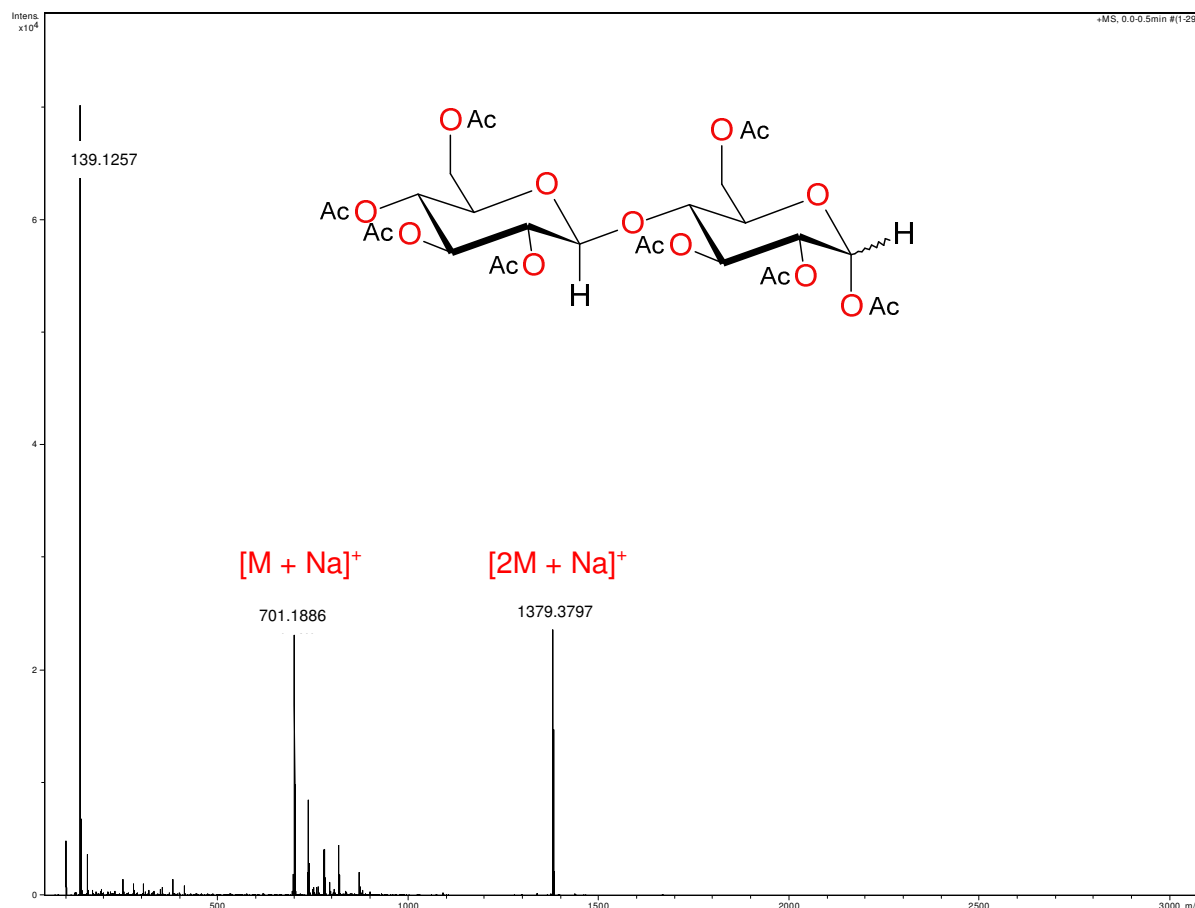


**Figure 83: MS Spectrum of Cellobiose in BMIMCl with Pyridine**

The molecular ion for cellobiose octaacetate (MW 678.59) can be identified as a sodiated ion,  $[M + Na]^+$ , visible as the peak observed at 701.18 m/z. A peak corresponding to the ion  $[2M + Na]^+$  was also detected at 1379.37 m/z. The  $[M + Na]^+$  ion located at 701.18 m/z was examined further by MS/MS to determine the fragmentation pattern, this data is located in the appendix.

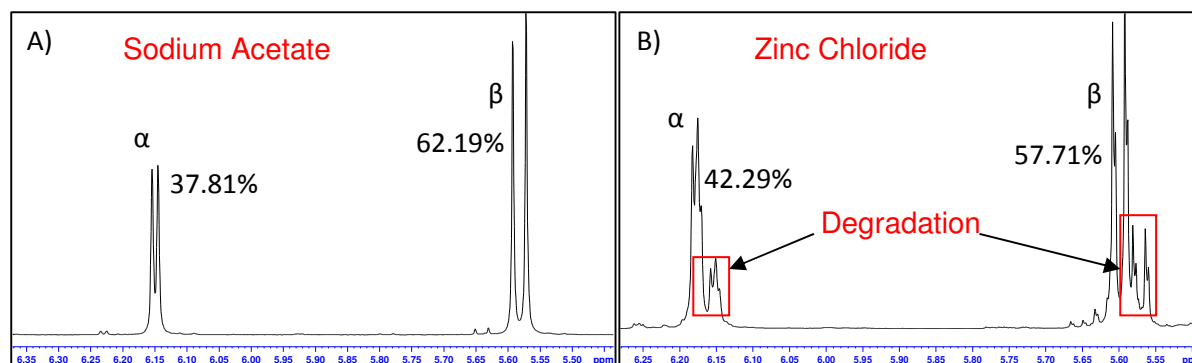


**Figure 84: Anomeric Region of  $^1\text{H}$  NMR Spectrum of Cellobiose Acetylated in BMIMCl  
A) Sodium Acetate and B) Zinc Chloride at 70°C in  $\text{CDCl}_3$**

The results obtained for the acetylation reactions catalysed by sodium acetate and zinc chloride however were not as expected. Examination of the  $^1\text{H}$  NMR spectra initially indicated the desired octaacetate product had been successfully synthesised in both reactions. Although the ratios of  $\alpha$  and  $\beta$  anomers did not conform to the proportions expected (Figure 84).

As previously noted the reaction catalysed by sodium acetate was expected to produce primarily the  $\beta$  product. It was identified however that the ratio of  $\alpha/\beta$  product was 37.81% and 62.19% respectively. Whilst the reaction catalysed with zinc chloride, instead of producing exclusively the  $\alpha$  product as predicted, exhibited a ratio of 42.29%  $\alpha$  anomer and 57.71%  $\beta$  anomer.

As with the pyridine catalysed extract, both the GC-MS and MS (with MS/MS) data confirmed the successful synthesis of the fully acetylated product for both the sodium acetate and zinc chloride catalysed reactions.

For the zinc chloride catalysed reaction a fully acetylated product was observed whilst the presence of a number of additional peaks ascribed as degradation products were also visible in the GC-MS chromatogram and the  $^1\text{H}$  NMR spectra (highlighted in Figure 84). A marked increase was also observed in the abundance of the peaks attributed to glucose pentaacetate as previously described with regards to the pyridine catalysed acetylation

product. Again the GC-MS chromatograms for the zinc chloride and sodium acetate catalysed reaction products are located in the appendix.

### 5.3.2 Acetylation of Other Disaccharides in BMIMCl

Following on from the acetylation of cellobiose a number of other commonly encountered disaccharides were also acetylated in BMIMCl, samples of each disaccharide (10% w/w in BMIMCl) were prepared via the general dissolution method and acetylated following the general acetylation protocol (see Chapter 2). The products were then extracted using the liquid – liquid extraction procedure (see Chapter 2).

#### 5.3.2.1 Trehalose

Trehalose (see Table 4, Chapter 3) is comprised of two  $\alpha$ -(1 $\rightarrow$ 1) linked glucose monomers. As trehalose is linked via carbon one for both glucose monomers the disaccharide is subsequently a non-reducing sugar.

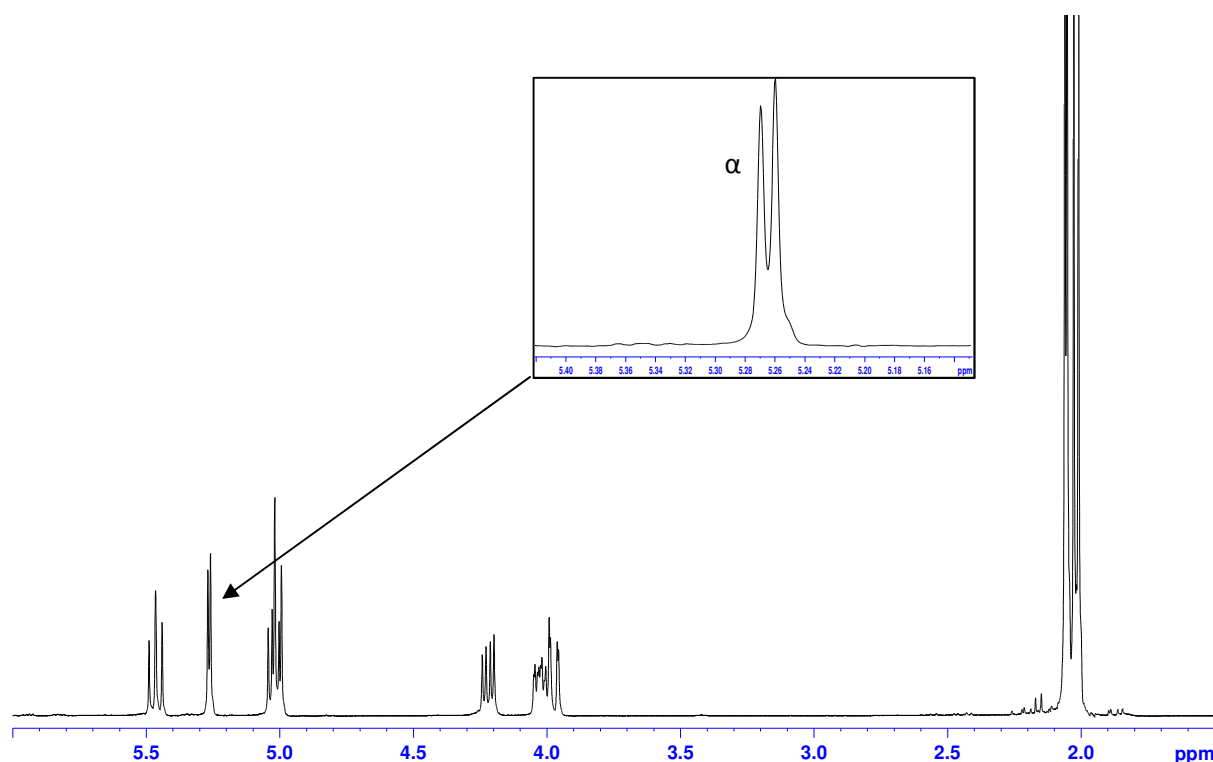


**Figure 85:  $^1\text{H}$  NMR Spectrum of Trehalose Acetylated in BMIMCl with Pyridine at 70°C in  $\text{CDCl}_3$ ; Inset - Magnified Region showing Single Anomeric Signal**



As expected the acetylated trehalose demonstrated a single anomeric signal in the  $^1\text{H}$  NMR spectrum (Figure 85) with a single sharp doublet visible at 5.26 ppm. Also as might have been predicted the GC-MS chromatogram (see Appendix) produced a single peak, further confirming the synthesis of a single species –  $\alpha,\alpha$ -(1 $\rightarrow$ 1) trehalose octaacetate<sup>192</sup>. It should be noted that no degradation was observed in either the NMR spectrum or the GC-MS chromatogram (including the presence of any degradation (glucose pentaacetate) post reaction during GC-MS analysis). This is due to the (1 $\rightarrow$ 1) bond present in trehalose; this bond is extremely strong and allows trehalose to withstand exposure to high temperatures and acidic conditions without breaking (degrading).

### 5.3.2.2 Lactose

Lactose (see Table 4, Chapter 3) is comprised of glucose and galactose linked through a  $\beta$ -(1 $\rightarrow$ 4) glycosidic bond. The acetylation of lactose has been studied many times in recent years incorporating both unconventional catalysts<sup>189,193</sup> and employing a variety of ionic liquid systems<sup>191</sup>.

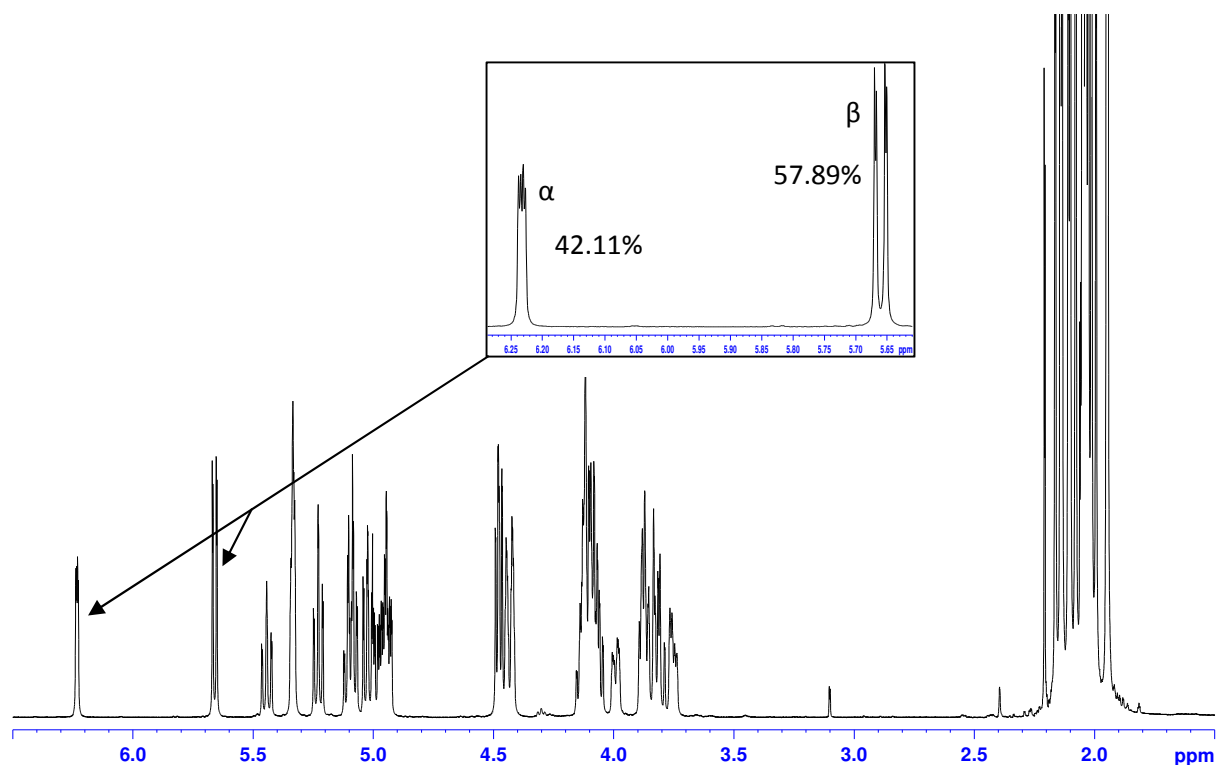


**Figure 86:  $^1\text{H}$  NMR Spectrum of Lactose Acetylated in BMIMCl with Pyridine at 70°C in  $\text{CDCl}_3$ ; Inset - Magnified Anomeric Region**

The interpretation of the  $^1\text{H}$  NMR spectrum (Figure 86) combined with the comparison of the spectra with an  $\alpha$ -lactose octaacetate standard (see Appendix) confirmed the synthesis of a variety of  $\alpha$ -anomers and  $\beta$ -anomers (42.11%  $\alpha$  / 57.89%  $\beta$ ). Analysis of the NMR spectra in conjunction with the GC-MS data (Figure 87) indicates that the disaccharide has undergone a degree of degradation during the acetylation reaction.

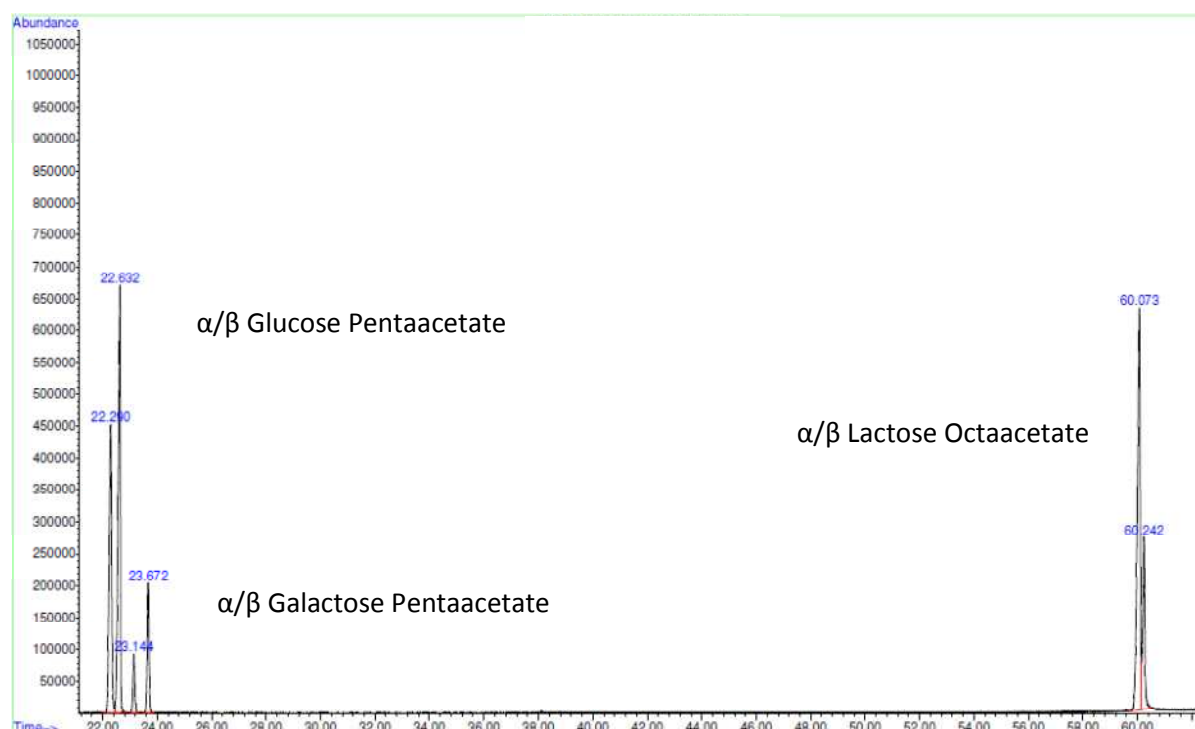


**Figure 87: GC-MS Chromatogram of Acetylated Lactose in BMIMCl with Pyridine**

There are multiple overlapping peaks observed in the NMR spectra along with four extra peaks (other than the two expected corresponding to  $\alpha/\beta$  lactose octaacetate) in the GC-MS chromatogram identified as arising from the presence of  $\alpha$  and  $\beta$  glucose pentaacetate and  $\alpha$  and  $\beta$  galactose pentaacetate. Again the GC-MS chromatogram suggests a substantial amount of degradation has occurred during the GC-MS analysis; this is confirmed by comparison with the chromatogram produced by the  $\alpha$ -lactose octaacetate standard (see Appendix). This indicates that the degradation is occurring primarily during the GC-MS analysis and not during the course of the acetylation reaction.

## 5.3.2.3 Sucrose

Sucrose (Figure 88) is comprised of one glucose and one fructose monomer linked together through an  $\alpha$ -(1 $\rightarrow$ 2) glycosidic bond. Again as with trehalose, sucrose is also classified as a non-reducing sugar<sup>192</sup>.

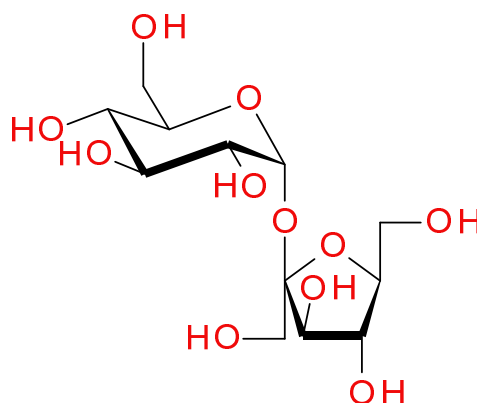


**Figure 88: Sucrose**

Sucrose, even more than the previously investigated disaccharides, has undergone extensive study in recent times in terms of both dissolution<sup>194,195</sup> and acetylation reactions in traditional solvents<sup>196</sup> and ionic liquids<sup>191</sup>.

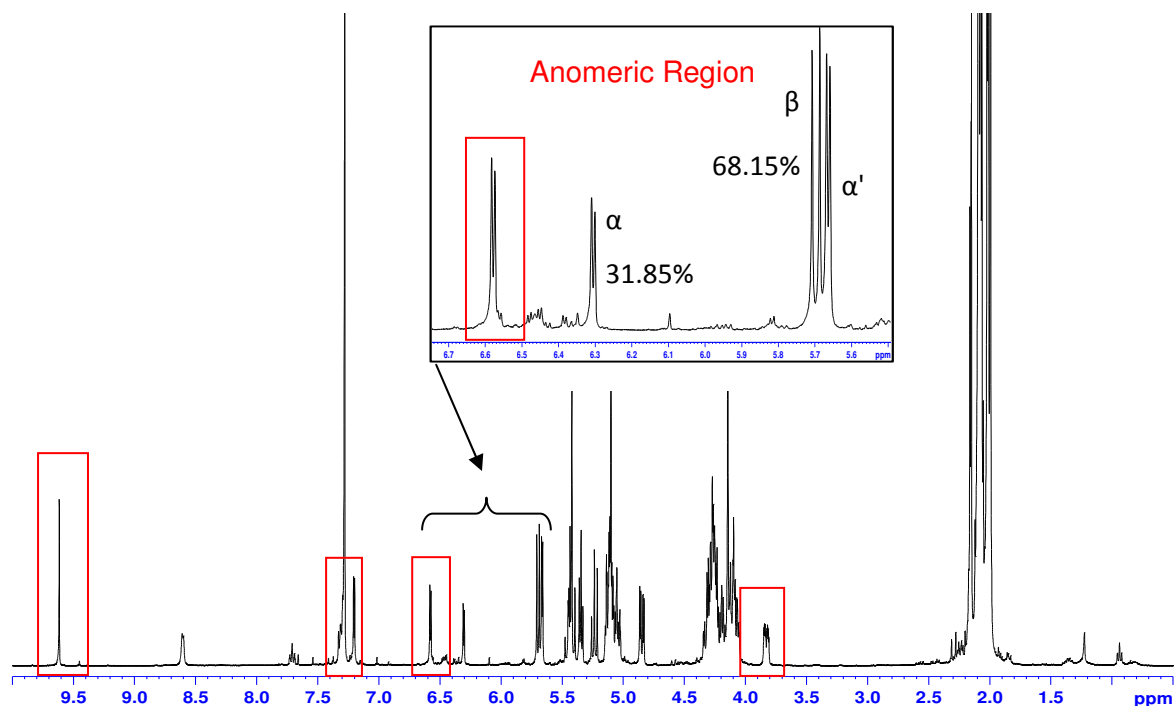


**Figure 89: <sup>1</sup>H NMR Spectrum of Sucrose Acetylated in BMIMCl with Pyridine at 70°C in CDCl<sub>3</sub>; Inset – Magnified Anomeric Region**

From the  $^1\text{H}$  NMR spectrum (Figure 89) it can be determined that the sucrose octaacetate has been formed but has also decomposed, as anomeric signals for both  $\alpha$  (31.85%) and  $\beta$  (68.15%) glucose pentaacetate (see Inset in Figure 88) are observed along with one (or possibly a mixture) of other compounds present from the degradation of fructose (identified by red boxes in Figure 89).

The data obtained from the GC-MS (Figure 90) analysis confirmed the synthesis of the sucrose octaacetate product by the presence of a single peak in the chromatogram at 56.777 minutes. Also identified from the chromatogram, once again, were two peaks corresponding to both  $\alpha$  and  $\beta$  glucose pentaacetate. However, comparison of the  $^1\text{H}$  NMR spectrum produced by the resulting reaction with a standard of  $\alpha$ -sucrose octaacetate (see Appendix) confirmed that a degree of the degradation observed in the spectrum occurred during the acetylation reaction.

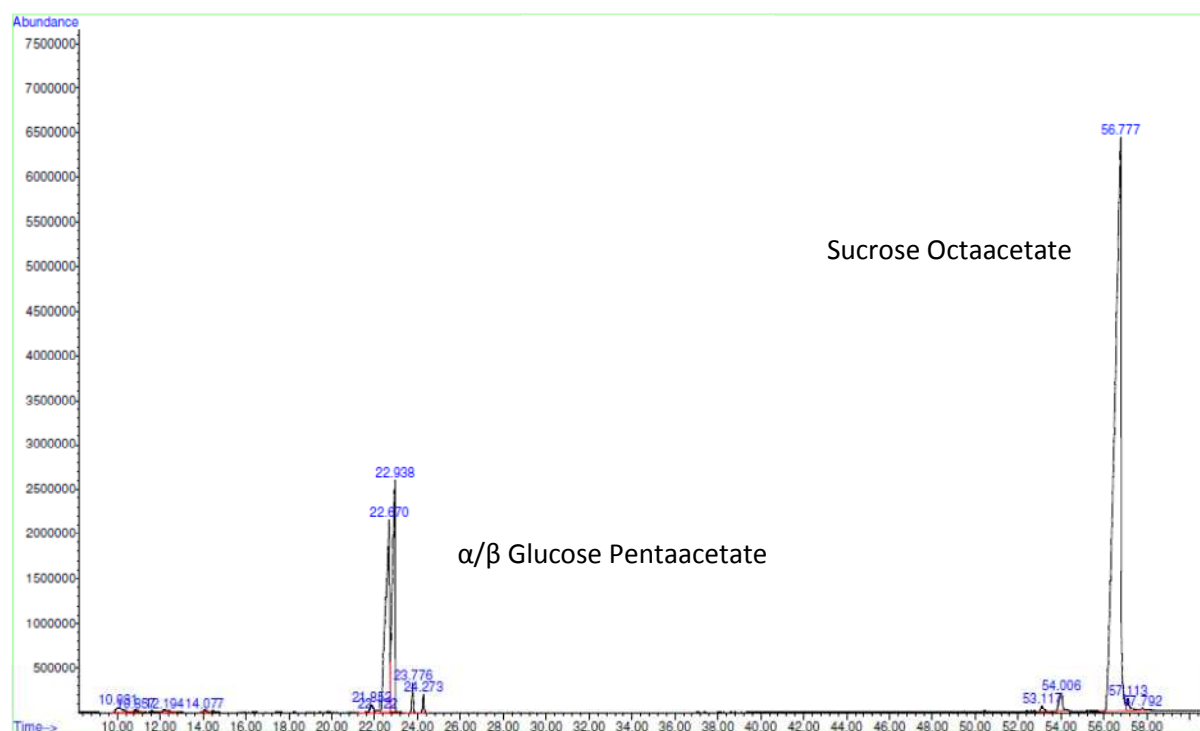


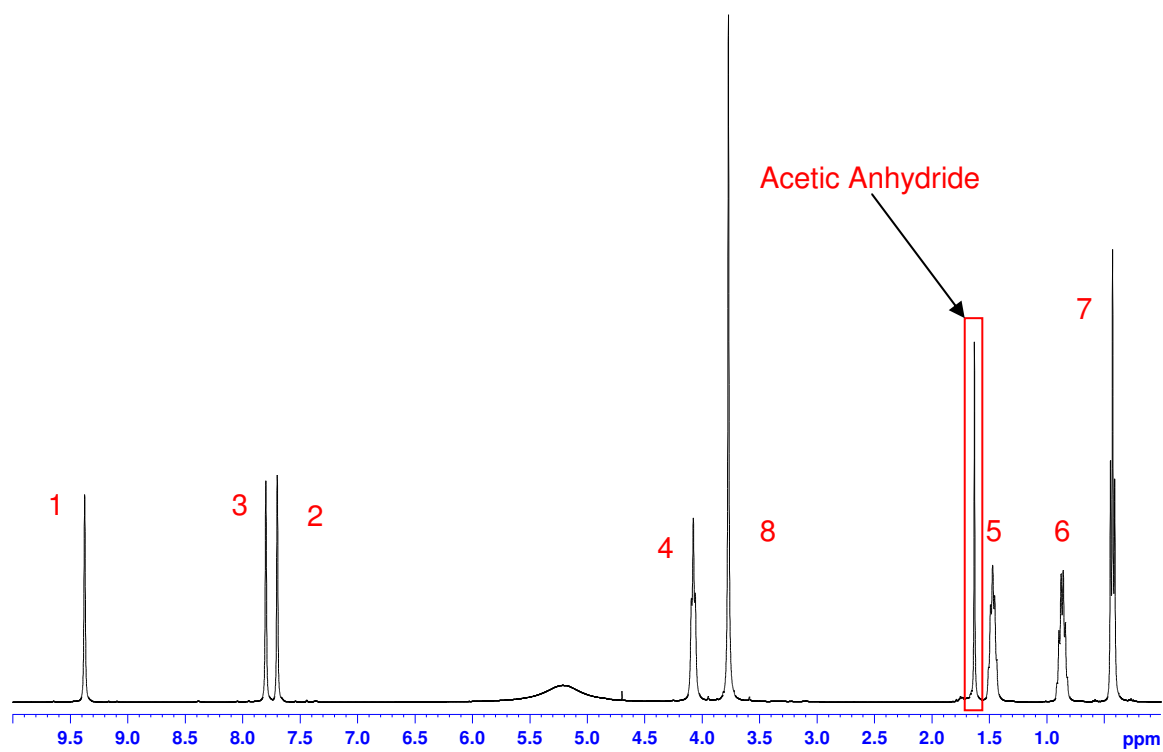
**Figure 90: GC-MS Chromatogram of Acetylated Sucrose in BMIMCl with Pyridine**

Given the complex nature of the products generated from the acetylation reactions, it was decided to abandon attempts to use the acetylation procedures for the derivatisation of EPS.

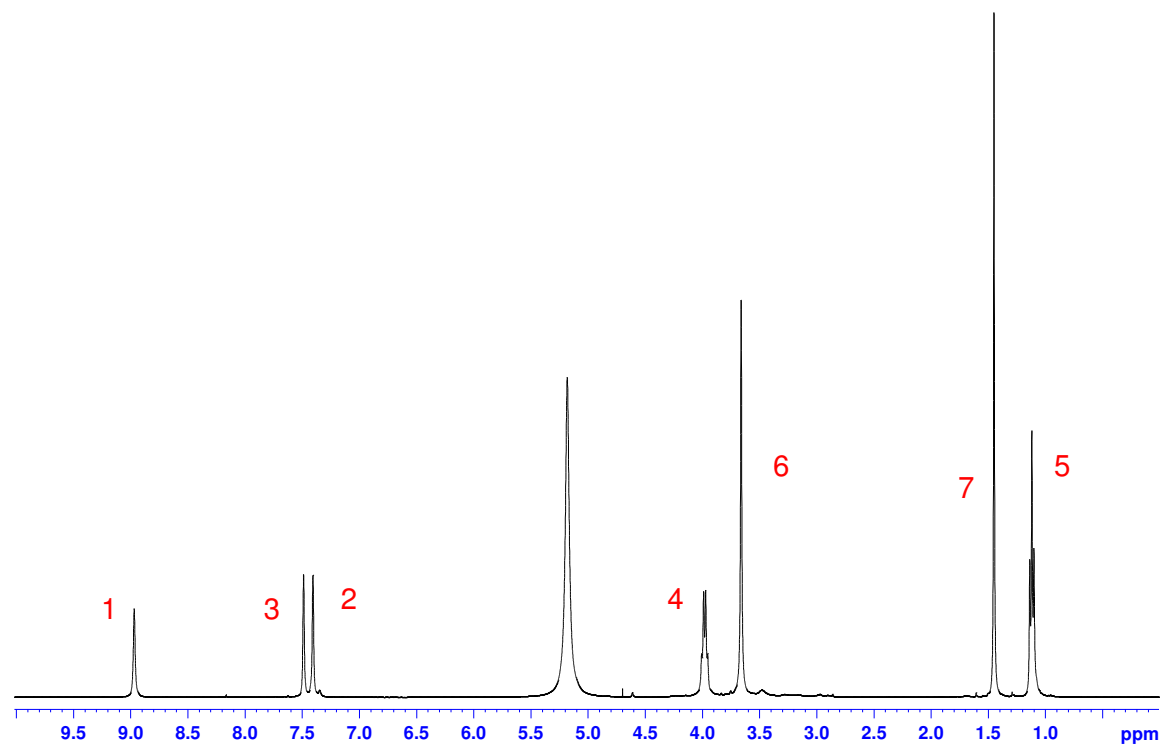
## 5.4 Appendices

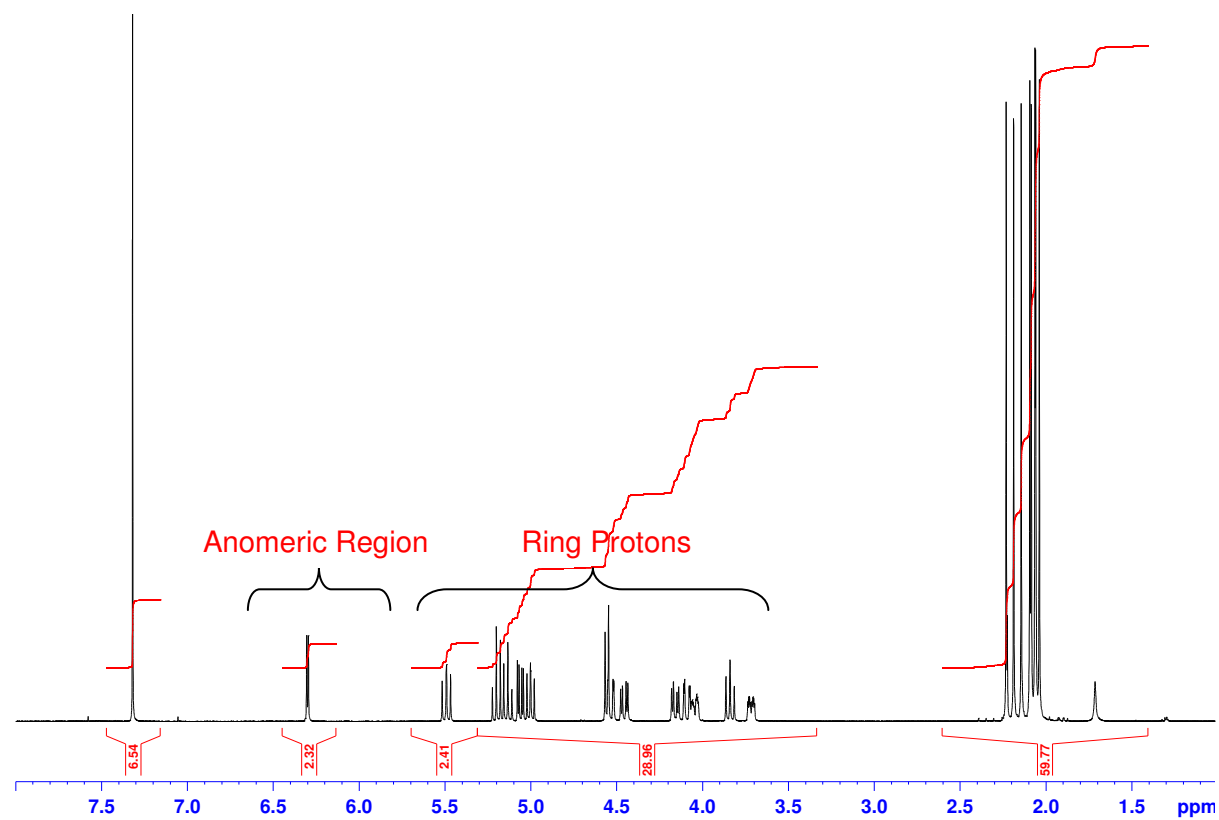
### 5.4.1 $^1\text{H}$ NMR Spectra of Recycled Ionic Liquids

#### 5.4.1.1 $^1\text{H}$ NMR Spectrum of Recycled BMIMCl with $\text{D}_2\text{O}$ insert at $25^\circ\text{C}$

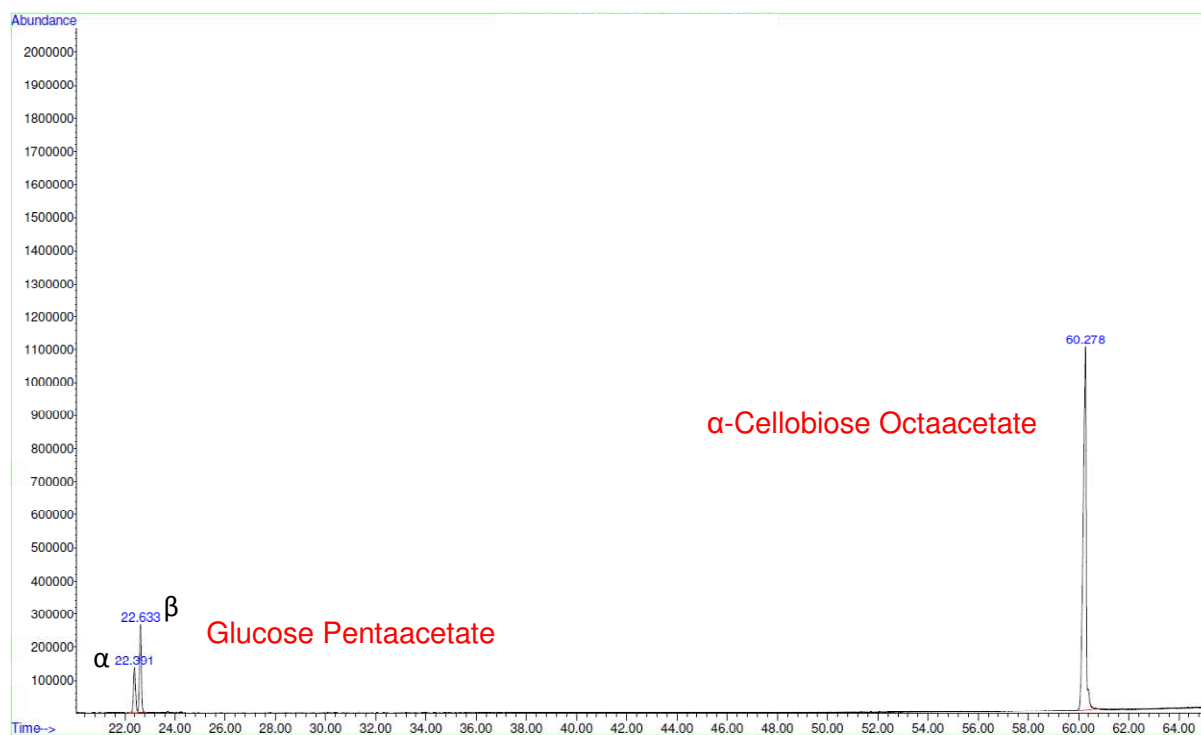


#### 5.4.1.2 $^1\text{H}$ NMR Spectrum of Recycled EMIMAc with $\text{D}_2\text{O}$ insert at $25^\circ\text{C}$



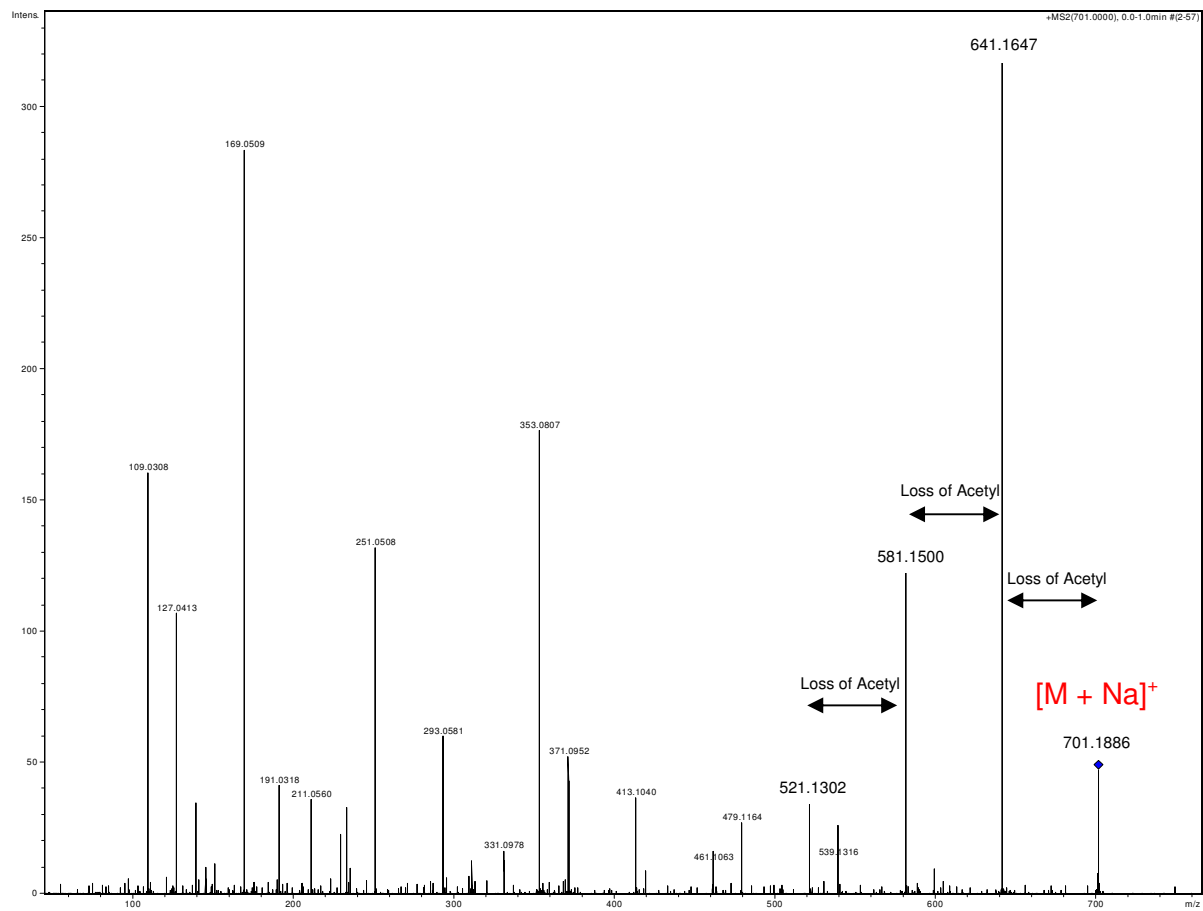
5.4.2  $\alpha$ -Cellobiose Octaacetate Standard5.4.2.1  $^1\text{H}$  NMR Spectrum with  $\text{CDCl}_3$  at 25 °C

## 5.4.2.1 GC-MS Chromatogram



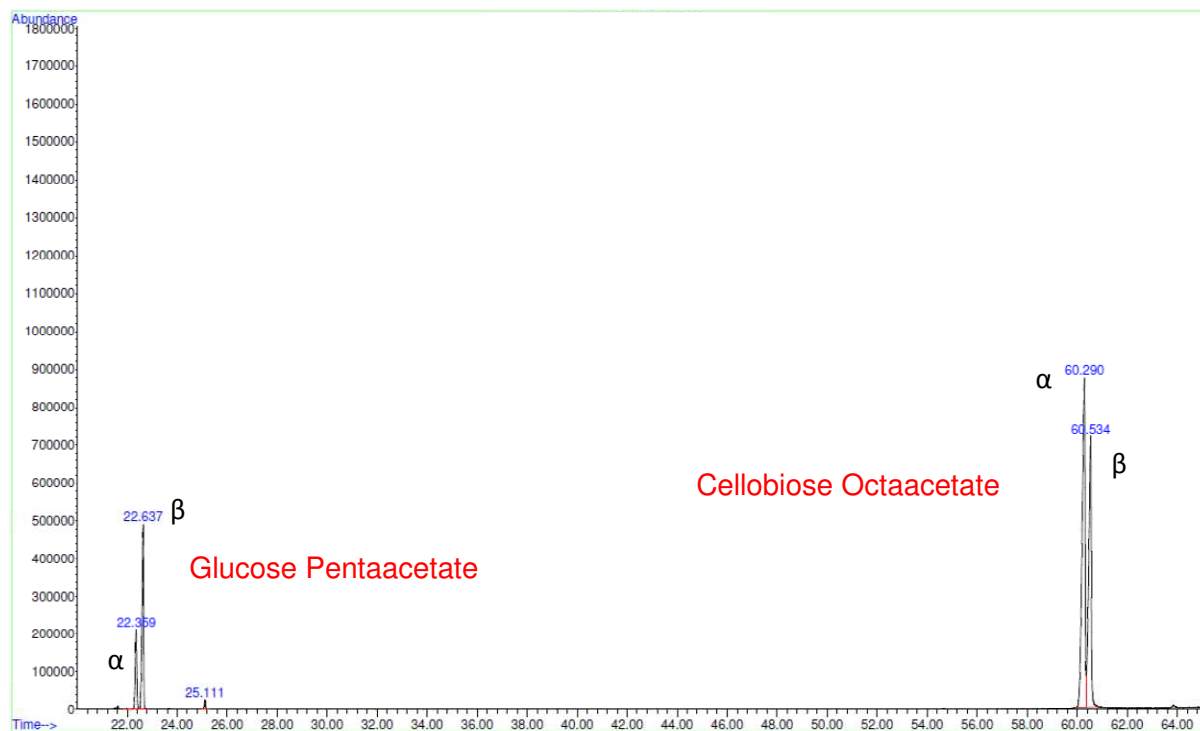
## 5.4.3 Cellobiose Acetylated in BMIMCl with Pyridine

## 5.4.3.1 MS/MS Spectrum

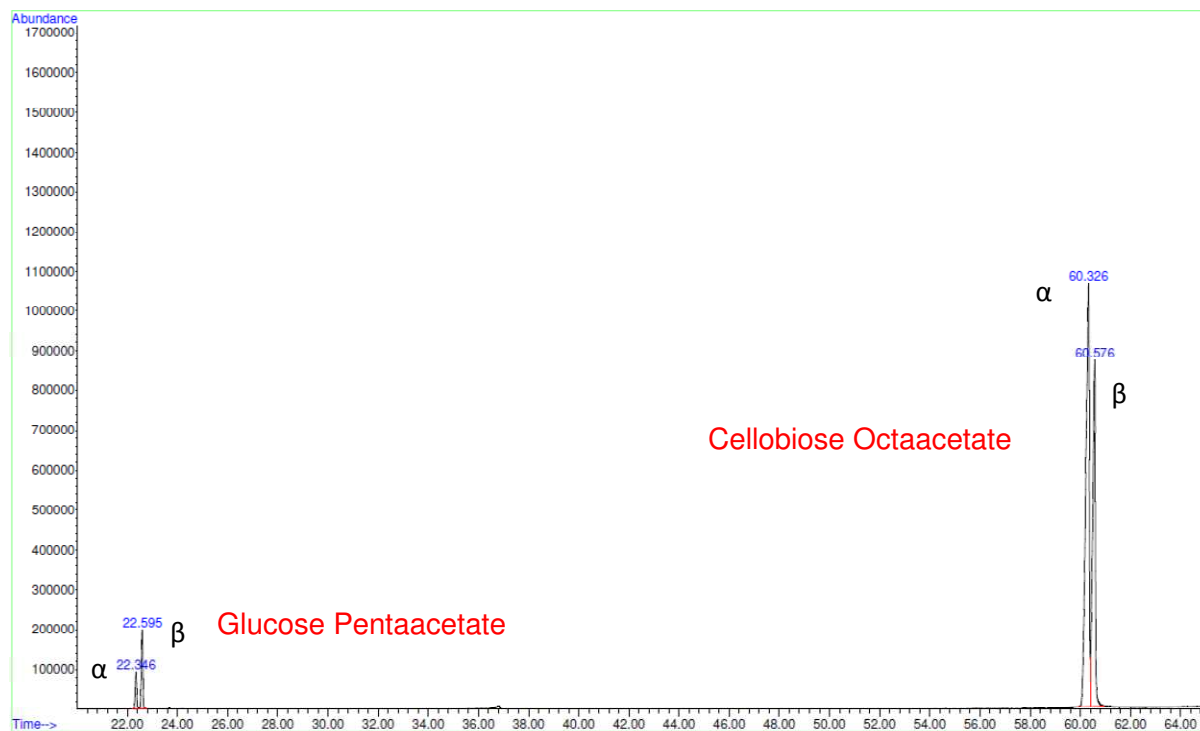


## 5.4.4 Zinc Chloride and Sodium Acetate Catalysed Acetylation Products

## 5.4.4.1 GC-MS Chromatogram Cellobiose Acetylated in BMIMCl with Zinc Chloride



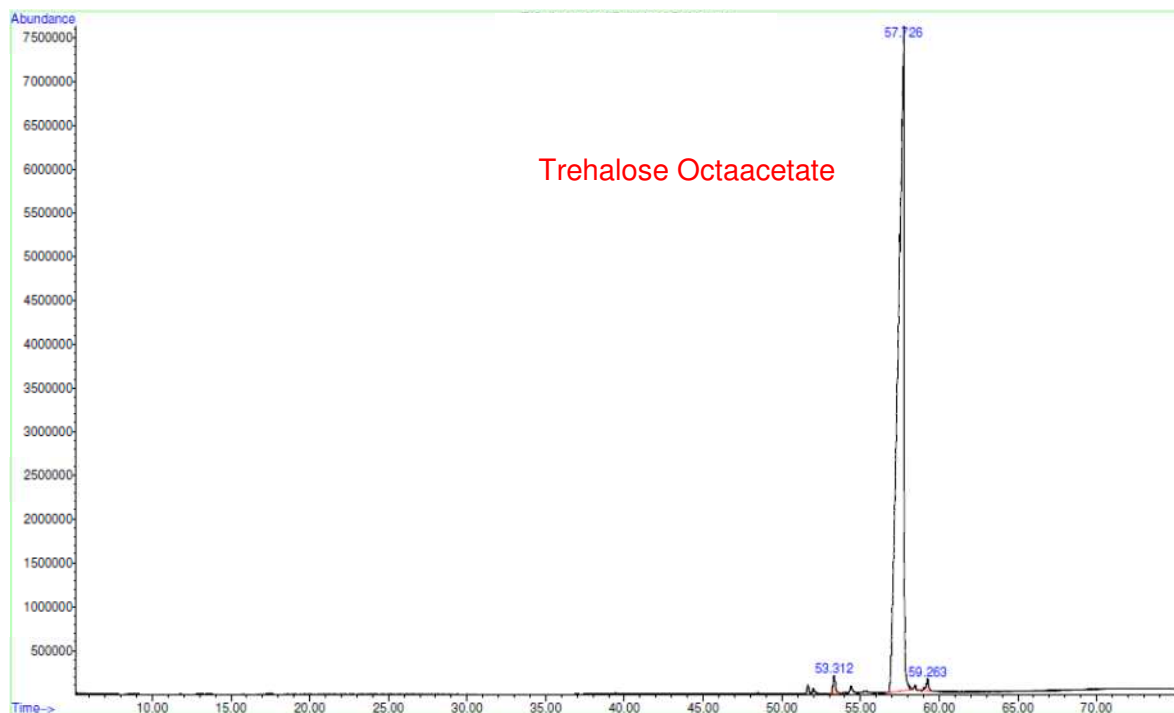
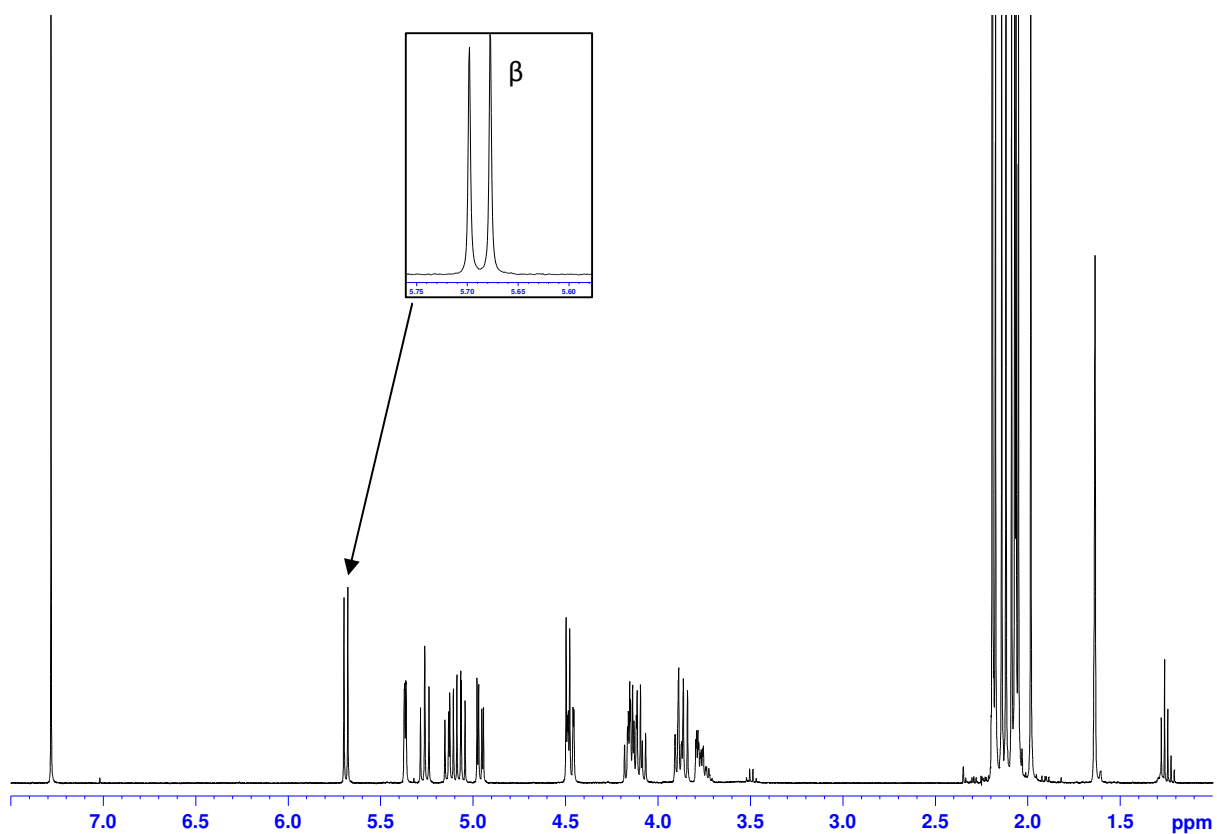
## 5.4.4.2 GC-MS Chromatogram of Cellobiose Acetylated in BMIMCl with Sodium Acetate



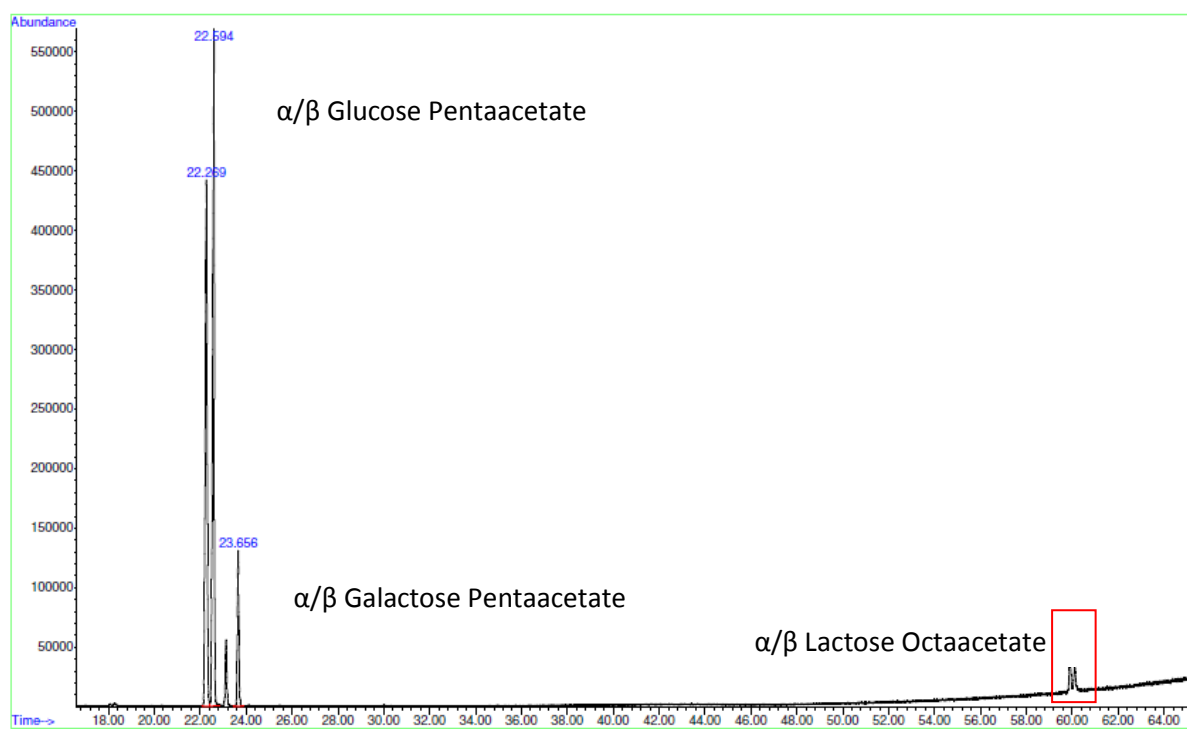
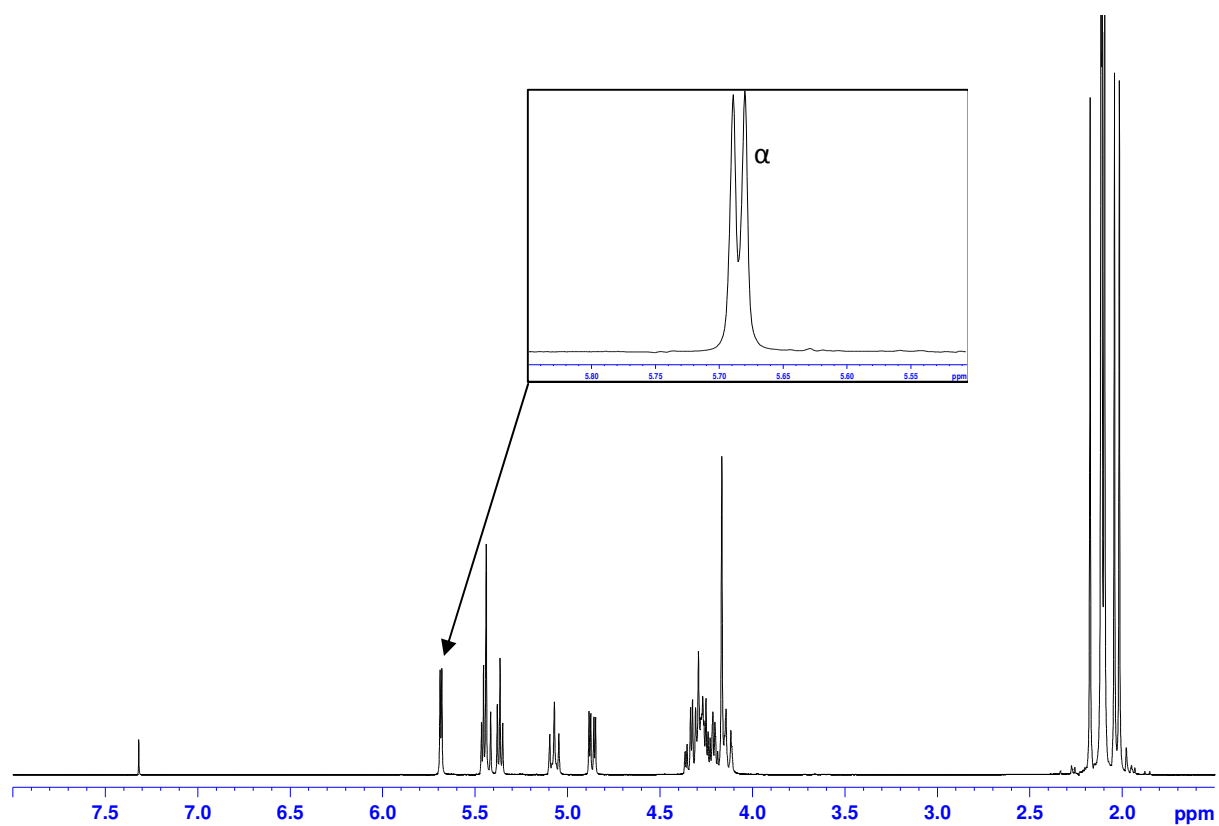


## 5.4.5 Trehalose Acetylated in BMIMCl with Pyridine

## 5.4.5.1 GC-MS Chromatogram

5.4.6  $\alpha$ -Lactose Octaacetate Standard5.4.6.1  $^1\text{H}$  NMR Spectrum with  $\text{CDCl}_3$  at 25  $^\circ\text{C}$ 

## 5.4.6.2 GC-MS Chromatogram

5.4.7  $^1\text{H}$  NMR Spectrum of Sucrose Octaacetate Standard with  $\text{CDCl}_3$  at  $25^\circ\text{C}$ 

## 6. References

1. McMurry, J. *Organic Chemistry*, 6th ed., [International student ed.], 2004.
2. Lindhorst, T. K. *Essentials of Carbohydrate Chemistry and Biochemistry*, 2nd ed.; Wiley VCH, 2000.
3. Garrett, R. H.; Grisham, C. M. *Biochemistry*; Brooks/Cole 1995.
4. Riiber, C. N.; Sorensen, N. A. *Norwegian Science Society Writings* **1933**, 7, 50.
5. Lemieux, R. U.; Kullnig, R. K.; Bernstein, H. J.; Schneider, W. G. *Journal of the American Chemical Society* **1958**, 80, 6098-6105.
6. Davis, B. G.; Fairbanks, A. J. *Carbohydrate Chemistry*; Oxford University Press: New York, 2002; Vol. 99.
7. Sinnott, M. L. *Carbohydrate Chemistry and Biochemistry: structure and mechanism*; RSC Publ.: Cambridge, 2007.
8. Lake, B. G.; Longland, R. C.; Gangolli, S. D.; Lloyd, A. G. *Toxicology and Applied Pharmacology* **1976**, 35, 113-122.
9. Amaechi, B. T.; Higham, S. M.; Edgar, W. M. *Archives of Oral Biology* **1998**, 43, 157-161.
10. Van Calsteren, M. R.; Pau-Roblot, C.; Begin, A.; Roy, D. *Biochemical Journal* **2002**, 363, 7-17.
11. Madigan, M. T.; Martinko, J. M. *Brock Biology Of Microorganisms* 11th ed.; Benjamin/Cummings Pub.Co, 2005.
12. Cui, S. W. *Food Carbohydrates: Chemistry, Physical Properties, and Applications*; CRC Taylor and Francis, 2005.
13. Davidson, R. L., Ed. *Handbook of Water-soluble Gums and Resins*; McGraw-Hill Education: New York, 1980.
14. Jansson, P.-e.; Kenne, L.; Lindberg, B. *Carbohydrate Research* **1975**, 45, 275-282.
15. Sutherland, I. W.; Johannis, P. K. In *Comprehensive Glycoscience*; Elsevier: Oxford, 2007; pp. 521-558.
16. Alberts, B.; Bray, D.; Johnson, A.; Lewis, J.; Raff, M.; Roberts, K.; Walter, P. *Essential Cell Biology*; Garland Publishing, Inc., 1998.
17. Whitman, W. B.; Coleman, D. C.; Wiebe, W. J. *Proceedings of the National Academy of Sciences* **1998**, 95, 6578-6583.
18. Monod, J. *Annual Review of Microbiology* **1949**, 3, 371-394.
19. Ghuysen, J. M.; Hackenbeck, R. *Bacterial Cell Wall*, 1st ed.; Elsevier Science Pub Co, 1994.

20. Gram, H. C. *Fortschritte der Medizin* **1884**, 2, 185-189.
21. Voet, D.; Voet, J. G.; Pratt, C. W. *Fundamentals of Biochemistry* John Wiley & Sons; Package edition 1999.
22. Horton, H. R.; Moran, L. A.; Scrimgeour, K. G.; Perry, M. D.; Rawn, J. D. *Principles of Biochemistry* 4th ed.; Pearson Prentice Hall, 2006.
23. Kay, W.; Petersen, B. O.; Duus, J. Ø.; Perry, M. B.; Vinogradov, E. *FEBS Journal* **2006**, 273, 3002-3013.
24. Glazer, A. N.; Nikaidō, H. *Microbial Biotechnology: Fundamentals of Applied Microbiology*, 2nd ed.; Cambridge University Press, 2007.
25. Sutherland, I. W. *Surface Carbohydrates of the Prokaryotic Cell*; Academic Press, 1977; Vol. London.
26. Sutherland, I. W. *Annual Review of Microbiology* **1985**, 39, 243-270.
27. Sutherland, I. W.; Rose, A. H.; Tempest, D. W. In *Advances in Microbial Physiology*; Academic Press, 1972; pp. 143-213.
28. Laws, A.; Gu, Y.; Marshall, V. *Biotechnology Advances* **2001**, 19, 597-625.
29. Narvhus, J.; Axelsson, L. *Lactic acid bacteria*, 2nd ed.; Academic Press, 2003.
30. Paul Ross, R.; Morgan, S.; Hill, C. *International Journal of Food Microbiology* **2002**, 79, 3-16.
31. van Vuuren, H. J. J.; Dicks, L. M. T. *American Journal of Enology and Viticulture* **1993**, 44, 99-112.
32. Steinkraus, K. H. *Antonie Van Leeuwenhoek International Journal of General and Molecular Microbiology* **1983**, 49, 337-348.
33. Marshall, V. M.; Cole, W. M. *Journal of Dairy Research* **1985**, 52, 451-456.
34. De Vuyst, L.; Degeest, B. *Fems Microbiology Reviews* **1999**, 23, 153-177.
35. Gruter, M.; Leeflang, B. R.; Kuiper, J.; Kamerling, J. P.; Vliegthart, J. F. G. *Carbohydrate Research* **1992**, 231, 273-291.
36. Leroy, F.; De Vuyst, L. *Trends in Food Science & Technology* **2004**, 15, 67-78.
37. Liu, S. Q. *International Journal of Food Microbiology* **2003**, 83, 115-131.
38. Banks, J. M. *International Journal of Dairy Technology* **2004**, 57, 199-207.
39. Williams, A. G.; Noble, J.; Banks, J. M. *International Dairy Journal* **2001**, 11, 203-215.
40. Marshall, V. M.; Rawson, H. L. *International Journal of Food Science & Technology* **1999**, 34, 137-143.
41. Cerning, J.; Bouillanne, C.; Landon, M.; Desmazeaud, M. J. *Sciences Des Aliments* **1990**, 10, 443-451.

42. Sharpe, M. E. *International Journal of Dairy Technology* **1979**, *32*, 9-18.
43. Kontusaari, S.; Forsén, R. *Journal of Dairy Science* **1988**, *71*, 3197-3202.
44. Somers, E. B.; Johnson, M. E.; Wong, A. C. L. *Journal of Dairy Science* **2001**, *84*, 1926-1936.
45. Bouman, S. *Journal of Food Protection* **1982**, *45*, 806.
46. Williamson, D. H. *Journal of Applied Bacteriology* **1959**, *22*, 392.
47. de Nadra, M. C. M.; de Saad, A. M. S. *International Journal of Food Microbiology* **1995**, *27*, 101-106.
48. Dueñas, M.; Irastorza, A.; Fernandez, K.; Bilbao, A. *Journal of Food Protection* **1995**, *58*, 76-80.
49. Oda, M.; Hasegawa, H.; Komatsu, S.; Kambe, M.; Tsuchiya, F. *Agricultural and Biological Chemistry* **1983**, *47*, 1623-1625.
50. Nagaoka, M.; Hashimoto, S.; Watanabe, T.; Yokokura, T.; Mori, Y. *Biological & Pharmaceutical Bulletin* **1994**, *17*, 1012-1017.
51. Kitazawa, H.; Yamaguchi, T.; Miura, M.; Saito, T.; Itoh, T. *Journal of Dairy Science* **1993**, *76*, 1514-1519.
52. Nakajima, H.; Suzuki, Y.; Kaizu, H.; Hirota, T. *Journal of Food Science* **1992**, *57*, 1327-1329.
53. Roberfroid, M. B.; Gibson, G. R. *Journal of Nutrition* **1995**, *125*, 1401-1412.
54. Gibson, G. R.; Probert, H. M.; Loo, J. V.; Rastall, R. A.; Roberfroid, M. B. *Nutrition Research Reviews* **2004**, *17*, 259-275.
55. Bello, F. D.; Walter, J.; Hertel, C.; Hammes, W. P. *Systematic and Applied Microbiology* **2001**, *24*, 232-237.
56. Ruas-Madiedo, P.; Hugenholtz, J.; Zoon, P. *International Dairy Journal* **2002**, *12*, 163-171.
57. Tsuda, H.; Miyamoto, T. *Food Science and Technology Research* **2010**, *16*, 87-92.
58. Fuller, R. *Journal of Applied Bacteriology* **1989**, *66*, 365-378.
59. Tissier, H., Institute Pasteur, 1900.
60. Mitsuoka, T. *Journal of Industrial Microbiology and Biotechnology* **1990**, *6*, 263-267.
61. Orla-Jensen, S. *Lait* **1924**, *4*, 468-474.
62. Scardovi, V. *Genus Bifidobacterium: Bifidobacterium* In *Bergey's Manual of Systematic Bacteriology*; Holt, J. G. Ed.; Williams & Wilkins, 1986; pp. 1418-1434.
63. Stiles, M. E.; Holzapfel, W. H. *International Journal of Food Microbiology* **1997**, *36*, 1-29.

64. Tamime, A. Y.; Richard, K. R. In *Encyclopedia of Food Microbiology*; Elsevier: Oxford, 1999; pp. 1355-1360.
65. Ruas-Madiedo, P.; Salazar, N.; de los Reyes-Gavilán, C. G.; Otto, H.; Patrick, J. B.; Mark von, I. In *Microbial Glycobiology*; Academic Press: San Diego, 2010; pp. 885-902.
66. Mayo, B.; van Sinderen, D. *Bifidobacteria: Genomics and Molecular Aspects*; Caister Academic Press., 2010.
67. Masco, L.; Huys, G.; De Brandt, E.; Temmerman, R.; Swings, J. *International Journal of Food Microbiology* **2005**, *102*, 221-230.
68. Scardovi, V.; Trovatelli, L. D. *Annual Reviews in Microbiology* **1965**, *15*, 19-29.
69. Servin, A. L. *Fems Microbiology Reviews* **2004**, *28*, 405-440.
70. Saavedra, J. M.; Bauman, N. A.; Perman, J. A.; Yolken, R. H.; Oung, I. *The Lancet* **1994**, *344*, 1046-1049.
71. Jiang, T.; Mustapha, A.; Savaiano, D. A. *Journal of Dairy Science* **1996**, *79*, 750-757.
72. Touré, R.; Kheadr, E.; Lacroix, C.; Moroni, O.; Fliss, I. *Journal of Applied Microbiology* **2003**, *95*, 1058-1069.
73. Ouwehand, A. C. *Antonie Van Leeuwenhoek International Journal of General and Molecular Microbiology* **2002**, *82*, 279-289.
74. Kleessen, B.; Sykura, B.; Zunft, H. J.; Blaut, M. *The American Journal of Clinical Nutrition* **1997**, *65*, 1397-402.
75. Arunachalam, K.; Gill, H. S.; Chandra, R. K. *European Journal of Clinical Nutrition* **2000**, *54*, 263-267.
76. Xiao, J. Z.; Kondo, S.; Takahashi, N.; Miyaji, K.; Oshida, K.; Hiramatsu, A.; Iwatsuki, K.; Kokubo, S.; Hosono, A. *Journal of Dairy Science* **2003**, *86*, 2452-2461.
77. Klaver, F. A. M.; Kingma, F.; Weerkamp, A. H. *Netherlands Milk Dairy Journal* **1993**, *47*, 151-164.
78. Desjardins, M. L.; Roy, D.; Goulet, J. *Milchwissenschaft-Milk Science International* **1991**, *46*, 11-13.
79. Gueimonde, M.; Delgado, S.; Mayo, B.; Ruas-Madiedo, P.; Margolles, A.; de los Reyes-Gavilan, C. G. *Food Research International* **2004**, *37*, 839-850.
80. Shah, N. P. *Journal of Dairy Science* **2000**, *83*, 894-907.
81. Lankaputhra, W. E. V.; Shah, N. P. *Cultured Dairy Products Journal* **1995**, *30*, 2-7.
82. Ruas-Madiedo, P.; Hernandez-Barranco, A.; Margolles, A.; de los Reyes-Gavilan, C. G. *Applied and Environmental Microbiology* **2005**, *71*, 6564-6570.
83. Sanchez, B.; Champomier-Verges, M. C.; Stuer-Lauridsen, B.; Ruas-Madiedo, P.; Anglade, P.; Baraige, F.; de los Reyes-Gavilan, C. G.; Johansen, E.; Zagorec, M.; Margolles, A. *Applied and Environmental Microbiology* **2007**, *73*, 6757-6767.

84. Marshall, V. M.; Tamime, A. Y. *International Journal of Dairy Technology* **1997**, *50*, 35-41.
85. Laws, A. P.; Marshall, V. M. *International Dairy Journal* **2001**, *11*, 709-721.
86. Duboc, P.; Mollet, B. *International Dairy Journal* **2001**, *11*, 759-768.
87. D'Ayala, G. G.; Malinconico, M.; Laurienzon, P. *Molecules* **2008**, *13*, 2069-21069.
88. Sutherland, I. W. *Biotechnology Advances* **1994**, *12*, 393-448.
89. Boels, I. C.; Kranenburg, R. v.; Hugenholtz, J.; Kleerebezem, M.; de Vos, W. M. *International Dairy Journal* **2001**, *11*, 723-732.
90. Jansson, P.-E.; Lindberg, B.; Sandford, P. A. *Carbohydrate Research* **1983**, *124*, 135-139.
91. Bhaskaracharya, R. K.; Shah, N. P. *Australian Journal of Dairy Technology* **2000**, *55*, 132-138.
92. Cerning, J. *FEMS Microbiology Letters* **1990**, *87*, 113-130.
93. Cerning, J. *Lait* **1995**, *75*, 463-472.
94. Stinglele, F.; Neeser, J. R.; Mollet, B. *Journal of Bacteriology* **1996**, *178*, 1680-1690.
95. Kranenburg, R. v.; Marugg, J. D.; Van Swam, I. I.; Willem, N. J.; De Vos, W. M. *Molecular Microbiology* **1997**, *24*, 387-397.
96. Welman, A. D.; Maddox, I. S. *Trends in Biotechnology* **2003**, *21*, 269-274.
97. Ielpi, L.; Couso, R. O.; Dankert, M. A. *Biochemistry International* **1983**, *6*, 323-333.
98. Postma, P. W.; Lengeler, J. W.; Jacobson, G. R. *Microbiological Reviews* **1993**, *57*, 543-594.
99. Sjoberg, A.; Hahnagerdal, B. *Applied and Environmental Microbiology* **1989**, *55*, 1549-1554.
100. Oba, T.; Doesburg, K. K.; Iwasaki, T.; Sikkema, J. *Archives of Microbiology* **1999**, *171*, 343-349.
101. Ruas-Madiedo, P.; de los Reyes-Gavilan, C. G. *Journal of Dairy Science* **2005**, *88*, 843-856.
102. Vedamuthu, E. R.; Neville, J. M. *Applied Environmental Microbiology*. **1986**, *51*, 677-682.
103. De Vuyst, L.; De Vin, F.; Vaningelgem, F.; Degeest, B. *International Dairy Journal* **2001**, *11*, 687-707.
104. Cerning, J.; Bouillanne, C.; Landon, M.; Desmazeaud, M. *Journal of Dairy Science* **1992**, *75*, 692-699.
105. Grobber, G. J.; Sikkema, J.; Smith, M. R.; de Bont, J. A. M. *Journal of Applied Microbiology* **1995**, *79*, 103-107.

106. Gasseem, M. A.; Sims, K. A.; Frank, J. F. *Lebensmittel-Wissenschaft und-Technologie* **1997**, *30*, 273-278.
107. Vaningelgem, F.; Van der Meulen, R.; Zamfir, M.; Adriany, T.; Laws, A. P.; De Vuyst, L. *International Dairy Journal* **2004**, *14*, 857-864.
108. Ricciardi, A.; Parente, E.; Crudele, M. A.; Zanetti, F.; Scolari, G.; Mannazzu, I. *Journal of Applied Microbiology* **2002**, *92*, 297-306.
109. Vliegthart, J. F. G.; Berg, D. J. C. v. d.; Robijn, G. W.; Janssen, A. C.; Giuseppin, M. L. F.; Vreeker, R.; Kamerling, J. P.; Ledebor, A. M.; *American Society for Microbiology*, 1995.
110. De Vuyst, L.; Vanderveken, F.; Van de Ven, S.; Degeest, B. *Journal of Applied Microbiology* **1998**, *84*, 1059-1068.
111. Laws, A. P.; Leivers, S.; Chacon-Romero, M.; Chadha, M. J. *International Dairy Journal* **2009**, *19*, 768-771.
112. Pham, P. L.; Dupont, I.; Roy, D.; Lapointe, G.; Cerning, J. *Journal of Applied and Environmental Microbiology* **2000**, *66*, 2302-2310.
113. Knoshaug, E. P.; Ahlgren, J. A.; Trempey, J. E. *Journal of Dairy Science* **2000**, *83*, 633-640.
114. Cerning, J.; Bouillanne, C.; Desmazeaud, M. J.; Landon, M. *Biotechnology Letters* **1986**, *8*, 625-628.
115. Garcia-Garibay, M.; Marshall, V. M. E. *Journal of Applied Microbiology* **1991**, *70*, 325-328.
116. Lemoine, J.; Chirat, F.; Wieruszeski, J. M.; Strecker, G.; Favre, N.; Neeser, J. R. *Applied and Environmental Microbiology* **1997**, *63*, 3512-3518.
117. Harding, L. P.; Marshall, V. M.; Elvin, M.; Gu, Y.; Laws, A. P. *Carbohydrate Research* **2003**, *338*, 61-67.
118. Yang, Z.; Huttunen, E.; Staaf, M.; Widmalm, G.; Heikki, T. *International Dairy Journal* **1999**, *9*, 631-638.
119. Doco, T.; Wieruszeski, J.-M.; Fournet, B.; Carcano, D.; Ramos, P.; Loones, A. *Carbohydrate Research* **1990**, *198*, 313-321.
120. Albersheim, P.; Nevins, D. J.; English, P. D.; Karr, A. *Carbohydrate Research* **1967**, *5*, 340-345.
121. Blake, J. D.; Richards, G. N. *Carbohydrate Research* **1970**, *14*, 375-387.
122. Neeser, J.-R.; Schweizer, T. F. *Analytical Biochemistry* **1984**, *142*, 58-67.
123. Biermann, C. J.; McGinnis, G. D. *Analysis of Carbohydrates by GLC and MS*; CRC Press, 1989.
124. Fox, A.; Morgan, S. L.; Hudson, J. R.; Zhu, Z. T.; Lau, P. Y. *Journal of Chromatography A* **1983**, *256*, 429-438.



125. Bishop, C.; Cooper, F.; Murray, R. *Canadian Journal of Chemistry* **1963**, *41*, 2245-2250.
126. Lee, Y. C. *Analytical Biochemistry* **1990**, *189*, 151-162.
127. Cataldi, T. R. I.; Campa, C.; De Benedetto, G. E. *Fresenius' Journal of Analytical Chemistry* **2000**, *368*, 739-758.
128. Rocklin, R. D.; Pohl, C. A. *Journal of Liquid Chromatography* **1983**, *6*, 1577-1590.
129. Currie, H. A.; Perry, C. C. *Journal of Chromatography A* **2006**, *1128*, 90-96.
130. Gerwig, G. J.; Kamerling, J. P.; Vliegthart, J. F. G. *Carbohydrate Research* **1978**, *62*, 349-357.
131. Laws, A. P.; Chadha, M. J.; Chacon-Romero, M.; Marshall, V. M.; Maqsood, M. *Carbohydrate Research* **2008**, *343*, 301-307.
132. Robijn, G. W.; Gallego, R. G.; vandenBerg, D. J. C.; Haas, H.; Kamerling, J. P.; Vliegthart, J. F. G. *Carbohydrate Research* **1996**, *288*, 203-218.
133. Robijn, G. W.; Vandenberg, D. J. C.; Haas, H.; Kamerling, J. P.; Vliegthart, J. F. G. *Carbohydrate Research* **1995**, *276*, 117-136.
134. Purdie T., I. J. C. *Journal of the Chemical Society, Transactions* **1903**, *83*, 1021-1037.
135. Howarth, W. N. *Journal of the. Chemical. Society.* **1915**, *107*, 8-16.
136. Hakomori, S. *Journal of Biochemistry* **1964**, *55*, 205-8.
137. Corey, E. J.; Chaykovsky, M. *Journal of the American Chemical Society* **1962**, *84*, 866-867.
138. Ciucanu, I.; Kerek, F. *Carbohydrate Research* **1984**, *131*, 209-217.
139. Bush, C. A.; Martin-Pastor, M.; Imberty, A. *Annual Review of Biophysics and Biomolecular Structure* **1999**, *28*, 269-293.
140. Duus, J. O.; Gotfredsen, C. H.; Bock, K. *Chemical Reviews* **2000**, *100*, 4589-4614.
141. Leeflang, B. R.; Faber, E. J.; Erbel, P.; Vliegthart, J. F. G. *Journal of Biotechnology* **2000**, *77*, 115-122.
142. Bubb, W. A. *Concepts in Magnetic Resonance Part A* **2003**, *19A*, 1-19.
143. Vliegthart, J. F. G.; Dorland, L.; Halbeek, H. v.; Tipson, R. S.; Derek, H. In *Advances in Carbohydrate Chemistry and Biochemistry*; Academic Press, 1983; pp. 209-374.
144. Karplus, M. *Journal of the American Chemical Society* **1963**, *85*, 2870-2871.
145. Bock, K.; Pedersen, C. *Journal of the Chemical Society, Perkin Transactions 2* **1974**, 293-297.
146. Wyatt, P. J. *Analytica Chimica Acta* **1993**, *272*, 1-40.

147. Badel, S.; Bernardi, T.; Michaud, P. *Biotechnology Advances* **2010**, *29*, 54-66.
148. Murugesan, S.; Linhardt, R. J. *Current Organic Synthesis* **2005**, *2*, 437-451.
149. Liu, Q. B.; Janssen, M. H. A.; van Rantwijk, F.; Sheldon, R. A. *Green Chemistry* **2005**, *7*, 39-42.
150. Swatloski, R. P.; Spear, S. K.; Holbrey, J. D.; Rogers, R. D. *Journal of the American Chemical Society* **2002**, *124*, 4974-4975.
151. Moulthrop, J. S.; Swatloski, R. P.; Moyna, G.; Rogers, R. D. *Chemical Communications* **2005**, 1557-1559.
152. Jones, D.; Pell, P. A.; Sneath, P. H. A. In *Maintenance of Microorganisms. A manual of laboratory methods*; Kirsop, B. E.; Snell, J. J. S. Eds.; Academic Press Inc. : London, 1984; pp. 35-40.
153. Sendra, E.; Fayos, P.; Lario, Y.; Fernández-López, J.; Sayas-Barberá, E.; Pérez-Alvarez, J. A. *Food Microbiology* **2008**, *25*, 13-21.
154. Yamamoto, Y.; Nunome, T.; Yamauchi, R.; Kato, K.; Sone, Y. *Carbohydrate Research* **1995**, *275*, 319-332.
155. Ciucanu, I.; Caprita, R. *Analytica Chimica Acta* **2007**, *585*, 81-85.
156. Chadha, M. J., University of Huddersfield, 2009.
157. Dunn, H., University of Huddersfield, 2002.
158. Bahary, W. S.; Hogan, M. P.; Jilani, M.; Aronson, M. P. In *Chromatographic Characterization of Polymers*; American Chemical Society, 1995; pp. 151-166.
159. Kaiser, K.; Benner, R. *Analytical Chemistry* **2000**, *72*, 2566-2572.
160. Lebet, V.; Arrigoni, E.; Amadò, R. *Zeitschrift für Lebensmitteluntersuchung und -Forschung A* **1997**, *205*, 257-261.
161. Lindberg, B.; Victor, G. In *Methods in Enzymology*; Academic Press, 1972; pp. 178-195.
162. Dutton, G. G. S.; Tipson, R. S.; Derek, H. *Applications of Gas-Liquid Chromatography to carbohydrates: Part I* In *Advances in Carbohydrate Chemistry and Biochemistry*; Academic Press, 1973; pp. 11-160.
163. Yu Ip, C. C.; Manam, V.; Hepler, R.; Hennessey, J. P. *Analytical Biochemistry* **1992**, *201*, 343-349.
164. Doares, S. H.; Albersheim, P.; Darvill, A. G. *Carbohydrate Research* **1991**, *210*, 311-317.
165. Sasaki, G. L.; Iacomini, M.; Gorin, P. A. J. *Anais Da Academia Brasileira De Ciencias* **2005**, *77*, 223-234.
166. Sasaki, G. L.; Gorin, P.A. J.; Souza, L.M.; Czelusniak, P.A.; Iacomini, M. *Carbohydrate Research* **2005**, *340*, 731-739.

167. Jansson, P.-E.; Kenne, L.; Widmalm, G. *Carbohydrate Research* **1987**, *168*, 67-77.
168. Robijn, G. W.; Wienk, H. L. J.; vandenBerg, D. J. C.; Haas, H.; Kamerling, J. P.; Vliegthart, J. F. G. *Carbohydrate Research* **1996**, *285*, 129-139.
169. Sutherland, I. W. *Biotechnology of Microbial Exopolysaccharides*; Cambridge University Press, 1990.
170. Friebolin, H. *Basic One- and Two-Dimensional NMR Spectroscopy* Fourth ed.; Wiley-VCH, 2004.
171. Harding, L. P.; Marshall, V. M.; Hernandez, Y.; Gu, Y.; Maqsood, M.; McLay, N.; Laws, A. P. *Carbohydrate Research* **2005**, *340*, 1107-1111.
172. Gorin, P. A. J., Mazurek, M. *Canadian. Journal of. Chemistry* **1975**, *53*, 1212-1223.
173. Ruas-Madiedo, P.; Gueimonde, M.; Margolles, A.; Reyes-Gavilan, C.; Salminen, S. *Journal of Food Protection* **2006**, *69*, 2011-2015.
174. Salazar, N.; Ruas-Madiedo, P.; Kolida, S.; Collins, M.; Rastall, R.; Gibson, G.; de Los Reyes-Gavilan, C. G. *International Journal of Food Microbiology* **2009**, *135*, 260-7.
175. Lee, Y. C. *Journal of Chromatography A* **1996**, *720*, 137-149.
176. Marshall, V. M.; Dunn, H.; Elvin, M.; McLay, N.; Gu, Y.; Laws, A. P. *Carbohydrate Research* **2001**, *331*, 413-422.
177. Heinze, T.; Dorn, S.; Schöbitz, M.; Liebert, T.; Köhler, S.; Meister, F. *Macromolecular Symposia* **2008**, *262*, 8-22.
178. Pinkert, A.; Marsh, K. N.; Pang, S. S.; Staiger, M. P. *Chemical Reviews* **2009**, *109*, 6712-6728.
179. Remsing, R. C.; Swatloski, R. P.; Rogers, R. D.; Moyna, G. *Chemical Communications* **2006**, 1271-1273.
180. Heinze, T.; Liebert, T. *Progress in Polymer Science* **2001**, *26*, 1689-1762.
181. Wu, J.; Zhang, J.; Zhang, H.; He, J.; Ren, Q.; Guo, M. *Biomacromolecules* **2004**, *5*, 266-268.
182. Kowsaka, K.; Okajima, K.; Kamide, K. *Polymer Journal* **1986**, *18*, 843-849.
183. Kowsaka, K.; Okajima, K.; Kamide, K. *Polymer Journal* **1988**, *20*, 1091-1099.
184. Biswas, A.; Shogren, R. L.; Stevenson, D. G.; Willett, J. L.; Bhowmik, P. K. *Carbohydrate Polymers* **2006**, *66*, 546-550.
185. Swalina, C.; Zauhar, R.; DeGrazia, M.; Moyna, G. *Journal of Biomolecular NMR* **2001**, *21*, 49-61.
186. Abbott, A. P.; Bell, T. J.; Handa, S.; Stoddart, B. *Green Chemistry* **2005**, *7*, 705-707.
187. Limousin, C.; Cleophax, J.; Petit, A.; Loupy, A.; Lukacs, G. *Journal of Carbohydrate Chemistry* **1997**, *16*, 327-342.

188. Szeja, W. *Polish Journal of Chemistry* **1980**, *54*, 1301-1304.
189. Bhaskar, P. M.; Loganathan, D. *Tetrahedron Letters* **1998**, *39*, 2215-2218.
190. Junot, N.; Meslin, J. C.; Rabiller, C. *Tetrahedron: Asymmetry* **1995**, *6*, 1387-1392.
191. Forsyth, S. A.; MacFarlane, D. R.; Thomson, R. J.; von Itzstein, M. *Chemical Communications* **2002**, 714-715.
192. Hudson, C. S.; Johnson, J. M. *Journal of the American Chemical Society* **1915**, *37*, 2748-2753.
193. Chen, C.-T.; Kuo, J.-H.; Li, C.-H.; Barhate, N. B.; Hon, S.-W.; Li, T.-W.; Chao, S.-D.; Liu, C.-C.; Li, Y.-C.; Chang, I. H.; Lin, J.-S.; Liu, C.-J.; Chou, Y. C. *Organic Letters* **2001**, *3*, 3729-3732.
194. Moreau, C.; Finiels, A.; Vanoye, L. *Journal of Molecular Catalysis a-Chemical* **2006**, *253*, 165-169.
195. Lima, S.; Neves, P.; Antunes, M. M.; Pillinger, M.; Ignatyev, N.; Valente, A. A. *Applied Catalysis* **2009**, *363*, 93-99.
196. Tiwari, P.; Kumar, R.; Maulik, P. R.; Misra, A. K. *European Journal of Organic Chemistry* **2005**, 4265-4270.

## 7. Publications